The role of endothelial cells in the regulation of the vascular response to Angiotensin II

Lampson Fan

Department of Cardiovascular Medicine
And
Christ Church College

A thesis submitted for the degree of Doctor of Philosophy in Cardiovascular Medicine

University of Oxford

Hilary Term 2013

Abstract

The role of endothelial cells in the regulation of the vascular response to Angiotensin II

Lampson Fan

Department of Cardiovascular Medicine and Christ Church College, University of Oxford

Submitted for the degree of D.Phil in Cardiovascular Medicine
Hilary Term 2013

Aortic dissection is a detrimental disease with a high mortality. However, the mechanisms regulating the susceptibility to aortic dissection remain unknown. We hypothesize that endothelial oxidative stress due to the activation of the reactive oxygen species (ROS)-generating Nox2 enzyme may play an important role in the development of aortic dissection. To investigate this, we generated transgenic mice (C57BL/6J background) with endothelial specific over-expression of Nox2 (Nox2 Tg) under the control of a tie-2 promoter. Expression of the human Nox2 transgene was confirmed by qRT-PCR to be found only in endothelial cells (EC) isolated from transgenic mice, and not in Wt EC or vascular smooth muscle cells (VSMC) and macrophages isolated from either genotype.

Wild-type (Wt) littermates and Nox2 Tg male mice (22-24 weeks old, n=11) were treated with saline or Ang II (1mg/kg/day) via subcutaneous mini-pump for 28 days. There was no significant difference in the pressor responses to Ang II between Wt and Nox2 Tg mice (Wt 121±7mmHg vs. Nox2-Tg 122±6mmHg). However, 5/11 Nox2 Tg mice developed aortic dissections compared to 0/11 Wt mice ($P<0.05$). Immunohistochemistry revealed significant increases in endothelial VCAM-1 expression, MMP activity and $CD45^+$ inflammatory cell recruitment in the aortas of Nox2 Tg mice after 5 days of Ang II infusion. Inflammatory cell recruitment was confirmed by FACS analysis of cells from digested aortas ($P<0.05$). Explanted aortas from Nox2-Tg mice had significantly greater secreted pro-inflammatory cytokine, Cyclophilin A (CypA) both at baseline and after 5 days of Ang II infusion compared to Wt littermates. Compared to primary Wt EC and VSMC, Nox2-Tg primary EC, but not primary VSMC, had increased ROS production which was accompanied by increased endothelial CypA secretion and ERK1/2 activation. Furthermore, conditioned media from Nox2-Tg EC induced greater ERK1/2 phosphorylation compared to conditioned media from Wt controls. Knockdown of CypA from sEND.1 endothelial conditioned media by siRNA knockdown abolished VSMC Erk1/2 phosphorylation.

In conclusion, we demonstrate for the first time that a specific increase in endothelial ROS through the over-expression of Nox2 was sufficient to induce aortic dissection in response to Ang II stimulation. Endothelial secreted CypA could be the signalling mechanism by which increased endothelial ROS regulates the inflammatory response and the susceptibility to aortic dissection.

Contents

Abstract **1**

Acknowledgements **9**

List of Figures **10**

List of Tables **14**

Chapter 1. Introduction **16**

1.1 Vascular Oxidative Stress and ROS **16**

1.1.1 Sources of O_2^- production 18

1.2 NADPH oxidases and their relevance in cardiovascular diseases **25**

1.2.1 Vascular smooth muscle cell NADPH oxidases 25

1.2.2 Endothelial NADPH oxidases 27

1.3 Angiotensin II infusion model of acute vascular inflammation **31**

1.3.1 Abdominal aortic aneurysm 32

1.3.2 Aortic dissection 33

1.3.3 Mechanism of Ang II induced aortic disease 38

1.4 Endothelial Nox2 over-expressing transgenic mice **44**

1.5 Original Hypothesis **46**

1.6 Aims **46**

Chapter 2. Materials and Methods **48**

2.1 Materials 48

2.1.1 Buffers and Media 48

2.2 Animal care and use 49

2.2.1 Nox2 Tg mice 49

2.2.2 DNA extraction 50

2.2.3 Genotyping PCR 50

2.2.4 Organ harvesting 52

2.2.5 Insertion of osmotic mini-pumps 52

2.3 Measurement of O_2^- 53

2.3.1 Dihydroethidium staining and high performance liquid chromatography 54

2.4 RNA techniques 55

2.4.1 RNA extraction 56

2.4.2 cDNA generation 56

2.4.3 Quantitative Real RT-PCR 57

2.5 Cell culture 59

2.5.1 sEND.1 cell culture 59

2.5.2 Isolation of bone marrow and peritoneal macrophages 59

2.6 Protein extraction and detection 61

2.6.1 Protein lysate preparation 61

2.6.2 Determination of protein content 61

2.6.3 Immunoblotting 62

2.7 Flow cytometry 64

2.7.1 Preparation of cell suspension from aorta 64

2.7.2 Staining procedure 64

2.7.3 Quantification of cell numbers 66

2.8 Statistical analysis 66

Chapter 3. Response of Nox2 Tg mice to Ang II infusion 68

3.1 Introduction 68

3.1.1 Hypothesis and Aims 70

3.2 Methods 70

3.2.1 Tail cuff blood pressure measurement 70

3.2.2 Analysis of aorta 71

3.3 Results 75

3.3.1 Nox2 transgene expression is endothelial specific 75

3.3.2 Blood pressure response to Ang II 77

3.3.3 Increased aortic dissection in Nox2 Tg mice in response to Ang II 79

3.3.4 Site of dissection was observed in the supra-renal aorta of Nox2 Tg mice ... 81

3.3.5 Increased elastic degradation in supra-renal aorta of Nox2 Tg mice 83

3.3.6 Assessment of the site of rupture using magnetic resonance imaging (MRI) 85

3.3.7 Increased BP in response to noradrenaline infusion had no effect on the development of aortic disease in Nox2 Tg mice 87

3.3.8 No significant difference in body weight or heart rate between wild-type and Nox2 Tg....93

3.4 Discussion....95

Chapter 4. Inflammatory response of Nox2 Tg aortas....101

4.1 Introduction....101

4.1.1 Hypothesis and Aims....103

4.2 Methods....103

4.2.1 Analysis of aorta....104

4.2.2 Magnetic resonance imaging (MRI)....110

4.3 Results....114

4.3.1 Increased endothelial VCAM-1 expression in the early stage of the development of Ang II-induced aorta dissection....114

4.3.2 Increased $CD45^+$ inflammatory cell recruitment in Nox2 Tg aortas as compared to wild-type aortas after 5 days of Ang II infusion....126

4.3.3 Increased metalloproteinase activity in Nox2 Tg aortas after 5 days of Ang II infusion 133

4.4 Discussion....136

4.4.1 Summary....139

Chapter 5. Characterisation of wild-type and Nox2 Tg primary endothelial cells and VSMCs....141

5.1 Introduction....141

5.2 Hypothesis and aims 142

5.3 Methods 142

5.3.1 Isolation of primary endothelial cells 142

5.3.2 Isolation of primary vascular smooth muscle cells 143

5.3.3 Preparation of conditioned media and stimulation of VSMCs 148

5.4 Results 148

5.4.1 Characterisation of primary endothelial cells 148

5.4.2 Characterisation of primary VSMCs 161

5.4.3 Evidence for secreted factors in the Nox2 Tg endothelial cell conditioned media which act to induce VSMC Erk1/2 phosphorylation and activation. 168

5.5 Discussion 170

Chapter 6. The mechanism of endothelial Nox2 regulation of VSMC activation: the role of secreted CypA 175

6.1 Introduction 175

6.2 Hypothesis and aims 176

6.3 Methods 177

6.3.1 Preparation of conditioned media from aorta 177

6.3.2 siRNA knockdown of CypA 177

6.4 Results 178

6.4.1 Detection of CypA 178

6.4.2 Ang II induced CypA secretion by sEND.1 cells in low glucose medium but not in high glucose medium (DMEM) 183

6.4.3 Nox2 Tg endothelial cells secreted higher levels of CypA at baseline compared to wild-type endothelial cells 185

6.4.4 Increased CypA secretion is associated with increased Erk1/2 phosphorylation in Nox2 Tg endothelial cells 188

6.4.5 No difference CypA secretion between wild-type and Nox2 Tg VSMCs .. 190

6.4.6 No significant difference Erk1/2 phosphorylation between wild-type and Nox2 Tg VSMCs in response to either acute or chronic Ang II stimulation 195

6.4.7 Exogenous CypA can induce Erk1/2 phosphorylation in VSMCs 198

6.4.8 sEND.1 endothelial CypA induced Erk1/2 phosphorylation that was abolished by knockdown of CypA. 201

6.4.9 CypA stimulation increased non-superoxide (O^{-}) ROS production 208

6.4.10 Increased CypA secretion by Nox2 Tg aortic vessel segments compared to wild-type aortic vessel segments 213

6.4.11 Increased CypA in Nox2 Tg aorta at both baseline and following Ang II infusion 215

6.5 Discussion 219

6.6 Summary 222

Chapter 7. General Discussion 224

7.1 Original hypothesis and aims 224

7.2 Summary of key findings 225

7.3 Proposed mechanism of endothelial O_2^- and CypA in Ang II induced aortic dissection 226

7.4 Future directions 226

7.5 Final conclusion 229

References 232

Appendices 252

Acknowledgements

I would like to firstly thank my supervisor Professor Keith Channon for the opportunity of the BHF CRE Clinical Fellowship and also to study for a D.Phil at his lab. I am extremely grateful for his inspiration, advice, and guidance throughout the D.Phil in accomplishing the research discussed in this thesis. I would like to extend my heartfelt thanks to Gillian Douglas for her kind and generous support, through the good and bad, and the occasional Christmas and bank holidays. The time, knowledge and patience that she has given to me over the last three years will forever be appreciated, even Glasgow FM. I would also like to thank Jennifer Bendall who provided not only the helping hand at the start of the project but also advice and support throughout the project.

I would like to express my sincerest gratitude to all members of the Channon Group, without whom this thesis would not have been possible. A big thank you for making the lab work such an enjoyable experience and for all the height jokes Mark Crabtree and Ashley Hale have invented over the last three year. A special thanks to Eileen McNeill for her help with FACS and experiments; Ashley Hale for helping out with pretty much everything, Mark Crabtree for the cell work; Joyti Patel as 1 of the 4 musketeers along with Surawee whose innocence has been tainted by Mark; Katrin who still sounds more German than Italian; Manish who is a dude and "MMP9" Regent Lee.

I would like to thank James Brown for technical support around the lab and reminders to wear lab coat and goggles; and to Carol Williams, Viv Clark and the technicians at the FGF for providing animal care. I also acknowledge the British Heart Foundation Centre of Research Excellence for the Clinical fellowship and Christ Church College for their support and generous allowances.

Finally, I would like to thank my family and friends for their support, especially my mum who has been a constant source of encouragement and helpful advice. I am truly grateful for my time at the Channon Lab and thank you to everyone who has made it such a wonderful learning experience.

List of Figures

Figure 2.1.....52

Figure 3.1.....73

Figure 3.2.....74

Figure 3.3.....76

Figure 3.4.....78

Figure 3.5.....80

Figure 3.6.....82

Figure 3.7.....84

Figure 3.8.....86

Figure 3.9.....88

Figure 3.10.....90

Figure 3.11.....92

Figure 4.1.....105

Figure 4.2.....107

Figure 4.3.....109

Figure 4.4.....112

Figure 4.5.....115

Figure 4.6.....**117**

Figure 4.7.....**118**

Figure 4.8.....**120**

Figure 4.9.....**121**

Figure 4.10.....**124**

Figure 4.11.....**125**

Figure 4.12.....**127**

Figure 4.13.....**128**

Figure 4.14.....**130**

Figure 4.15.....**131**

Figure 4.16.....**132**

Figure 4.17.....**134**

Figure 4.18.....**135**

Figure 5.1.....**145**

Figure 5.2.....**147**

Figure 5.3.....**150**

Figure 5.4.....**152**

Figure 5.5.....**154**

Figure 5.6.....**155**

Figure 5.7.....**157**

Figure 5.8.....**159**

Figure 5.9.....**160**

Figure 5.10.....**162**

Figure 5.11.....**164**

Figure 5.12.....**166**

Figure 5.13.....**167**

Figure 5.14.....**169**

Figure 6.1.....**179**

Figure 6.2.....**181**

Figure 6.3.....**182**

Figure 6.4.....**184**

Figure 6.5.....**186**

Figure 6.6.....**187**

Figure 6.7.....**189**

Figure 6.8.....**191**

Figure 6.9.....**192**

Figure 6.10.....**194**

Figure 6.11.....**196**

Figure 6.12.....**197**

Figure 6.13.....**199**

Figure 6.14.....**200**

Figure 6.15.....**202**

Figure 6.16.....**203**

Figure 6.17.....**205**

Figure 6.18.....**207**

Figure 6.19.....**209**

Figure 6.20.....**210**

Figure 6.21.....**212**

Figure 6.22.....**214**

Figure 6.23.....**216**

Figure 6.24.....**218**

Figure 7.1.....**230**

List of Tables

Table 2.1 Buffers and media 49

Table 2.2 Primer list 51

Table 2.3 TaqMan® Gene Expression Assays. 57

Table 2.4 Antibodies used for immunoblotting. 63

Table 2.5 Antibodies used for flow cytometry. 65

Chapter 1:
Introduction

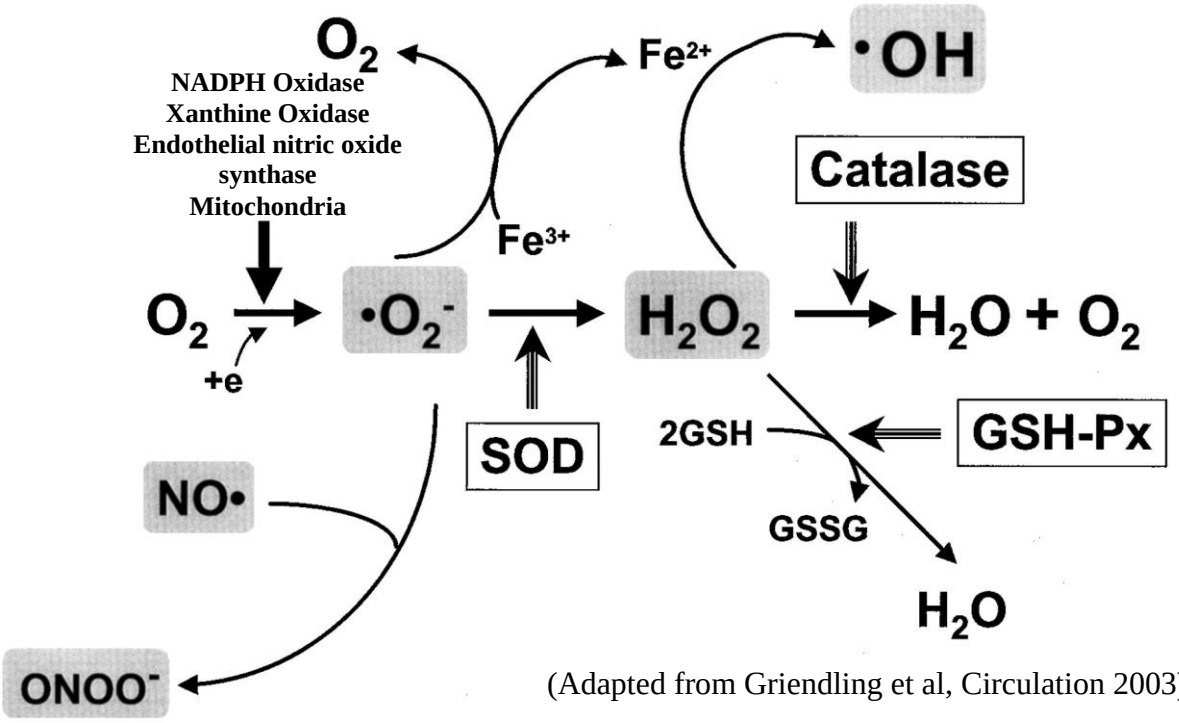
Chapter 1. Introduction

1.1 Vascular Oxidative Stress and ROS

Vascular oxidative stress has been recognised as a key factor in the pathogenesis of many diseases including atherosclerosis, diabetes and hypertension (Cai and Harrison, 2000). It was firstly defined in 1985 by Sies H as "An imbalance between oxidants and antioxidants in favour of the oxidants, potentially leading to damage" (Seis, 1985). Oxidants in the cell consist of reactive oxygen or nitrogen species, a group of radical or non-radical entities released by mitochondrial respiratory chain or by cellular enzymatic activities. The major reactive oxygen species (ROS) relevant to vascular disease are superoxide (O_2^-) peroxynitrite ($ONOO^-$), hydroxyl ($OH^\cdot$) anions and H_2O_2. When released in excess quantities, these oxygen species trigger a variety of cellular response including cell dysfunction, alteration of proliferation, cell death and damage to genomic or mitochondrial DNA. It is vital therefore to have robust defence against the formation of these damaging oxygen species.

The overall balance between oxidative (ROS generating) and reductive (ROS scavenging) process constitutes cellular "redox state". When the rate of formation of ROS exceeds the scavenging or depredating capacity of the antioxidant defence system, oxidative stress occurs (Irani, 2000; Kunsch and Medford, 1999). The antioxidant mechanisms can be divided into non-enzymatic molecules and antioxidant enzymes. Non-enzymatic molecules serve as ROS degrading molecules (ROS scavengers) including uric acid, ascorbic acid, α-tocopherol, and sulfhydryl-containing molecules such as glutathione (Liu et al., 1997). Antioxidant enzymes include catalase, glutathione peroxidase and superoxide dismutase (SOD). There are three types of SOD: mitochondria manganese-containing SOD

(MnSOD), cytosolic copper-zinc SOD (CuSOD) and an extracellular SOD. A summary of the key ROS producing enzymes and anti-oxidant enzymes is shown in Diagram 1.1 (Griendling and FitzGerald, 2003).



(Adapted from Griendling et al, Circulation 2003)

Diagram 1.1 Enzymatic sources of vascular ROS and defence mechanisms.
Oxidases convert O_2 to O_2^- which can be dismuted to H_2O_2 by superoxide dismutase (SOD). H_2O_2 can be converted to H_2O by glutathione peroxidise (GSH-Px) or catalase.

Recently, it has become clear that ROS such as O_2^- and H_2O_2 have several other important roles in the regulation of cellular function, such as the modulation of specific redox-sensitive signal transduction pathways and transcriptional regulatory networks (Griendling and Harrison, 1999; Irani, 2000; Kunsch and Medford, 1999). Evidence for this can be found from the studies of non-phagocytic cells. For example, in T lymphocytes, ROS influence the activity of the transcription factor, NF-κB, by releasing its inhibitory subunit

IκB and causing a rapid activation of protein kinase C (PKC) resulting in cell proliferation (Irani, 2000) . In rabbit kidney epithelial cells, H_2O_2 has been found to activate c-Jun N-terminal kinase (JNK), which is involved in redox signalling (Cui and Douglas, 1997). In cardiac myocytes, H_2O_2 has been discovered as secondary messenger involved in the response of cardiomyocyte to endothelin-1 (Cheng et al., 1999).

Many of the biological effects of ROS are concentration dependent so at lower concentrations, ROS may function as secondary messengers to regulate cellular physiological activities. However, at levels above the physiological concentration, ROS are deleterious to cells and cause cellular oxidative damage. The different ROS species also have distinct roles. O_2^- is usually generated though the donation of one electron from molecular O_2 and is unstable in aqueous solution with half-life of a few milliseconds. Most of O_2^- are therefore rapidly dismuted to H_2O_2 so when O_2^- production is low such as in the resting cell, most of the biological effect are likely to be secondary to H_2O_2 which is more stable, diffusible and cell membrane permeable. H_2O_2 is therefore likely to be more relevant than O_2^- in the modulation of basal signal transduction pathways. O_2^- also reacts with NO at a slightly slower rate than SOD ($7x10^{-9}$ vs. $2x10^{-9}$ $mol.L^{-1}.s^{-1}$) (Forman and Fridovich, 1973; Huie and Padmaja, 1993) so when NO are in the high nanomolar range it may outcompete SOD to generate $ONOO^-$ which results in NO inactivation and cellular dysfunction. At very high levels O_2^- could react with iron-sulphur centres within proteins and release iron which reacts with H_2O_2 to generate the highly reactive $OH^{\cdot}$ leading to oxidative stress associated tissue injury.

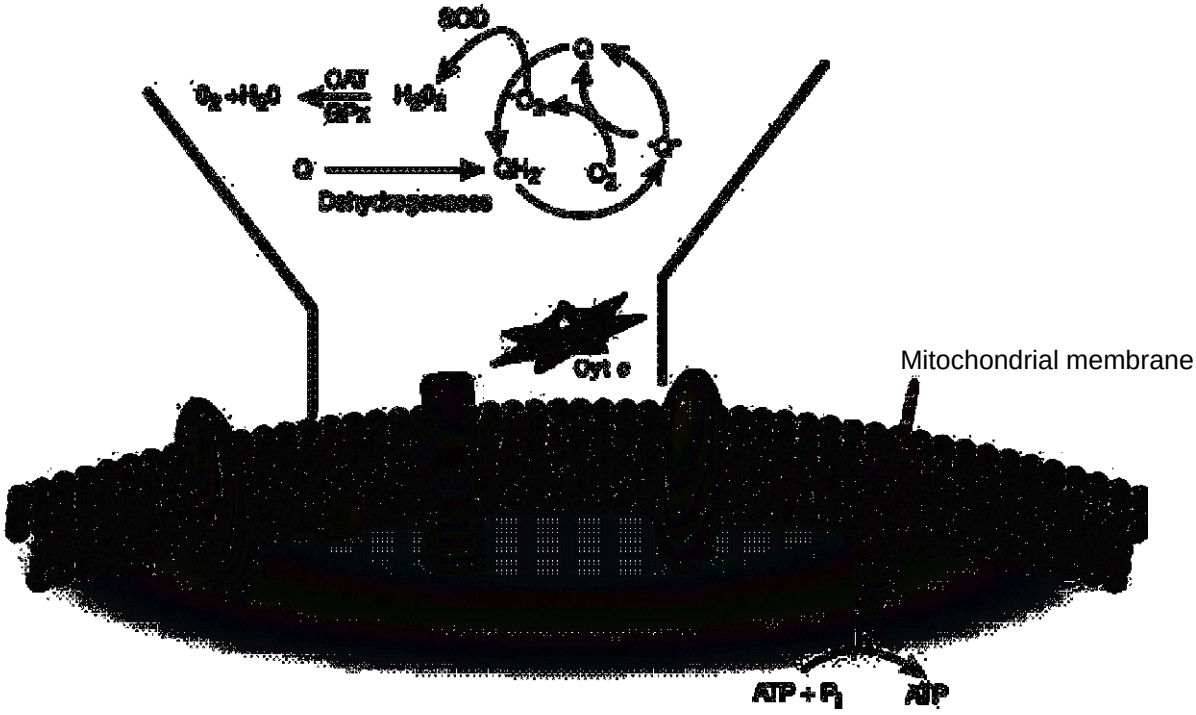
1.1.1 **Sources of O_2^- production**

There are many sources of ROS generation inside the cells including the mitochondria, Xanthine oxidase (XO), uncoupled Nitric Oxide Synthases, Cytochrome p-450 and

NADPH oxidases. Other enzymes such as lipooxygenases may also generate ROS (Dröge, 2002).

1.1.1.1 Mitochondria

The mitochondrial respiratory chain can be a major source of O_2^- generation. During aerobic metabolism, energy of mitochondrial electron transport is converted to the high energy ATP bonds via the multi-component NADH dehydrogenase complex. Molecular oxygen serves as the electron acceptor from co-enzyme Q (part of Complex III) and forms O_2^-, which is dismuted by SOD to form H_2O (Diagram 1.2) (Finkel and Holbrook, 2000).



Adapted from Finkel et al, Nature, 2000

Diagram 1.2 Schematic representation of the mitochondrial electron transport chain generation of O_2^-.
Electrons from complex I or II dehydrogenases are transferred to coenzyme Q forming the unstable intermediate $\cdot Q^-$ which can then transfer electrons directly to molecular oxygen to form O_2^-. The superoxide is enzymatically dismuted by SOD to form hydrogen peroxide that in turn is metabolized by catalase and glutathione reductase to water and molecular oxygen.

It has been calculated around 1-4% of O_2 may be incompletely reduced resulting in O_2^- formation mainly at complex I and III.

In situations of metabolic disturbance there is increased mitochondrial O_2^- production which contributes to the development of cardiovascular diseases. For example, hyperglycaemia induces mitochondrial O_2^- production which activates hexosamine and polyol pathways and damages peripheral organs leading to diabetic complications (Du et al., 2000). Mitochondrial generation of O_2^- also plays an important role in ischaemia-reperfusion injury where the increased O_2^- contributes to the activation of NF-KB, secretion of IL6 and increased endothelial permeability (Pearlstein et al., 2002).

1.1.1.2 Xanthine Oxidoreductase

Xanthine oxidoreductase (XOR) is a ubiquitously expressed molydboflavoenzyme which acts to catalyse the oxidation of hypoxanthine to xanthine and xanthine to urate. It exists in two inter-convertible forms: xanthine dehydrogenase (XD) which is constitutively expressed in cells, and xanthine oxidase (XO) which is generated through reversible thiol oxidation of sulfhydryl residues on XD or via irreversible cleavage of a segment of XD during episodes of ischaemia, hypoxia or inflammatory stimuli such as TNF-α (Meneshian and Bulkley, 2002). Unlike XD, XO requires molecular O_2 as electron acceptor thereby generating O_2^- during the catalytic reaction.

XOR is expressed on the luminal surface of endothelial cells in most organs and is upregulated by interferon-γ (Dupont et al., 1992). There is increasing evidence supporting an important role for XOR in endothelial dysfunction and development of vascular disease. For example, allopurinol (inhibitor of XOR) increased NO-stimulated blood flow and reversed endothelial dysfunction in smokers and diabetics (Butler et al., 2000; Guthikonda et al., 2003). XOR activity was also found to be elevated by >200% in diseased arteries of

patients with heart failure and inversely correlated with endothelial-dependent vasodilatation (Landmesser et al., 2002). However, the largest clinical trial, OPT-CHF study, in which over 400 patients were recruited and randomised to receive either oxypurinol or placebo did not demonstrate overall improvement in moderate to severe heart failure although there was some benefit in the subgroup of patients with elevated serum uric acid (Hare et al., 2008).

1.1.1.3 Cytochrome P-450

Cytochrome P-450 (CYP) enzymes are well known hemo-containing hepatic endoplasmic reticular flavoenzymes that can metabolise cholesterol, vitamins, steroids and many medicinal drugs through oxidation, peroxidation and reduction in an oxygen and NADPH dependent manner (Fleming, 2001). CYPs are predominately expressed in the liver but it has become clear that some specific forms of CYPs are primarily expressed in extra-hepatic tissues such as the lung and kidneys. In the vascular system, the predominant CYP involved are CYP2 and CYP4 gene families which modulate vascular function through the generation of vasodilatory metabolites. For example, 20-HETE generated by CYP4A in VSMCs is a main determinant of myogenic response in renal and cerebral arteries (Gebremedhin et al., 2000; Zou et al., 1994). It has also been shown CYP2 epoxygenases (most notably CYP 2C8/9) expressed in endothelial cells generate epoxyeicosatrienoic acids (EETs) which is an integral part of endothelium-derived hyperpolarisation factor (EDHF) response that mediates NO and prostaglandin independent vasodilatation observed in coronary, mesenteric and renal arteries (Fleming, 2001). This was shown in porcine coronary arteries in which incubation with anti-sense oligonucleotides directed against the coding region of CYP 2C markedly reduced CYP 2C mRNA and protein; and significantly

attenuated EDFH-mediated relaxation without affecting the vaso-relaxation response to NO or NO donors (Fisslthaler et al., 1999).

Recent evidence have shown that CYP also generates superoxide, hydrogen peroxide and hydroxyl radicals when the electrons for the reduction of the central heme iron are transferred to the bound oxygen in an NADPH dependent reaction (Bondy and Naderi, 1994; Puntarulo and Cederbaum, 1998). It is interesting to note that CYP 2C which has been identified to produce EDHF involved in vasorelaxation is a significant source of ROS in porcine coronary arteries (Fleming et al., 2001). As ROS is potentially a vasoconstrictor due to the inactivation of NO, the role of CYP in vascular disease is likely to be complex.

1.1.1.4 Uncoupled Nitric Oxide Synthases

Nitric Oxide Synthases (NOS) are homodimeric oxidoreductases that produce NO through the oxidation of L-arginine by the reduction of O_2. The essential co-factor of NOS, tetrahydrobiopterin (BH_4) has been shown to have a critical role as the determinant of NOS activity. Therefore, when BH_4 availability is limited, NOS becomes "uncoupled" and generates superoxide instead of NO (Alp and Channon, 2004). In addition, BH_4 itself is highly susceptibility to oxidation, so the loss of BH_4 in response to increased ROS production from other enzymatic sources such as NADPH oxidases has been shown to amplify oxidative stress through the loss of NO production and increase in NOS-dependent O_2^- production (Landmesser et al., 2003). Similarly, peroxynitrite generated through the reaction between NO and O_2^- may also oxidise BH_4 and represent another mechanism by which NOS becomes uncoupled (Alp and Channon, 2004). In addition to degradation and increased catabolism, BH_4 levels may also be depleted due to reduced synthesis through modifications of GTP cyclohydrolase I (GTPCH) activity, which is the rate limiting enzyme in the biosynthesis of BH_4. Elevated O_2^- production from uncoupled NOS has been

implicated in the development of several diseases including atherosclerosis, diabetes and hypertension (Alp et al., 2003; Vasquez-Vivar et al., 2003).

1.1.1.5 NADPH oxidases

NADPH oxidases were originally discovered in neutrophils as enzymatic sources for the generation of O_2^- required for the respiratory burst needed to kill invading organisms (Thrasher et al., 1994). When the system is defective, little or no O_2^- is produced, microbial killing is impaired and the individual is severely immune-compromised with recurrent life threatening sepsis, hypergammaglobuniaemia and systemic granulomatous infiltration. This condition is known as chronic granulomatous disease (CGD), an inherited genetic disorder (Landing and Shirkey, 1957; Quie et al., 1968). Apart from microbiocidal function, O_2^- produced by neutrophils are also implicated in the pathogenesis of many diseases such as rheumatoid arthritis and ischemia-reperfusion injury (Li and Shah, 2004).

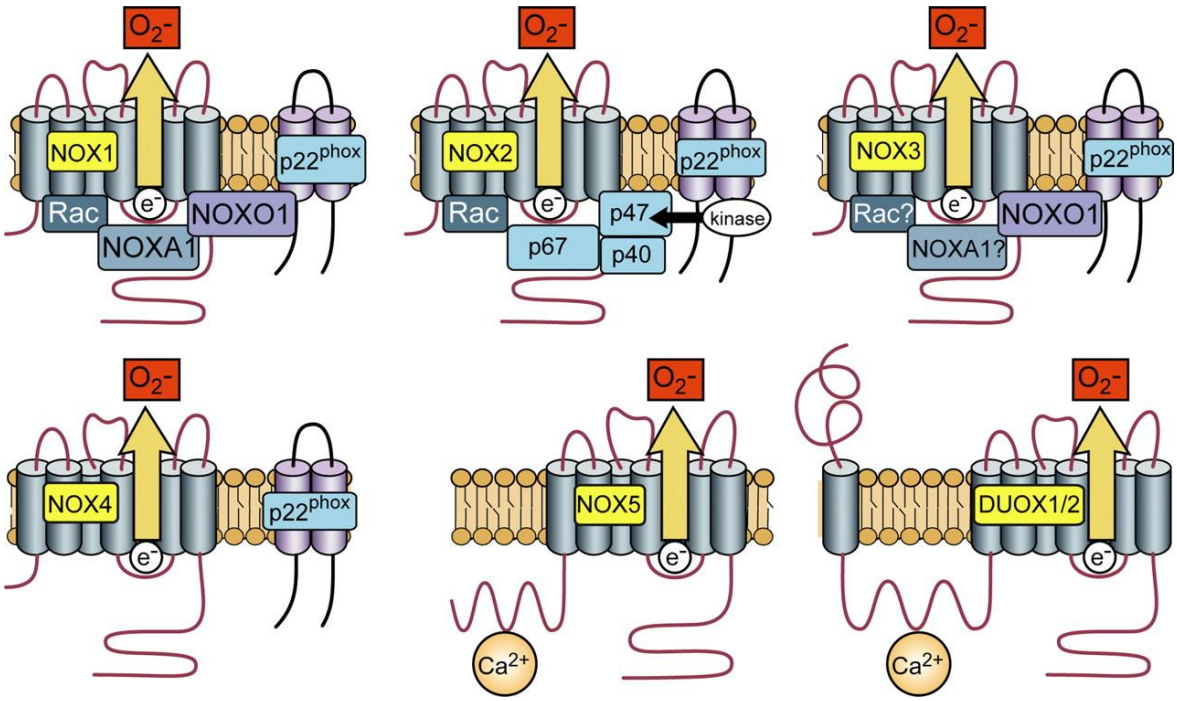
The molecular structure and regulatory mechanism of neutrophil NADPH oxidase has been extensively studied and well characterised. It is a multicomponent enzyme consisting of membrane associated cytochrome b_{558} (a heterodimer composed of $p22^{phox}$ and $gp91^{phox}$) and several regulatory subunits ($p47^{phox}$, $p67^{phox}$, $p40^{phox}$, and Rac1 or Rac2). NADPH oxidase is dormant in resting neutrophils as the plasma membrane preparations from neutrophils have no NADPH oxidase activity. Neutrophil NADPH oxidase acquires catalytic activity when the cells are exposed to stimuli such as phorbol esters, opsonised microbes or peptides from degraded bacterial proteins. Following cellular activation, the cytosolic components ($p47^{phox}$, $p67^{phox}$, $p40^{phox}$, and Rac1 or Rac2) translocate to the plasma membrane and associate with the cytochrome complex to form the active enzyme complex.

NADPH oxidase generates superoxide by transferring electrons from NADPH to molecular O_2.

$$NADPH + 2O_2 \leftrightarrow NADP^+ + 2O_2^- + H^+$$

Seven isoforms have been identified so far in the Nox family e.g., Nox1-5 and Duox1-2 (Diagram 1.3) (Bedard and Krause, 2007). In the vasculature, endothelial cells (EC) mainly express Nox2 and Nox4 whereas vascular smooth muscle cells (VSMC) predominantly express Nox1 and Nox4.

Diagram 1.3



Adapted from Bedard and Krause, Physiol Rev, 2007

Diagram 1.3 NADPH isoforms.
Although the NADPH oxidase isoforms are similar in structure, they differ in activation mechanisms. $p22^{phox}$ is required in the activation of Nox 1, Nox 2, Nox 3 and Nox 4; Rac for Nox1, Nox2, Nox2; NOXO1 for Nox1 and Nox 3; NOXA1 for Nox 1 and possibly Nox 3. Nox5 and Duox1/2 are activated by Ca^{2+} and do not appear to require subunits.

1.2 NADPH oxidases and their relevance in cardiovascular diseases

1.2.1 **Vascular smooth muscle cell NADPH oxidases**

Vascular smooth muscle cells (VSMCs) NADPH oxidases have been the focus of studies over recent years (Clempus and Griendling, 2006). Similar to the phagocytic oxidase, the VSMC NADPH oxidases are membrane located as 98% of the oxidase activity was detected in the membrane fraction (Griendling et al., 2000). All VSMC Nox isoforms require $p22^{phox}$ whilst the catalytic unit could be Nox1, Nox2, Nox4 or Nox5 (Ambasta et al., 2004). Treatment of cultured VSMC with Ang II or TNFα increased $p22^{phox}$ mRNA expression and oxidase activity, and the Ang II-stimulated oxidase activity can be decreased to 50% by antisense $p22^{phox}$ transfected into these cells (De Keulenaer et al., 1998a; Rajagopalan et al., 1996). The distribution of the catalytic unit is tissue specific so in aortic VSMCs, only Nox1 and Nox4 are expressed.

An important characteristic of VSMC Noxs in comparison to neutrophil Nox system is that VSMC Noxs have basal activity as well as agonist induced activity (Sorescu et al., 2001). The basal activity is likely to come from the Nox4 isoform whereas the agonist induced activity is mostly from the Nox1 isoform (Sorescu et al., 2001).

1.2.1.1 Nox1

Nox1 has been implicated in the development of many cardiovascular diseases such as hypertension and abdominal aortic aneurysm formation. It is found to be upregulated in experimental models of hypertension such as renin transgenic rats (Wingler et al., 2001), Dalh salt-sensitive rats (Nishiyama et al., 2004) and clipping of renal arteries (Wang et al., 2007). Knockout of $p47^{phox}$, an essential subunit for Nox1, prevents hypertension induced

by bone morphogenetic protein-4, a Nox1 dependent endothelial agonist. More directly, Nox1 knockout prevented the sustained rise in blood pressure in response to Ang II (Matsuno et al., 2005b); and also reduced formation of Ang II induced abdominal aortic aneurysm (Gavazzi et al., 2007). However, in the renin over-expressing mouse model of hypertension, Nox1 knockout had no effect on either vascular hypertrophy (Matsuno et al., 2005a) or blood pressure (Yogi et al., 2008). Nox1 over-expression in VSMCs on the other hand leads to exacerbated blood pressure increase and vascular hypertrophy in response to Ang II (Dikalova et al., 2005). These mice have impaired endothelial dependent relaxation which suggests cross-talk between VSMCs and the release of endothelial NO (Dikalova et al., 2010).

There is emerging evidence for the role of Nox1 in other vascular diseases. In atherosclerosis for example, the role of Nox1 was examined by crossing male Nox1 knockout mice ($Nox1^{+/-}$) mice onto the $ApoE^{-/-}$ background to generate $Nox1^{+/-}ApoE^{-/-}$ mice and feeding these mice high fat diet for 18 weeks to examine for the development of atherosclerotic plaques in the aorta (Sheehan et al., 2011). The deficiency of Nox1 resulted in 15% reduction in aortic arch lesions which was associated with reduced macrophage infiltration compared to $ApoE^{-/-}$ control.

1.2.1.2 Nox4

Recent studies have suggested that Nox4 could be involved in the differentiation and the maintenance of VSMCs phenotype: Nox4 mediates TGF-β mediated transformation of fibroblasts into contractile fibroblasts (Cucoranu et al., 2005) and knockdown of Nox4 by SiRNA down-regulated the differentiation markers such SM-α actin, SM-MHC and calponoin (Clempus et al., 2007). However, the evidence available for the role of Nox4 in VSMCs is still very much in the preliminary stage.

1.2.2 **Endothelial NADPH oxidases**

NADPH oxidases are well established enzymatic sources of endothelial O_2^- (Al-Mehdi et al., 1998; De Keulenaer et al., 1998b; Meyer et al., 1999). Similar to VSMC NADPH oxidases, endothelial NADPH oxidases produce consistently a low basal level of O_2^- without exogenous stimulation. The activity of endothelial NADPH oxidase can be increased in response to high concentration of LDL (Meyer and Schmitt, 2000); cytokines such as TNFα (Murphy et al., 1992), cyclic strain (Howard et al., 1997), pulsatile stretch (Hishikawa and Lüscher, 1997) and oscillatory shear (De Keulenaer et al., 1998b).

Endothelial cells express mainly Nox2 and Nox4 and evidence have shown they have distinct roles and regulatory mechanisms. Nox2 in endothelial cells is structurally similar to Nox2 in neutrophils and requires binding of the regulatory subunits for their activation. Nox2 is upregulated by agonists such as Ang II, shear stress and oxidised-LDL and is the predominant source of agonist induced NADPH oxidase derived O_2^- in endothelial cells (Lassègue et al., 2012). Nox4 on the other hand has distinctly different structure and regulatory mechanisms to Nox2. One of the major differences is that Nox4 is constitutively active and does not require the binding of cytosolic regulatory subunits for its activity. Secondly, the main product of Nox4 is H_2O_2 rather than O_2^- (Dikalov et al., 2008) suggesting that Nox4 mainly accounts for the basal ROS required for maintaining normal endothelial function, such as cell proliferation and migration.

1.2.2.1 Nox 4

The first targeted endothelial Nox4 study was by Ray et al. when they generated an endothelial specific Nox4 over-expressing transgenic mouse (Ray et al., 2011). These mice exhibited significantly enhanced endothelial dependent acetylcholine or histamine induced vasodilatation from increased H_2O_2 production and reduced basal blood pressure which

was normalised by the use of antioxidants. The key mechanism was attributed to the EDHF effect of H_2O_2 and reduced NO inactivation. In support of the protective effect of Nox4, $Nox4^{-/-}$ mice had reduced ischemia-induced angiogenesis and increased vascular inflammation, media hypertrophy and endothelial dysfunction in response to Ang II stimulation (Schröder et al., 2012). This was associated with reduced NO synthase expression, NO production, and hemeoxygenase-1 expression which was a protective factor against hypoxia. Others have shown endothelial Nox4 over-expression enhanced recovery from hind limb ischaemia and increased eNOS expression (Craige et al., 2011). Collectively, these studies suggest a vaso-protective effect of endothelial Nox4 through activation of eNOS, increase in production of NO, generation of H_2O_2 as an EDHF and increase in anti-hypoxia factors such as HO-1.

1.2.2.2 Nox 2

The role of endothelial Nox2 in vascular diseases has been extensive studied in hypertension given its ability to inactivate NO and affect vascular remodelling. It is found to be upregulated in the vessel wall in many forms of hypertension (Cifuentes et al., 2000; Lassègue et al., 2012; Wang et al., 2001). In $Nox2^{-/-}$ mice, basal blood pressure is reduced (Wang et al., 2001) and infusion of Nox2 ds-tat, an inhibitor of Nox2, reduced the hypertensive effect of Ang II (Rey et al., 2001).

Nox2 has also been extensively studied in atherosclerosis where Nox2-derived O_2^- is involved in oxidation of LDL and uptake in macrophage and VSMC proliferation (Meyer and Schmitt, 2000). Clinical studies have shown that the expression of the $p22^{phox}$ subunit of NADPH oxidase is upregulated in human coronary arteries and is correlated with the progression of atherosclerotic lesions (Azumi et al., 1999; Cahilly et al., 2000). The C242T polymorphism of $p22^{phox}$, which alters NAPDH oxidase superoxide activity in human

vessels, was found to be associated with increased risk of coronary artery disease (Guzik et al., 2000; Inoue et al., 1998). Experimental studies however, are more controversial. Kirk et al (Kirk et al., 2000) showed that there was no difference in atherosclerotic lesion formation in $Nox2^{-/-}$ ascending aortas compared to $ApoE^{-/-}$ mice. In contrast, a more recent study (Judkins et al., 2010b) found 50% reduction in the atherosclerotic lesion in descending aortas of $Nox2^{-/y}ApoE^{-/-}$ mice compared to $ApoE^{-/-}$ controls. Cell specific Nox2 knockout studies will be required to account for the contradictory findings for the role of Nox2 in atherosclerosis.

There is also increasing evidence for the role of endothelial Nox2 in the development of aortic disease such as abdominal aortic aneurysms. In human abdominal aneurysmal tissues, $p22^{phox}$ expression was observed to be upregulated and associated with increased macrophage infiltration and matrix metalloproteinase (MMP) activity (Ejiri et al., 2003). In mouse experimental models, knockout of $p47^{phox}$ reduced aortic superoxide production and the incidence of aortic aneurysm formation (Thomas et al., 2006). In addition, there was a reduction in macrophage infiltration and MMP-2 activity. The use of pharmacological inhibitor of Nox2 such as apocynin suppressed aortic aneurysm formation (Xiong et al., 2009). Interestingly, the use of Vitamin E, a non-specific ROS scavenger, also demonstrated attenuation of abdominal aortic aneurysm formation (Gavrila et al., 2005). However, none of these previous studies have used a targeted cell approach and as Nox2 is highly expressed in many different cells including phagocytic cells, endothelial cells and adventitial fibroblasts, it was not possible to address the question of the importance and contribution of endothelial Nox2. It is also unclear whether an increase in endothelial ROS alone is sufficient to drive the development of diseases observed in these studies. This is an important question, since endothelial ROS production and endothelial

dysfunction are predictive of cardiovascular events and long-term clinical outcome (Schachinger et al., 2000). Further understanding of the role of endothelial ROS may identify new therapeutic targets in the prevention and treatment of cardiovascular diseases.

Recently, the role of endothelial ROS in atherosclerosis was investigated by Dr Douglas (Douglas et al., 2012). Atherosclerosis is a chronic inflammatory vascular disease and $ApoE^{-/-}$ is the most commonly used and established model for the study of atherosclerosis. As mentioned previously, the role of Nox2 in atherosclerosis is still unclear with contradictory experimental findings. This is likely caused by of the use of global Nox2 deficiency which affects multiple cells in the vasculature including endothelial cells, inflammatory cells and adventitial fibroblasts. To address the question of endothelial Nox2 and ROS contribution to the development of atherosclerosis, Dr Douglas crossed the Nox2 Tg mice, where the Nox2 transgene was over-expressed specifically in the endothelial cells, with $ApoE^{-/-}$ mice and examined for atherosclerotic plaque development following high fat diet (Douglas et al., 2012). There was no difference in blood pressure at baseline but Nox2-Tg $ApoE^{-/-}$ mice had significantly greater vascular superoxide production compared to $ApoE^{-/-}$ controls. It was observed at 9 weeks there was an increase in endothelial VCAM-1 expression and macrophage recruitment which indicated an important role for endothelial Nox2 in the initiation of atherosclerosis. Interestingly, no difference in atherosclerotic plaque progression was observed subsequently suggesting that endothelial Nox2 derived superoxide played a limited role once the plaque has already formed.

The study by Dr Douglas on atherosclerosis showed a role for endothelial ROS at the early stage of disease development. It suggested that the impact of endothelial ROS maybe

greater in models of acute inflammatory disease where the initial injury determines to a greater extent the progression of the disease.

1.3 Angiotensin II infusion model of acute vascular inflammation

The most commonly used model for acute inflammation is the Angiotensin II (Ang II) infusion model. Ang II is an oligopeptide derived from the precursor molecule angiotensinogen. It plays an important role in the renin-angiotensin system causing vasoconstriction and the release of aldosterone from the adrenal cortex. Ang II can also induce vascular inflammation through affecting all stages of the inflammatory response: increased vascular permeability, leukocyte recruitment and activation of tissue-repair process (Table 1) (Marchesi et al., 2008). The key mechanisms by which Ang II mediate these effects include the upregulation of ROS and activation of pro-inflammatory transcription factors such as nuclear factor (NF)-κB.

Ang II

Increased vascular Permeability	**Increased vascular Inflammation**	**Increased vascular repair**
Increase in prostaglandins, VEGF	Increase in inflammatory adhesion molecules (E-selectin, P-selectin, integrins VCAM-1, ICAM-1), cytokines (MCP-1, IL-6, IL-8, TNF-α MIP-2, CCL5, CXCR2, PAI-1)	Increased growth factors (EGF, PDGF, IGF, TGF-β) and metalloproteinases (MMP-2, MMP-9)

Table 1 Summary of the effects of Ang II on vascular inflammation
Ang II affects all stages of the inflammatory process: vascular permeability through upregulation of prostaglandins and vascular endothelial growth factor (VEGF); recruitment of inflammatory cells through cytokine and chemokines and vascular repair through mediators of cell growth such as epidermal growth factor.

Ang II modulates ROS predominantly through the activation of NADPH oxidase via AT1 receptors found in both endothelial cells and VSMCs. The precise signalling pathway is still unknown although it is dependent on the phosphorylation of $p47^{phox}$ by protein kinase C (Marchesi et al., 2008) which in turn is regulated by three different phospholipases: phospholipase C (Karathanassis et al., 2002), phospholipase D (Touyz and Schiffrin, 1999) and phospholipase A_2 (Zafari et al., 1999). Any changes to NADPH oxidase therefore would likely have a significant effect on Ang II mediated vascular inflammation.

The effect of Ang II induced vascular inflammation is variable and dependent on the mouse model used. The most commonly described pathology is the development of abdominal aortic aneurysm (AAA) and aortic dissection.

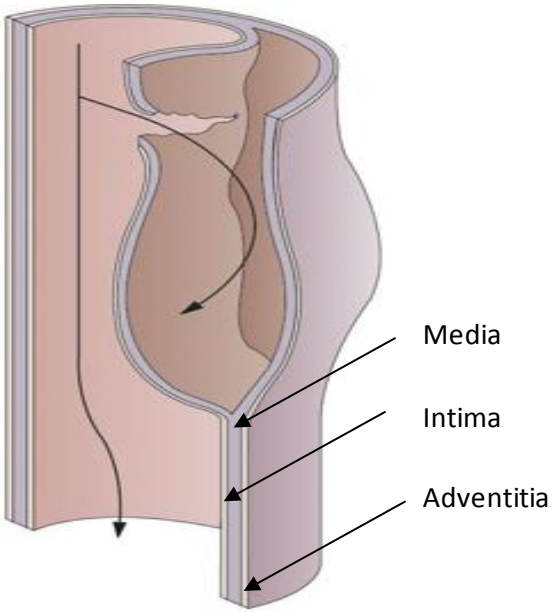
1.3.1 **Abdominal aortic aneurysm**

Vascular aneurysms are chronic inflammatory disease in which there is a localised dilation of an artery with more than 50% increase over its normal diameter (Johnston et al., 1991). The commonest form of aneurysm is abdominal aortic aneurysm (AAA) where abdominal

aorta has a diameter >3cm compared to the normal diameter of 2cm. AAA is highly prevalent in patients with advanced coronary artery disease which suggests an association of risk factors for both diseases. High risk of rupture is associated with >5cm of diameter and patients with aneurysm >5.5cm are generally advised for surgical repair (Ernst, 1993).

1.3.2 **Aortic dissection**

Aortic dissection on the other hand is an acute vascular disease where there is bleeding into and along the wall of the aorta (Scott, 2002). It is associated with medial wall degeneration followed by a tear in the vessel intima leading to propagation of blood down the vessel and formation of a false lumen between the intima and the media (Diagram 1.4) (LeMaire and Russell, 2011). Aortic dissection has an incidence of around 2000 cases per year in the United States and 3000 in Europe, and is most often seen in men aged 40 to 70 (Mehta et al., 2002; Nienaber et al., 2004). Several risk factors have been identified to be associated with the development of this disease including hypertension, atherosclerosis, aortic dilatation and connective tissue disorders.(LeMaire and Russell, 2011) However, despite advances in techniques for diagnosis and treatment the mortality rate of aortic dissection remains high, approximately 50% in the first 48 hours and up to 70% in the first week after the dissection (Setacci et al., 2010). Furthermore, much of the underlying mechanisms of aortic dissection are still not well understood which limits the capacity for the development of future therapeutic strategies.



Adapted from LeMaire et al, Nat. Rev. Cardiol, 2010

Diagram 1.4 Development of aortic dissection
Aortic dissection develops from a tear in the intima which is followed by tracking of blood between the intima and media and the subsequent formation of a false lumen.

1.3.2.1 Mouse models of AAA and aortic dissection

Unlike in humans where AAA and aortic dissection are separate clinical entities, the distinction is far less clear in mice. Mice also do not spontaneously develop AAA or aortic dissection in contrast to human so either pharmacological agents or genetic modifications are required to induce the development of aortic disease. Examples of genetic modifications include TIMP-$1^{-/-}$ mice (Silence et al., 2002), $LDL^{-/-}$ or $ApoE^{-/-}$ mice fed a high fat diet for a prolonged period (6 months) (Tangirala et al., 1995), or mutation in the fibrillin-1 allele where a cysteine was substituted for glycine at position 1039 ($Fbn1^{C1039G/+}$) resulting in a systemic disorder of the connective tissue (Marfans syndrome). Patients with Marfans syndrome commonly present with progressive aortic

root dilatation, aortic dissection and aneurysm formation. (Habashi et al., 2006). For pharmacological induction of aortic disease the most commonly used agents are: elastase which involves infusion of pancreatic elastase into the aorta (Curci and Thompson, 1999); calcium chloride through direct placement of concentrated solution over the aorta (Chiou et al., 2001); and Ang II infusion delivered via subcutaneous osmotic mini-pumps. The advantages and disadvantages of each model system are listed below.

Agent	Advantages	Disadvantages
Elastase infusion	Reliable induction of aneurysm Consistent pathology	Difficult surgery Variable depending on elastase preparation
Calcium chloride	Simple surgery and cost effective	Highly variable pathology Longer time to develop pathology
Ang II	More physiological as no direct damage to aortic wall More relevant to the human disease as Ang II is implicated in the development of human aortic dissection and Ang II receptor blockers have been shown to slow down the progression of Marfan's syndrome in both human (Habashi et al., 2006) and mice (Brooke et al., 2008).	Heterogeneous pathology Comparatively expensive

Ang II infusion has therefore become the most wided used and studied model for aortic aneurysm and dissection with over 60 studies since year 2000. The dose ranged between 1.44mg/kg/day (1000ng/kg/min) to 3mg/kg/day. Due to the increasing use of the Ang II infusion model in different genetically modified mouse models, it's becoming clear that there is a range of different pathologies induced by Ang II. A common feature uniform to all the studies is that the pathology is located in the supra-renal aorta, the segment of aorta between the diaphragm and the renal arteries (Ayabe et al., 2006; Bruemmer et al., 2003; Daugherty et al., 2000; Gavazzi et al., 2007; Gavrila et al., 2005; Manning et al., 2003; Rateri et al., 2011; Saraff et al., 2003; Satoh et al., 2009; Thomas et al., 2006; Tieu et al., 2009; Uchida et al., 2010; Wang et al., 2010; Xiong et al., 2009; Zhang et al., 2009). This is different to human AAA which is located typically in the infra-renal aorta. Many factors likely contribute to this difference in location of pathology including haemodynamics.

1.3.2.2 Aortic dissection precedes aortic abdominal aneurysm in ApoE$^{-/-}$

With recent advances in imaging techniques it is now possible to analyse in detail the different stages of Ang II induced aortic disease. It was first described by Saraff et al. that when sections of mouse AAA were analysed serially from 1-56 days of Ang II infusion, a rupture in the vessel media and haematoma contained by the adventitia could be observed after 7 days (Saraff et al., 2003). This was followed subsequently by inflammatory cell recruitment in the peri-adventitial space and organisation of the haematoma. Remodelling then occurs with deposition of elastin, development of new vessels and formation of an aneurysm. The notion that aortic dissection precedes abdominal aortic aneurysm formation is supported by later studies using in-vivo ultrasound (Barisione et al., 2006) and MRI (Klink et al., 2011) which demonstrated the rupture of vessel media around 6 days after Ang II infusion and subsequent development of aneurysm in the same region. Daugherty el

al. (Daugherty et al., 2011) therefore proposed the following model for the development of Ang II induced AAA in ApoE$^{-/-}$. It is debatable whether an aneurysm formed following dissection should still be termed abdominal aortic aneurysm or a pseudo-aneurysm but the pathology is still an aneurysm as there is dilation of the lumen.

Sequential characteristics of AAA development in ApoE$^{-/-}$ mice

Days of Ang II infusion	Pathological findings
48h	Macrophage infiltration and some elastin degradation
4-10 days	Medial rupture and formation of haematoma
>14 days	Luminal expansion, organisation of the haematoma, aortic vessel remodelling
>28 days	Atherosclerotic lesions

1.3.2.3 Ang II induced different pathologies in C57Bl/6J

Majority of Ang II infusion studies used hyperlipidaemic mice, ApoE$^{-/-}$ or LDL$^{-/-}$, based on the rationale that hyperlipidaemia is a known risk factor in human AAA and hyperlipidaemic mice have an increased rate of AAA formation (Daugherty et al., 2000). However, hyperlipidaemic mice have high background systemic inflammation which makes study of the individual pathways involved difficult. Recent studies have therefore started using C57BL/6J for their Ang II experiments. In these mice, interestingly, different aortic pathologies have been described. In two of the studies, 1.44mg/kg/day dose of Ang II was used for 28 days but one study described only medial thickening (Owens et al., 2010) whilst the other described the development of abdominal aortic aneurysm in 20% of the mice (Wang et al., 2010). The third study used 3.6mg/kg/day dose of Ang II and described the pathology as aortic dissection with a clear site of dissection and extension of

the false lumen up the whole length of the aorta (Tieu et al., 2009). Blood pressure induced by Ang II was similar across all 3 studies. This heterogeneity in pathologies induced by Ang II suggests the involvement and activation of many different mechanisms.

1.3.3 **Mechanism of Ang II induced aortic disease**

1.3.3.1 Blood pressure

The mechanism by which Ang II causes aortic disease, AAA or dissection, is still not clear. It has been shown however, that it is not related to the increase in blood pressure caused by Ang II. Many studies have used noradrenaline to increase blood pressure to a similar level as observed with Ang II and have observed no development of aortic disease in noradrenaline treated mice (Cassis et al., 2009; Fukai et al., 1999; Gavazzi et al., 2007; Owens et al., 2010). The study by Cassis et al. also used hydralazine to lower blood pressure in Ang II treated mice which did not prevent the development of aortic disease. On the surface, the mouse findings contradict human studies where reducing blood pressure using either β-blocker or calcium channel blocker is associated with improved outcome in aortic dissection (Suzuki et al., 2012) but it should be taken into account that mouse studies examined early stages of aortic disease in mice which did have any underlying disease whereas human studies are long term studies of patients who already have vascular diseases. No studies in animal models so far have investigated the effect of increased blood pressure on aortic disease after the dissection or aneurysm has occurred.

1.3.3.2 Matrix metalloproteinases (MMP)

Matrix metalloproteinases are endopeptidases classified according to their substrate specificity. MMP-2 and MMP-9 for example, are gelatinases which are mainly specific for

the breakdown of gelatin in the vascular wall. They act to degrade extracellular matrix leading to weakening of the vessel wall. The main MMPs that have been found to be upregulated in Ang II induced vascular diseases are MMP-2 and MMP-9 (Thompson and Baxter, 1999). MMP-9 is an inducible enzyme secreted by mononuclear phagocytes localized to human AAA tissue and cultures of human AAA tissue have found large secreted quantities of MMP-9 (McMillan et al., 1995b; Newman et al., 1994; Thompson et al., 1995). MMP-2 is expressed by VSMCs and adventitial fibroblasts located in areas adjacent to mononuclear phagocytes (Davis et al., 1998; McMillan et al., 1995a). Inhibition of MMPs by the broad-spectrum antibiotics doxycycline or knockout of MMP-2 and MMP-9 inhibited the development of aortic aneurysm (Longo et al., 2002; Manning et al., 2003; Pyo et al., 2000). In addition, over-expression of tissue inhibitor of matrix metalloproteinase (TIMP-1), reduced the formation of aortic aneurysm (Allaire et al., 1998) whereas knockout of TIMP-1 enhanced the development of AAA (Eskandari et al., 2005). Regulation of MMPs by Ang II is not well understood but it is likely to be dependent on the MAPK pathway (Jiménez et al., 2009) and also ROS production from NADPH oxidase (Grote et al., 2003; Luchtefeld et al., 2005).

1.3.3.3 Inflammatory cells and cytokines

Daugherty et al. have previously described inflammatory cell recruitment to be an early event in the development of AAA. One of the key processes of inflammatory cell recruitment is the production of cytokines, signalling protein molecules that modulate the immune response. There is increasing evidence for the role of specific cytokines in mediating Ang II induced aortic dissection. The most well studied cytokines involved in Ang II induced aortic disease are IL6, MCP-1, TGF-β and more recently, Cyclophilin A.

1.3.3.3.1 MCP-1

MCP-1 is a cytokine produced by macrophages in response to Ang II stimulation and acts as a monocyte chemotactic factor which signals through the CCR2 receptor. It has been shown that knockout of CCR2 receptor significantly reduced Ang II induced aneurysm formation but not CCR3 or CCR5 which are not targets for MCP-1 (Ishibashi et al., 2004; MacTaggart et al., 2007). Using conditioned media from whole aorta, Tieu et al, demonstrated significant elevation of secreted MCP-1 in aortas from mice treated with Ang II and this was associated with macrophage recruitment and development of aortic dissection. They showed also that $CCR2^{-/-}$ mice had significantly reduced MCP-1 secretion and incidence of aortic dissection which was restored following adoptive transfer of $CCR2^{+}$ monocytes. These studies therefore, demonstrated an important role for MCP-1 in macrophage recruitment and amplification of inflammatory response required for the development of aortic disease.

1.3.3.3.2 IL-6

Interleukin 6 is a pro-inflammatory cytokine secreted by many cell types including endothelial cells, vascular smooth muscle cells, T cells and macrophages. It is secreted at high levels by abdominal aortic aneurysmal tissue and is associated with high risk of abdominal aneurysm rupture (Jones et al., 2001; Juvonen et al., 1997). However, its contribution to aortic disease has only been recently described by Tieu et al. where they demonstrated a significant increase in IL6 secretion by aortas in response to Ang II stimulation and knockout of IL6 significantly reduced the inflammatory response and Ang II induced aortic dissection. Further studies are required to elucidate fully the role of IL-6 in vascular diseases.

1.3.3.3.3 TGF-β

Transforming factor beta (TGF-β) is a secreted protein which controls proliferation and cellular differentiation and plays a major role in cardiovascular disease, immunological responses, cancer and Marfans syndrome (Cucoranu et al., 2005; Finder et al., 1995; Neptune et al., 2003; Wang et al., 2010). The contribution of TGF-β to aortic disease is paradoxical. In humans, TGF-β signalling is upregulated in Marfans syndrome (Neptune et al., 2003) and mutations of *TGF-β1* and *TGF-β2* that lead to increased TGF-β activity results in Loeys-Dietz syndrome which shares many clinical features of Marfans syndrome (Loeys et al., 2006; Pannu et al., 2005). These observational findings in humans are supported by evidence from mouse models of Marfans syndrome where a mutation was introduced into the *Fibrillin-1* gene leading to an increase in TGF-β activity and the development of aortic aneurysm (Habashi et al., 2006). This was attenuated by TGF-β antagonists such as TGF-β neutralising antibody or Ang II receptor I blocker. In another study, treatment of $ApoE^{-/-}Cxcl10^{-/-}$ mouse model of AAA with anti- TGF-β neutralizing antibody also reduced Ang II induced aortic dilatation (King et al., 2009). However, in a more recent study by Wang et al, treatment with anti TGF-β neutralizing antibody enhanced monocytes invasion, increased the rate of Ang II induced AAA from 20% to 90% and significantly reduced survival rate from 100% to <20% (Wang et al., 2010). This suggests TGF-β plays distinct roles in different aortic diseases and is highly dependent on the mouse model used. Further studies are required to elucidate the mechanism underlying this difference in the behaviour of TGF-β.

1.3.3.3.4 Cyclophilin A

Recently, a new cytokine, Cyclophilin A (CypA), has been found to play an important role in Ang II-induced aortic disease. CypA is a 18 kDa protein belonging to a family of highly conserved and ubiquitous proteins termed immunophilins (Galat, 1993). It was firstly identified in 1984 as the main target for the immunosuppressive drug: cyclosporine A (Handschumacher et al., 1984) which acts to inhibit the cis-trans isomerisation of peptidyl-prolyl catalytic activity (PPIase activity) of CypA (Steinmann et al., 1991). The PPIase activity of CypA is crucial in protein folding as the trans-state is much more favourable compared to the Cis-state but the energy required for the isomerisation is too high for spontaneous conformational change thus making the cis-trans isomerisation the rate limiting step in protein folding (Herzberg and Moult, 1991).

CypA was firstly identified to be a vascular cytokine by Berk et al. when they discovered CypA as a secreted factor that was increased with the use of a ROS inducing compound, LY83583 (Liao et al., 2000). They later observed conditioned media containing CypA and purified human CypA stimulated Erk1/2 activity and DNA synthesis in a concentration dependent manner which was abolished on immunodepletion of CypA (Jin et al., 2000). Secretion of CypA is a highly regulated process which depends on vesicle transport and plasma membrane binding. Inhibition of RhoGTPases, enzymes critically involved in signaling pathways linked to actin cytoskeletal arrangement (Mackay and Hall, 1998), through the expression of dominant negative mutants inhibited ROS dependent CypA secretion (Suzuki et al., 2006). CypA was also found to be co-localized with vesicle-associated membrane protein (VAMP) in response to ROS stimulation and gene silencing of VAMP-2 by SiRNA significantly inhibited CypA release (Suzuki et al., 2006).

Secreted CypA is a potent chemo-attractant for inflammatory cells in vitro (Sherry et al., 1992; Xu et al., 1992). It has also been shown to induce cytokine release such as IL-6 from inflammatory cells (Payeli et al., 2008) Moreover, another study of CypA using a monocytes cell line revealed CypA induced expression of MMP-9, IL-6 and TNF-α through the activation of NF-κB by Erk1/2 pathway (Yuan et al., 2010). Recently, Satoh et al. demonstrated that the increase in IL-6 and MCP-1 induced by Ang II in primary VSMCs was abolished in VSMCs isolated from $CypA^{-/-}$ mice (Satoh et al., 2009). CypA can also activate endothelial cells through the upregulation of VCAM-1 (Jin et al., 2004) and stimulate VSMCs to increase MMP activity (Satoh et al., 2009). Knockout of CypA in $ApoE^{-/-}$ mice completely abolished Ang II induced aortic dissection and aneurysm formation (Satoh et al., 2009). Berk et al. proposed in their model that VSMCs act as the central co-coordinator in regulating and amplifying the vessel response to Ang II. When Ang II binds to its receptor in VSMCs, ROS production by NADPH oxidase is increased which leads to secretion of CypA, pro-MMP and translocation of MT1-MMP to the cell membrane. Secreted CypA then acts to increase Erk1/2 phosphorylation and superoxide production in VMSCs and also the recruitment of $CD45^{+}$ inflammatory cells.

The mechanism of CypA signalling is still unclear. One possible mechanism is the receptor mediated signalling pathways. Several candidate receptors have been proposed and amongst them, the extracellular matrix metalloproteinase inducer (EMMPRIN) has been investigated the most (Arora et al., 2005; Pushkarsky et al., 2001). EMMPRIN is highly expressed and upregulated in monocytes and play a key role in MMP activation (Yuan et al., 2010). Several studies have shown binding of CypA to EMMPRIN (Chen et al., 2005; Pushkarsky et al., 2001) and blocking of EMMPRIN prevents CypA mediated cellular effects such as cytokine secretion (Yuan et al., 2010). However, more studies are

required to conclusively demonstrate EMMPRIN is the key receptor that mediated CypA intracellular effects.

1.4 Endothelial Nox2 over-expressing transgenic mice

In order to investigate the contribution and role endothelial ROS in Ang II induced aortic disease, a novel transgenic mouse model of endothelial specific over-expression of human Nox2 transgene under the control of the murine Tie2 promoter was generated (Bendall et al., 2007) (Diagram 1.5).

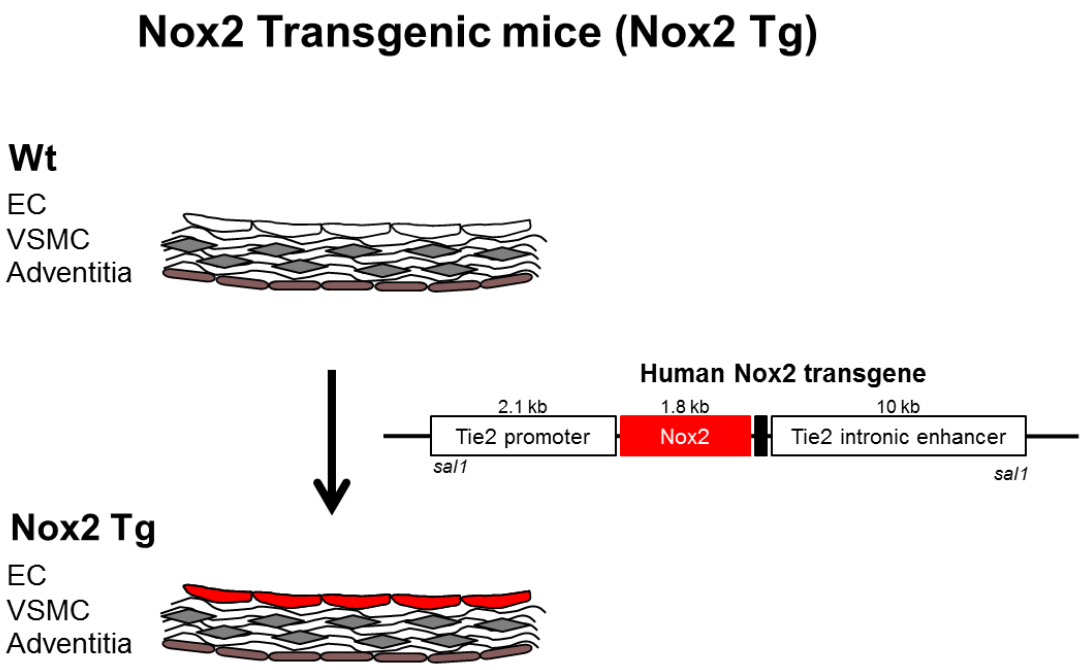


Diagram 1.5 Generation of Nox2 Tg mice

The Tie2 promoter and its intronic enhancer were used in the construction of the Nox2 transgene so that expression of the Nox2 transgene could be targeted specially to the vascular endothelium. The transgene underwent pronuclear microinjection into fertilized eggs of wild-type C57BL/6xCBA mice. The transgenic founders were backcrossed for 10 generations onto C57BL/6J strain.

The Nox2 Tg mice have been characterised previously (Bendall et al., 2007). The incorporation of the Nox2 transgene was confirmed using fluorescent in-situ hybridisation and 2 strains were identified with the integration site on chromosome 17 and chromosome 12. When expression of human Nox2 mRNA was analysed, the strain with integration in chromosome 17 had significantly greater expression than the other strain so these mice were selected for breeding.

At baseline, Nox 2 Tg aortas have significantly greater total Nox2 mRNA and protein levels compared to the wild-type littermate. This was associated with increased aortic O_2^- production which was abolished by endothelial removal. On DHE staining, increased superoxide production was localised to the endothelium providing further evidence that the transgene was endothelial specific. Interestingly, there appeared to be a compensatory rise in endothelial eNOS protein and mitochondrial superoxide dismutase in response to the increase in ROS production in Nox2-Tg mice. There was no difference in basal blood pressure between wild-type and Nox2 Tg mice. However, at a sub-pressor dose of Ang II, there was a significant elevation of blood pressure in the Nox2-Tg mice indicating the endothelial specific increase in ROS was sufficient to potentiate the haemodynamic response to Ang II as compared to the wild-type controls. Nox2 Tg mouse is therefore a unique and novel model to study the role of endothelial ROS on the development of acute and chronic vascular diseases.

1.5 Original Hypothesis

The work in this PhD thesis tests the main hypothesis that endothelial Nox2 and Nox2-derived ROS are sufficient to modify the initiation and development of structural vessel disease. Specifically I hypothesize that endothelial ROS modifies susceptibility to aortic dissection in response to Ang II through pathways including:

- Promotion of vascular inflammation
- Increased inflammatory cell recruitment and metalloproteinase activity
- Increased inflammatory cytokine secretion

1.6 Aims

This aim of this thesis is to investigate the role of endothelial Nox2 and ROS in the initiation and development of Ang II induced aortic dissection using the endothelial specific Nox2 over-expressing mice, Nox2 Tg. The specific aims are:

- To characterise the response of Nox2 Tg mice to Ang II infusion
- To investigate the role of endothelial Nox2 in the regulation of aortic inflammatory response
- To characterise the differences between wild-type and Nox2 Tg mice at the cellular level including endothelial cells and VSMCs

Chapter 2:
Materials and Methods

Chapter 2. Materials and Methods

All materials and general methods used are contained in this chapter. Some specifics techniques are discussed in more detail in the relevant chapters.

2.1 Materials

2.1.1 Buffers and Media

Buffer/Media	Reagents	Supplier
TE buffer	10mM Tris-HCl pH 8.0, 1 mM ethylenediaminetetraacetic acid (EDTA)	Sigma-Aldrich
TAE buffer	2 M Tris Acetate, 100 mM Na_2EDTA	National Diagnostics Ltd
DNA lysis buffer	10 mM Tris-HCl pH 8.5, 0.45 % Non-idet P40, 0.45 % Tween-20, 0.2 mg/ml Proteinase K	Sigma-Aldrich, Bioline
PBST	PBS with 0.05 % Tween-20	Lonza, Sigma-Aldrich
FACS buffer	PBS containing 0.2 % Bovine Serum Albumin (BSA) and 2 mM EDTA	Lonza, Sigma-Aldrich
FACS fixative	2 % formaldehyde in PBS	Sigma
Lavage buffer	PBS containing 5 mM EDTA	Lonza
MACS buffer	PBS containing 0.5 % BSA and 2 mM EDTA	Lonza, Sigma-Aldrich
DMEM complete growth media (Low glucose 1g or High glucose 4.5g)	DMEM supplemented with 1 % penicillin-streptomycin, 1 % L-glutamine and 10 % foetal bovine serum (FBS)	Lonza, Sigma-Aldrich
VSMC growth media	DMEM supplemented with 1 % penicillin-streptomycin, 1 % L-glutamine and low endotoxin 20 % foetal bovine serum	Invitrogen, Lonza, Sigma-Aldrich

	(FBS)	
VSMC digestion buffer	DPBS with Ca^{2+} and Mg^{2+}	Lonza
Endothelial growth media	EBM-2 supplemented with EMG2 BulletKit (5% FBS, hEGF, VEGF, hFGF-B, R^3-IGF-1, hydrocortisone, Gentamycin/Amphotericin-B and ascorbic acid; Lonza, product code CC-3202)	Lonza
Aorta FACS digestion buffer	D-PBS with Ca^{2+} and Mg^{2+} with 20mM HEPES	Lonza
Aorta FACS wash buffer	DPBS without Ca^{2+} and Mg^{2+} with 0.2% BSA and 2mM EDTA	Lonza
Transfer buffer	200mM Tris Base with 2M Glycine	Sigma-Aldrich

Table 2.1 Buffers and media

Sigma-Aldrich (Gillingham, UK); Bioline (London, UK); National Diagnostics Ltd (distributed by Thermo Fisher Scientific, Loughborough, UK);Lonza (Slough, UK); Pierce (Loughborough, UK); Invitrogen (Paisley, UK)

2.2 Animal care and use

All animal experiments were conducted in accordance with the UK Home Office Animals (Science Procedures) Act 1986 (HMSO UK) under the project licence 30/2562 and Personal Licence 60/11690.

All mice were housed in individually ventilated cages at 21°C with a 12-hour light/dark cycle and controlled temperature (20-22°C), and fed standard chow (19.67% protein, 4.13% oil and 3.22% fibre; B&K Universal Ltd, Aldbrough, UK) and water *ad libitum*.

2.2.1 **Nox2 Tg mice**

Endothelial-targeted Nox2 over-expressing (Nox2 Tg) mice were generated by Dr Bendall in our laboratory (Bendall et al., 2007) in which a human Nox2 transgene was specifically

over-expressed in endothelial cells under the murine Tie2 (endothelial specific) promoter. Founder mice were backcrossed onto the C57BL/6J strain for greater than ten generations. Heterozygotic breeding was used with wild-type C57BL/6J bought from Harlan UK Limited (Bicester, UK) to produce litters containing either heterozygote Nox2 Tg or wild-type C57BL/6J mice. Male Nox2 Tg mice and their wild-type littermate controls between 18-24 weeks of age were used for all experiments.

2.2.2 **DNA extraction**

Mouse ear notches were digested for a minimum of 5 hours at 55°C in 500 µl of DNA lysis buffer. DNA was purified by extraction with 500 µl of phenol:chloroform:isoamyl alcohol (25:24:1) (Sigma-Aldrich, UK) and then vortexed vigorously before centrifugation at 16,000 g for 15 minutes. The clear upper layer was transferred into a new Eppendorf tube and DNA was precipitated by the addition of 50 µl of 3 M sodium acetate (pH 5.2) and 1ml of chilled 100% ethanol for 30 minutes at -80°C. The samples were centrifuged at 13,000 rpm for 10 minutes and then washed twice with 1 ml of 70% ethanol and centrifugation at 13,000 rpm in between each wash. After the final wash, the DNA pellet was air dried and resuspended in 80µl TE buffer.

2.2.3 **Genotyping PCR**

Nox2 Tg mice were genotyped using the primers listed in Table 2.2. Products were run on a 2.5% agarose gel prepared by dissolving agarose in 1x TAE buffer and adding ethidium bromide to a final concentration of 5%. Once the gel had set, PCR products were loaded and run at 125V in 1x TAE buffer for 45 min. DNA was visualised using UV illumination. Bioline hyperladder IV (Bioline) was used to identify the PCR product size

Primer	Primer Sequence
Gp91RTRF1	GTCACACCCTTCGCATCCATTCTCAAGTCAGT
Gp91RTR1	CTGAGACTCATCCCAGCCAGTGAGGTAG
D14Mit62F	AGGACTCAATGAGCAGGGAA
D14Mit62R	ACTCTCCTGCCACCCCTC

Table 2.2 Primer list

All primers were brought from Sigma Europe.

Reaction Mix

H_2O	8.5µl
BioMix Red (Bioline)	12.5µl
Primers	0.5µl each (4µl in total)
DNA	2µl

Thermocycle Sequence

Step 1	95ºC 15 min
Step 2	94ºC 1 min
Step 3	64ºC 1 min
Step 4	72ºC 5s
Step 5	Go to step 2, 25 cycles
Step 6	72ºC 10 min
Step 7	10ºC 1 min
Step 8	End

Expected Products

Wt	125bp
Tg	225bp

Figure 2.1

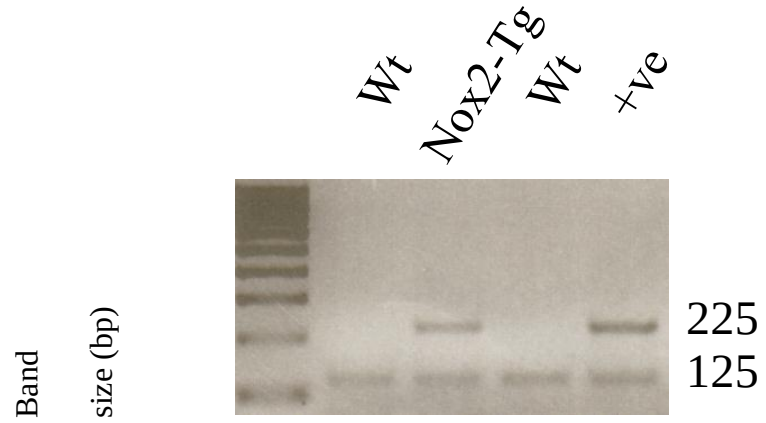


Figure 2.1 Genotyping of genomic DNA from Nox2 Tg and wild-type mice.
PCR product from Nox2 Tg is 225bp; the product from wild-type is 125bp. As all Nox2 Tg mice used in this project are heterozygotes, both the 225 and 125bp bands are seen.

2.2.4 **Organ harvesting**

Mice were culled by inhalation of isoflurane (>25%). The chest cavity was opened and a small incision in the right atrium was made to allow perfusion with ice-cold PBS (and 4% paraformaldehyde if the tissue harvested was for histology). Organs were harvested and either snap frozen in liquid nitrogen or placed into ice-cold serum free DMEM for cell isolation. For histology, organs were placed into 4% paraformaldehyde or frozen on dry ice in OCT.

2.2.5 **Insertion of osmotic mini-pumps**

Subcutaneous osmotic mini-pumps (Alzet® Model 1002, 14 days; 1004, 28 days; distributed by Charles River) were used for Saline, Angiotensin II (Sigma-Aldrich, Gillingham, UK) or Noradrenaline infusion (Sigma-Aldrich, Gillingham, UK). Nox2 Tg and wild-type mice were anaesthetised by inhalation with 2 % isoflurane in 95 % oxygen. Mice received buprenorphine at the time of surgery. Osmotic mini-pumps containing either sterile saline, Ang II (1mg/kg/day) or Noradrenaline (10mg/kg/day) were implanted

subcutaneously in the midscapular region. Mini-pump surgery was performed by Dr Gillian Douglas.

To ensure individual animals received appropriate doses according to their weight, Ang II was made up in sterile saline using the following formulae:

$$\frac{\text{Dose (}\mathbf{1}\text{ mg) x weight (kg; averaged for similar weights)}}{\text{Pump rate over 24 hours}} = \mathbf{mg/\mu l}$$

Pump rate 14 day pumps, 6µl/day

28 day pumps, 3 µl/day

Mice were monitored throughout the study for adverse effects such as muscle weakness or wound breakdown. Animals showing signs of discomfort, distress or significant weight loss that could not be alleviated were culled by a Schedule 1 method.

Special precautions were taken for noradrenaline-treated mice due to severe peripheral vasoconstriction which resulted in reduced ability of these mice to thermo-regulate. Mice were in ventilated cage without warming following surgery and monitored hourly in the first day.

2.3 Measurement of O_2^-

Although superoxide (O_2^-) is short lived as compared to other ROS, it remains the precursor of many other biologically important reactive oxygen species. Detecting O_2^- production by cells provided us with important information about cell and organ redox-

status. Many assays have been developed to measure the levels of O_2^- production by cells and organs. The main method used in this PhD research project is Dihydroethidium high performance liquid chromatography (DHE HPLC).

2.3.1 Dihydroethidium staining and high performance liquid chromatography

Dihydroethidium, DHE, is a cell permeable compound that interacts with intracellular O_2^- to form oxyethidium (Zhao et al., 2003) which then binds to nucleic acids to emit bright red fluorescence detectable by fluorescent microscope. However, the sensitivity and specificity of DHE fluorescent microscope detection of superoxide is low and subjective to the experience of researchers. The data it provides are more qualitative rather than quantitative.

During the last decade, DHE high performance liquid chromatography (DHE HPLC) has been adapted and developed by Fink et al. for specific and quantitative detection of O_2^- (Fink et al., 2004). It relies on the oxidation of dihydroethidium to the fluorescent DNA binding and membrane permeable compound ethidium and 2-hydroxythdium which is specific for detecting O_2^- (Benov et al., 1998; Bindokas et al., 1996). DHE based assay has several advantages over other assays of ROS measurement:

- It is not subjected to redox recycling
- Unaffected by reductants such as glutathione
- Provides accurate ROS measurements

Recent evidence has shown 2-dihydroethidium peak detected by the fluorescence pump to be more specific to $O_2^{\cdot -}$ production especially from NADPH oxidases whereas ethidium

peak detected by the UV pump corresponds more to H_2O_2 production (Fernandes et al., 2007). The main disadvantages of DHE HPLC are that it is relatively expensive and requires specialist expertise to set-up the system; and also requires greater quantities of tissue/cells compared to other methods.

For the work in this thesis, cells were pre-incubated with either serum-free DMEM alone as controls, or in the presence of pegylated superoxide dismutate (Peg-SOD; Sigma) at 100 U/ml, or tiron, a non-specific superoxide scavenger at 10 mM or DPI, flavoprotein inhibitor at 20 µM for 30 min. Cells were then washed twice with pre-warmed PBS, and incubated with or without Ang II (10^{-7} M) in serum free DMEM containing DHE (25 µM, Invitrogen) for 20 min. Cells were then harvested and spun at 13,000 RPM. Ice cold methanol (200 µl) was added into the pellet followed by 100 µl of 0.1 M HCl. The supernatant was removed for the analysis of O_2^- production using HPLC. Separation of DHE was done using a gradient HPLC system (Jasco, UK) with an ODS3 reverse phase column (250 mm, 4.5 mm, Hichrom UK) and quantified using a fluorescence detector set at 510 nm (excitation) and 595 nm (emission). Chromatography peaks were quantified by measuring the area under the curve using the Azure software. The 2-hydroxyethdium peak around 12 minutes was deemed to be specific to O_2^- production according to the methods published previously (Crabtree et al., 2009; Fernandes et al., 2007). Peg-SOD was used to verify that that the peak at 12 minutes was O_2^- specific.

2.4 RNA techniques

All RNA experiments were carried out using certified RNase-free filter tips on a clean bench area and molecular biology grade water (Sigma-Aldrich, Gillingham, UK) to avoid contamination by nucleic acids and RNase.

2.4.1 **RNA extraction**

For the isolation of RNA, cells were lysed directly in 1ml of TRIzol reagent (Sigma-Aldrich, Gillingham, UK) and placed immediately on ice. For frozen tissue, samples were homogenised in 1ml of TRIzol reagent. All samples were subjected to 1 cycle of freeze-thaw to promote cell lysis. Chloroform (200ul per 1ml of TRIzol) was added to each sample, vortexed briefly and centrifuged at 13,000 rpm for 15 min at 4˚C. The colourless aqueous phase containing RNA was carefully removed and transferred to a new tube. An equal volume of 70% ethanol was added to precipitate the RNA. Purification of RNA was done using either the RNeasy® Mini-kit (tissue samples) or RNeasy® Micro-kit (cell samples) (Qiagen, Crawley, UK) with on-column DNase I treatment using an RNase-Free DNase Set (Qiagen, Crawley, UK) to remove any genomic DNA contamination according to manufacturer's instructions. Extracted RNA was quantified by measuring absorbance at 260 nm using a NanoDrop ND-1000 Spectrophotometer (Thermo Fischer Scientific, Loughborough, UK). RNA was either immediately stored at –80°C to prevent degradation or reversed transcribed to cDNA which is more stable.

2.4.2 **cDNA generation**

Total RNA was transcribed to cDNA using Quantitect Reverse Transcription Kit (Qiagen, Crawley, UK) according to manufacturer's instructions. Briefly, RNA samples were incubated with gDNA Wipeout Buffer for 2 min at 42ºC to remove contaminating genomic DNA. Reverse transcriptase master mix containing reverse transcriptase, RT buffer and primer mix was added to the samples, incubated for 15 min at 42ºC and then 3 min at 95ºC to inactivate reverse transcriptase. As a negative control to check for contaminating genomic DNA, reverse transcriptase (RT) was replaced with water in some samples. Synthesized cDNA was diluted to 2.5ng/µl and stored at –80°C.

2.4.3 **Quantitative Real RT-PCR**

2.4.3.1 TaqMan Probes

All real time RT-PCRs were performed with TaqMan® gene expression assays (Applied Biosystems, Warrington, UK) which contained primers and a probe complementary to the target cDNA sequence (Table 2.3).

Gene	Reference Sequence Accession no.	ABI product number
Human Nox2	NM_000397.3	Hs00166163_m1
Mouse Nox2	NM_007807.4	Mm01287742_m1
Mouse Nox4	NM_015760.4	Mm00479246_m1
Mouse Cd68	NM_009853.1	Mm00839636_g1
Mouse myosin heavy polypeptide 11, SMC (Myh11)	NM_013607.2 NM_001161775.1	Mm00443013_m1
Mouse Cd31(PECAM)	NM_001032378.1 NM_008816.2	Mm00476702_m1
Mouse GAPDH	NM_008084.2	4352932E

Table 2.3 TaqMan® Gene Expression Assays.

All assays used in qRT-PCR are listed with accession numbers and product number. TaqMan® probes are commercial products, designed and optimized by Applied Biosystems (Warrington, UK); sequences are not available.

The probes are labelled with a 5' reporter fluorophore (e.g. FAM™ or VIC®) and a 3' quencher. The reporter and quencher stay in close proximity which suppresses the reporter fluorescence. The probe anneals between the forward and reverse primers of the target DNA sequence and during the extension step, the Taq polymerase cleaves the TaqMan probe from the target by its 5'exonuclease activity. This results in the separation of the reporter fluorophore from the quencher which increases the fluorescence signal of the

reporter. The increase in fluorescence is directly proportional to the amount of probe cleavage.

2.4.3.2 qRT-PCR Method

11.25 µl of cDNA (4.4 ng/µl) was mixed with a mastermix (13.75 µl) containing 12.5 µl 2xTaqMan® Universal Master Mix (Applied Biosystems, Warrington, UK) and 1.25 µl 20xTaqMan® gene expression assay. Each sample was assayed at least in duplicate and negative controls containing water instead of cDNA were included to check for the presence of contaminating cDNA. For all reactions a housekeeping gene was used to control for the variability between different samples. cDNA were amplified with an iCycler IQ real-time detection system (Bio-Rad Laboratories Ltd, Hemel Hempstead, UK) in 96-well plates (Bio-Rad Laboratories Ltd, Hemel Hempstead, UK) using the following parameters:

Step 1:
50 °C for 2 minutes *(Taq polymerase activation)*
95°C for 10 minutes *(denaturation)*
Step 2: 50 cycles
95°C for 15 seconds *(annealing)*
60°C for 1 minute *(extension)*

There is an exponential increase in product during the real time RT-PCR which results in an increase in reporter dye fluorescence with each cycle of the PCR. As the reaction components become limiting, the rate of target product accumulation decreases until a plateau is reached and there is no further increase in PCR product. The threshold cycle (Ct) value corresponds to where a detectable increase in fluorescence crosses an arbitrary threshold and is proportional to the amount of initial PCR template. The threshold is set in the linear phase of the amplification plot. Relative quantification of gene expression was performed using the comparative Ct method (ΔCt). Gene expression data were normalised

to the house keeping gene, GAPDH, by the formula:

Gene of interest (GOI) Ct value – Housekeeping gene (HK) Ct value = ΔCt

As each cycle represents a doubling of the PCR product, an increase of the Ct value by 1 represents a 2-fold change in expression. Therefore **ΔCt** data are represented as $\mathbf{2}^{-\Delta Ct}$.

2.5 Cell culture

All cell culture experiments were performed in sterile conditions using laminar flow hoods and disposable tissue culture grade plastics. Tissue culture flasks and plates were purchased from Greiner Bio-One, Corning and Appleton Woods. Cell cultures were kept in incubators at 37°C with humidity saturated atmosphere containing 5% CO_2.

2.5.1 sEND.1 cell culture

The sEND-1 mouse endothelioma cell line was originally derived from subcutaneous haemangioma (Williams et al., 1988). sEND.1 cells were grown in Complete Medium. When confluent, cells were detached using 0.05% Trypsin EDTA and passaged 1 in 15 or plated out in the desired density of 10^5 cells in 6 well plates or 10^4 cells in 12 well plates.

2.5.2 Isolation of bone marrow and peritoneal macrophages

All mice were culled by isoflurane. Characterisation of the isolated macrophages was done by Dr J Patel (in our lab).

2.5.2.1 Isolation of bone marrow cells

Mice were culled and both the skin and muscle were removed from lower limbs. The femur and tibia were stripped of remaining tissue in a petri dish and the bones were cut at the joint using a scalpel. Using a 25 G needle and a 1 ml syringe filled with ice-cold PBS, the bone marrow was expelled, disaggregated with a Pasteur pipette and a single cell suspension prepared by passing through a 70 µm cell strainer with the plunger of a 1 ml

syringe. The cell suspension was centrifuged at 3,000 rpm for 5 minutes at 4 ºC to pellet the cells.

2.5.2.2 Isolation of bone marrow derived macrophages (BMDMs)

Bone marrow cells were isolated as described in Section 2.4.2.1 into DMEM-F12. A single bone marrow cell suspension from 1 mouse was plated in 2 petri dishes with 10 ml macrophage growth media in each dish. Conditioned media from L929-cells was used as a source of macrophage colony stimulating factor (M-CSF). 5 ml of macrophage growth media was added to each dish after 3 days of culture. On day 7, BMDMs were harvested for western blot analysis.

2.5.2.3 Isolation of resident peritoneal macrophages

Mice were culled as previously described and a small incision was made along the abdomen to expose the peritoneum. 10 ml ice-cold lavage buffer was injected into the peritoneal cavity using a 25 G needle and 10 ml syringe. The abdomen was agitated to detach adherent cells into the lavage solution. The lavage fluid was spun at 2,500 rpm to pellet the cells for western blot analysis.

2.5.2.4 Isolation of BioGel-elicited peritoneal macrophages

20-24 weeks old Nox2 Tg and wild-type mice were injected with 1 ml of 2 % BioGel polyacrylamide beads in PBS (Bio-Rad Laboratories Ltd, Hemel Hempstead, UK) into the peritoneum. Macrophages and other phagocytic cells are recruited to the peritoneal cavity but fail to phagocytose Biogel beads due to their large size (50 μm). BioGel intra-peritoneal injections were performed by Dr E. McNeill.

2.6 Protein extraction and detection

2.6.1 **Protein lysate preparation**

Cells were lysed directly in ice-cold CellLytic^{TM} mammalian tissue lysis buffer (Sigma-Aldrich, Gillingham, UK) containing EDTA-free Protease Inhibitor cocktail (Roche, Herts., UK) and phosphatase inhibitor if detection of phosphorylation was required. The wells were scraped with the plunger of a 1 ml syringe and the lysates were transferred to Eppendorf tubes on ice. Tissue samples were homogenized using a hand-held electric homogenizer in cell lysis buffer with protein and phosphatase inhibitors. All samples were freeze-thawed 3 times for further cell lysis and centrifuged at 13,000 rpm for 10 minutes at 4 °C. The supernatants were used for protein concentration measurement as described in Section 2.5.2. Lysates were stored at -20 °C.

2.6.2 **Determination of protein content**

Total protein content in lysate (10µl) was quantified using the BCA™ Protein Assay kit (Thermo Fisher Scientific, Loughborough, UK) with BSA standards according to the manufacturer's instructions. The Bicinchoninic Acid (BCA) protein assay is a highly sensitive colorimetric assay. The assay solution contains Cu^{2+} ions which are reduced to Cu^{+} by peptide bonds in the protein sample. The amount of Cu^{2+} being reduced is proportional to the amount of protein present in the solution. BCA chelates Cu^{+}, forming a purple-coloured product that strongly absorbs light at a wavelength of 562 nm. For the generation of a standard curve, protein standards ranging from 0.125 to 2 mg/ml were prepared from bovine serum albumin (BSA) (Sigma Aldrich, Inc.) using the same buffer as that was used for sample preparation (e.g. RIPA for western blotting). For the assay itself, 10µl of standards and samples in duplicates were added to 190µl of working reagent, incubated for 30 min at 37ºC and read in a microplate reader at 562nm.

2.6.3 **Immunoblotting**

Protein lysates was prepared using NuPage® LDS Sample Buffer (Invitrogen, Paisley, UK) and NuPage® Reducing Agent according to manufacturer's instructions and heated for 10 min at 70ºC. Lysates were resolved by SDS-PAGE (NuPAGE® 4-12 % Bis-Tris pre-cast gel) to separate denatured proteins in the lysate according to their molecular weight. Molecular weight rainbow markers (Amersham, distributed by VWR UK) were loaded to determine product band sizes. Protein samples were transferred onto polyvinylidene difluoride (PVDF) membranes (Millipore, Watford, UK) using wet transfer. Membranes were washed in PBST and blocked in 5 % milk in PBST for 1 hour at room temperature. The membrane was washed briefly and then incubated overnight with primary antibodies. Protein bands were visualized using HRP-conjugated secondary antibodies and chemiluminescence (SuperSignal; Thermo Fisher Scientific, Loughborough, UK).

Membranes were stripped for 30 minutes at 50°C in 6.25 mM Tris (pH 6.8) with 2% SDS and 100 mM ß-mercaptoethanol to re-probe membranes with a different primary antibody. Following stripping, membranes were washed for 30 min in PBST, blocked in PBST with 5% milk and incubated with antibodies as described below.

Target	Conjugate	Specificity	Species	Working Concentration	Product number	Supplier
Primary Antibodies						
Nox2	-	Mouse	Mono	1:1000	58698	BD
Nox4	-	Mouse	Rabbit	1:1000		KCL
CypA	-	Mouse	Rabbit	1:10,000	BML-SA296	Enzo
Erk1/2	-	Mouse	Rabbit	1:500	sc-154	Santa Cruz
p-Erk1/2	-	Mouse	Rabbit	1:500	197G2	Cell Signalling
VCAM-1	-	Mouse	Mono	1:1000	MAB6432	R&D
F4/80	-	Mouse	Rabbit	1:1000	sc-25830	Santa Cruz
CD102	-	Mouse	Mono	1:1000	Af774	R&D
GAPDH	-	Mouse	Mono	1:5000	MAB374	Millpore
SM-α actin	-	Mouse	Mono	1:5000	Sc-130617	Santa Cruz
α-actinin	-	Mouse	Mono	1:5000	Sc-15335	Santa Cruz
Secondary Antibodies						
Rabbit IgG	HRP	Rabbit	Goat	1:5000	W4011	Promega
Mouse IgG	HRP	Mouse	Rabbit	1:5000	W402B	Promega
Goat IgG	HRP	Goat	Donkey	1:5000	sc-2020	Santa Cruz

Table 2.4 Antibodies used for immunoblotting.

Santa Cruz (distributed by Insight Biotechnology Ltd, Middlesex, UK); Cell signalling (distributed by New England Labs, Hitchin, UK); Millipore (distributed by VWR); Promega (Southampton, UK); Enzo Life Sciences (Exeter, UK); BD Biosciences (Oxford, UK); Nox4 is a gift from Prof Shah (King College London, UK).

2.7 Flow cytometry

2.7.1 **Preparation of cell suspension from aorta**

Aortas from renal arteries to the aorta arch were dissected clean of adhering fat and connection tissue and placed into ice cold aortic digestion buffer. The vessels were cut into small 3-4 mm segments and incubated in a digestion mix containing 60U/ml Hyaluronidase (Sigma), 450U/ml Collagenase I (Sigma), 125U/ml Collagenase XI (Sigma) and 60U/ml DNase I (Sigma) at 37ºC for 1 hour. The digestion solution was passed through a 70µM cell strainer and the remaining aortic pieces were mashed through the strainer with the soft end of 1ml syringe plunger. The solution was transferred into a FACS tube and centrifuged at 1,200 rpm for 5 min at 4ºC for staining.

2.7.2 **Staining procedure**

Cells were resuspended in FACS wash buffer and red cells were lysed using Erylyse (1 part Tris 0.17M pH 7.2, 9 part Ammonium Chloride 0.16M) at room temperature for 3 min. Cells were then pelleted and washed with FACS wash buffer before incubation with 1/100 Fc receptors blocking antibody, Fcγ III/IIR, for 15 min at 4ºC. Fc receptors were blocked to reduce Fc-mediated antibody binding. Cells were stained at saturating antibody concentrations for specific cell markers with flourochrome-conjugated antibodies in FACS buffer (Table 2.6) for 15 minutes on ice in the dark. Where available, corresponding isotype control antibodies were added at the same concentration as the antibody of interest. Cells were washed with FACs buffer and centrifuged for 3,000 rpm for 5 minutes at 4 ˚C before being fixed with 250 µl of FACS fixative. Data was acquired using a CyAn Analyser flow cytometer (Beckman Coulter Ltd, UK) and then analysed using Summit (Dako, Ely, UK) and FlowJo (Tree Star Inc., USA) software. Unstained samples were used to set the voltages for individual experiments. Cells were initially gated using forward

(FSC) and side scatter (SSC) to exclude cell debris, red blood cells or dead cells and then gated for the respective populations. Compensation was performed using positive control samples stained for each color.

Target	Conjugate	Clone	Isotype	Working Concentration	Product number	Supplier
Primary Antibodies						
CD11b	PerCP Cy5.5	M1/70	Rat1gG2b	1 µg/ml	550993	BD Biosciences
F4/80	APC	BM8	Rat IgG2a	1 µg/ml	123115	BioLegend
CD45	PE-Cy7	30-F11	Rat1gG2b	1 µg/ml	552848	BD Biosciences
CD14	PE	Sa2-8	Rat IgG2a	0.25 µg/ml	12-0141-81	eBioscience
CCR2	APC	475301	Rat1gG2b	0.2 µg/ml	FAB5538A	R&D Systems
Isotype control antibodies						
Rat IgG2b	PerCP Cy5.5	RTK4530	Rat IgG2b	1 µg/ml	400631	BioLegend
Rat IgG2a	PE	eBR2A	Rat IgG2a	2 µg/ml 0.25 µg/ml	12-4321-41	eBioscience
Rat IgG2a	APC	RTK2758	Rat IgG2a	1 µg/ml	400511	BioLegend
Rat IgG2b	APC	141945	Rat IgG2b	2 µg/ml 0.2 µg/ml	IC013A	R&D Systems
Rat IgG2b	PE-Cy7	A95-1	Rat IgG2b	1 µg/ml	552849	BD Biosciences

Table 2.5 Antibodies used for flow cytometry.

APC: allophycocyanin, PE: phycoerythrin. BD Biosciences (Oxford, UK); BioLegend (distributed by Cambridge Bioscience Ltd, Cambridge, UK); eBioscience (Hatfield, UK); R&D Systems (Abingdon, UK).

2.7.3 **Quantification of cell numbers**

A known number of flourochrome-conjugated calibration beads (CaliBRITE; BD Biosciences, Oxford, UK) were added to each test sample to obtain total cell counts. FACS analysis was carried out by Dr E. McNeill.

2.8 Statistical analysis

For in vivo experiments, data were obtained from at least six mice/per group. For ex-vivo and in vitro experiments, data were obtained from at least 3 independent experiments. Data with Normal distribution are expressed as mean and SEM and tested for significance using Student's t-test or ANOVA with Dunnett's post-test to compare each group to the control group. Non-parametric data are expressed as median with inter-quartile range and tested for significance using Mann-Whitney or Kruskal-Wallis test. Categorical data are tested using Fisher's exact test. $P<0.05$ was considered statistically significant.

Chapter 3:

Response of Nox2 Tg mice to Ang II infusion

Chapter 3. Response of Nox2 Tg mice to Ang II infusion

3.1 Introduction

Vascular oxidative stress has been implicated in the development of many cardiovascular diseases including hypertension, atherosclerosis and heart failure (Gavrila et al., 2005; McCormick et al., 2007; Miller et al., 2002; Xiong et al., 2009). One of the main sources of ROS are NADPH oxidase (Nox) found in many vascular cell types including endothelial cells (EC) and vascular smooth muscle cells (VSMC). Endothelial cells (EC) mainly express Nox2 and Nox4 whereas vascular smooth muscle cells (VSMC) predominantly express Nox1 and Nox4 (Ago et al., 2004; Buul et al., 2005; Griendling, 2004).

Endothelial Nox2 is upregulated by agonists such as Ang II, shear stress and oxidised-LDL and is the predominant source of NADPH oxidase derived O_2^- in endothelial cells (Al-Mehdi et al., 1998; De Keulenaer et al., 1998a; Lassègue et al., 2012; Meyer and Schmitt, 2000). Nox4 on the other hand mainly accounts for the basal ROS required for maintaining normal endothelial function, such as cell proliferation and migration (Anilkumar et al., 2008; Griendling, 2004; Lassegue and Griendling). Nox2 has also been observed to be upregulated in diseases states such as hypertension and atherosclerosis (Judkins et al., 2010a; Jung et al., 2004). However it is still unclear whether the increases in the levels of endothelial Nox2 expression and endothelial ROS production play a causative role in the pathogenesis of these diseases or is merely a consequence of the disease process. A question left unanswered in particular is whether an increase in endothelial ROS alone is sufficient to promote disease progression.

To address this question, a novel mouse model of endothelial specific targeted Nox2 over-expression (Nox2-Tg) (Bendall et al., 2007) was generated and infused with Ang II. It addition to its pressor effects, Ang II is also a well-known potent activator of the Nox2 enzyme and also an inducer of acute vascular inflammation. It has been studied extensively as a model of aortic dissection and abdominal aortic aneurysm (AAA) formation in hyperlipidaemic mice such as $ApoE^{-/-}$ (Ayabe et al., 2006; Cassis et al., 2009; Daugherty et al., 2000; Saraff et al., 2003). One of the key factors that were found to sensitize the vessel response to Ang II in hyperlipidaemic mice was the increased ROS production and vascular inflammation due to hyperlipidaemia. It is known Ang II modulates ROS predominantly through the activation of NADPH oxidase via AT1 receptors found in both endothelial cells and VSMCs. Endothelial ROS may therefore have a specific role in mediating Ang II induced aortic disease.

3.1.1 **Hypothesis and Aims**

In order to test the hypothesis that that an increase in endothelial ROS production through the over-expression of Nox2 in the endothelium (Nox2 Tg) is sufficient to promote Ang II induced aortic dissection I aim in this chapter to:

- Evaluate the blood pressure response and the development of acute vascular diseases in Nox2 Tg mice in response to Ang II infusion.
- Characterise the development of vascular pathology induced by Ang II infusion.

3.2 Methods

General methods are described in the Chapter 2. Only methods and reagents used specifically in the experiments for this chapter are described below.

3.2.1 **Tail cuff blood pressure measurement**

Systolic blood pressure was measured in the morning using Visitech ^{R} computerized tail-cuff system (Visitech, USA) in conscious mice following subcutaneous insertion of osmotic mini-pumps containing either saline, noradrenaline (10mg/kg/day) or Ang II (1mg/kg/day). Tail of mice were pulled through a plastic pressure cuff and taped down to reduce movement. Blood pressure sensor was then placed over the tail. Mice were trained for 1 week before readings were recorded at 2 day intervals (Thomas et al., 2006). Twenty readings were taken per mouse of which the first 10 readings were discarded. An average of the remaining 10 readings was used to calculate the mean systolic blood pressure in each group. Heart rate was also recorded and analysed in a similar manner to blood pressure.

3.2.2 **Analysis of aorta**

3.2.2.1 Microscopic photographs of aorta

Mice were terminally anaesthetised using isoflurane. The chest cavity was opened and the aorta was perfused through the left ventricle with PBS followed by 4% paraformaldehyde (PFA) then placed into a petri-dish for inspection of structural morphology and damages under a dissection microscope with a digital camera attachment. Aortas were photographed and placed in 4% PFA for fixation.

3.2.2.2 Immunohistochemistry

Following overnight fixation in 4% PFA, aortas was transferred to 70% ethanol and the section from the diaphragm to the left renal artery (supra-renal aorta) were transferred to a biopsy processing cassette (Fisher Scientific, Loughborough, UK) with the diaphragmatic side facing the top, placed in a tissue processing machine (Bavimed Histomaster) and dehydrated through graded ethanol solutions (30min 70%, 2x 30min 95%, 3x 30min 100%, 3x 30min histoclear) and infiltrated with paraffin. Aortas were then embedded in paraffin blocks. Sequential sections of 7 μm thickness were cut with a microtome (Leica RM2155; Leica Microsystems) from the first appearance of the renal artery until no aorta was observed. Sections were mounted onto adhesive poly-L-lysine coated slides (VWR, Leicestershire, UK). Approximately 300 sections were cut for each aorta and the renal artery was used for orientation so sections at the same anatomical point could be taken for analysis.

Sections were de-paraffinised with histoclear (National Diagnostics Ltd, Hull, UK), hydrated through graded ethanol solutions and stained with Masson's Trichome stain

(VWR, Leicestershire, UK) to inspect structural changes or Elastin Van Gieson stain to examine elastic lamina degradation. For Masson's Trichome, staining for muscle fibres (azophloxine; red), collagen (light green SF; green) and cytoplasm (tungstophosphoric acid orange G; orange) with nuclear staining with Ehrlich's Haematoxylin solution (Clin-Tech Limited, Guilford, UK) was performed according to the manufacturer's instructions. For Elastin Van Gieson, staining for elastic fibre (blue-black), nuclei (blue), collagen (red) and other tissue (yellow) was also performed according to manufacturer's instructions. Sections were dehydrated through graded ethanol solutions and cover-slipped with Neo-Mount® anhydrous mounting medium (VWR, Leicestershire, UK).

Aortic sections were visualised and imaged using a coolSNAP-pro camera (Roper Scientific) and Leica DMRBE microscope using x5, x10, x20, x40 and x60 objectives. For sections stained with Masson's Trichome, mean medial area was measured at 3 separate anatomical sites, 0.3mm, 0.9 mm and 1.5 mm, above and below the left renal artery. For Elastin Van Gieson, length of elastin breakdown was measured over 2 anatomical sites above the renal artery (0.3mm and 0.9mm). Elastin breakdown was quantified by measuring the length of all elastic degradation and then dividing the total by the circumference of the vessel. Example of an elastin break is shown in Figure 3.1. All image analysis was performed using Image Plus-Pro software (Media Cybernetics, USA).

Figure 3.1

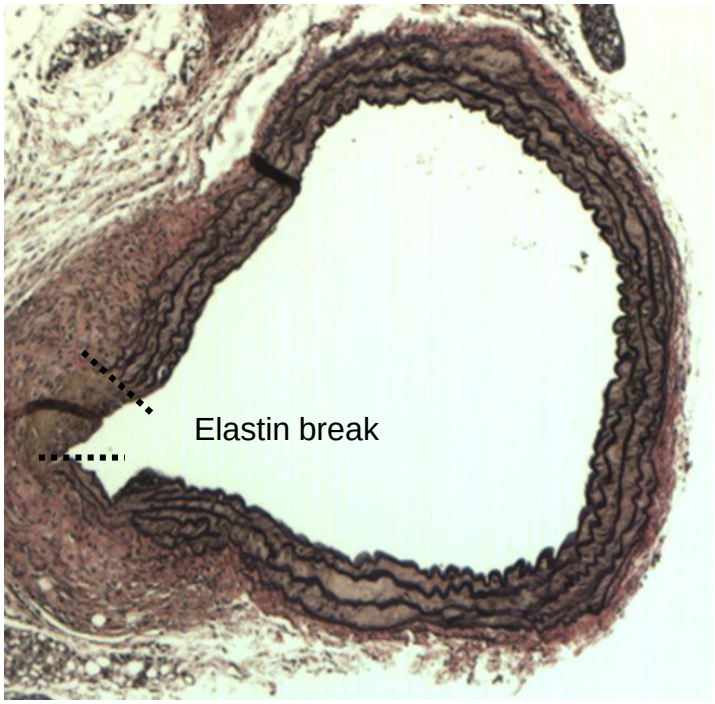


Figure 3.1 Example of elastin degradation

Elastin degradation is marked by the 2 dotted black lines. The length of break is measured and then divided by the circumference of the vessel.

3.2.2.3 Magnetic resonance imaging (MRI)

For aortic MRI, aortas were harvested from terminal isoflurane anaesthetised mice, fixed in 4% PFA and glued onto a wooden cocktail stick. This was embedded in small glass tubes with 2 ml of 2.5% high specification agarose (Schneider et al., 2003). Once the agarose is set, 2ml of 4% PFA enriched with 1:250 gadolinium is added followed by 5 ml of 2.5% agarose with 1:250 gadolinium. The aortas were then scanned by MRI overnight by Dr J. Schneider using the imaging sequence developed as described previously (Schneider et al., 2003) . Amira (Visage Imaging, USA) was used to analyse the images and reconstruct the aorta as 3D images.

Figure 3.2

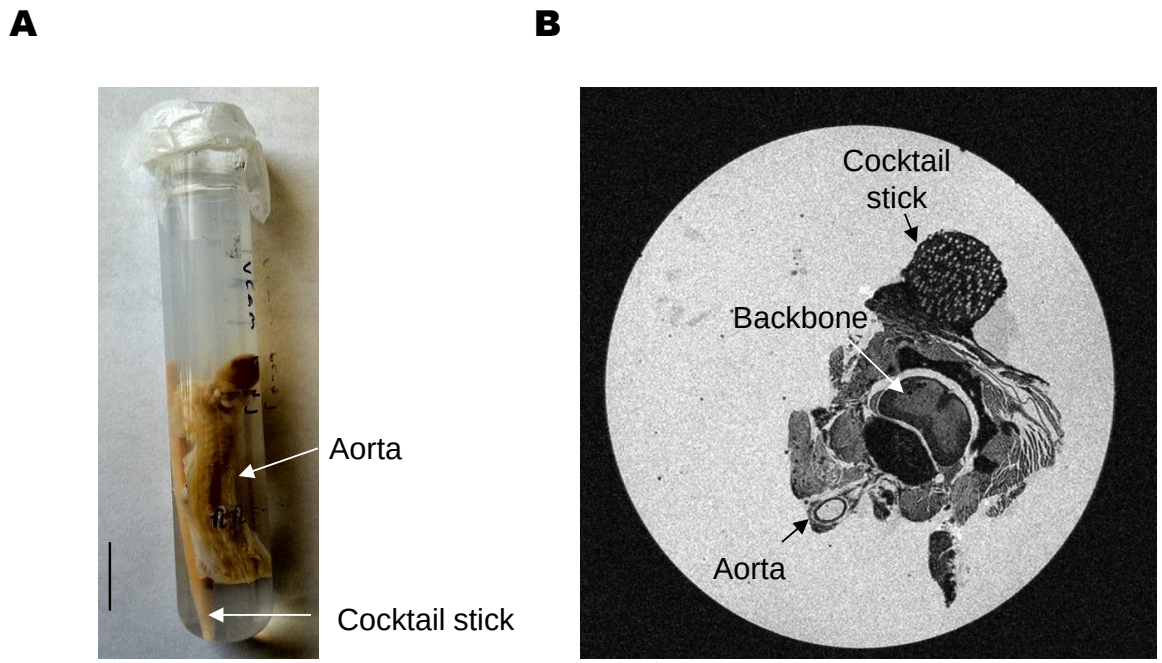


Figure 3.2 Sample preparation for MRI

Black bar – 1cm. **(A)** Photograph of a small glass tube with aorta embedded inside on a cocktail stick. **(B)** Representative MRI image of an aorta scanned inside the small glass tube.

3.3 Results

3.3.1 **Nox2 transgene expression is endothelial specific**

It was important first to confirm that the expression of Nox2 human transgene was endothelial specific in Nox2 Tg mice as other studies have shown Tie-2 promoter can be expressed in monocytes. To achieve this, primary endothelial cells, vascular smooth muscle cells and macrophages were isolated, RNA were extracted and used for quantitative RT-PCR as described in Chapter 2. I confirmed primary cell type specificity using cell specific markers: PECAM (CD31) for endothelial cell, myosin heavy polypeptide 11 for VSMC and CD68 for macrophages (Figure 3.3). Human Nox2 transgene expression was detected only in endothelial cells but not in VSMCs or macrophages isolated from the Nox2-Tg mice or in any cell types isolated from wild-type mice. Mouse Nox2 was detected to a similar extent in endothelial cells and macrophages indicating that endothelial specific over-expression of human Nox2 did not alter the levels of endogenous mouse Nox2.

Figure 3.3

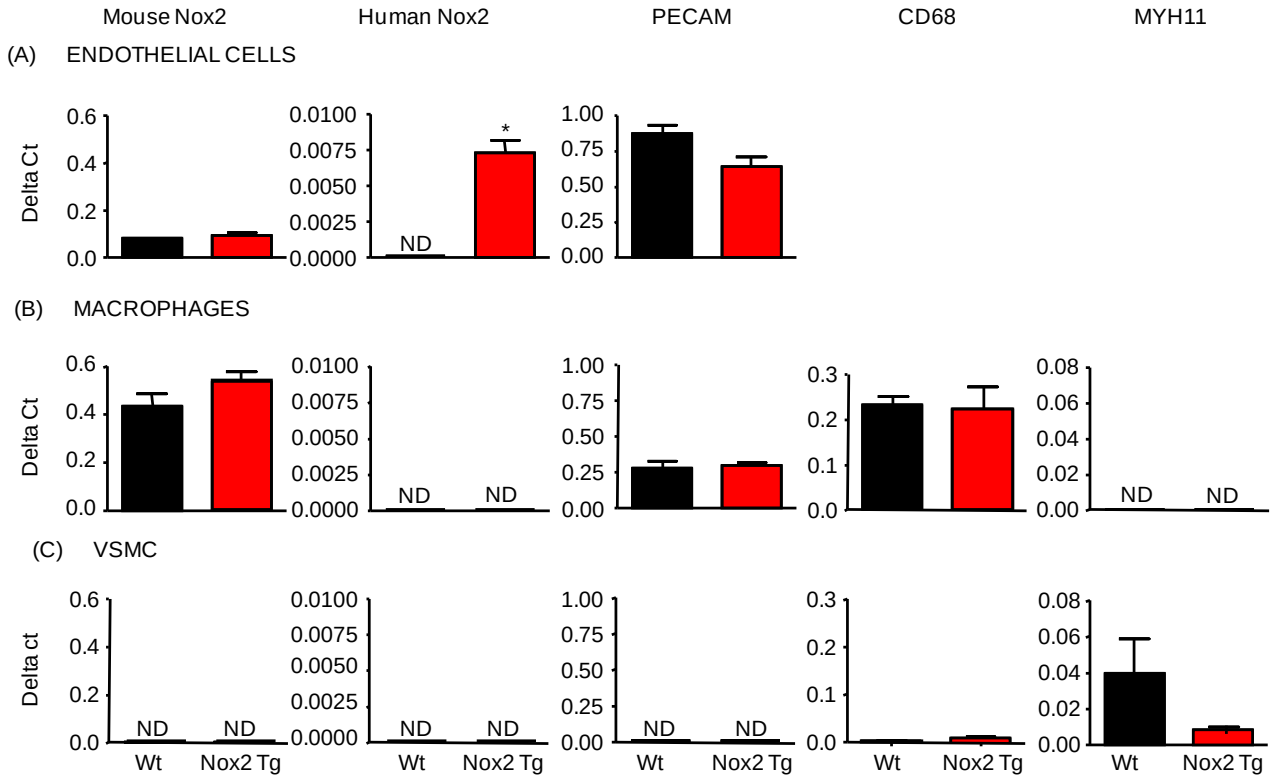


Figure 3.3 Nox2 transgene expression is endothelial specific.

RNA was extracted from primary endothelial cell isolated from lung, macrophages isolated from bone marrow and VSMCs isolated from aorta. Mouse Nox2, human Nox2, PECAM (endothelial cell marker), CD68 (macrophage marker) and MYH 11 (VSMC marker) were measured by fluorescence real time quantitative RT-PCR. **(A)** Endothelial cells. **(B)** Macrophages. **(C)** VSMC. Fold change was expressed as ΔCt relative to GAPDH. ND – Not detected. Data are expressed as mean±SEM. * $p<0.05$, n=4 per group. The human Nox2 transgene was only observed in Nox2 Tg endothelial cells, and not in Nox2 Tg VSMCs or macrophages or from any cells isolated from wild-type mice. Endogenous mouse endothelial Nox2 expression was unaffected by the Nox2 transgene.

3.3.2 **Blood pressure response to Ang II**

Ang II is a potent vasoconstrictor that causes a significant and sustained rise in systolic blood pressure (BP) (Cassis et al., 2009; Fukai et al., 1999; Gavazzi et al., 2007; Owens et al., 2010). To determine whether the increase in endothelial ROS production in Nox2 Tg mice had any effect on the pressor response to Ang II, Ang II (1mg/kg/day) was delivered subcutaneously via osmotic mini-pumps. BP was measured using Visitech tail cuff system as described in the methods section. There was no significant difference in either baseline systolic BP, 97.2±2.5 versus 95.0±2.9 mmHg in Nox2-Tg and wild-type mice respectively, or systolic BP following Ang II infusion which peaked with an increase of approximately 20mmHg both for wild-type (120.7±6.6 mmHg) mice and Nox2-Tg mice (121.2±6.7 mmHg) after 7 days of Ang II treatment (Figure 3.4). There was no difference in heart rate at baseline, 680±16 vs. 696±19 or after Ang II infusion, 660±27 vs. 682±20 between wild-type and Nox2 Tg.

Figure 3.4

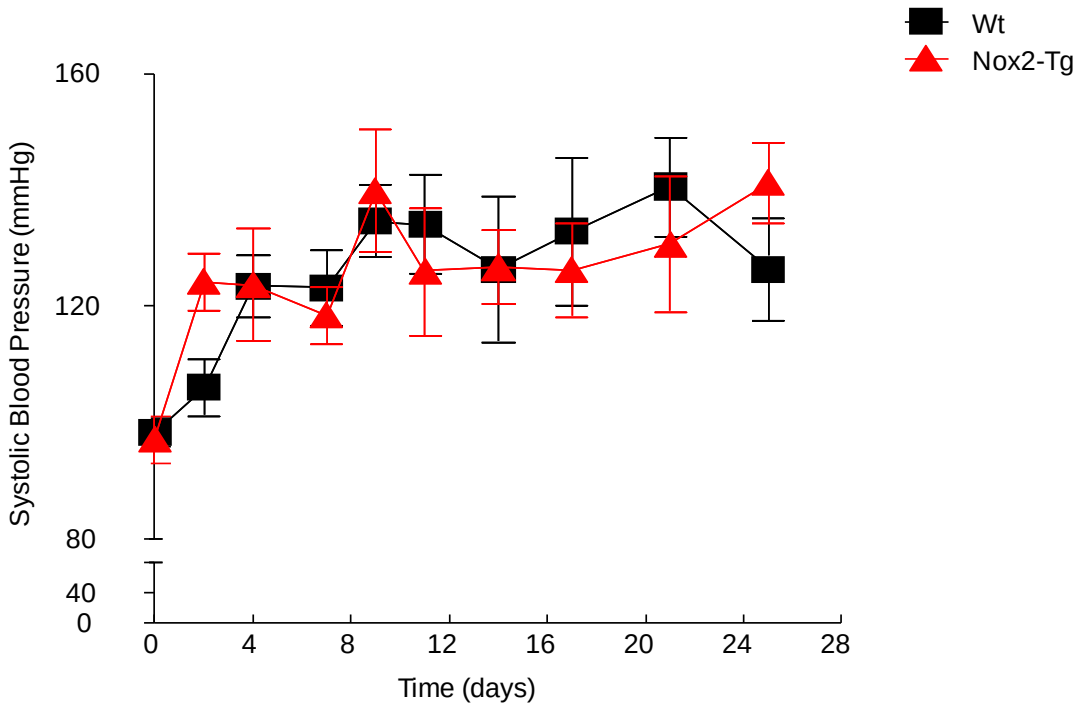


Figure 3.4 No difference in systolic blood pressure response to Ang II between Wt and Nox2 Tg

Systolic blood pressure of mice was recorded over 28 days of Ang II infusion (1mg/kg/day) using the Visitech Tail Cuff system. Mice were trained for 1 week prior to mini-pump implantation. Data are expressed as mean±SEM, n=11 per group. No difference in systolic blood pressure was observed between wild-type and Nox2 Tg at either baseline or following Ang II infusion.

3.3.3 **Increased aortic dissection in Nox2 Tg mice in response to Ang II**

Aortas were harvested from terminal anaesthetised wild-type and Nox2 Tg mice after 28 days of Ang II infusion. Surprisingly, despite no significant differences in systolic BP response between two groups, macroscopic aortic disease was observed in 45% (5/11) of Nox2-Tg mice compared to none (0/11) in the wild-type littermates ($p<0.05$; Figure 3.5 A, B). It commonly spanned the entire length of the descending aorta but most of the gross distortion was observed in the supra-renal aorta, between the diaphragm and the renal arteries.

Figure 3.5

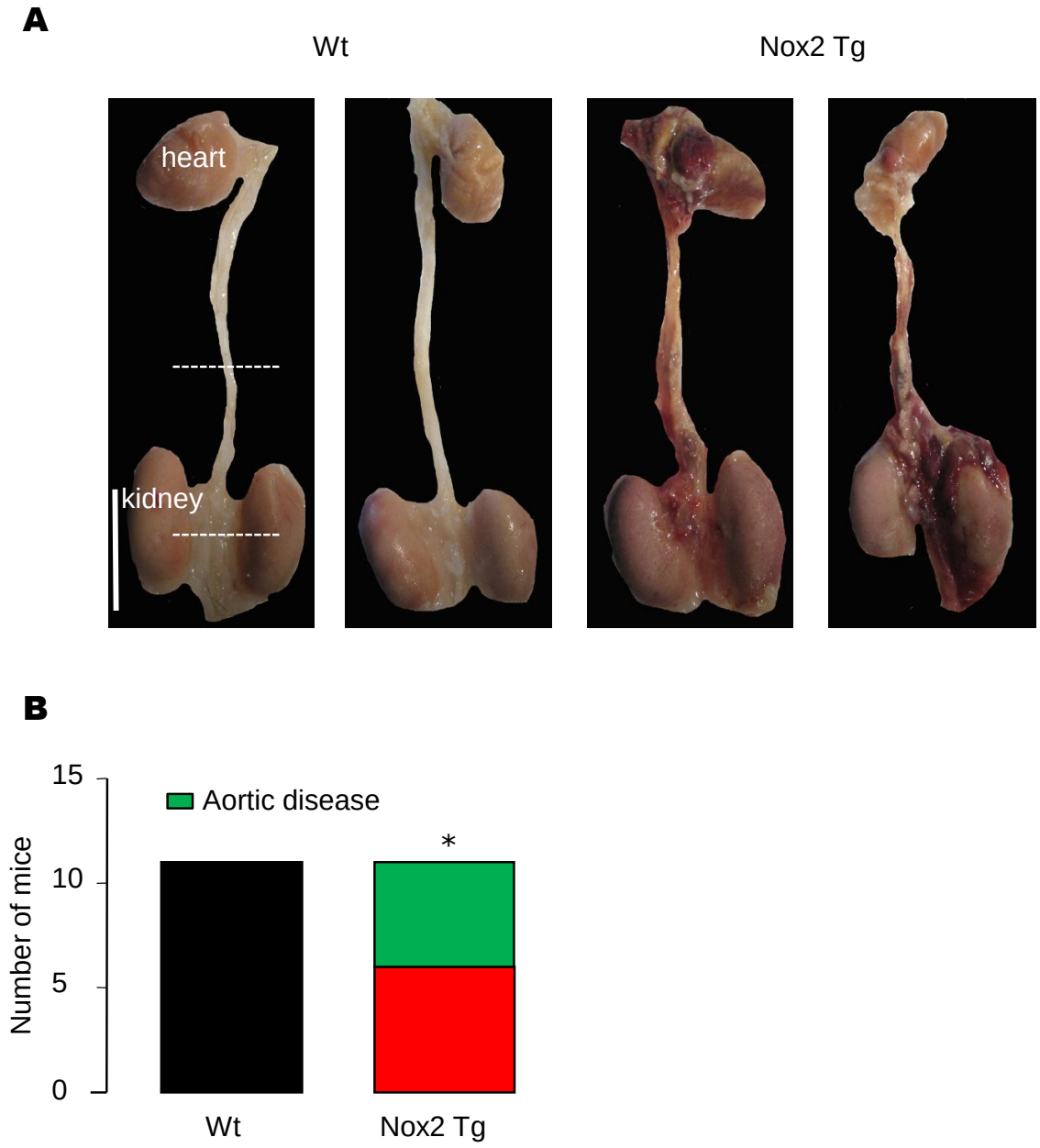


Figure 3.5 Increased aortic disease in Nox2 Tg in response to Ang II

20-24 weeks old Wt and Nox2 Tg littermate mice were infused with Ang II (1mg/kg/day) via subcutaneous osmotic mini-pumps for 28 days. Aortas were harvested and photographed at the end of the 28 day period. **(A)** Representative images of Wt and Nox2 Tg aortas. White bar – 1cm. Dotted white line – top, diaphragm; bottom, left renal artery. **(B)** Number of observed aortic disease in Wt and Nox2 Tg. *$p<0.05$, n=11 per group. Almost 50% of Nox Tg mice developed aortic disease following Ang II infusion for 28 days compared to none in the wild-type.

3.3.4 **Site of dissection was observed in the supra-renal aorta of Nox2 Tg mice**

Wild-type and Nox2 Tg aortas were embedded in paraffin, serially sectioned and stained with Masson's Trichrome stain to provide further information on the pathology of aortic dissection observed in Nox2 Tg mice. A rupture point was observed in the supra-renal aorta segment between the diaphragm and renal arteries, which is consistent with findings reported by other studies (Cassis et al., 2009; Daugherty and Cassis, 2004; Gavazzi et al., 2007). On analysis of the aortic media from 3 separate anatomical locations defined by the left renal artery, there was a significant reduction in medial area in the Nox2 Tg suprarenal aorta segment compared to wild-type controls ($p<0.05$). Interestingly, there was no significant difference in the aortic medial area below the renal arteries between wild-type and Nox2 Tg mice (Figure 3.6 A, B) suggesting the pathology was localised to the supra-renal area.

Figure 3.6

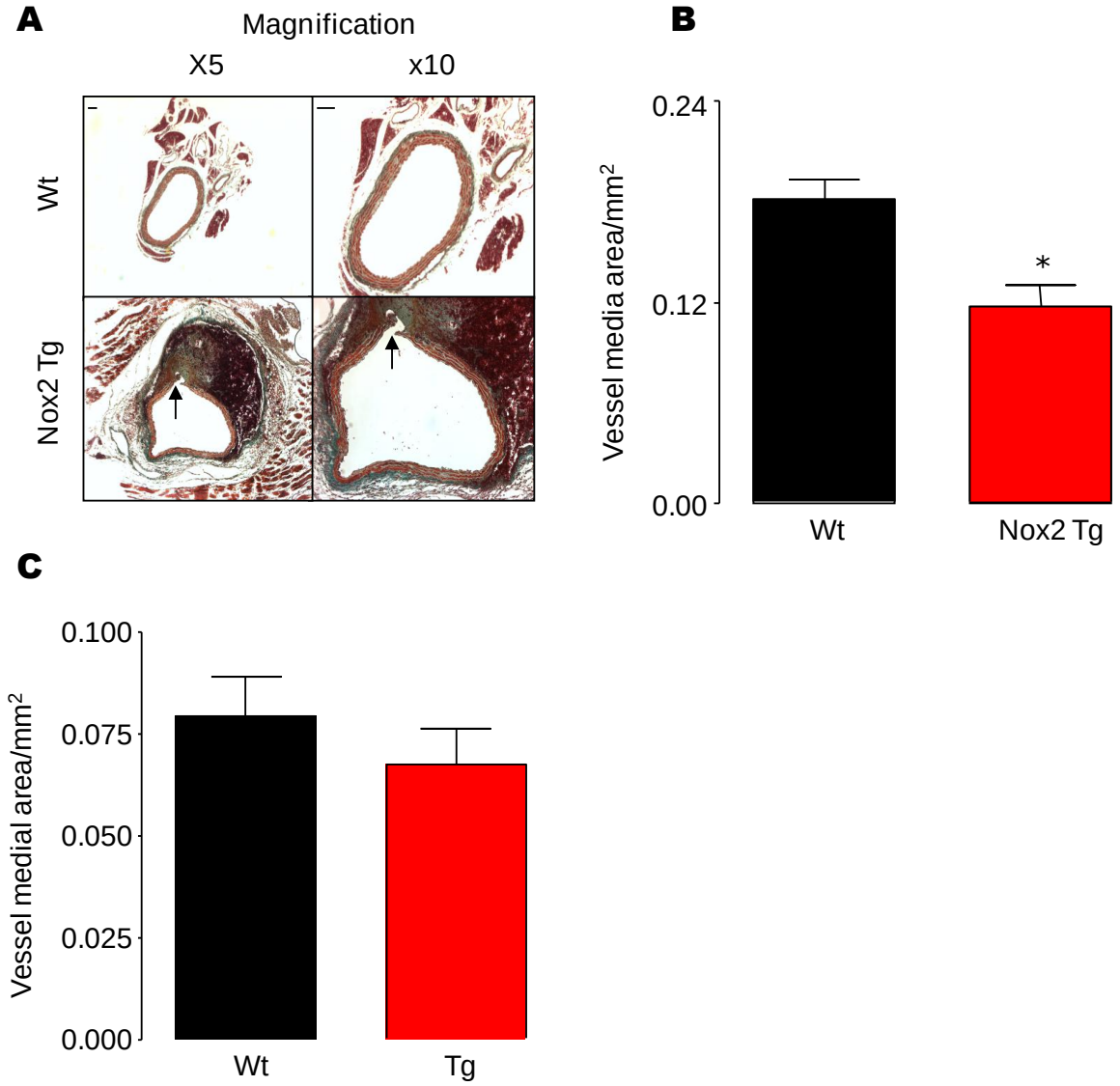


Figure 3.6 Reduced medial area in Nox2 Tg supra-renal aorta

Aortas from Nox2 Tg and Wt after 28 days of Ang II infusion were embedded in paraffin, sectioned and stained with Masson's Trichrome stain. **(A)** Representative images of aortic sections from the supra-renal aorta taken at x5 or x10 magnification demonstrating the site of dissection, black arrow. Black bar – 40 µm. **(B)** Quantification of vessel medial area from 3 anatomical positions above the left renal artery (LRA). Data are expressed as mean±SEM. *$p<0.05$, n=6-8 per group. **(C)** Quantification of vessel medial area below the LRA at 2 anatomical positions defined by LRA. Data are expressed as mean±SEM, n=6-8 per group. The point of rupture was observed in the Nox2 Tg supra-renal aorta. Supra-renal but not infra-renal aortic medial area was reduced in Nox2 Tg aortas compared to the wild-type.

3.3.5 **Increased elastic degradation in supra-renal aorta of Nox2 Tg mice**

Following the observation that the aortic medial area was reduced in Nox2 Tg supra-renal segment I next examined elastin degradation which contributes to weakening of the aorta wall and development of aortic disease. Sections of supra-renal aortas from wild-type and Nox2 Tg mice were stained with Elastic Van Gieson stain. The aorta normally has several continuous layers of elastic lamina. However in diseased aortas from Nox2 Tg mice, breaks in the elastic lamina were observed indicating elastin degradation and complete breakdown of all layers were observed at the point of rupture (Figure 3.7 A). Elastin degradation was quantified by measuring the total lengths of elastin break divided by the circumference of the vessel. I found a significant increase in elastin degradation in Nox2 Tg aortic sections compared to the wild-type controls, (Figure 3.7B, $p<0.05$).

Figure 3.7

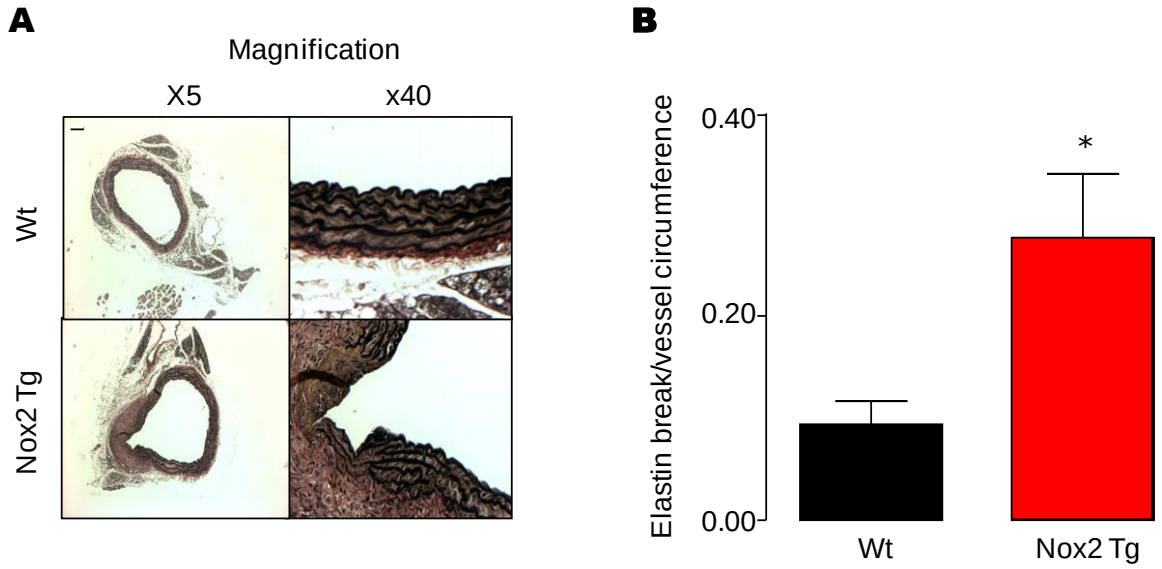


Figure 3.7 Increased elastic degradation in Nox2 Tg aortas

Wt and Nox2 Tg aortic sections taken from set anatomical positions defined by the left renal arteries were stained with Elastin-Van-Gieson stain. **(A)** Representative images of aortic sections demonstrating increased elastin breakdown in Nox2 Tg taken at x5 and x40 magnification. Black bar – 40 µm. **(B)** Quantification of elastin degradation presented as length of elastic break over vessel circumference. Data are expressed as mean±SEM. *$p<0.05$, n=6-8 per group.

3.3.6 **Assessment of the site of rupture using magnetic resonance imaging (MRI)**

Although histological aortic sections gave good insight into aortic pathology, it only provided limited information on 3D structure which is important in understanding underlying mechanism of the disease. To obtain further 3D information, we harvested supra-renal aortas on backbone from Nox2 Tg mice following Ang II infusion for 5 days. Aortas were embedded in the glass tube as described in Methods and then scanned overnight with magnetic resonance imaging. Magnetic resonance images were analysed and reconstructed in 3D using Amira. As expected, the point of rupture was found to be in the supra-renal aorta (Figure 3.8). The haematoma was located outside of the aortic media. It extended upwards from the left renal artery and severely compressed the lumen area in the supra-renal aorta. Patency of the aorta was still maintained which explained the tolerance of the mouse to the aortic disease.

Figure 3.8

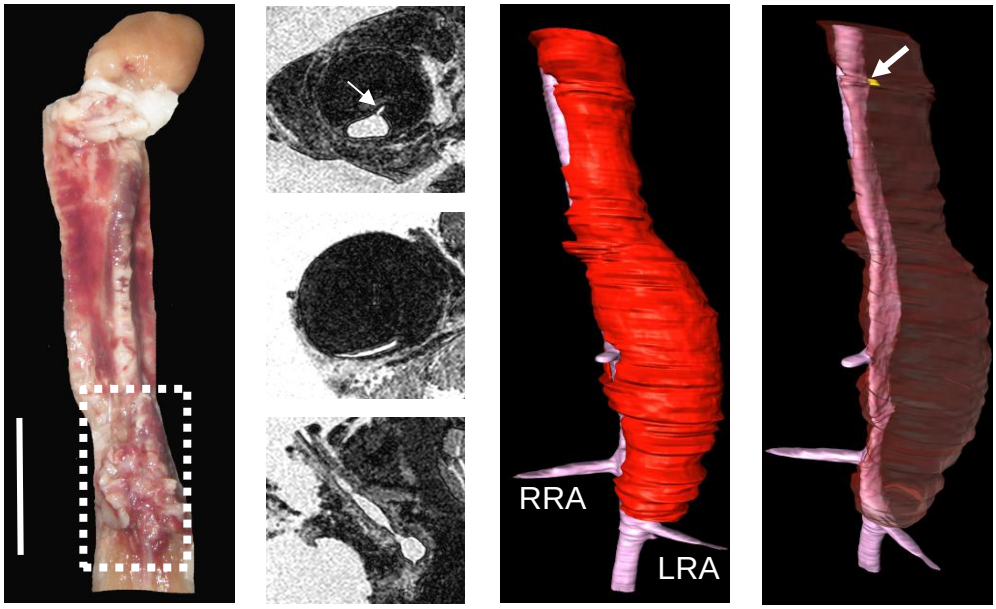


Figure 3.8 Magnetic resonance imaging (MRI) of diseased Nox2 Tg supra-renal aorta

20-24 week-old Nox2 Tg mice were infused with Ang II for 5 days. Aortas were harvested, embedded in glass tubes and scanned overnight with MRI. White bar – 1cm. Left first panel: Representative photograph of Nox2 Tg diseased aorta. White box – supra-renal aorta. Second Column panels: MRI cross sections at top, middle and bottom of supra-renal aorta. White arrow – site of dissection. Third and fourth panels: 3D reconstructed aorta. RRA – right renal artery; LRA – left renal artery; aorta- pink; surrounding haematoma – red; point of rupture – yellow dot and white arrow. The site of rupture was confirmed in the supra-renal aorta. The haematoma was located outside of the aortic media and spread upwards from the LRA. Gross compression of the aortic lumen was observed (Middle MRI panel).

3.3.7 **Increased BP in response to noradrenaline infusion had no effect on the development of aortic disease in Nox2 Tg mice**

It was shown in Figure 3.3 that Ang II causes an increase in BP in both wild-type and Nox2 Tg mice. In order to investigate if the increases in aortic disease observed in Nox2 Tg mice were due to the rise in blood pressure or some other Ang II specific effect, I infused mice with noradrenaline, a catecholamine that increases BP through α-adrenergic receptor mediated contraction of vascular smooth muscle cells, and is commonly used in mouse models to investigate isolated effects of BP on the development of vascular disease (Cassis et al., 2009; Fukai et al., 1999; Gavazzi et al., 2007; Owens et al., 2010). Unlike Ang II, noradrenaline does not elicit a vascular inflammatory response.

In order to find the dose of noradrenaline that would induce a rise in blood pressure similar to that of Ang II (1mg/kg/day), wild-type mice were infused initially either with 4.4 or 5.4mg/kg/day dose of noradrenaline. Saline and Ang II infused mice were used as controls (Figure 3.9 A). There was no increase in BP over 14 days in noradrenaline treated group compared to saline-treated group. In contrast, Ang II treated group had a large increase in BP which was consistent to the previously experiments. For the next cohort of wild-type mice, the dose of noradrenaline was increased to 8, 10 or 12 mg/kg/day (Figure 3.9 B). There was a modest rise in BP in all three doses of noradrenaline treated groups with a mean of 110mmHg however, mice in the 12mg/kg/day cohort (2/3) had greater rate of sudden death without aorta pathology on post-mortem.

Figure 3.9

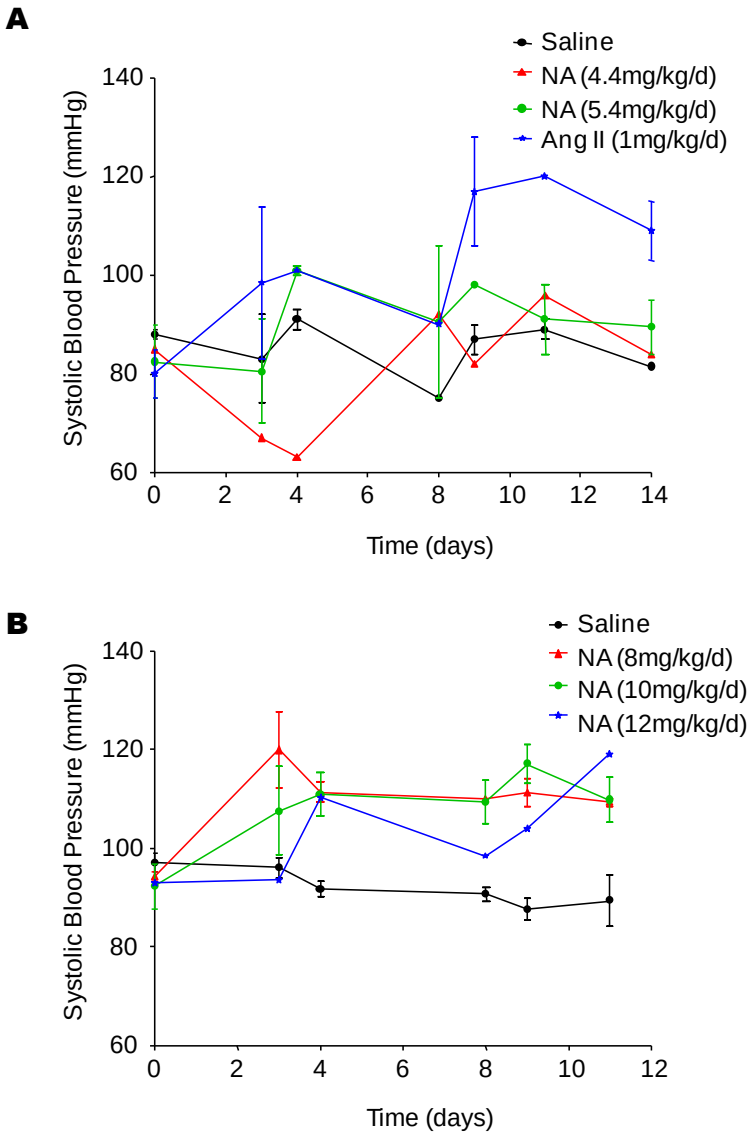


Figure 3.9 Development of method for noradrenaline (NA) infusion (1)

20-24 week-old Wt mice were implanted subcutaneously with osmotic mini-pumps containing noradrenaline (NA) at different doses. Blood pressure was measured for 14 days with the Visitech Tail Cuff system. **(A)** Mean systolic blood pressure following NA infusion at 4.4 and 5.4mg/kg/day, Ang II infusion at 1mg/kg/day or saline infusion. Data are expressed as mean±SEM. **(B)** Mean systolic blood pressure following either NA infusion at 8, 10 or 12mg/kg/day or saline infusion. Data are expressed as mean±SEM. Infusion at of noradrenaline at 8mg/kg/day or above induced a significant increase in systolic blood similar to that of 1mg/kg/day of Ang II infusion. All mice at least n=2-3 per group before start of the experiment but due to deaths, some groups only had 1 mouse surviving to the end of the experiment.

Based on these results, a further cohort of wild-type mice was infused with 8 or 10mg/kg/day of noradrenaline (Figure 3.10). There was a significant increase in blood pressure to a similar degree in both doses of noradrenaline treated groups compared to saline contrails. Noradrenaline at dose of 10mg/kg/day had a higher peak systolic blood pressure than 8mg/kg/day. Therefore, 10mg/kg/day of noradrenaline were subsequently chosen as the dose of noradrenaline for future experiments.

It is worth noting that noradrenaline had a significant and immediate effect on peripheral vasoconstriction at doses above 8mg/kg/day which impacted on thermal regulation and increased the risk of sudden death especially at dose of 12mg/kg/day. It was observed that the recovery of remaining mice was significantly better at room temperature instead of the warmed recovery unit. Mice were therefore, subsequently kept at room temperature in normal ventilated racks without warming.

Figure 3.10

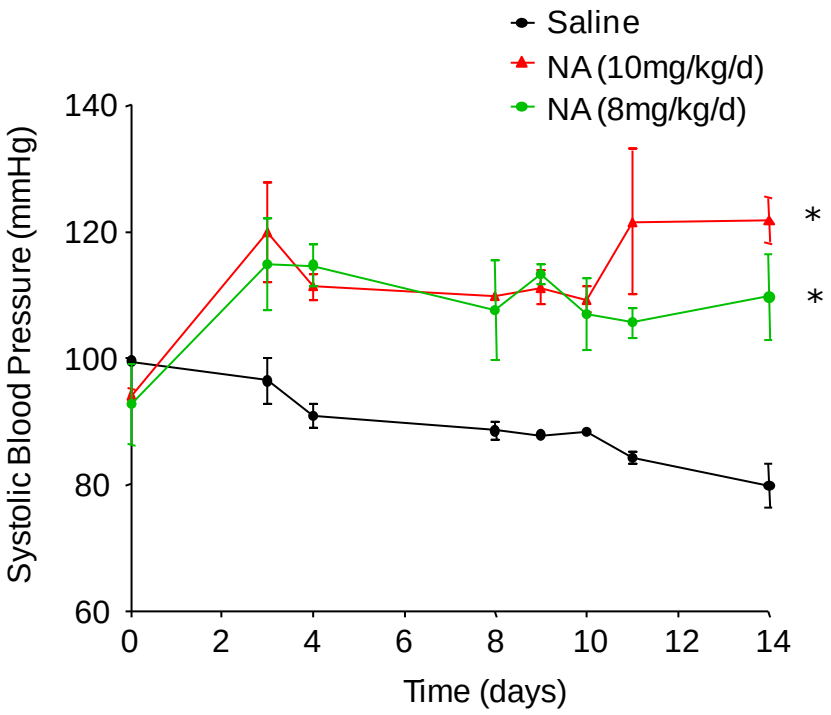


Figure 3.10 Development of method for noradrenaline (NA) infusion (2)

20-24 week-old Wt mice were implanted subcutaneously with osmotic mini-pumps containing either noradrenaline (NA) at doses of 8 and 10mg/kg/day or saline. Data are expressed as mean±SEM. *p<0.05, n=3-4 per group. Greater peak systolic blood pressure was achieved with 10mg/kg/day of Ang II.

Wild-type and Nox2 Tg littermates at 20-24 weeks of age were infused with noradrenaline (10mg/kg/day), Ang II (1mg/kg/day) or saline for 14 days (Figure 3.11 A). Mice were terminally anaesthetised on day 14 following BP measurement and aortas were harvested for analysis. Similar to previous experiments, Ang II increased systolic BP to the same extent in wild-type and Nox2 Tg mice however, 3/5 Nox2 Tg mice developed aortic dissection as compared to none in the wild-type group (n=5 per group). Noradrenaline infusion induced a similar rise in systolic BP as observed in Ang II treated wild-type and Nox2 Tg mice. However, in contrast to Ang II, no aortic dissections were observed in Nox2 Tg mice infused with noradrenaline (n=6, Figure 3.11 B). The limitation here is that the average blood pressure induced by nor-adrenaline was lower than that of Ang II although not statistically different. Higher doses of nor-adrenaline were not possible due to the increased risk of sudden death and the likelihood to exceed Home Office severity limit.

Figure 3.11

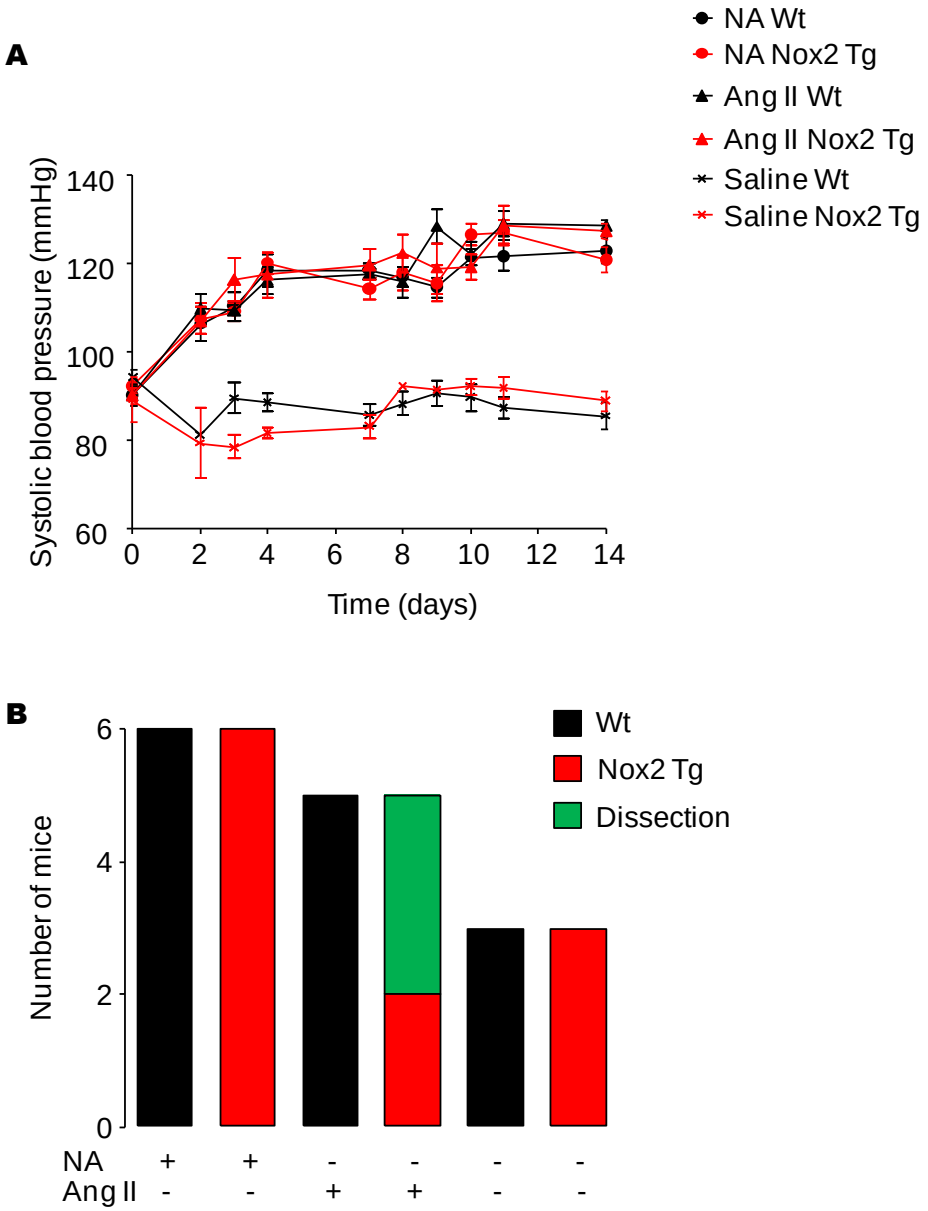


Figure 3.11 Noradrenaline induced a similar rise in blood pressure as Ang II but did not result in the development of aortic dissection

20-24 week-old Wt and Nox2 Tg mice were implanted subcutaneously with osmotic mini-pumps containing noradrenaline (10mg/kg/day), Ang II (1mg/kg/day) or saline. Aortas were harvested for analysis on day 14 following blood pressure measurements. **(A)** Mean systolic blood pressure over 14 days. Data are expressed as mean±SEM. **(B)** Number of aortic dissections observed in NA, Ang II or saline treated groups. n=3 saline, n=5-6 other groups. No aortic dissection was observed in noradrenaline treated groups in contrast to Ang II despite achieving similar rises in systolic blood pressure.

3.3.8 **No significant difference in body weight or heart rate between wild-type and Nox2 Tg**

All mice were weighed before insertion of osmotic mini-pumps. No difference in weight was observed between wild-type and Nox2 Tg in all treatment groups. Heart rate was recorded by the Visitech blood pressure system along with systolic blood pressure. No difference was observed in heart rate between wild-type and Nox2 Tg during saline, Ang II or NA infusion (Table 3.1).

Table 3.1: Weight, systolic blood pressure and heart rate of Wt and Nox2 Tg mice following 14 days of Ang II infusion

	Saline		Ang II (1mg/kg/day)		Noradrenaline (10mg/kg/day)	
	Wt	Nox2 Tg	Wt	Nox2 Tg	Wt	Nox2 Tg
Body weight (g)	35.5±1.95	37±2.3	34.2±1.2	31.1±0.8	32.1±1.5	35.3±1.22
Blood pressure (mmHg)	95.0±2.9	97.2±2.5	120.7±6.6	121.2±6.7	114.4±3.2	115.2±3.2
Heart rate (bpm)	708±21	742±11	696±22	704±9	667±13	645±8

Data are mean±SEM, n=3 for saline groups, n=6-11 all others.

3.4 Discussion

In this chapter, I investigated the effects of a specific increase in endothelial ROS on the development of Ang II mediated aortic disease, using the Nox2 Tg mouse model where the Nox2 transgene was specifically over-expressed in endothelial cells. The key findings were:

- Increased endothelial ROS in Nox2 Tg mice led to a significant increased incidence of aortic disease in response to Ang II.
- The rupture point was identified in the supra-renal aorta which had reduced medial area and increased elastin degradation.
- The increase in Ang II induced aortic disease appeared to be independent of the blood pressure effects of Ang II.

Increased vascular reactive oxygen species (ROS) production is implicated in chronic endothelial dysfunction and the development of cardiovascular diseases including hypertension, atherosclerosis and heart failure (Cai and Harrison, 2000). Global gene deletion of Nox2 reveals that ROS production is required for the progression of atherosclerosis (Judkins et al., 2010a) and vascular remodeling. However, it remains unclear whether increased ROS production by specific cell types is sufficient to drive disease pathogenesis, or whether the increase in cellular ROS is merely a consequence of disease progression.

Endothelial cell ROS production is a key component of the abnormal endothelial function characteristic of vascular disease states, but it is not known to what extent endothelial cell-specific ROS directly contributes to progression of structural vascular diseases. This is an important question, since endothelial ROS production and endothelial dysfunction are

predictive of cardiovascular events and long-term clinical outcome (Schachinger et al., 2000).

The endothelial specific Nox2 Tg mouse mimics the increase in endothelial Nox2 observed in vascular diseases thus provides a powerful tool to test whether increased endothelial Nox2 expression, and the consequent increase in endothelial cell ROS production, is sufficient to modify the vascular response to Ang II. The specificity of the endothelial Nox2 transgene was confirmed by quantitative real-time PCR which demonstrated that the Nox2 transgene was only detected in endothelial cells and not in VSMCs or in macrophages isolated from Nox2 Tg mice or any cells isolated from wild-type mice.

I found that treatment with Ang II at 1mg/kg/day in wild-type C57BL/6J did not lead to the development of aortic disease. However, in Nox2-Tg mice, the same dose of Ang II induced 45% incidence of aortic disease. This is 2 times higher than the 20% incidence reported in other studies using a higher dose of Ang II (1.44-3mg/kg/day) in C57BL/6J mice (Tieu et al., 2009; Wang et al., 2010). The endothelial specific Nox2 overexpression was therefore sufficient to induce greater incidence of aortic disease with a lower dose of Ang II which highlights the role of endothelial ROS and endothelial dysfunction in the initiation and development of the vascular disease.

The increase in aortic disease in Nox2 Tg mice was associated with reduced vessel medial thickness and increased aortic elastin degradation suggesting the activation of matrix metalloproteinases (MMPs). Regulation of MMPs by Ang II is not well understood but it is likely to be dependent on the MAPK pathway (Jiménez et al., 2009) and also ROS production from NADPH oxidase (Grote et al., 2003; Luchtefeld et al., 2005). The main MMPs that have been found to be upregulated in Ang II induced vascular disease are

MMP-2 and MMP-9 (Thompson and Baxter, 1999). MMP-9 is an inducible enzyme secreted by mononuclear phagocytes (McMillan et al., 1995b; Newman et al., 1994; Thompson et al., 1995) whereas MMP-2 is expressed by VSMCs and adventitial fibroblasts in areas adjacent to mononuclear phagocytes (Davis et al., 1998; McMillan et al., 1995a). The roles of MMPs are examined further in the next chapter.

The pathology observed in Nox2 Tg mice were classified as aortic dissection rather than AAA based on the observations that:

1) Pathology occurred early on, between day 5 to day 6, which is too early for the development of aortic aneurysm (AAA typically develops after 14-28 days of Ang II infusion).
2) A clear rupture point could be identified in the supra-renal aorta by both immunohistochemistry and by MRI as evidenced by the complete breakdown of elastin and rupture of the vascular wall. This was defined as the dissection point. The localisation of aortic pathology to the supra-renal segment was consistent with findings from other studies. (Ayabe et al., 2006; Bruemmer et al., 2003; Daugherty et al., 2000; Gavazzi et al., 2007; Gavrila et al., 2005; Manning et al., 2003; Rateri et al., 2011; Saraff et al., 2003; Satoh et al., 2009; Thomas et al., 2006; Tieu et al., 2009; Uchida et al., 2010; Wang et al., 2010; Xiong et al., 2009; Zhang et al., 2009). It is still unclear why the aortic pathology localises to the supra-renal segment in mice. Only one study so far had investigated the response of different aortic segments to Ang II (Owens et al., 2010). In this study, the authors observed ascending aorta to respond by medial hyperplasia instead of hypertrophy found in the other segments. The region specific difference was attributed to differential expression of Id3 (inhibitor of differentiation) in the aorta. Other factors such as haemadynamics are likely also to play a role.

3) The haematoma typically tracked most of the way up the vessel suggesting the formation of a false lumen.
4) The aortic lumen was severely compressed by the haematoma which is typically not observed in AAA.

We have previously shown that Nox2 Tg mice had increased pressor response to Ang II (0.4mg/kg/day) (Bendall et al., 2007). Interestingly, at higher dose of Ang II (1mg/kg/day) there was no longer a difference in blood pressure between wild-type and Nox2 Tg mice. Ang II mediates its increase in blood pressure mainly through AT1 receptors on VSMCs which is the predominant cell type in the vascular wall. At low doses of Ang II, endothelial ROS may still have a comparable effect as Ang II on VSMCs whereas at higher doses, the response of VSMCs to Ang II is likely to overwhelm any influences exerted by endothelial ROS. This would suggest the change in blood pressure in response to Ang II was not the cause of the increase in aortic dissection observed in Nox2 Tg mice. Furthermore, we infused noradrenaline to achieve a similar rise in systolic BP as Ang II and observed no aortic dissection in noradrenaline treated Nox2 Tg mice compared to ~50% in Ang II treated Nox2 Tg mice. These results further indicate that Ang II-induced aortic dissection was independent to its pressor effect, which is consistent with findings from previous studies (Cassis et al., 2009; Fukai et al., 1999; Gavazzi et al., 2007; Owens et al., 2010).

On the surface, the mouse data contradict human studies: patients with aortic dissection often have high blood pressure and lowering the blood pressure in these patients results in better long term outcomes; reducing blood pressure in patients with Marfans syndrome reduced progression of the disease (Mehta et al., 1995). However, human studies are long term studies of disease progression in patients who already have the disease whereas mouse studies examined disease development in previously healthy mice. It would be interesting if noradrenaline was given to mice after the development of aortic aneurysm. It

is possible increases in blood pressure may then have an effect on the rupture of the aneurysm.

Chapter 4:
Inflammatory response of Nox2 Tg aortas

Chapter 4. Inflammatory response of Nox2 Tg aortas

4.1 Introduction

I have shown previously in Chapter 3 that:

- Increased endothelial ROS in Nox2 Tg mice led to a significant increased incidence of aortic dissection in response to Ang II.
- The dissection point was identified in the supra-renal aorta which had reduced media area and increased elastin degradation.
- The increase in Ang II induced aortic dissection was independent of the blood pressure effects of Ang II.

Ang II induces vascular inflammation by affecting all stages of the inflammatory response: increased vascular permeability, leukocyte recruitment and activation of tissue repair process. The initial phase of inflammation is an increase in vascular permeability associated with exudation of protein-rich fluid. Ang II induces the release of prostaglandins such as PGE2 and PGI2 and vascular endothelial growth factor (VEGF) which are the main effectors mediating the increase in vascular permeability (Harris et al., 2004).

The next phase in the inflammatory cascade is leukocyte recruitment which involves leukocyte rolling from the bloodstream and adhering to the vascular wall (margination) and then migrating through the vascular wall (diaspedesis). Ang II regulates leukocyte recruitment through AT_1 and AT_2 receptors (Marchesi et al., 2008) and the upregulation of adhesion molecules such as VCAM-1 which allows leukocytes to bind firmly to the endothelial surface. In endothelial cells (ECs) Ang II up-regulates the expression of

VCAM-1 through pathways involving NFκB and ROS (Fleming et al., 2001). Partial knockout of VCAM-1 significantly attenuated the development of inflammatory vascular diseases such as atherosclerosis (Cybulsky et al., 2001). Ang II also promotes EC-Leukocyte interactions with release of cytokines and chemokines such as IL-8 which recruits neutrophils through the CXCR2 receptor. Blocking of CXCR2 receptors significantly inhibited the recruitment of inflammatory cells (Nabah et al., 2007). Ang II can therefore directly increases leukocyte recruitment through the release of vascular pro-inflammatory mediators.

The pro-inflammatory role of Ang II is further supported by the anti-inflammatory protective effects of Ang II inhibitors such as losartan. In both human Marfans syndrome and mouse models of Marfans syndrome, losartan (Ang II receptor blocker) reduced the development of AAA (Brooke et al., 2008; Habashi et al., 2006). In hyperlipidimic rabbits, losartan reduced aortic intima proliferation and macrophage infiltration (Chen et al., 2002) and in patients with premature atherosclerosis, irbesartan reduced serum levels of VCAM-1 and TNF-α (Navalkar et al., 2001).

Ang II also influences collagen metabolism and extracellular matrix composition by the activation of matrix metalloproteinase (MMP) activity. The main MMPs that have been found to be upregulated in Ang II induced vascular disease are MMP-2 and MMP-9 (Thompson and Baxter, 1999). Inhibition of MMPs by the broad-spectrum antibiotics doxycycline or knockout of MMP-2 and MMP-9 inhibited the development of aortic aneurysm (Longo et al., 2002; Manning et al., 2003; Pyo et al., 2000).

4.1.1 **Hypothesis and Aims**

One of the key mechanisms by which Ang II mediate its pro-inflammatory effects is the upregulation of ROS through NADPH oxidase. Increasing endothelial ROS through Nox2 over-expression could potentially have a significant impact on all aspects of Ang II induced vascular inflammation including EC-leukocyte interaction, leukocyte recruitment and MMP activation and provide an explanation for the observed increase in aortic dissection in Nox2 Tg mice.

To test the hypothesis that increases in endothelial ROS potentiate Ang II induced vascular inflammation, I examined the key components of the inflammatory pathway including endothelial activation and expression of adhesion molecules, inflammatory cell recruitment and matrix metalloproteinase (MMP) activity.

The main aims of this chapter are:

- To investigate VCAM-1 expression in wild-type and Nox2 Tg aortic in response to Ang II.
- To evaluate inflammatory cell recruitment in wild-type and Nox2 Tg aorta using CD45 as leukocyte marker
- To examine matrix metalloproteinase activity in wild-type and Nox2 Tg aorta using in-situ zymography

4.2 Methods

General methods are described in the Chapter 2. Only methods and reagents used specifically in the experiments for this chapter are described below.

4.2.1 **Analysis of aorta**

4.2.1.1 Immunofluorescence confocal microscopy

Supra-renal aorta was briefly perfusion fixed with 4% PFA, dissected and transferred into plastic moulds (VWR, UK) filled with OCT (VWR, UK) with the diaphragmatic end facing upwards. Moulds were frozen on dry ice and stored at -20ºC for sectioning. Serial 10μm sections were cut with Leica CM-3050-S Cryostat from the first appearance of the renal artery until no aorta was observed. Sections were mounted onto adhesive poly-L-lysine coated slides (VWR, Leicestershire, UK). Approximately 400 sections were cut for each aorta and the renal artery was used for orientation so sections at the same anatomical point could be taken for analysis.

4.2.1.1.1 VCAM-1 staining

Aortic sections were air-dried for 10 minutes at room temperature and then blocked with DAKO blocking solution (DAKO laboratories) containing 10% horse serum (Vector Laboratories) for 2 hours at room temperature. Sections were washed with PBS and then incubated with Rat anti-mouse VCAM-1 antibody, 1:50 dilution, (Cambridge Bioscience, UK) for 2 hours. Following three washes (5 min/each) with PBS, rabbit anti-rat secondary antibody (BD Pharmingen, UK) conjugated to Alexa-568 flourochrome (red fluorescence) was added onto the sections and incubated for 1 hour at room temperature. Sections were mounted in Mowiol (Sigma-Aldrich, UK) and DAPI (1:1000, Invitrogen, UK) and dried overnight. VCAM-1 fluorescence was examined using Zeiss 510 MetaHead confocal fluorescence microscope. Settings for laser power, gain and offset were optimised using the negative control so that DAPI (blue fluorescence) was clearly visible but not any background red fluorescence. All VCAM-1 staining was done in a blinded batch design

with the images taken at x40 and x60 objectives with the same setting for the confocal microscope to minimise operator bias. Images were analysed using Image Pro-Plus software by which the red fluorescence intensity was measured and then divided by the length of the vessel. Lung and aorta from ApoE$^{-/-}$ mice which have high systemic background inflammation and VCAM-1 expression in the endothelial cells were used as positive controls. Optimal VCAM-1 detection was observed using primary antibody at 1:50 dilution (Figure 4.1).

Figure 4.1

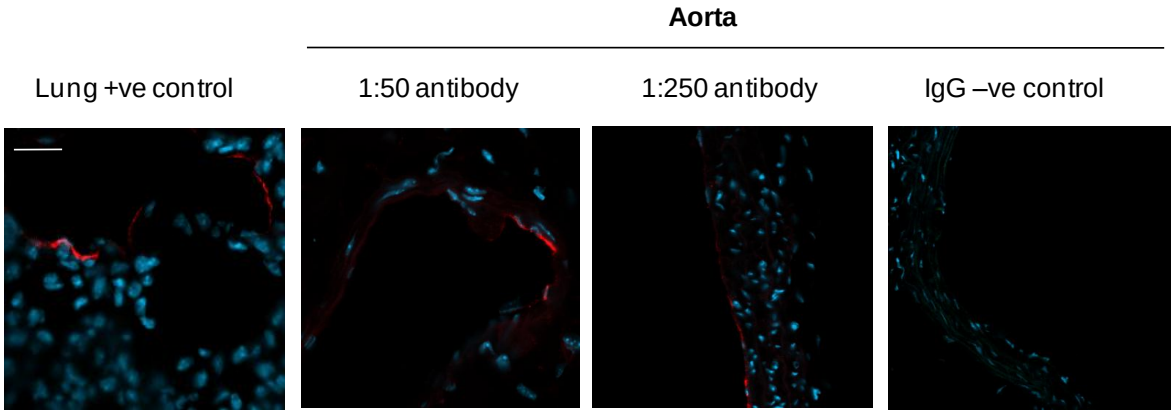


Figure 4.1 Optimisation of VCAM-1 staining

Representative images at x60 magnification taken with Zeiss 510 MetaHead confocal fluorescence microscope from lung positive control incubated with 1:50 anti-VCAM-1 antibody; aortas incubated with either 1:50 or 1:250 dilution of anti-VCAM-1 antibody or 1:50 Rat IgG negative control. White bar - 40µm.

4.2.1.1.2 CD45 staining

CD45 is a pan-leukocyte marker commonly used to assess for the presence of inflammatory cells. Sections were air-dried and fixed in acetone for 10 minutes. Following fixation, sections were rehydrated with PBS for 10 min and then blocked with DAKO blocking solution (DAKO laboratories, UK) and 10% horse serum (Vector Laboratories, UK) for 2 hours. CD45 staining with rat anti-mouse CD45 antibody (BD Pharmingen, UK) for the assessment of inflammatory cells was initially poor after 2 hours of primary antibody incubation and 1 hour of secondary antibody even in the positive control cryosections from $ApoE^{-/-}$ lung and aorta, which have high systemic background inflammation and $CD45^{+}$ cells (Figure 4.2 A). No $CD45^{+}$ cells were visible in these sections. I next used immunohistochemistry with Vector® Red Substrate Kit (Vector Labs, UK) which has greater sensitivity due to the amplification of the signal by the avidin/biotin interaction according to manufacturer's instructions to improve the detection of $CD45^{+}$ cells (Figure 4.2 B). However, $CD45^{+}$ staining was only marginally improved with vector red staining. Longer incubation period (24 hours) was then tried with immunofluorescence staining, which dramatically improved detection of $CD45^{+}$ cells (Figure 3.2 C). No CD45 staining was observed in the IgG control. Subsequent CD45 staining was therefore performed with 24 hours primary antibody incubation, 1 hour secondary antibody incubation and mounted in Mowiol and DAPI. Staining was done in a blinded batch design and images were taken with Zeiss 510 MetaHead confocal fluorescence microscope with the same settings to minimise operator bias. Images were analysed using Image Pro-Plus software. Cell with red fluorescence surrounding DAPI nuclei were defined as $CD45^{+}$. Data was expressed as number of $CD45^{+}$ cells over the vessel adventitial area.

Figure 4.2

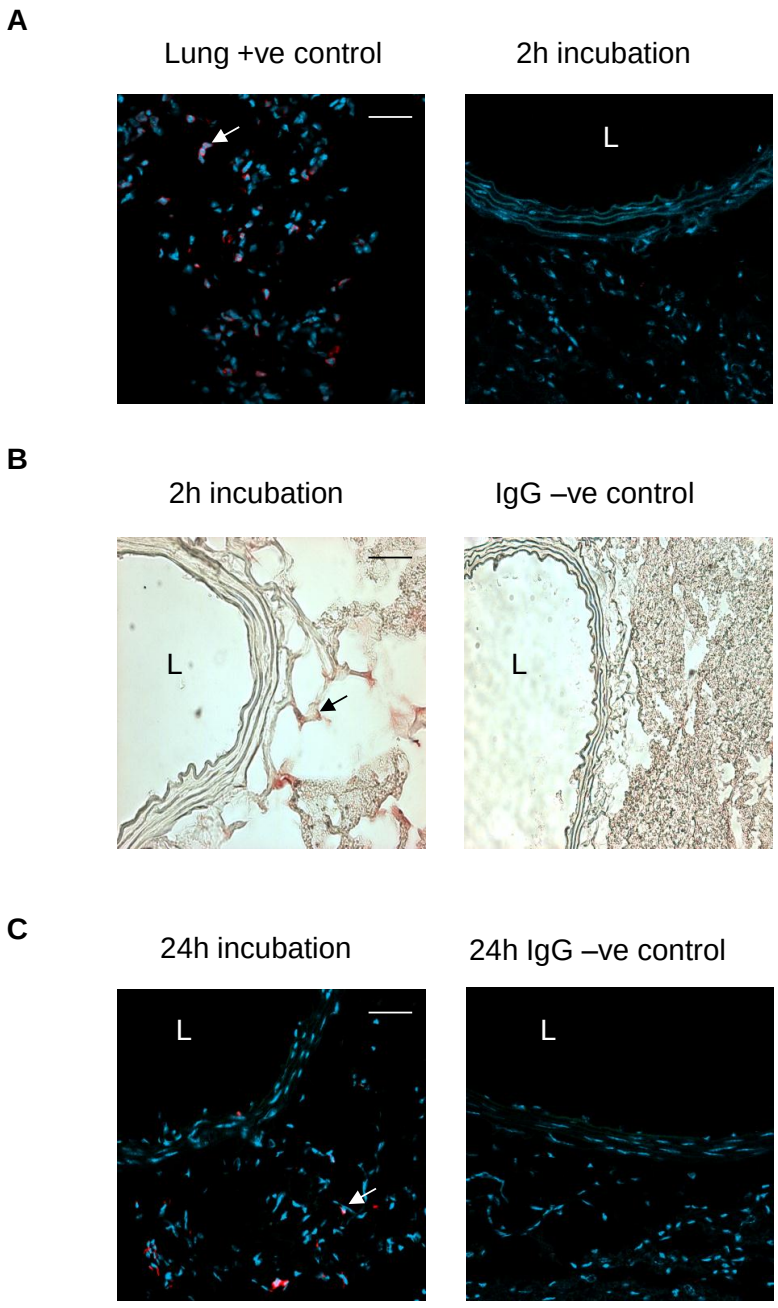


Figure 4.2 Optimisation of CD45 staining

ApoE$^{-/-}$ sections from lung and aorta were probed with CD45 antibody. White/black bar - 40µm. **(A)** Representative images of lung and aorta with 2 hour CD45 antibody incubation taken at x40 magnification. DAPI (nuclei): blue; CD45 stain: red. Only cells with both DAPI and CD45 stain, white arrow, were defined as CD45^{+} cells. **(B)** Vector red stain of aorta incubated with either CD45 or IgG antibodies for 2h. CD45^{+} cells: red, black arrow. **(C)** Immunofluorescence staining of aorta incubated with CD45 or IgG antibodies for 24h. CD45^{+} cells: red with DAPI (blue), white arrow.

4.2.1.1.3 In-situ zymography

For the assessment of matrix metalloproteinase (MMP) activity, an in-situ zymography kit, EnzChek® Gelatinase/Collagenase Assay Kit (Invitrogen, UK), was used (Goodall et al., 2001; Satoh et al., 2009). The kit contains DQ™ gelatin which on cleavage by MMPs, produce highly fluorescent peptides that are directly proportional to the proteolytic activity of MMP. This could be observed under microscope as green fluorescence at wavelength of 468nm. The assay was optimised using cryosections from $ApoE^{-/-}$ lung and aorta as they have active inflammation and high MMP activity (Figure 4.3). Aortic sections were incubated for 1 hour with DQ gelatin in Tris-$CaCl_2$ buffer (50mM Tris, 10mM $CaCl_2$, 1µM $ZnCl_2$). The sections were washed with PBS and mounted in Mowiol with DAPI. DQ™ gelatin used at a concentration of 100µg/ml produced the best result, and MMP activity was completely inhibited by the MMP inhibitor phenanthroline (1mM). All in-situ zymography was therefore performed with 1 hour incubation of DQ™ gelatin at 100µg/ml concentration in a blinded batch design. Images were taken with Zeiss 510 MetaHead confocal fluorescence microscope with the same settings to minimise operator bias. Images were analysed using Image Pro-Plus software.

Figure 4.3

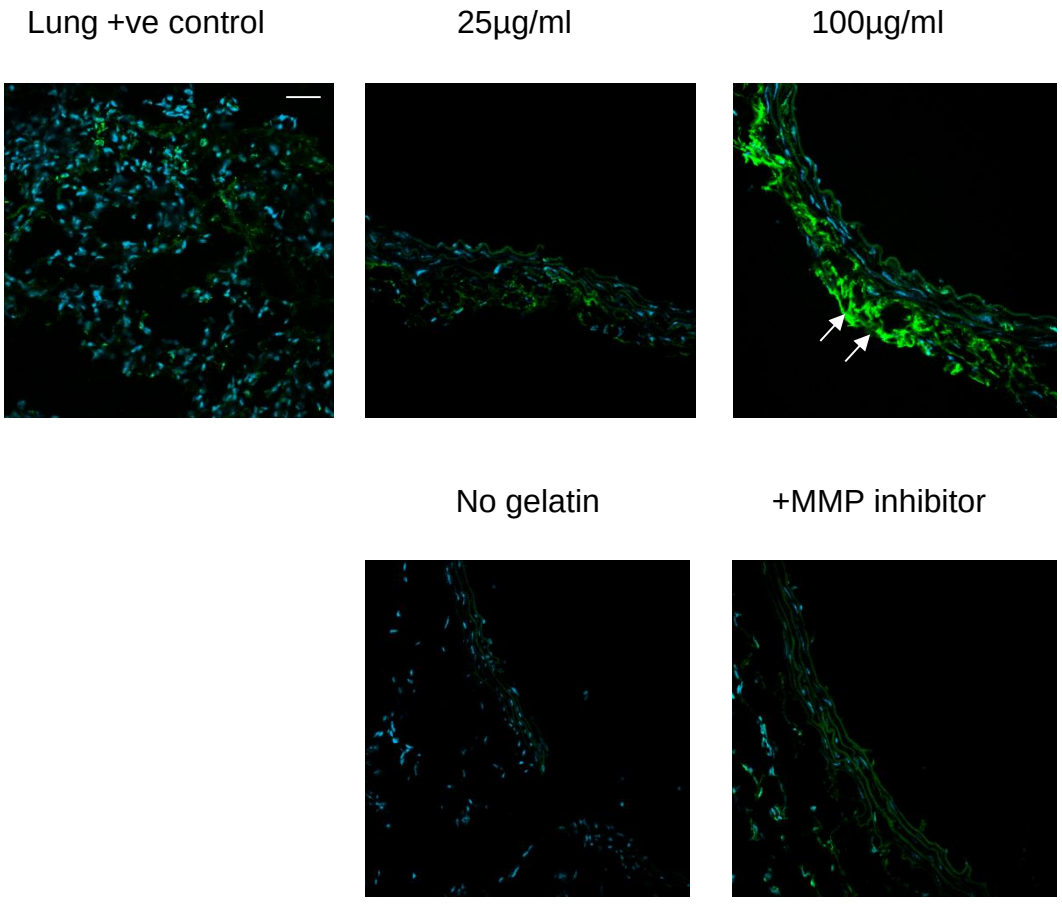


Figure 4.3 Optimisation of in-situ zymography

Representative images taken at 40X magnification of lung positive control, aortas incubated with 25 or 100µg/ml DQ gelatin, negative control with no gelatin and with MMP inhibitor, phenanthroline (1mM) and 100µg/ml DQ gelatin. White bar – 40 µm.

4.2.1.1.4 CD68 staining

CD68 is a glycoprotein expressed on monocytes and macrophages and commonly used as a marker for these cells. In order to further characterise the contribution of monocyte/macrophages to $CD45^+$ inflammatory cells recruited to the vessel wall, aortic sections were examined for CD68 expression. Sections were washed with PBS and then incubated with rat anti-mouse CD68 antibody (BD Pharmingen, UK) for 2 hours, 1:100 dilution, (Cambridge Bioscience, UK) for 2 hours. Following three washes (5 min/each) with PBS, rabbit anti-rat secondary antibody (BD Pharmingen, UK) conjugated to Alexa-568 flourochrome (red fluorescence) was added onto the sections and incubated for 1 hour at room temperature. Sections were mounted in Mowiol (Sigma-Aldrich, UK) and DAPI (1:1000, Invitrogen, UK) and dried overnight. CD68 fluorescence was examined using Zeiss 510 MetaHead confocal fluorescence microscope. Settings for laser power, gain and offset were optimised using the negative control so that DAPI (blue fluorescence) was clearly visible but not any background red fluorescence. Images were analysed using Image Pro-Plus software similar to CD45 staining.

4.2.2 **Magnetic resonance imaging (MRI)**

4.2.2.1 In-vivo injection of microparticles of iron oxide (MPIO)

Magnetic resonance imaging of antibody-conjugated microparticles is a novel imaging technique for the detection of vessel inflammation developed by Professor Choudhury at Oxford (Akhtar et al., 2010; McAteer et al., 2008; McAteer et al., 2004; Schneider et al., 2004) . VCAM-1/p-selectin or IgG conjugated MPIOs were prepared by Dr McAteer. Mice were terminally anaesthetised with isoflurane and the chest cavity opened to expose the heart while still-beating. Using an insulin syringe, 200µl of diluted VCAM-1 or IgG

MPIO (1:12.5 dilution), were injected into the left ventricle and allowed to circulate for 10 min. Blood was then collected from the right ventricle and the mouse was perfused with 10ml of PBS followed by 10ml of 4% PFA. The whole aorta down to the femoral bifurcation was harvested on the backbone and transferred for fixation in 4% PFA or frozen in OCT for immunofluorescent staining as described previously.

PFA fixed aorta was then either embedded in paraffin for histology as described previously or transferred to glass tubes for MRI scan.

4.2.2.2 Magnetic resonance imaging (MRI) – Low resolution

Aortas were dissected and placed onto a custom made rack (Figure 4.4). This was embedded in the glass tube with 20ml of 2.5% of high specification agarose (Fisher, UK). 2 ml of 4% PFA with 1:250 gadolinium was added to the tube followed by 50ml of 2.5% high specification agarose enriched with 1:250 dilution of gadolinium. The gel was allowed to set overnight before scanning by MRI, performed by Dr J. Schneider, and images were analysed using Image Pro-Plus software.

Figure 4.4

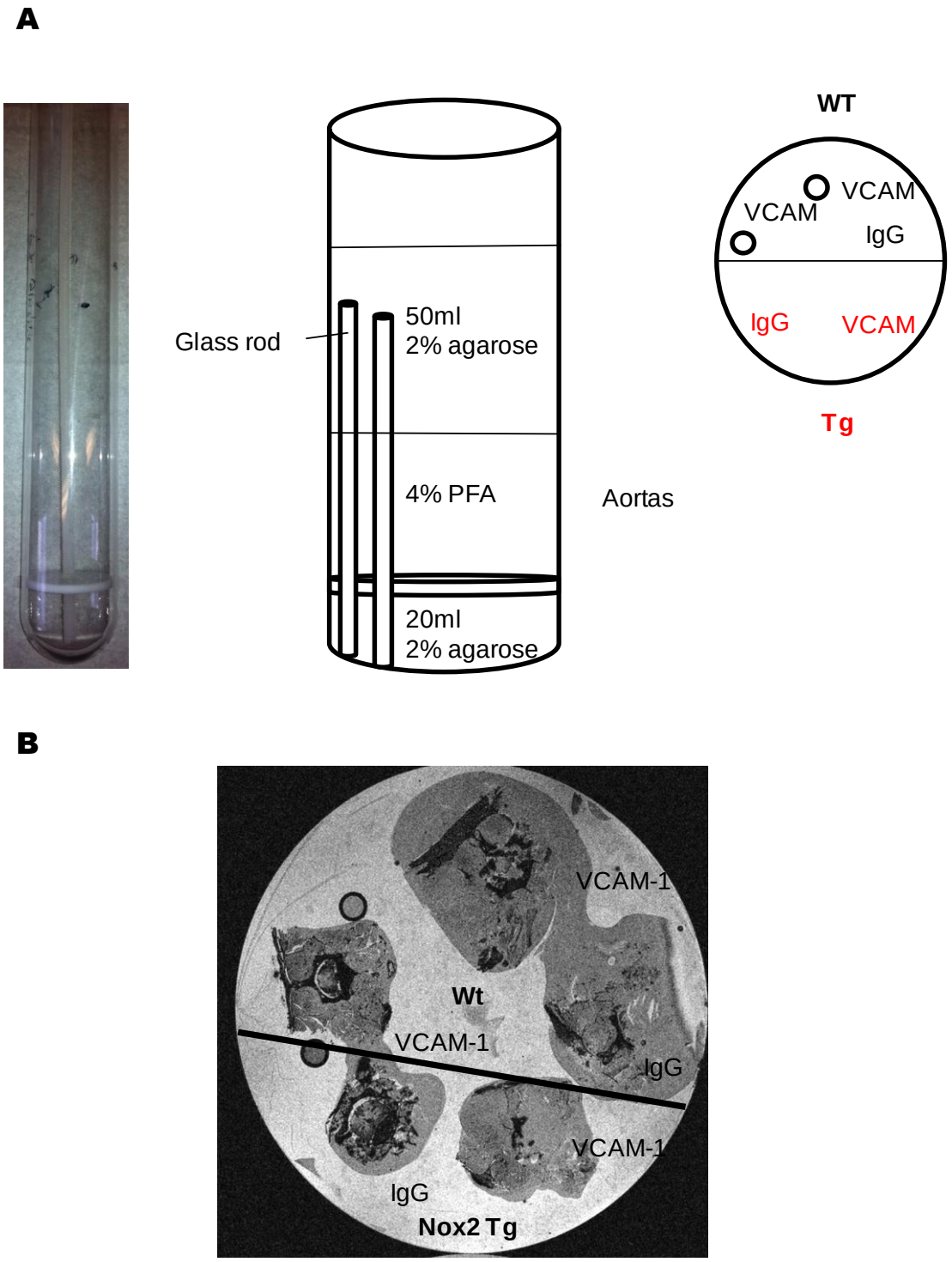


Figure 4.4 Large tube for MRI scans of aorta

(A) Representative photograph of the large tube and setup for MRI of aortas. 2 glass rods were inserted for orientation. Maximum of 5 aortas were scanned at any one time. **(B)** Example MRI image of aortas scanned in the large glass tube.

4.2.2.3 MRI aorta – High resolution

To increase the MRI resolution, aortas on backbone were embedded individually in small glass tubes with 2 ml of 2.5% High specification agarose. Once the agarose was set, 2ml of 4% PFA enriched with 1:250 gadolinium was added followed by 5 ml of 2.5% agarose with 1:250 gadolinium. The aortas were then scanned by overnight by MRI. Amira (Visage Imaging, USA) was used to reconstruct the aorta in 3D images.

4.3 Results

4.3.1 Increased endothelial VCAM-1 expression in the early stage of the development of Ang II-induced aorta dissection

4.3.1.1 VCAM-1 expression was elevated after 3 days of Ang II infusion in Nox2 Tg aortas with further increases at 5 days

Ang II is known to induce Nox2-dependent vascular oxidative stress and inflammation which are associated with the development of aortic dissection. I hypothesized that endothelial Nox2 over-expression may therefore potentiate the pro-inflammatory effects of Ang II. To test this hypothesis, I examined for endothelial expression of VCAM-1, a marker of endothelial cell activation in aorta from wild-type and Nox2 Tg mice following treatment with either saline or Ang II for 3 or 5 days. Supra-renal aortas were harvested at the end of the experiments, embedded in OCT, frozen on dry ice and serially sectioned for the detection of VCAM-1 expression by immunohistochemistry. The nuclei were labelled with DAPI (blue colour) to visualise the cells. There was a significant 3 fold greater increase in VCAM-1 expression (red fluorescence) in the aortas of Nox2-Tg mice after 3 days of Ang II treatment compared to wild-type and saline controls (Figure 4.5 A and B, $p<0.05$). After 5 days of Ang II treatment, the expression of VCAM-1 was increased in both the wild-type and Nox2 Tg aortas but the difference remained at 3 fold ($p<0.05$).

Figure 4.5

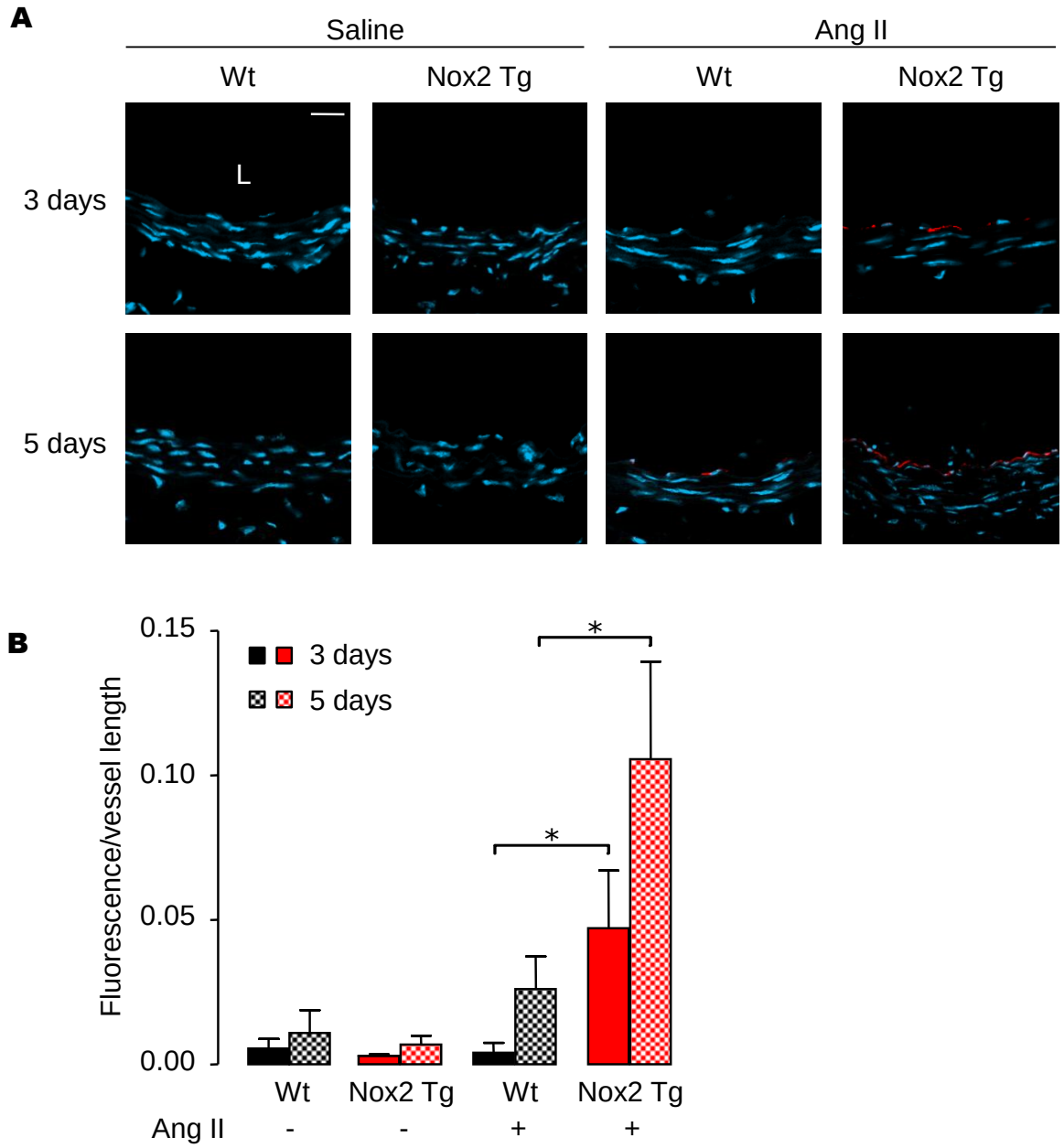


Figure 4.5 Increased VCAM-1 expression in Nox2 Tg aorta after only 3 days of Ang II infusion

20-24 weeks old mice were infused with either saline or Ang II (1mg/kg/day) for 3 or 5 days. Supra-renal aortas were harvested and frozen in OCT. 10µm cryosections were stained for VCAM-1 expression. **(A)** Representative images presented at x40 magnification with lumen facing upwards. Blue fluorescence: DAPI; Red fluorescence: VCAM-1. White bar - 40µm. L – lumen. **(B)** Fluorescence intensity was quantified using ImagePro Plus and presented as fluorescence over the length of vessel. Data are expressed as mean±SEM. *$p<0.05$; n=6-8 per group.

4.3.1.2 MRI of aorta injected with anti-VCAM-1 conjugated MPIO revealed greater VCAM-1 expression around the site of dissection

Wild-type and Nox2 Tg mice were infused with Ang II for 5 days and anti-VCAM-1 or IgG conjugated MPIOs were injected through the left ventricle as described in methods. Aortas were embedded in paraffin, sectioned and stained with H & E stain and examined for the presence of MPIO (Figure 4.6). There was greater MPIO (yellow beads) binding in Nox2 Tg aortas injected with anti-VCAM-1 MPIOs compared to the wild-type. Neither the wild-type nor Nox2 Tg aortas showed significant binding of IgG control MPIOs. To confirm that the anti-VCAM-1 conjugated MPIO binds to areas of VCAM-1 expression, a further cohort of Nox2 Tg mice were infused with Ang II for 5 days and injected with anti-VCAM-1 conjugated MPIO. The aorta was frozen in OCT, serially sectioned, stained for VCAM-1 expression and examined under Zeiss confocal fluorescent microscope. MPIOs are auto-fluorescent at a wavelength of 488nm and visualised as green fluorescence. VCAM-1 expression was visualised by red fluorescence.

MPIOs were observed to bind to areas where VCAM-1 was expressed as indicated by the arrows in Figure 4.7. IgG control MPIOs was not observed to bind to aortic areas of VCAM-1 expression.

Figure 4.6

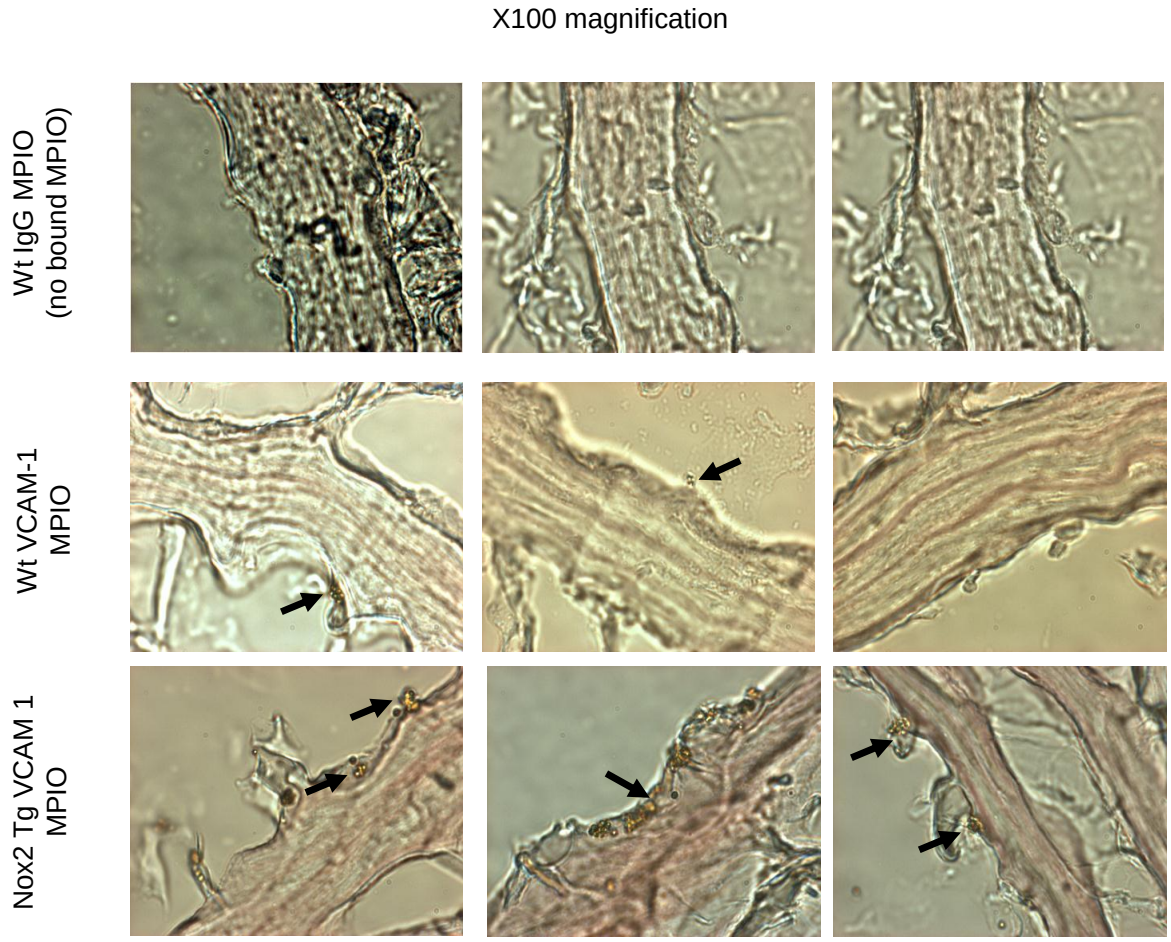


Figure 4.6 Increased anti-VCAM-1 MPIO in Nox2 Tg aorta

20-24 weeks-old Wt and Nox2 Tg littermates were infused with Ang II for 5 days. Anti-VCAM-1 or IgG conjugated MPIO were injected through the left ventricle. Aortas were harvested, embedded in paraffin, sectioned to 7µm and stained with H&E to examine for MPIO binding. Representative images were taken at x100 magnification. Top row: Wt aorta injected with anti-IgG MPIO; Middle row: Wt aorta injected with anti-VCAM-1 MPIO; Bottom row: Nox2 Tg aorta injected with anti-VCAM-1 MPIO. Black arrows: bound MPIO.

Figure 4.7

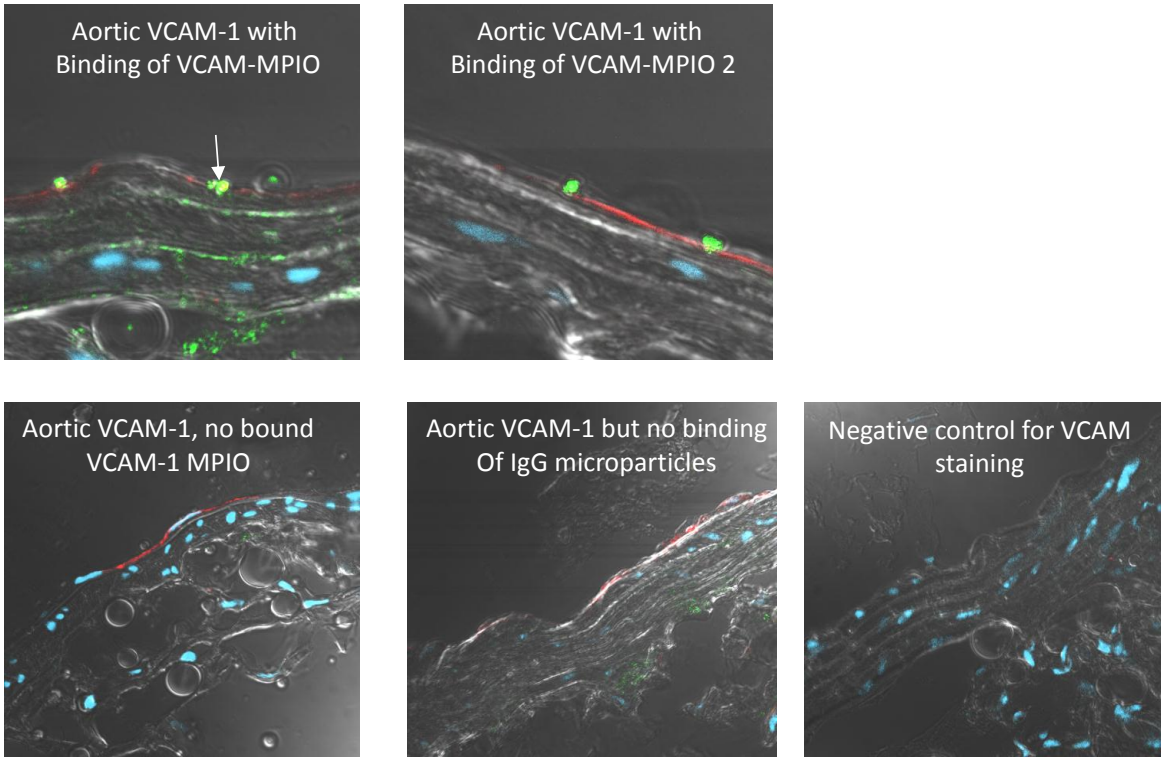


Figure 4.7 Anti-VCAM-1 MPIOs binds to aortic areas of VCAM-1 expression

Nox2 Tg mice were infused with Ang II for 5 days and injected with either anti-VCAM-1 or IgG conjugated MPIOs. Aortas were harvested, frozen in OCT, sectioned to 10µm, and stained for VCAM-1. Representative images taken at x40 magnification with Zeiss confocal fluorescent microscope. VCAM-1: red; MPIO: green round fluorescence and white arrow; nuclei: blue (DAPI).

Following confirmation of the specificity of MPIOs, the next trial cohort of wild-type and Nox2 Tg mice (n=3 Wt, n=2 Nox2 Tg) were infused with Ang II for 5 days and 50% of Nox2 Tg mice were observed to have developed aortic dissection. Aortas were embedded in large glass tube as described in the method and scanned overnight with MRI. Following MRI, aortas were embedded in paraffin, serially sectioned and stained with H & E. MPIO binding was examined under the microscope and manually counted. Corresponding MRI images at the same anatomical position as the sections were identified using the left renal artery as a marker to check the correlation between MPIO binding and MRI signal (Figure 4.8). There were greater VCAM-1 MPIO binding in dissected Nox2 Tg aortas compared to non-dissected Nox2 Tg and wild-type aortas. MPIOs were also observed to accumulate in the haematoma suggesting trafficking across the rupture site and binding to cells expressing p-selectin such as platelets. The lumen of the dissected aorta was severely compressed as previously observed with histology in Chapter 1. Although the MPIO binding to VCAM-1 was apparent when compared to the negative control, aortas injected with IgG MPIOs, the MPIO signal on MRI was poor due to the low resolution and it was difficult to distinguish small differences in MPIO binding based on MRI e.g. between 9 and 20 MPIOs (Figure 4.10). High resolution MRI was therefore needed.

Figure 4.8

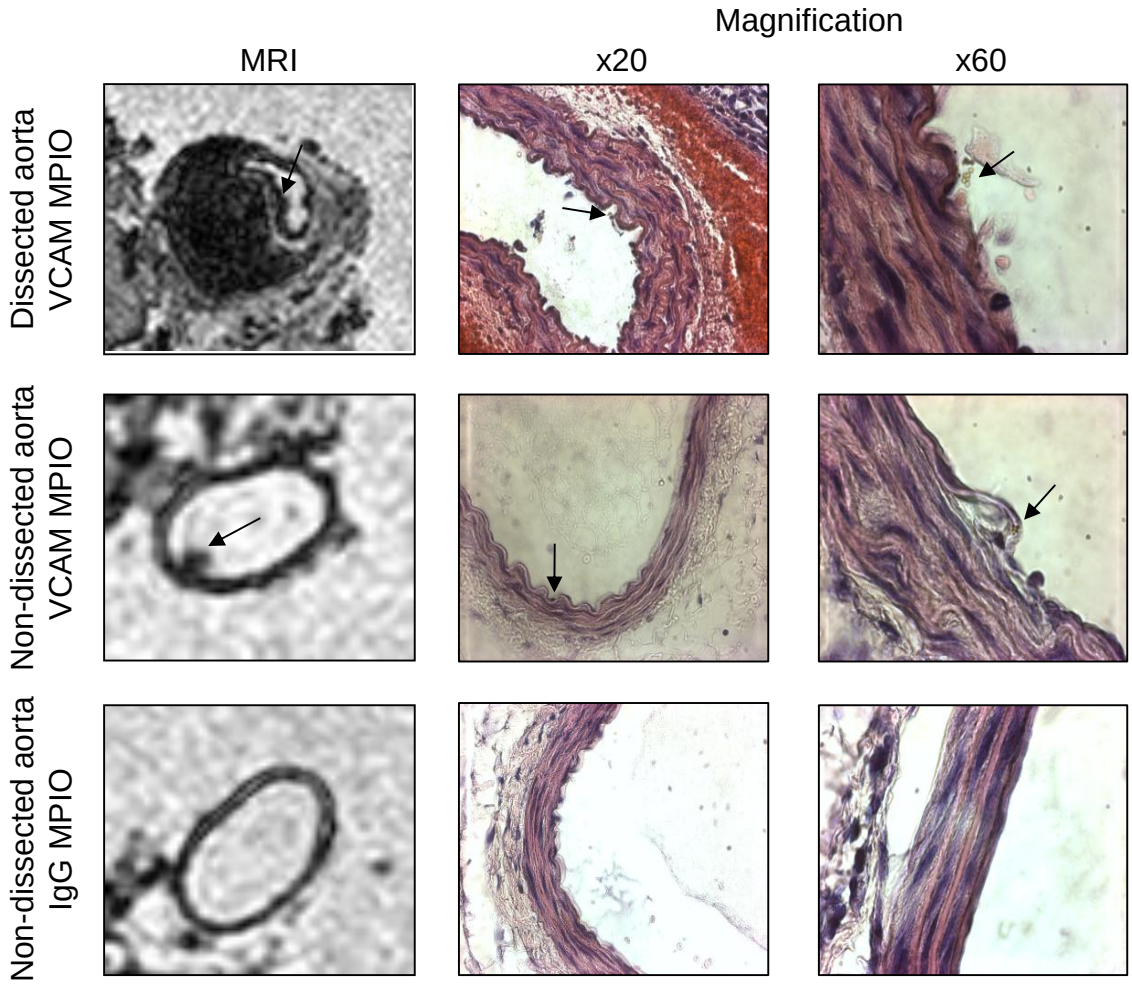
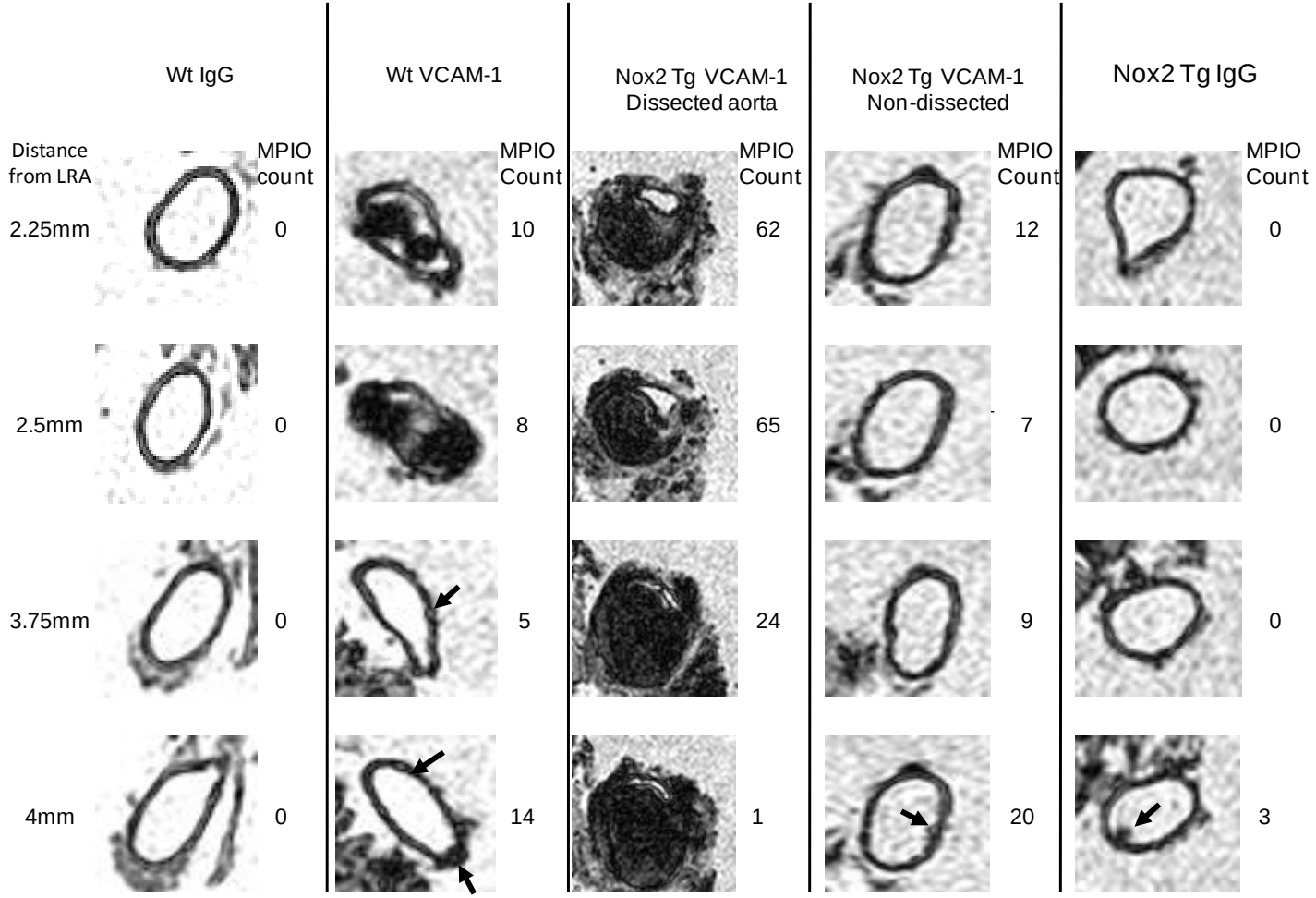


Figure 4.8 Increased MPIO binding in dissected aorta compared to non-dissected aorta and IgG control

Wt and Nox2 Tg mice were infused with Ang II for 5 days. Aortas were embedded in a large glass tube and scanned overnight with MRI. Following MRI, aortas were embedded in paraffin, sectioned (7µm) and stained with H&E. Representative MR cross-sections of Nox2 Tg aortas with corresponding histology images taken at the same anatomical positions. Top row: dissected aorta injected with anti-VCAM-1 MPIO; Middle row: non-dissected aorta injected with anti-VCAM-1 MPIO; Bottom row: non-dissected aorta injected with IgG MPIO. Black arrow – MPIO.

Figure 4.9



MPIO count were obtained from corresponding H&E sections, not from MR images.

Figure 4.9 MPIO signal is weak when scanned in large glass tube

Aortic sections from Wt and Nox2 Tg infused with Ang II for 5 days at set distances from the left renal artery (2.25mm, 2.5mm, 3.75 and 4mm) were stained with H&E, examined under the microscope and MPIOs bound to the aortic wall were counted manually (MPIO count). Corresponding MR images at the same anatomical positions were identified using left renal artery as a landmark. Left 2 columns: MR cross-sections of Wt aortas injected with either IgG or anti-VCAM-1 conjugated MPIO; Right 3 columns: MR cross-sections of Nox2 Tg aortas injected with either IgG or anti-VCAM-1 conjugated MPIO. Black arrow – shadow cast by MPIO.

For high resolution MRI, aortas were harvested following 5 days of Ang II treatment, injected with either IgG or VCAM-1/p-selectin conjugated microparticles and embedded in small glass tubes as described in the methods and scanned overnight. MRI cross-sections of the aorta were analysed and reconstructed in 3D using Amira (Figure 4.10, aorta in pink; surrounding haematoma in red; MPIO in green; dissection point in yellow dot and indicated by white arrow). There was greater MPIO binding and VCAM-1 expression in the dissected aorta around the site of dissection (yellow dot and white arrow). Interestingly, even in the Nox2 Tg aorta which did not dissect, there was an increase in VCAM-1 expression suggesting that VCAM-1 upregulation was not a consequence of dissection but rather a preceding event (Figure 4.11 A). There was very little microparticle binding in the aorta injected with IgG conjugated control MPIO (Figure 4.11 B). Together, these data indicated that endothelial activation was an early event of Ang II infusion in Nox2-Tg aortas and VCAM-1 expression was greatest in the area where the aortic dissection occurs.

Figure 4.10

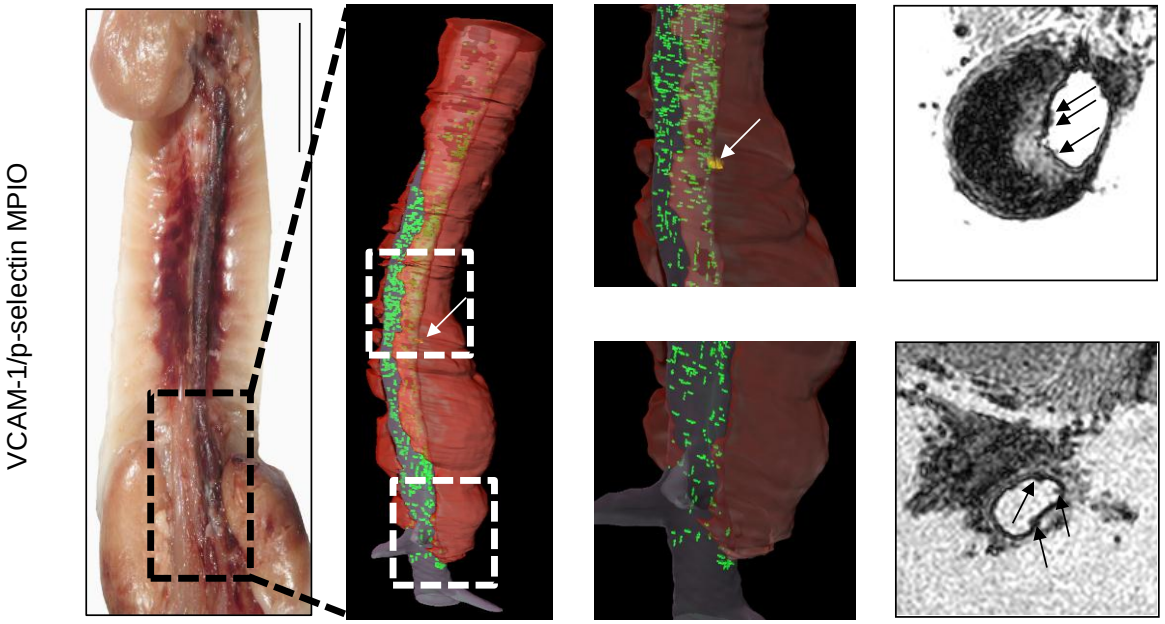


Figure 4.10 Increased VCAM-1 expression at site of dissection in Nox2 Tg supra-renal aorta.

20-24 weeks-old Nox2 Tg mice were infused with Ang II for 5 days and injected with either anti-VCAM-1 or IgG conjugated MPIO. Aorta were harvested on backbone, embedded in small glass tubes and scanned overnight. First panel – photograph of dissected aorta injected with VCAM-1 conjugated MPIO. Black bar – 1cm. Black dotted box – Area of MR Scan. Pink- aortic vessel; red – surrounding haematoma; green – MPIO; white arrow and yellow marker – point of dissection. White dotted box – area of magnification shown in the next panels. Right panels – original MR images. Black arrow – MPIO.

Figure 4.11

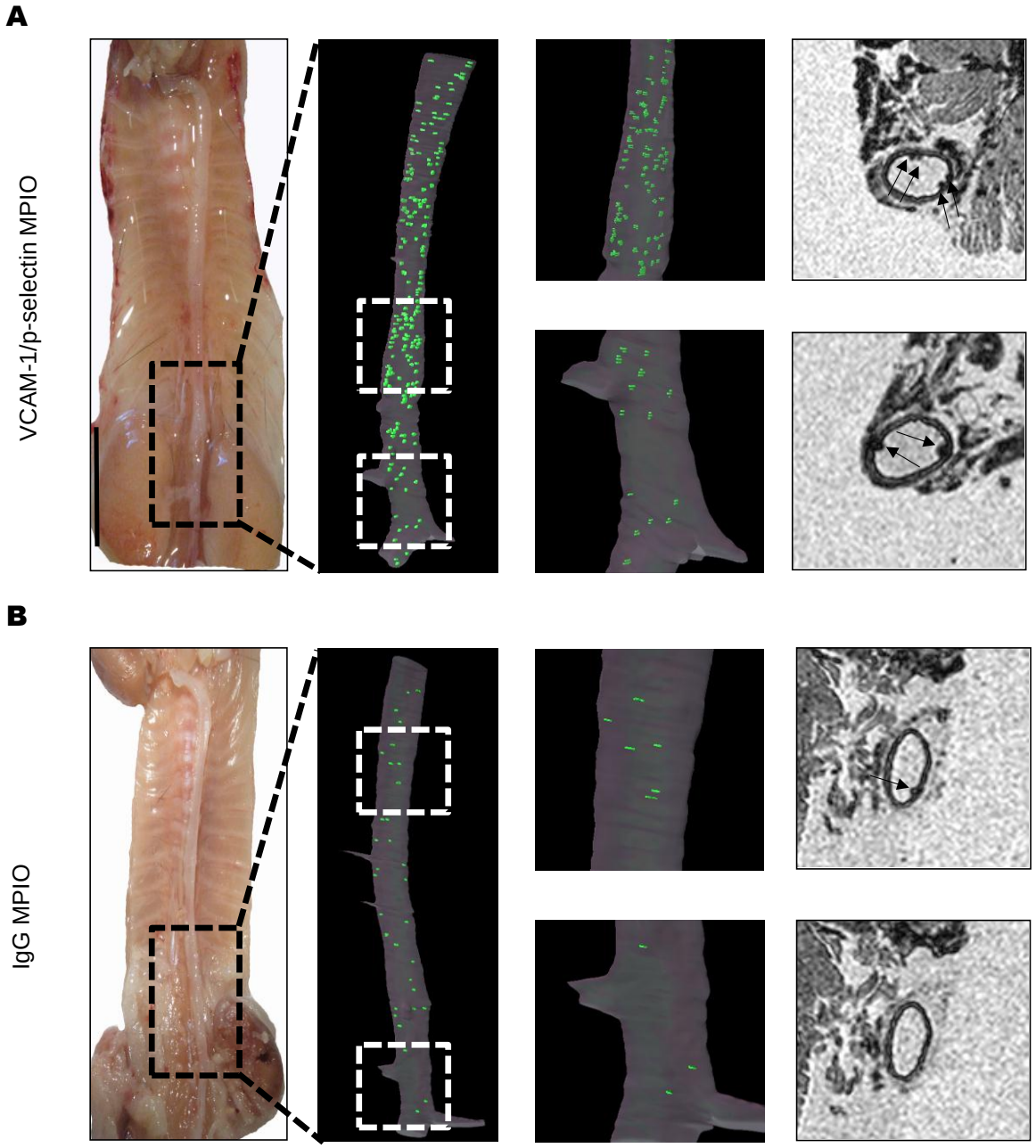


Figure 4.11 Increased VCAM-1 expression and no binding of IgG MPIO in non-dissected Nox2 Tg supra-renal aorta

Non-dissected aorta injected with **(A)** VCAM-1/p-selectin or **(B)** IgG conjugated MPIO. Black bar – 1cm. Black dotted box – Area of MR Scan. Pink- aortic vessel; Green – MPIOs; white dotted box – area of magnification shown in the next panels. Right panels – original MR images. Black arrow – MPIO.

4.3.2 **Increased CD45$^+$ inflammatory cell recruitment in Nox2 Tg aortas as compared to wild-type aortas after 5 days of Ang II infusion**

4.3.2.1 CD45$^+$ cells by immunofluorescence

Previous studies have shown an important role for VCAM-1 in vascular inflammation (Cook-Mills et al., 2011). To investigate the effect of the increased VCAM-1 expression in Nox2-Tg aortas on inflammatory cell recruitment I examined the number of CD45$^+$ leukocytes after 3 and 5 days of saline or Ang II infusion using immunofluorescence and confocal microscopy. I found CD45$^+$ leukocytes (red fluorescence) recruitment was significantly increased in Nox2-Tg aortas after 5 days of Ang II treatment ($p<0.05$) compared to wild-type and saline treated controls (Figure 4.12 A, B). In contrast to VCAM-1 expression there was no difference in CD45$^+$ cell recruitment after 3 days of Ang II infusion (Figure 4.13 A, B) suggesting leukocyte recruitment occurred after endothelial VCAM-1 expression.

Figure 4.12

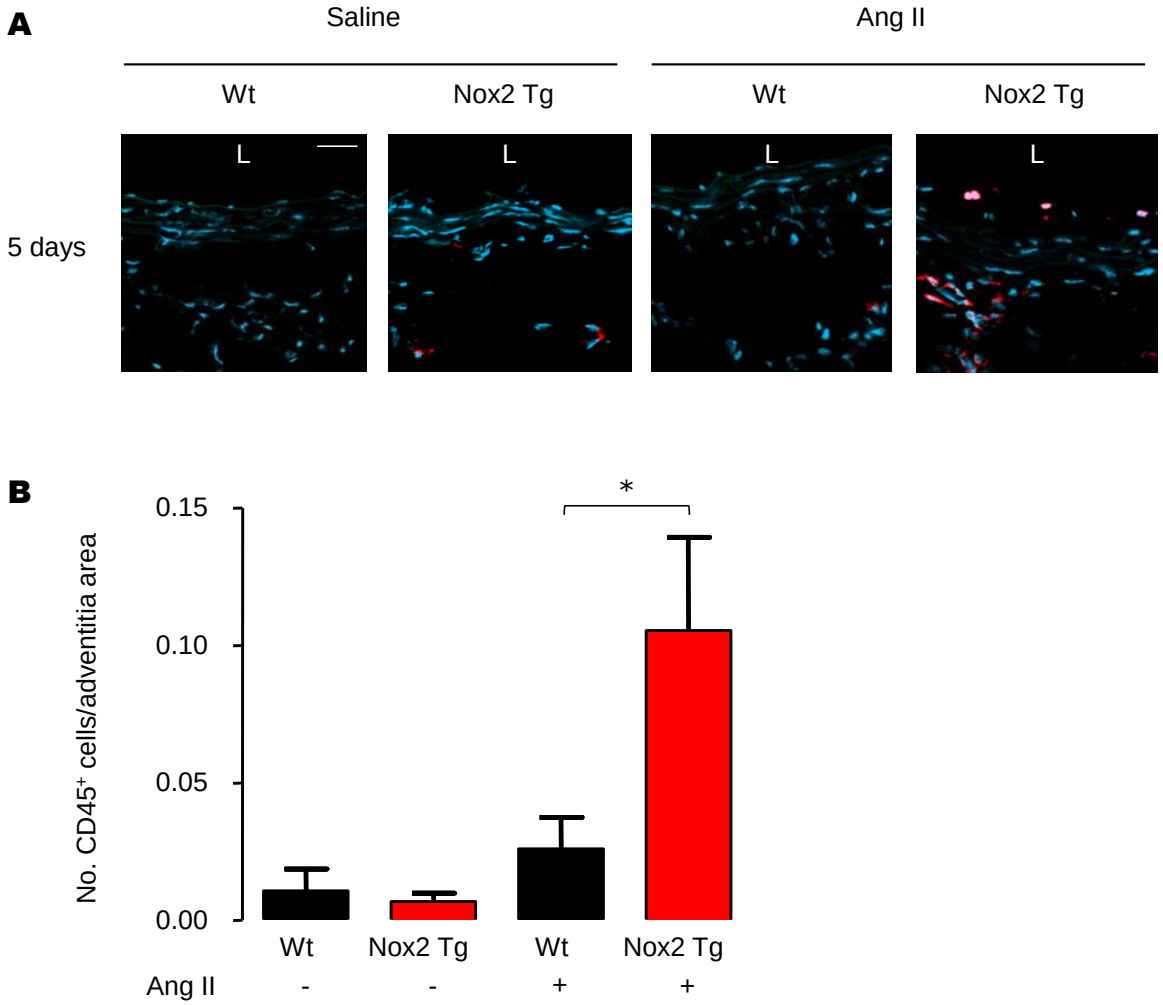


Figure 4.12 Increased CD45$^+$ cell recruitment in Nox2 Tg aorta after 5 days of Ang II infusion.

20-24 weeks-old Wt and Nox2 Tg mice were infused with saline or Ang II for 5 days. Supra-renal Aortas were harvested and frozen in OCT. 10µm cryosections were stained for CD45 expression. White bar – 40 µM. **(A)** Representative images presented at x40 magnification. Blue fluorescence: DAPI; Red fluorescence: CD45. **(B)** CD45$^+$ cell number presented as number of cells over adventitial area. Data are expressed as mean±SEM. *p<0.05, n=6-8 per group.

Figure 4.13

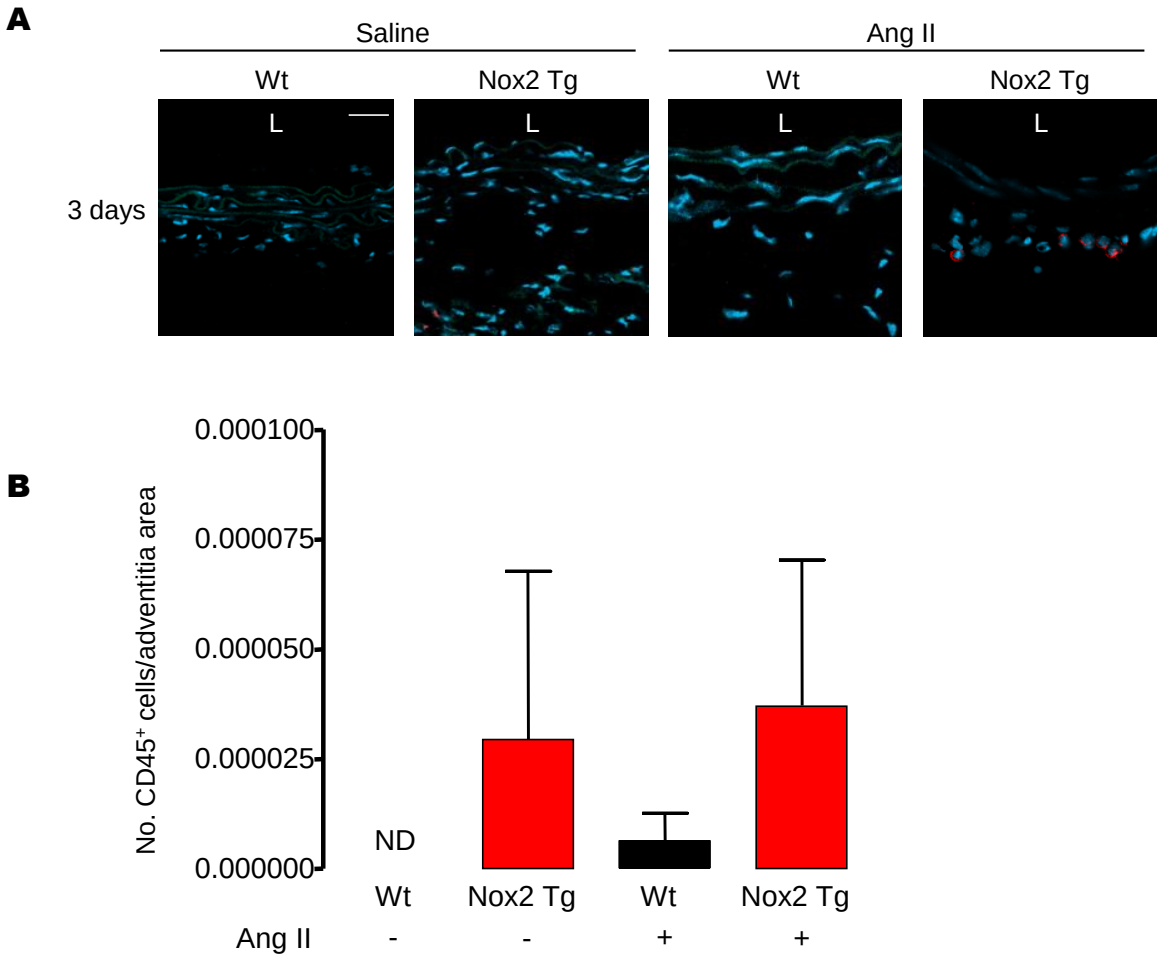


Figure 4.13 No difference in CD45$^+$ cells after 3 days of Ang II infusion between Wt and Nox2 Tg

Wt and Nox2 Tg mice were infused with saline or Ang II for 3 days. **(A)** Representative images presented at x40 magnification. White bar – 40 µm. Blue fluorescence: DAPI; Red fluorescence: CD45. **(B)** CD45$^+$ cell number presented as number cells over adventitial area. Data are expressed as mean±SEM, n=6-8 per group.

4.3.2.2 CD45$^+$ cell quantification by flow cytometric analysis of cells from digested aorta

In order to further examine CD45$^+$ cell recruitment to the aorta, cells were isolated by enzymatic digestion of aortas after 5 days of Ang II infusion and CD45$^+$ cells quantified using flow cytometry (Tieu et al., 2009). The CD45$^+$ cell population was gated using the isotype control (Figure 4.14 A, B). There was a significant increase in CD45$^+$ cells in Nox2-Tg aortas ($2.49x10^7 \pm 1.5x10^7$) following Ang II treatment compared to wild-type controls ($3.9x10^4 \pm 8x10^3$, $p<0.01$). There was no difference in CD45$^+$ cell numbers at baseline between wild-type ($1.8x10^4 \pm 2x10^3$) and Nox2-Tg ($2.3x10^4 \pm 7x10^3$) aortas.

CD45 is a pan-leukocyte marker expressed on all leukocytes including myeloid cells and lymphocytes. In order to ascertain the type of CD45$^+$ cells recruited to the aorta, additional cell markers established in other studies such as CD14 and CD11b were used (Tieu et al., 2009). No significant increase in the number of CD14$^+$/CD11b$^+$ macrophages or leukocytes expressing CCR2 receptor was observed in the aortic cell suspension following Ang II stimulation. No difference was observed either in the proportion of CCR2$^+$ cells in contrast to the study by Tieu et al. where they found a large proportion of recruited aortic inflammatory cells in response to Ang II to be CD14$^+$/CD11b$^+$ macrophages with high expression of CCR2 receptor (Figure 4.15 A, B; Figure 4.16).

Figure 4.14

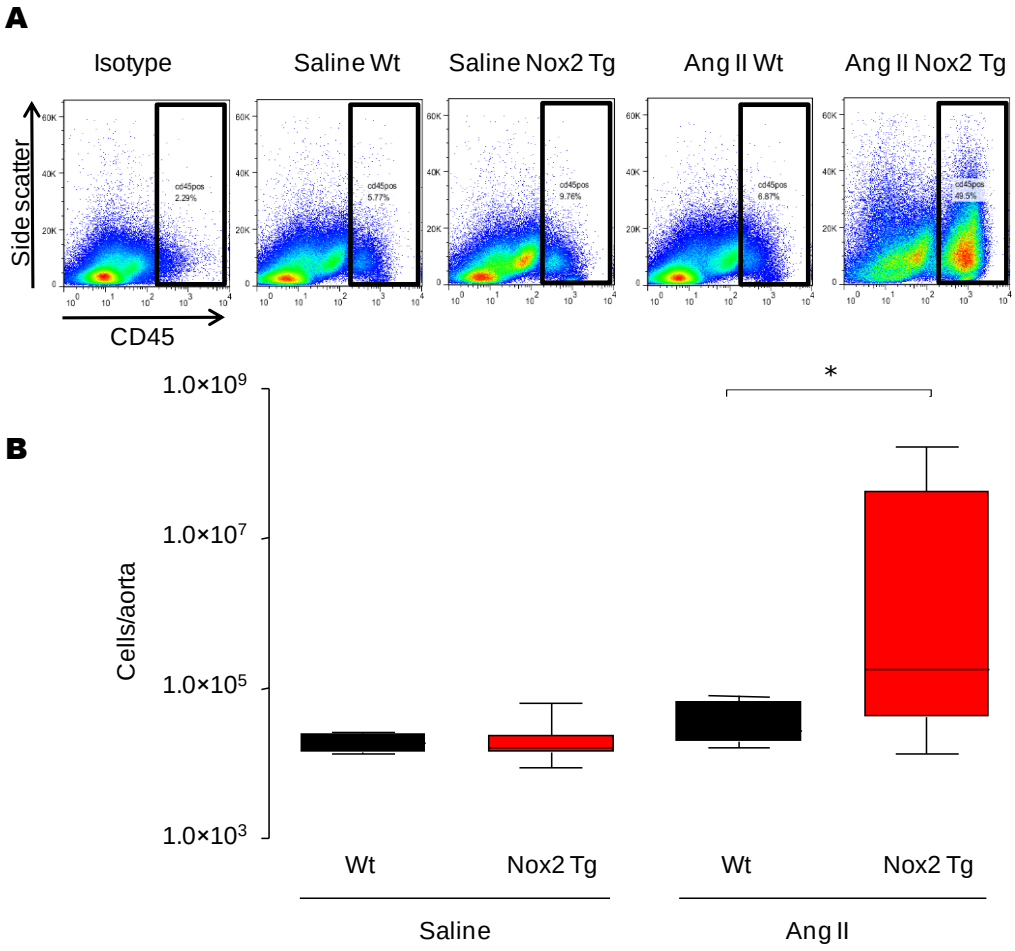


Figure 4.14 Greater CD45$^+$ inflammatory cell recruitment in Nox2 Tg explanted aorta after Ang II infusion for 5 days

20-24 weeks old Wt and Nox2 Tg mice were infused with Ang II for 5 days. Aorta from arch to the renal arteries were harvested and digested into cell suspension. Cells suspension was probed with CD45 antibody and counted by flow cytometry. **(A)** CD45$^+$ cell population was gated using CD45 isotype control. Black box indicates CD45$^+$ cell population. **(B)** Data presented as cells per aorta on a logarithmic scale. Data are expressed as median±interquartile range. *$p<0.05$, n=4 for saline, n=7-8 for other groups.

Figure 4.15

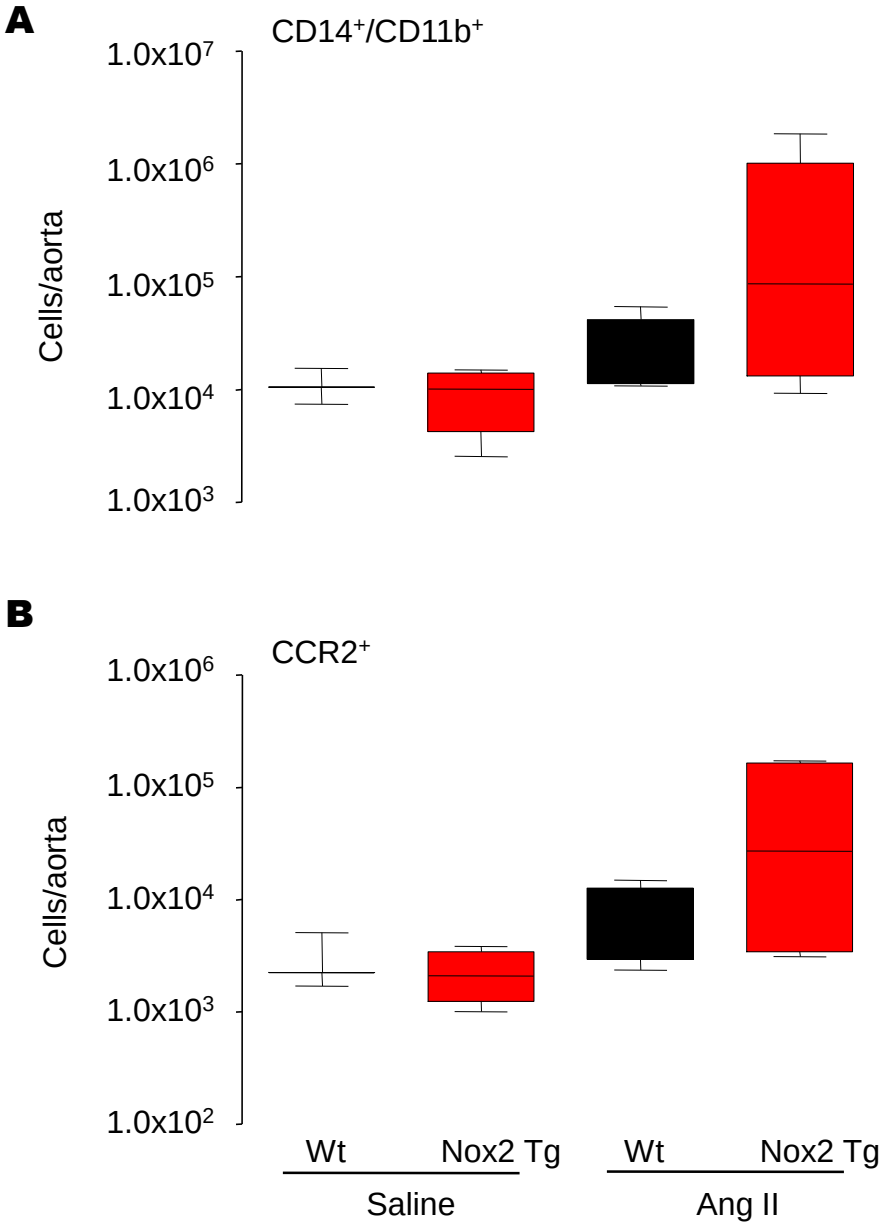


Figure 4.15 No significant increase in $CD14^+/CD11b^+$ macrophages or cells expressing CCR2 receptor

Cell suspension from digested Wt and Nox2 Tg aortas were probed with CD14, CD16 and CCR2 antibodies and counted by flow cytometry. n=4 for saline, n=7-8 for other groups. **(A)** Number of $CD14^+/CD11b^+$ cells presented on logarithmic scale. Data are expressed as median±interquartile range. **(B)** Number of $CCR2^+$ cells presented on logarithmic scale. Data are expressed as median±interquartile range.

Figure 4.16

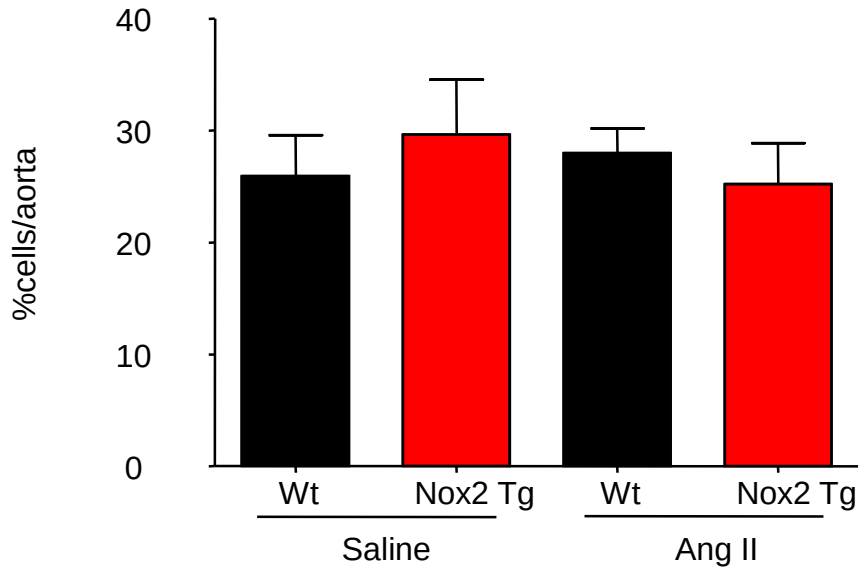


Figure 4.16 No significant increase in % CCR2$^+$ cells

Cells prepared as Figure 4.17 and probed with CCR2 antibody. Percentage of CCR2$^+$ cells expressed as mean±SEM.

4.3.3 **Increased metalloproteinase activity in Nox2 Tg aortas after 5 days of Ang II infusion**

Metalloproteinases (MMP) play a key role in vessel remodelling and aortic dissection. I therefore examined MMP activity using in-situ zymography. Frozen sections were incubated with fluorescently labelled gelatin which produced green fluorescence on cleavage by MMPs. MMP activity was found to be significantly increased in Nox2-Tg aortas after 5 days of Ang II infusion compared to wild-type controls (Figure 4.17 A and B, $p<0.05$,) although a small difference was observed even at day 3 (Figure 4.18 A, B). MMP activity was predominately localised to the adventitia where the $CD45^+$ inflammatory cells were present but there was also activity in the aortic media, suggesting contribution of MMPs from both recruited inflammatory cells and VSMCs. No MMP activity was observed aortas from saline-treated animals. Specificity was confirmed using the MMP inhibitor, phenanthroline (1mM) which completely inhibited MMP activity.

Figure 4.17

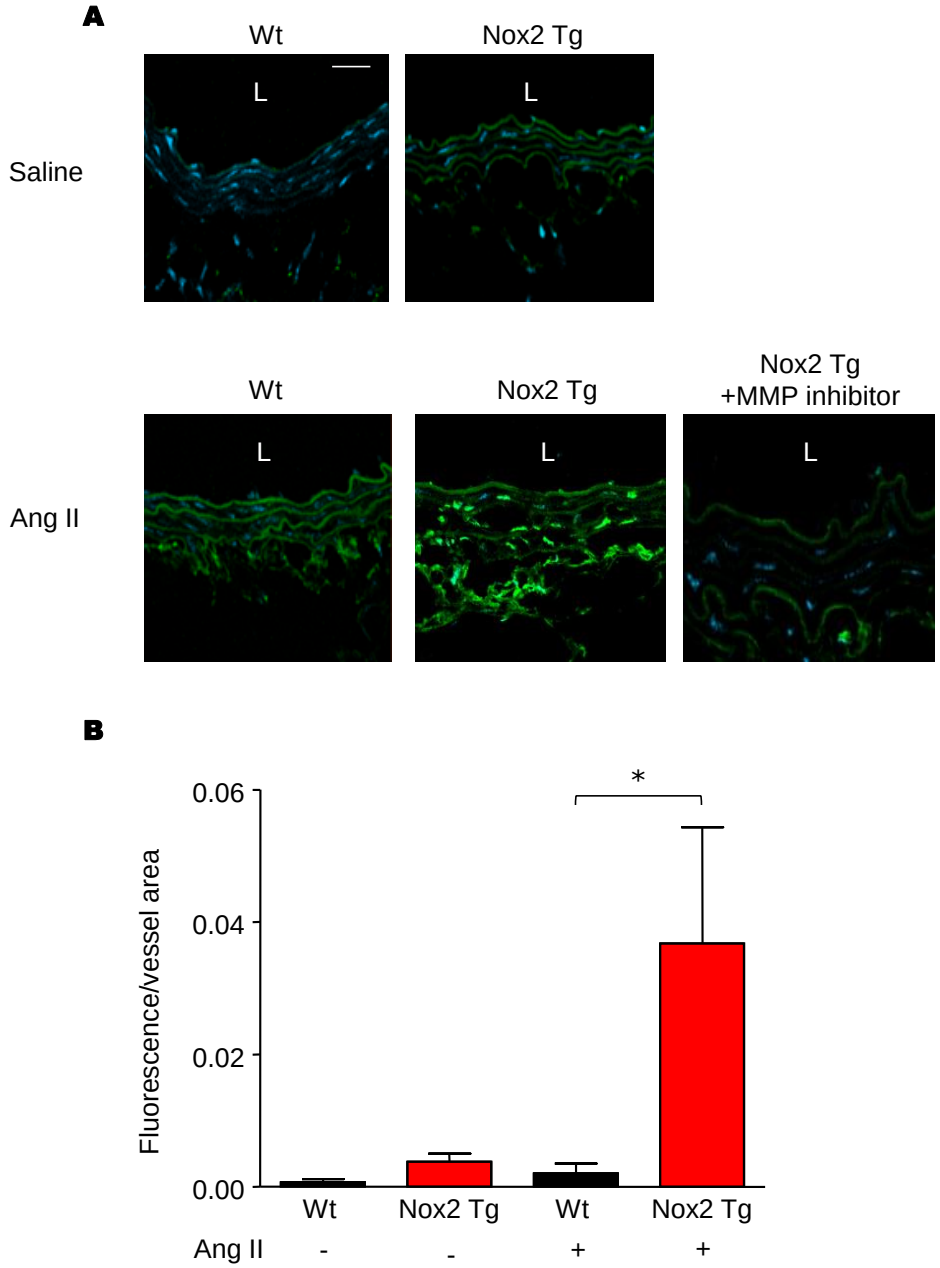


Figure 4.17 Greater MMP activity in Nox2 Tg aorta after 5 days of Ang II infusion compared to Wt

20-24 weeks old Wt and Nox2 Tg mice were infused with Ang II for 5 days. Supra-renal aortas were frozen in OCT and sectioned at 10µm/slice. In-situ zymography was used to detect MMP activity. **(A)** Representative images presented at x40 magnification. White bar – 40 µm. Blue: DAPI; Strong Green: MMP activity. Phenanthroline (1mM) was used as the MMP inhibitor. L- lumen **(B)** Fluorescence presented as fluorescence intensity over vessel area. Data are expressed as mean±SEM. *$p<0.05$, n = 6-8 per group.

Figure 4.18

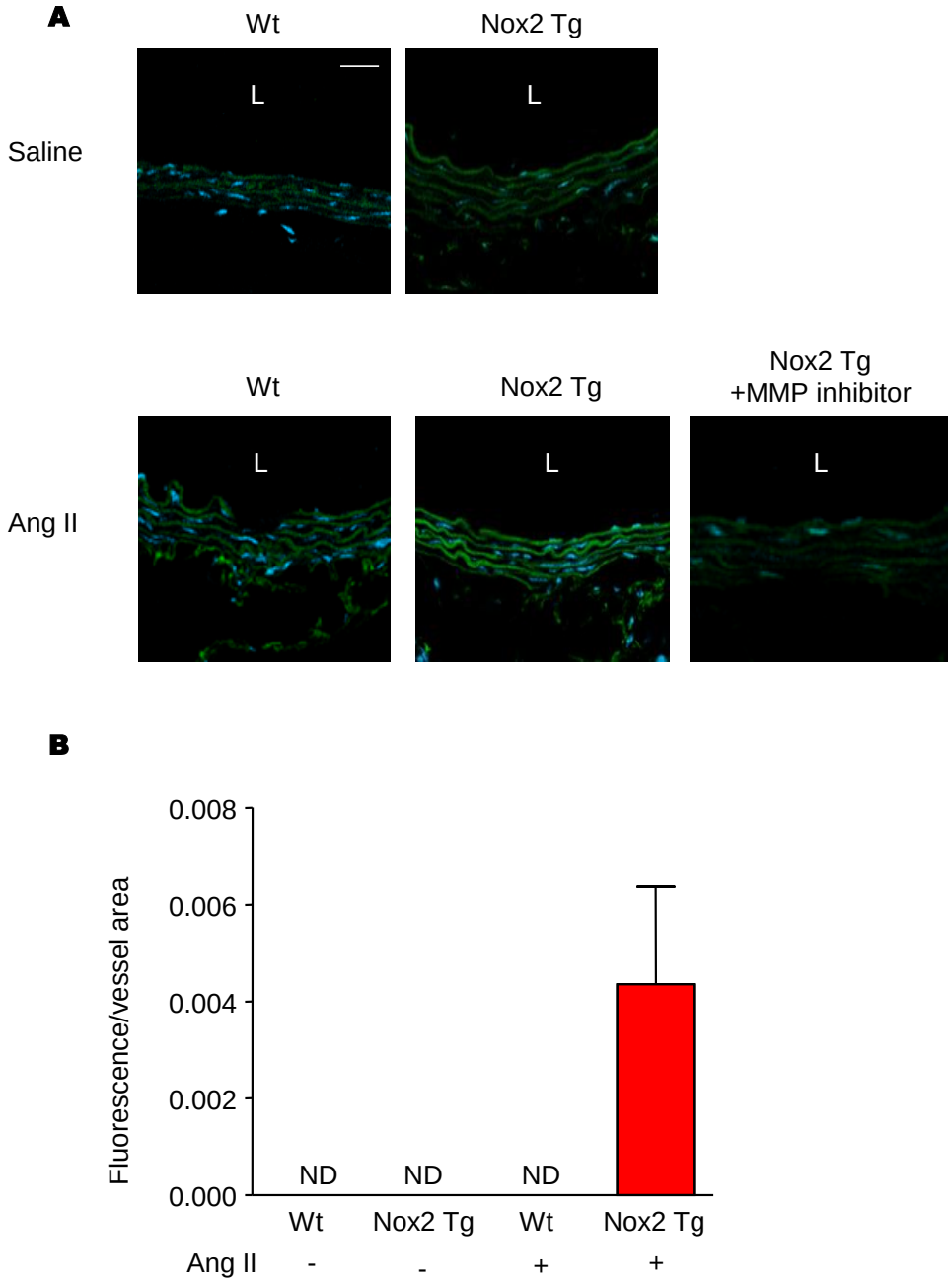


Figure 4.18 Small increases in MMP activity in Nox2 Tg aortas after 3 days of Ang II infusion

20-24 weeks old mice were infused with Ang II for 3 days. **(A)** Representative images presented at x40 magnification. White bar – 40 µm. Blue: DAPI; Strong Green: MMP activity. Phenanthroline (1mM) was used as the MMP inhibitor. L- lumen **(B)** Fluorescence presented as fluorescence intensity over vessel area. ND – not detected. Data are expressed as mean±SEM, n = 6-8 per group.

4.4 Discussion

In this chapter, I investigated the effects of increased endothelial ROS on the potentiation of Ang II induced vascular inflammation. The key findings were

- Greater upregulation of VCAM-1 expression in Nox2 Tg aortas compared to wild-type after 3 days of Ang II infusion.
- Greatest VCAM-1 expression at the site of dissection.
- Greater $CD45^+$ inflammatory cell recruitment in Nox2 Tg aorta after 5 but not 3 days of Ang II infusion compared to wild-type
- Increased matrix metalloproteinase (MMP) activity in Nox2 Tg aortas after 5 days of Ang II infusion.

Vascular inflammation is a critical step in the development of aortic dissection. Leukocyte adhesion is primarily mediated by endothelial surface expression of adhesion molecules e.g. VCAM-1 (Cook-Mills et al., 2011). In order to investigate the role of vascular inflammation in the initiation and development of aortic dissection in Nox2 Tg, the aorta had to be studied at a time point before the development of dissection. It has been established from previous imaging studies that Ang II induced aortic dissection occurred between day 5 and 6 (Klink et al., 2011; Saraff et al., 2003). Accordingly, VCAM-1 expression, CD45 recruitment and MMP activity in wild-type and Nox2 Tg mice were studied after 3 and 5 days of Ang II infusion.

My results showed clearly that no macroscopic aortic changes or dissections were observed after 3 days of Ang II infusion. Endothelial VCAM-1 expression, however, was already significantly increased at day 3 of Ang II infusion in Nox2-Tg aortas compared to wild-type controls, indicating that Nox2 Tg endothelial cells were activated. Endothelial

VCAM-1 expression was increased after 5 days of Ang II infusion in both the wild-type and Nox2 Tg, but a 3 fold greater difference in Nox2 Tg was observed.

On further analysis, it was interesting to find that the upregulation of VCAM-1 expression in Nox2 Tg aortas was similar to the rate of dissection: around 50% had significant increases in VCAM-1 expression whilst the other 50% had little increase. It raised the possibility that if a longer course of Ang II treatment was given, the 50% of Nox2 Tg aortas with increased VCAM-1 expression might develop aortic dissection. This hypothesis was supported by results from MRI of anti-VCAM-1 conjugated MPIOs which demonstrated an increase in the density of VCAM-1 expression around the dissection site in Nox2 Tg aortas. In non-dissected Nox2 Tg aortas, there was also increased MPIO binding and VCAM-1 expression, which provided further evidence that VCAM-1 expression was not a consequence of aortic dissection but a preceding event. In-vivo injections of anti-VCAM-1 conjugated MPIOs and serial MRI scans would be required to establish whether VCAM-1 expression predicted the occurrence of aortic dissection.

Ang II increases inflammatory cell recruitment through mechanisms including VCAM-1 upregulation, increased ROS and NFκB (Fleming et al., 2001). In Nox2 Tg aortas, increased VCAM-1 expression was followed by a significant increase in $CD45^+$ cell recruitment as measured by both immunohistochemistry and FACS analysis of digested aorta after 5 days of Ang II infusion. There was no significant difference in $CD45^+$ cells between wild-type and Nox2 Tg after 3 days of Ang II treatment. In contrast to the report by Tieu et al. (Tieu et al., 2009), I did not find a significant increase in $CD14^+/CD11b^+$ macrophages. There was a significant increase in $CD11b^+$ cells which suggested that neutrophils were the predominant inflammatory cells recruitment to the site of dissection. A neutrophil marker would be required to confirm this finding. One explanation for the apparent discrepancies could be the duration of Ang II treatment. In the study by Tieu et

al, the aortas were harvested after 6 days of Ang II treatment whereas in my study, the aortas were harvested after 3 or 5 days of Ang II treatment. Neutrophils are the first inflammatory cells to be recruited to sites of injury which is then followed by lymphocytes and macrophages (Nathan, 2006). It is possible therefore the difference between the studies was because the inflammatory cells were measured at different time points in the vascular inflammatory response to Ang II.

Interestingly, $CD45^+$ cells were mostly located in the adventitia suggesting that they were not recruited from the luminal side of the aorta but rather from the vasa vasorum. Vasa vasorum is a network of capillaries within the adventitia of large diameter vessels such as the aorta (Mulligan-Kehoe, 2010). There is increasing evidence for a role of the vasa vasorum in the development of aortic diseases (Zhang et al., 2009; Zhao et al., 2004), and several studies have suggested the recruitment of inflammatory cells was from vasa vasorum in the adventitia rather than from luminal side of the vessel through the intima (Maiellaro and Taylor, 2007). In the "outside-in" paradigm, chronic inflammatory signals stimulate the adventitial fibroblast to undergo phenotypic switch which results in increased inflammatory cytokine production, MMP activation and upregulation of vasa vasorum endothelial VCAM-1 and the recruitment of inflammatory cells (Okamoto et al., 2001),. This is important because it suggests adventitia as an active component in the development of vascular disease.

The significance of $CD45^+$ inflammatory cell recruitment to the Nox2 Tg aorta was demonstrated by the co-localised increase in matrix metalloproteinase (MMP) activity. MMPs are the effector enzymes that degrade the extracellular matrix in the connective tissue, leading to weakening of the vessel wall and the development of structural vessel disease such as aortic dissection and aneurysm formation (Raffetto and Khalil, 2008). The main MMPs that have been found to be upregulated in Ang II induced vascular disease are

MMP-2 and MMP-9 (Manning et al., 2003; Satoh et al., 2009). Inhibition of these MMPs through pharmacological (e.g. doxycycline) or genetic modifications attenuated the development of aortic disease in experimental mouse models (Longo et al., 2002; Manning et al., 2003; Pyo et al., 2000). In Nox2 Tg aortas, MMP activity was observed to be mainly in the adventitia and vessel media suggesting contribution from both adventitial inflammatory cells and VSMCs.

4.4.1 **Summary**

Together, the results in this chapter indicate that endothelial activation is an early event of Ang II induced aortic dissection, preceding inflammatory cell infiltration. Therefore, endothelial activation driven by Nox2-derived ROS production could be an initiating event in the development of Ang II-induced aortic dissection. This is a novel discovery adding to the conventional theory whereby VSMCs are presumed to be the main initiators of pathways leading to the development of aortic dissection in response to Ang II (Dimmeler and Zeiher, 2000; Gavazzi et al., 2007; McCormick et al., 2007; Satoh et al., 2009; Tieu et al., 2009).

Chapter 5:

Characterisation of wild-type and Nox2 Tg primary endothelial cells and VSMCs

Chapter 5. Characterisation of wild-type and Nox2 Tg primary endothelial cells and VSMCs

5.1 Introduction

In the previous chapters I demonstrated that an increase in endothelial ROS through the over-expression in Nox2 in Nox2 Tg mice lead to an increased incidence of aortic dissection, which was associated with increases in endothelial VCAM-1 expression, inflammatory cell recruitment from the adventitia and matrix metalloproteinase activity. Endothelial cells were therefore able to modulate the response of the whole aortic vessel to Ang II stimulation. There are two main potential mechanisms by which endothelial cells can achieve this: direct cell-to-cell interaction or via secreted paracrine factors. However, due to the existence of the elastic lamina and thickness of the aorta, the interaction between endothelial cells, VSMCs and the cells in the adventitia is more likely to be mediated by paracrine factors rather than direct cell-cell interaction. In order to determine precisely which mechanism is responsible for translating the changes in endothelial ROS to changes in the whole vessel, primary aortic cell types would have to be examined directly.

It is often unclear whether interventions in the in-vivo systems such as a transgene expressed in the animal tissues could be translated into in-vitro systems. Therefore, it was crucial to isolate the primary cells from transgenic mice and characterise these cells to make sure that they retained some of the same characteristics as what was observed in-vivo.

5.2 Hypothesis and aims

In order to test the hypothesis that isolated primary endothelial cells and VSMCs from Nox2 Tg and wild-type mice would retain some of the same characteristics as in-vivo I aim in this chapter:

- To develop methods for the isolation of primary endothelial cells and VSMCs.
- To characterise the primary cells in respect of:
    - Gene expressions of human Nox2 transgene, endogenous mouse Nox2 and Nox4.
    - Protein expressions of Nox2 and Nox4.
    - Production of reactive oxygen species (ROS).

5.3 Methods

Most of the methods used in this chapter have been described in Chapter 2. Only methods and reagents used specifically in the experiments for this chapter are described below.

5.3.1 **Isolation of primary endothelial cells**

Endothelial cell were isolated from the lungs of mice using CD31 (PECAM, endothelial cell marker) immunomagnetic bead selection. Animals were sacrificed by an overdose of inhaled isoflurane and lungs were harvested into ice-cold DMEM, finely minced and digested in DMEM containing 0.18 U/ml liberase TM (purified collagenase, Roche) and 0.1 mg/ml DNase I (Roche) for 60 minutes at 37°C with gentle agitation every 15 minutes. The remaining visible tissue pieces were sheared by trituration through a 5 ml pipette, passed through a 100 μm cell strainer (BD Biosciences) and then washed with PBS containing 10% FBS. The digestion mix was centrifuged at 1,200 rpm at room temperature for 5 minutes. The cell pellet was resuspended in 10 ml MACS buffer, passed through a 40 μm cell strainer (BD Biosciences), centrifuged at 250 g in room temperature for 5 minutes

and resuspended in 500 µl MACS buffer. 1µg/ml of rat anti-mouse CD31 monoclonal antibody (BD Biosciences) was added for 15 minutes at 4°C. MACS buffer (500 µl) was then added and the cells were centrifuged at 300 g for 5 minutes at room temperature. The cell pellet was resuspended in 500 µl MACS buffer and 70 µl MACS® MicroBeads were added. After 15 minutes incubation at 4°C the sample was centrifuged at 300 g for 5 minutes at room temperature. The cell pellet was resuspended in 500 µl MACS and added onto a MACS® MS cell separation column in a magnetic field. After washing the column 3 times with 500 µl MACS buffer, MicroBead labelled CD31 positive cells were eluted from the column by removing it from the magnetic field and washing out the cells using MACS buffer. The cells were centrifuged at 300 g for 5 minutes at room temperature, resuspended in 500 µl endothelial cell medium EGM®-2-MV supplemented with FCS, hEGF, VEGF, hFGF-B, R^3-IGF-1, hydrocortisone, Gentamycin/Amphotericin-B and ascorbic acid, and seeded in 0.5% gelatin coated 12 well dishes (3.8 cm^2 growth area). Primary endothelial cells were cultured for a maximum of 3 days.

5.3.2 **Isolation of primary vascular smooth muscle cells**

Vascular smooth muscle cells (VSMC) were isolated from murine thoracic aorta. Mice were sacrificed by an overdose of inhaled isoflurane, and aortas were perfused by ice-cold PBS. The descending aorta was dissected, cleaned of adhering fat and adventitia. The aorta was then opened longitudinally and placed in ice-cold DMEM. The endothelial cell layer was removed using a cell scraper and the aorta was cut into 1-2 mm segments. At this point, VSMCs could be isolated either by cultured explant or by enzymatic digestion.

5.3.2.1 Cultured explant

Aortic segments were placed lumen side down onto gelatin coated 6 well plates. DMEM with 10% FBS (500 µl) was carefully added into the well so that the segments were not

displaced. The aortic tissue was allowed to adhere to the bottom of the culture well overnight and a further 500 µl of media was then added. VMSCs began to grow out from the stuck down aortic tissues after 5 days of culture. Two weeks were required to obtain a full well of VSMCs.

5.3.2.2 Enzymatic digestion

Aortic segments were digested for 1 hour at 37ºC in 1.5 mg/ml collagenase II (Worthington Biochemical Corp, USA, distributed by Lorne Laboratories, Reading, UK). The digestion mix was passed through a 100 µM cell strainer (BD Biosciences) and plated into a 6 well plate coated with 1% gelatin in 1 ml of VSMC media. One week was required to obtain a full well of VSMCs.

5.3.2.3 Comparison of cultured explant and enzymatic digestion

Both techniques of VSMC isolation have been used extensively in the literature. Enzymatic digestion, however, has the advantage that less time is required to obtain the same number of VSMCs. To ensure that the purity of VSMCs was not affected by enzymatic digestion, VSMCs isolated using the two methods in matched wild-type aortas were labelled with a VSMC specific marker, SM-α-actin and assessed for purity using confocal microscopy. SM α-actin positive VSMCs (red fluorescence; DAPI (nuclei) - blue) were similar between the two methods (Figure 5.1).

Figure 5.1

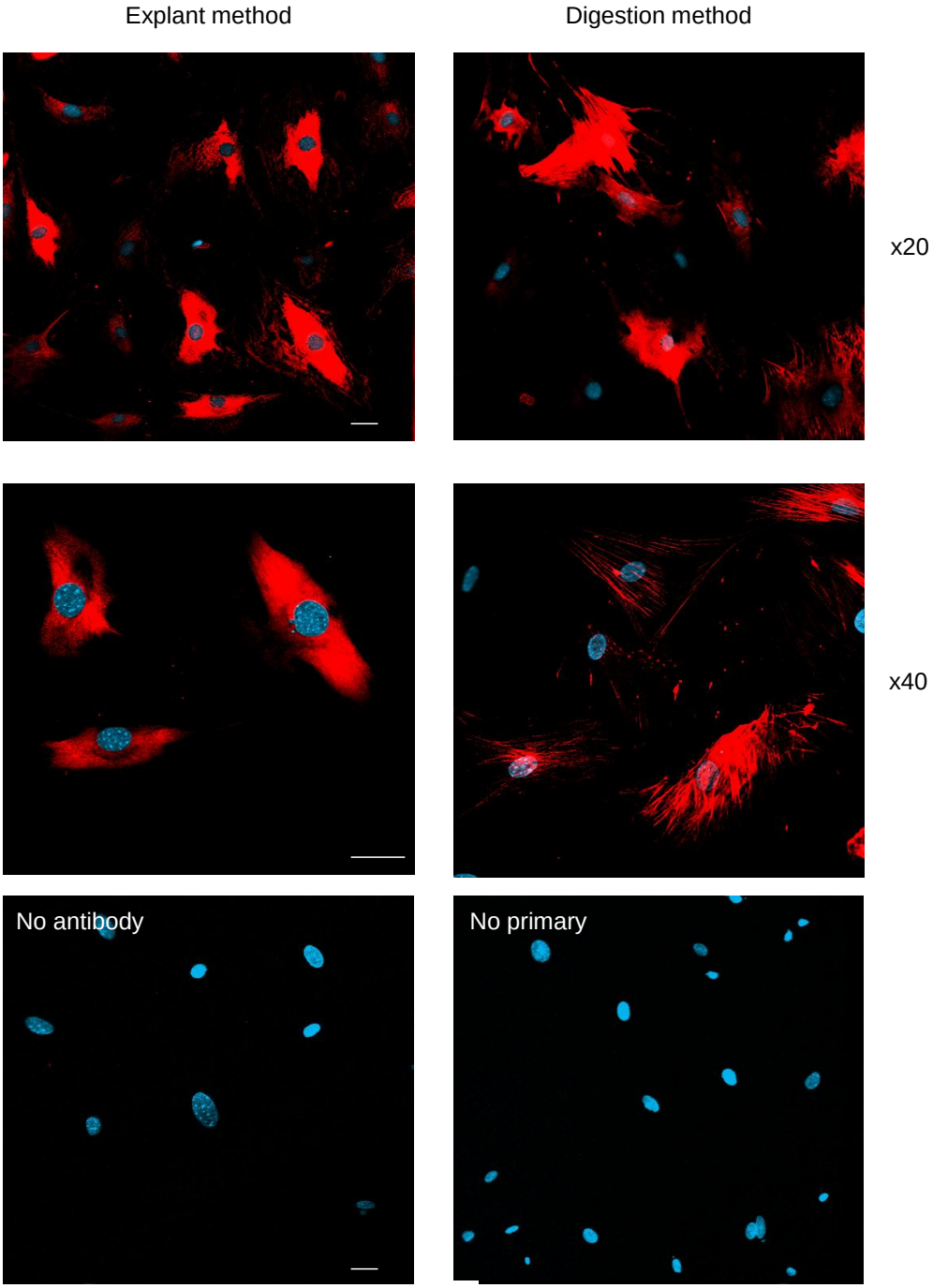


Figure 5.1 No difference in SM α-actin stain between VSMCs isolated from cultured explant or enzymatic digestion

Representative images of VSMCs stained with SM α-actin antibody and visualised under confocal microscopy (details seeing method). Nuclei were stained blue (DAPI); SM α-actin was in red. Top row: x20 magnification; middle row: x40 magnification; bottom row: controls. White bar - 20μm. There was no significant difference in the purity of VSMCs (SM α-actin positive) between cells isolated using two different methods.

5.3.2.3.1 Immunofluorescence VSMCs staining

Primary VSMCs (1 x 10^4 cells) were plated on a glass coverslip coated with 1:1000 fibronectin (Sigma-Aldrich, UK) placed in the wells of a 12 well tissue culture dish. Following overnight incubation, cells were washed with PBS, fixed with 4% PFA and then incubated with 0.1% triton-100 (Sigma-Aldrich, UK) for 4 mins. Cells were blocked with 10% FBS/PBS and incubated with primary anti-mouse SM α-actin antibody (1 µg/ml concentration; Santa Cruz, UK) for 30 minutes. After washing, cells were incubated with Alex-568 conjugated secondary rat-anti-mouse IgG antibody (1:500 dilutions) for 30 mins. Coverslips with stained cells were then removed from the well and mounted onto adhesive poly-L-lysine coated slides (VWR, Leicestershire, UK), dried overnight and examined using Zeiss confocal fluorescence microscope.

5.3.2.3.2 Specificity of SM α-actin

The specificity of SM α-actin was verified using primary VSMCs and 3 different other cell types: sEND.1 (an endothelial cell line); MEF and NH-3t3 (two fibroblast cell lines). Only primary VSMCs stained positive for SM α-actin (red fluorescence) (Figure 5.2).

Figure 5.2

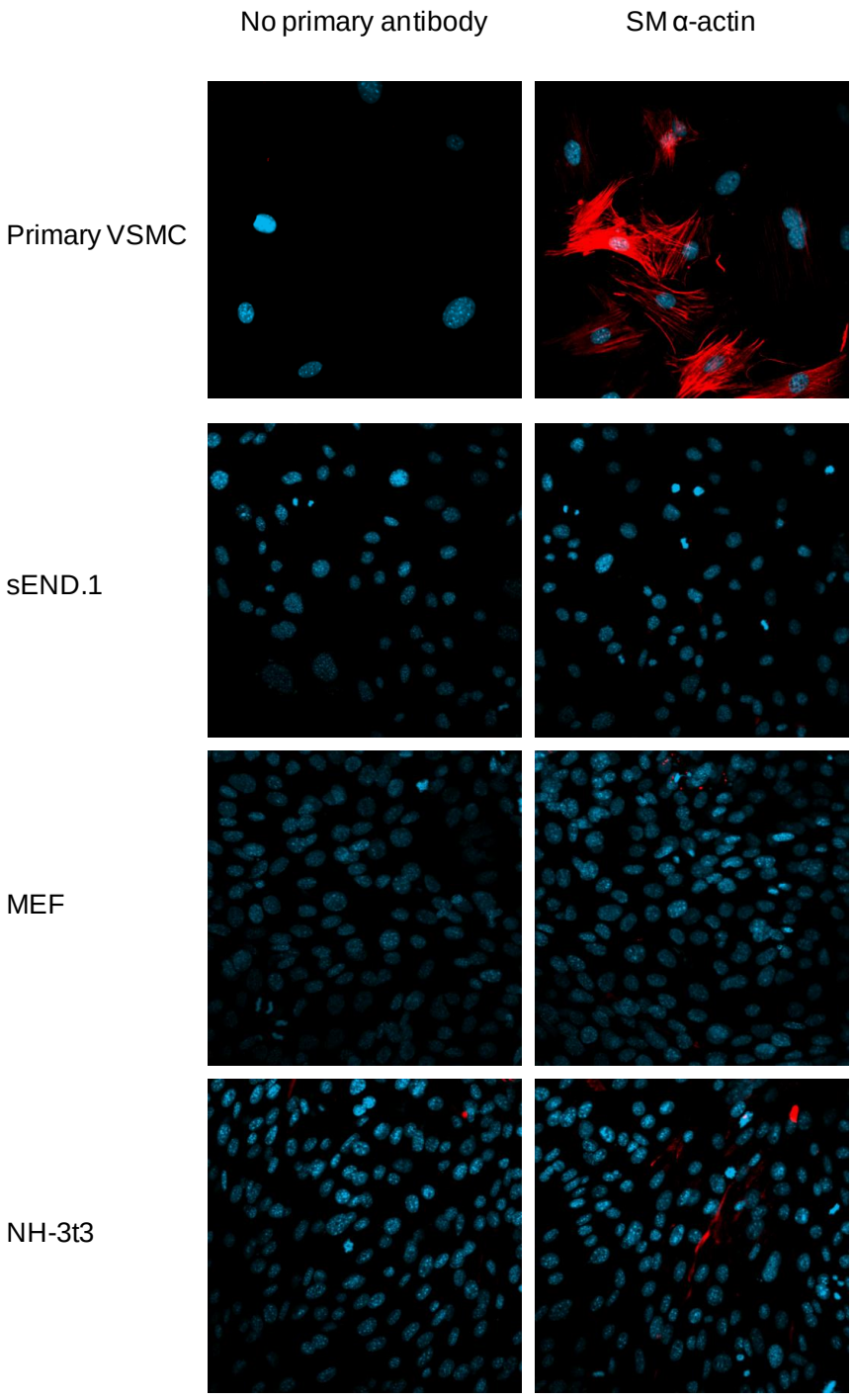


Figure 5.2 SM α-actin is VSMC specific

Representative images of VSMCs, sEND.1 (endothelial cells), MEF and NH-3t3 cells (fibroblasts) stained with SM α-actin antibody. Images were taken at x20 magnification. White bar - 20µm. SM α-actin: red fluorescence; nuclei: blue fluorescence (DAPI). Only VSMCs stained positive for SM α-actin.

5.3.3 Preparation of conditioned media and stimulation of VSMCs

Conditioned media was obtained from primary endothelial cells following 24 hours of incubation with serum free DMEM. The media were spun sequentially at 2,000, 3,000 and 13,000 RPM to remove cell debris and then concentrated 10 fold using an ultra-filter (Amicon-Ultra 0.5 ml, 10k; Millipore, UK). VSMCs at passage 2 were plated into 12 well plates and on confluency, concentrated conditioned media (20 µl) obtained from endothelial cultures were added into each well of VSMCs and incubated for 20 min. VSMCs were harvested immediately into ice cold lysis buffer containing protease and phosphatase inhibitors (Roche, UK). Following 3 cycles of freeze-thaw, lysates were used for western blot and probed for phosphorylated Erk1/2, total Erk1/2 and GAPDH.

5.4 Results

5.4.1 Characterisation of primary endothelial cells

Primary endothelial cells were isolated from the lungs of wild-type and Nox2 Tg mice as described in the methods. To reduce variability, primary endothelial cells isolated from several mice per group were pooled and split equally into 12 well plates.

5.4.1.1 Human Nox2 transgene was detectable at day 3 of culture

Primary endothelial cells isolated from wild-type and Nox2 Tg mice were cultured for 3 days and harvested for quantitative RT-PCR (qRT-PCR). The expression of CD31 (PECAM, an endothelial cell marker) was used as positive control. Human Nox2 transgene was detectable in Nox2 Tg endothelial cells, but not in wild-type primary endothelial cells after 3 days of culture. However, when compared to the previous qRT-PCR experiment results shown in Chapter 3 (Figure 3.3) where freshly isolated Nox Tg endothelial cells were used immediately for RNA extraction, 3 days of culture reduced human Nox2

transgene expression by 3 fold (Figure 5.3). There was no significant difference in the levels of mRNA expressions of endogenous mouse Nox2 and Nox4 between wild-type and Nox2 Tg endothelial cells.

Figure 5.3

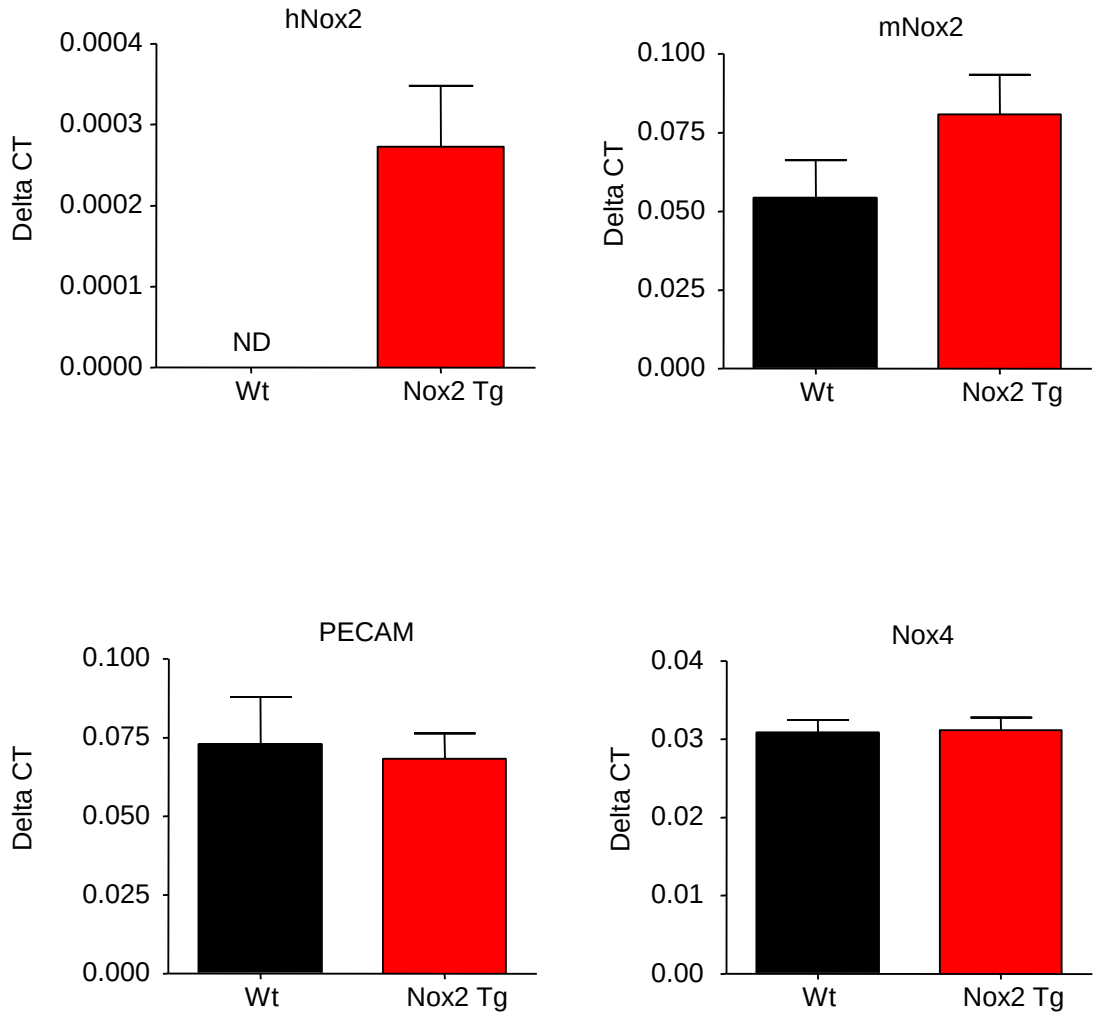


Figure 5.3 Human Nox2 transgene was only expressed in Nox2 Tg endothelial cells

Primary endothelial cells were isolated and cultured for 3 days. Cells were then harvested and examined for human Nox2 (hNox2), mouse Nox2 (mNox2) and Nox4 with PECAM as endothelial specific marker. Data are expressed as mean±SEM, n=3 independent experiments. ND – not detected. The human Nox2 transgene was only detected in endothelial cells isolated from Nox2 Tg mice. There was no significant difference in the gene expression of PECAM, mouse Nox2 and Nox4 between Wt and Nox2 Tg endothelial cells.

5.4.1.2 Increased total Nox2 protein expression in Nox2 Tg endothelial cells

Endothelial cells were isolated from wild-type and Nox2 Tg mice as described previously and lysed in lysis buffer (Sigma-Aldrich) after 3 days of culture. Western blots of endothelial lysates were probed for Nox2, Nox4, F4/80 (macrophage marker), CD102 (an endothelial marker) and SM α-actin (VSMC marker). The specificity of Nox2 protein was confirmed using lysates from primary macrophages isolated from the same mouse as the positive control, and lung tissue from Nox2 knockout mice as the negative control (Figure 5.4 A).

There was an increase in total Nox2 protein in Nox2 Tg endothelial cells compared to wild-type endothelial cells, however, no difference in the protein level of Nox4 was observed (Figure 5.4 B). Macrophages were used as negative control for Nox4. Endothelial cell specificity was verified by the presence of CD102 and lack of SM α-actin and F4/80 protein expression. Equal endothelial protein loading was demonstrated by CD102.

Figure 5.4

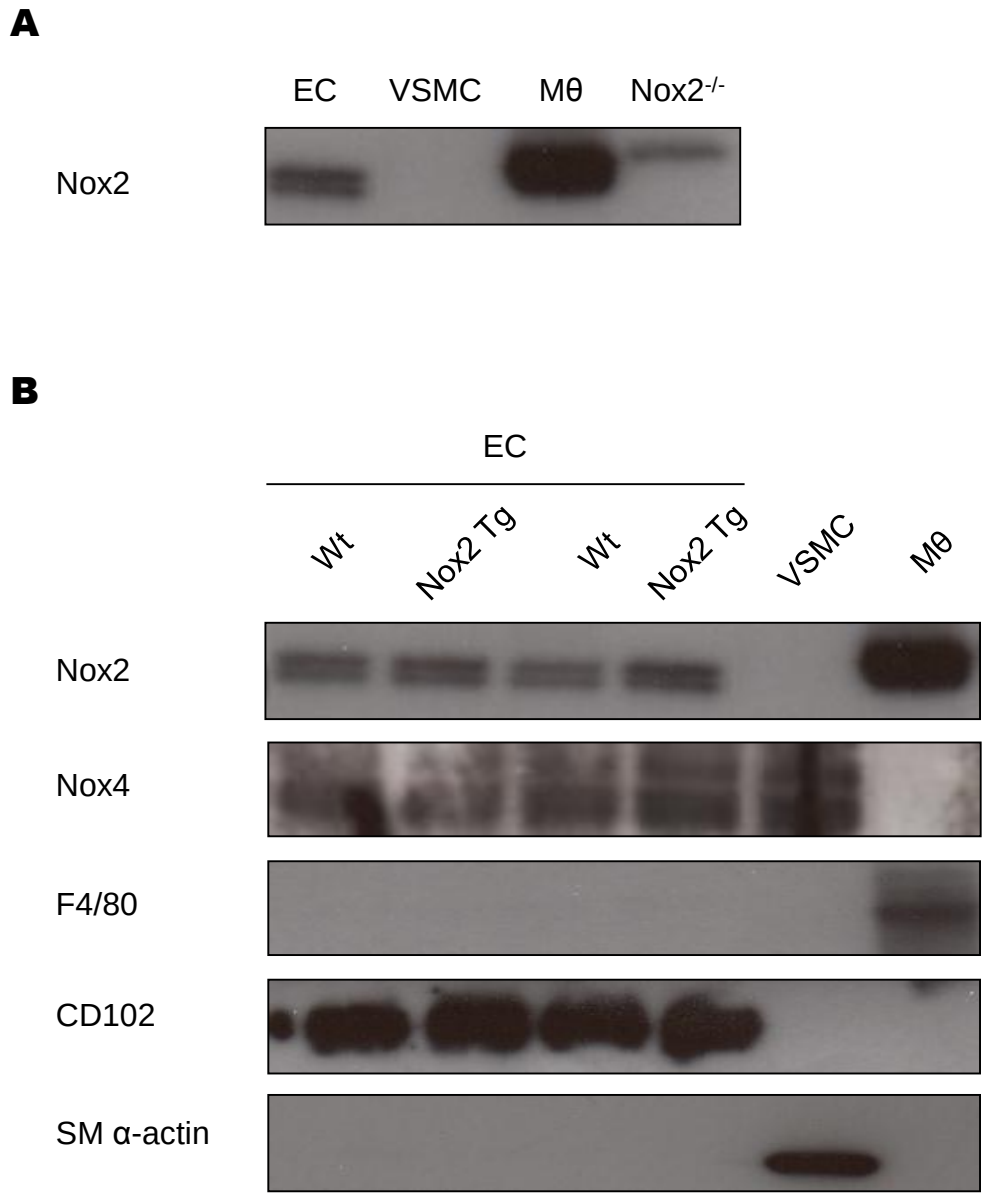


Figure 5.4 Increased total Nox2 protein in Nox2 Tg endothelial cells

Representative western blots of endothelial cells (EC) after 3 days of culture. **(A)** Specificity of the Nox2 antibody was checked using EC, VSMC, macrophages (Mθ) and Nox2 knockout tissue ($Nox2^{-/-}$). Nox2 protein was only detected in EC and Mθ. **(B)** Protein expression of Nox2, Nox4, F4/80 (macrophage marker), CD102 (EC marker), SM α-actin (VSMC marker) in EC, VSMC and primary macrophage (Mθ). There was increased Nox2 protein in Nox2 Tg endothelial cells compared to the wild-type. No difference was observed in Nox4 protein level.

5.4.1.3 Measurement of reactive oxygen species production

I have confirmed so far the presence of human Nox2 transgene and an increase in the protein levels of total Nox2 in primary endothelial cell isolated from Nox2 Tg mice after 3 days of culture. To examine whether this had a functional effect, the production of superoxide was measured from these cells using DHE HPLC.

sEND.1 cells, 1 $x10^5$, were seeded into 12 well plates and stimulated with Ang II over a range of time points (0, 5, 15, 30 min). A chromatography peak appearing around 12 minutes corresponded to the 2-hydroxyethdium peak and a second peak appearing around 15 minutes corresponded to the ethidium peak (Figure 5.5). A time dependent increase in 2-hydroxythethidium production was observed in response to Ang II (10^{-7} M) stimulation which was abolished almost completely by pre-incubation with 100 units/ml of pegylated superoxide dismutase (Peg-SOD) (Figure 5.6). As Peg-SOD catalytically dismuted O_2^- to oxygen and hydrogen peroxide, this would suggest the assay is specific for the measurement of O_2^- production. The residual 2-OH peak in Peg-SOD treated cells likely represented a combination of oxidation of the original DHE reagent and incomplete protection from oxidation by Peg-SOD.

Figure 5.5

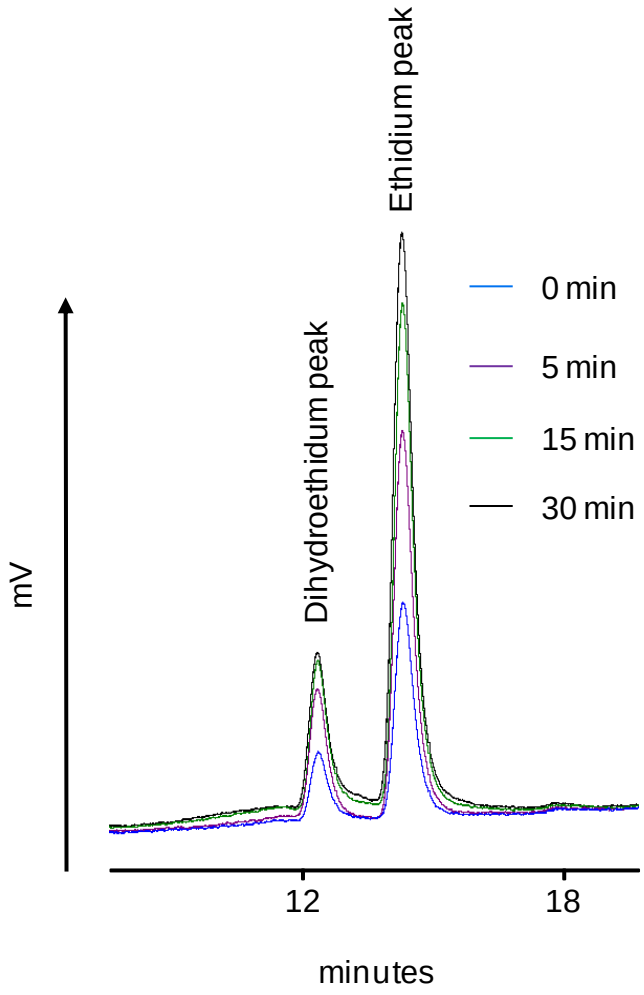


Figure 5.5 Time dependent increase in 2-hydroxyethidium peak in response to Ang II stimulation

Representative DHE HPLC traces for the detection of Ang II-induced O_2^- production by sEND.1 cells, which corresponded to the 2-hydroethidium peak appearing at ~12 minutes. The ethidium peak represented the production of other ROS species. Ang II increased the both 2-hydroethidium and ethidium peaks in a time dependent manner.

Figure 5.6

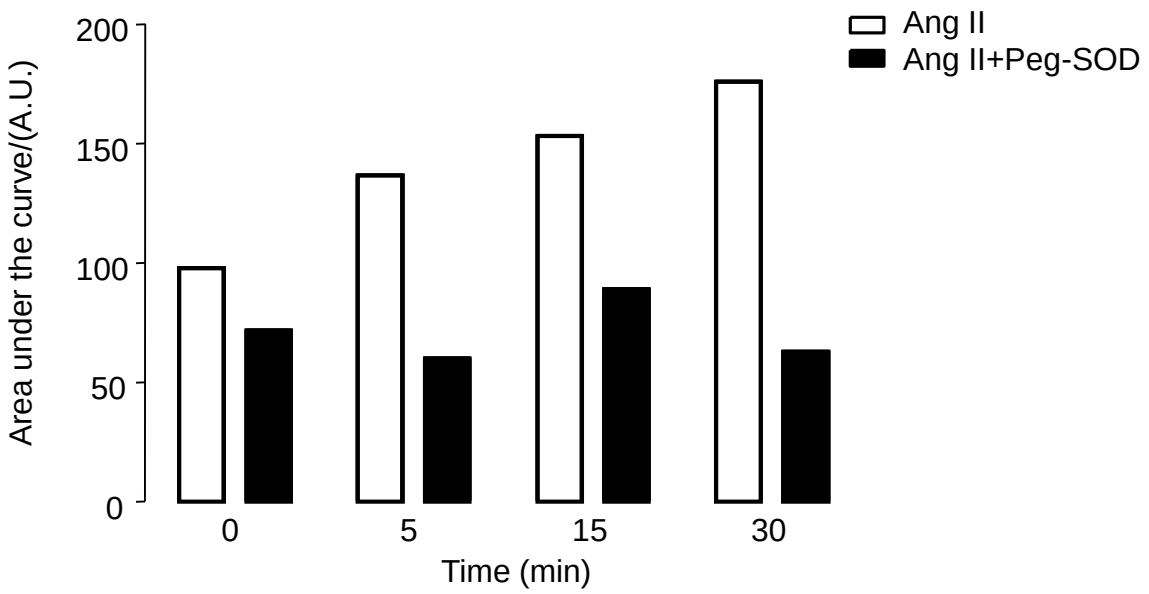


Figure 5.6 Increases in 2-hydroxyethdium peak in response to Ang II were abolished by pegylated superoxide dismutase

sEND.1 cells were pre-incubated with Peg-SOD (100 units/ml) for 30 min before treatment with Ang II for 0, 5 15 and 30 min. The production of 2-hydroxyethidium fluorescence detected by DHE HPLC was quantified using area under the curve. A.U. – arbitrary units. Ang II stimulation induced a time-dependent increase in 2-hydroxyethidium peak that was inhibited in the presence of Peg-SOD.

5.4.1.4 Tiron but not DPI inhibited ROS production to a similar extent as Peg-SOD in Ang II treated sEND.1 cells

To further test the specificity of the DHE HPLC assay to detect O_2^- production, other inhibitors of O_2^- were used including diphenyleneiodonium chloride (DPI), which is a flavo-protein inhibitor and inhibits both nitric oxide and NADPH oxidase; and tiron, which is a O_2^- scavenger. sEND.1 cells were pre-incubated with the inhibitors for 30 minutes before stimulation with Ang II (10^{-7} M) for 20 minutes (Figure 5.7).

Ang II induced a 1.5 fold increase in O_2^- production (2-hydroxyethidium peak) that was inhibited by tiron to a similar extent as Peg-SOD (Figure 5.7). However, DPI showed no inhibition and instead, there was an increase in the 2-hydroxyethidium peak even in the untreated cells. When DPI treated cells were examined under the fluorescence microscope, I observed that there was a significant number of floating dead cells which was not observed in tiron and peg-SOD treated groups. Peg-SOD was used as the inhibitor of O_2^- for future experiments as it is more physiological and relevant to biological systems than tiron.

Figure 5.7

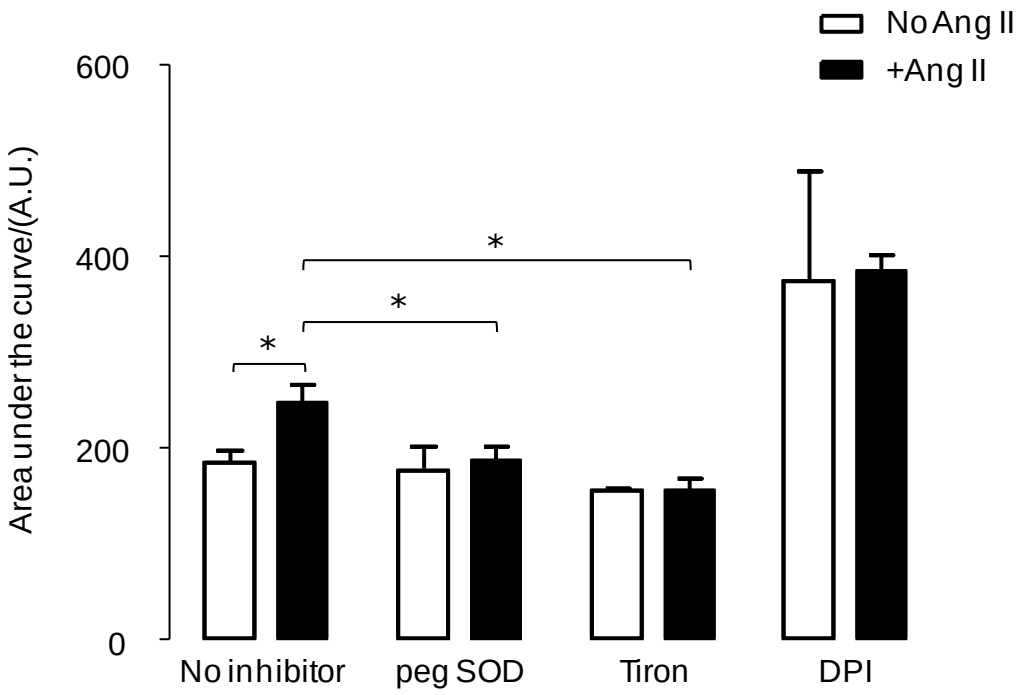


Figure 5.7 Tiron but not DPI reduced ROS production to a similar extent as Peg-SOD in Ang II treated sEND.1 cells

sEND.1 cells were pre-incubated with Peg-SOD (100 units/ml), Tiron (1 mM), or DPI (20 µM) for 30 minutes before stimulation with Ang II for 20 min. O_2^- production was detected by DHE fluorescence HPLC method. 2-hydroxyethidium peaks were quantified using area under the curve and presented as mean±SEM. *$p<0.05$, n=3 independent experiments. A.U. - arbitrary units. Peg-SOD and tiron inhibited the 2-hydroxyethidium peaks to a similar degree.

5.4.1.5 Increased superoxide production in Nox2 Tg endothelial cells compared to wild-type

From the initial experiments with sEND.1 cells, it was established that Ang II (10^{-7} M) induced an increase in superoxide production which was significantly inhibited by pre-incubation of cells with Peg-SOD. Next, I examined superoxide production by primary endothelial cells isolated from wild-type and Nox2 Tg mice.

Primary endothelial cells were isolated from the lungs of wild-type and the Nox2 Tg mice as described in Chapter 2. Cells were cultured for 3 days and at day 3, cells were pre-incubated in DMEM alone as control, or with Peg-SOD for 30 min. Cells were then stimulated in the presence or absence of Ang II for 20 min and then harvested for the measurement of ROS production by DHE HPLC. The 2-hydroxyethdium peak was quantified as area under the curve (Figure 5.8).

There was a significantly higher level of ROS production in untreated (baseline) Nox2 Tg endothelial cells compared to wild-type control cells (Figure 5.9 A). This increase in baseline ROS production by unstimulated Nox2 Tg endothelial cells was abolished by Peg-SOD suggesting O_2^- as the dominant ROS. When the cells were stimulated with Ang II, there was a greater increase (3 fold) in ROS production by Nox2 Tg endothelial cells compared to the increase (2 fold) in ROS production by wild-type controls. Peg-SOD inhibited the levels of ROS production by both wild-type and Nox2 Tg endothelial cells down to baseline (Figure 5.9 B).

Figure 5.8

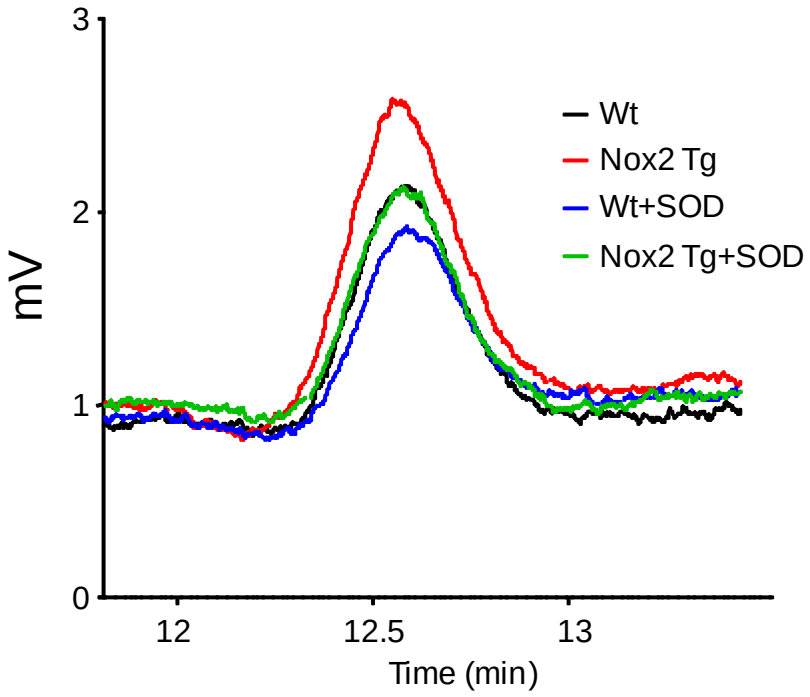


Figure 5.8 Increased ROS at baseline in Nox2 Tg endothelial cells

Representative traces of 2-hydroxyethidium peak (O_2^- production) detected by DHE HPLC in primary endothelial cells isolated from wild-type and Nox2 Tg mice. Nox2 Tg endothelial cells produced higher levels of baseline O_2^- as compared to the levels of wild-type control cells. Pre-incubation of cells with peg-SOD reduced the levels of O_2^- production in both wild-type and Nox2 Tg endothelial cells.

Figure 5.9

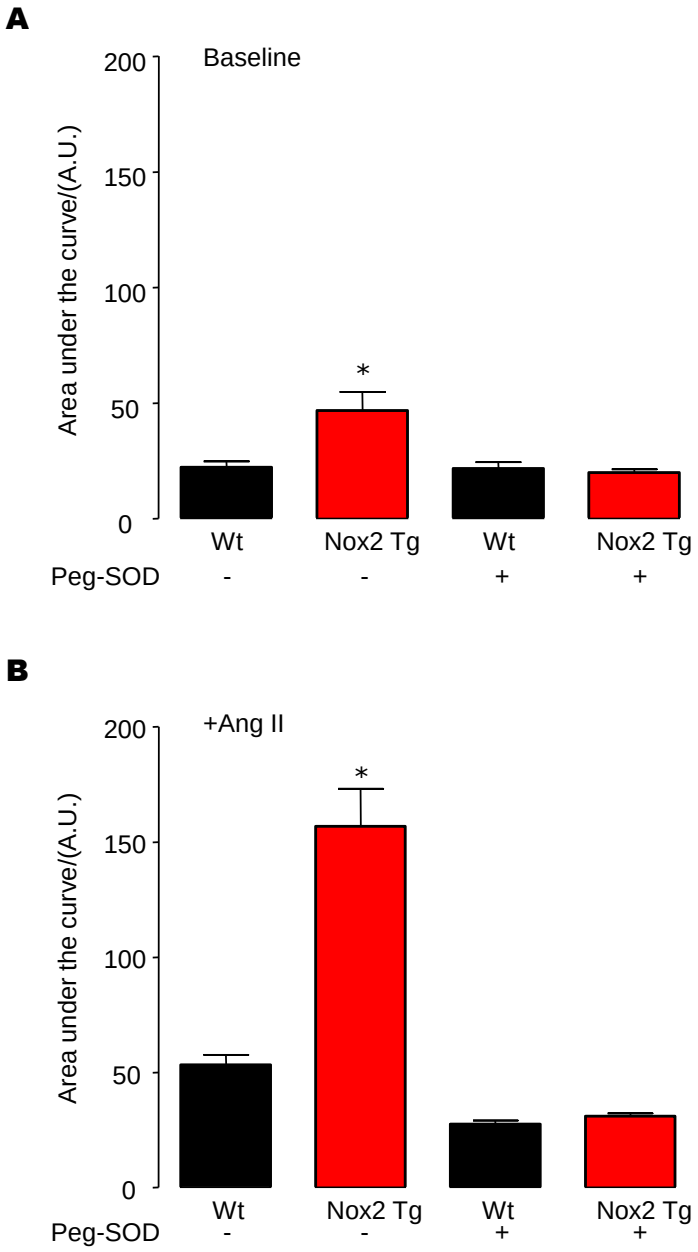


Figure 5.9 Greater endothelial ROS in Nox2 Tg endothelial cells at both baseline and in response to Ang II compared to Wt

Primary endothelial cells were pre-incubated with Peg-SOD or in DMEM alone as control and then stimulated with or without Ang II. O_2^- production was detected by DHE HPLC and quantified by area under the curve of the 2-hydroxyethidium peak. Data are expressed as mean±SEM. A.U. – arbitrary units. *$p<0.05$, n=3 independent experiments and 8 mice/per group were used for each experiment. **(A)** Baseline O_2^- by wild-type and Nox2 Tg endothelial cells in DMEM control media. **(B)** Ang II (10^{-7} M) induced O_2^- production in wild-type and Nox2 Tg endothelial cells. Peg-SOD was used to verify the assay specificity for the detection of O_2^-.

5.4.2 Characterisation of primary VSMCs

Primary VSMCs were isolated from the aorta of wild-type and Nox2 Tg mice as described in the methods. To reduce variability, primary VSMCs were isolated from the same animal used for endothelial cell isolation and VSMCs isolated from several mice of the same genotype were pooled before being split equally into 12 well plates.

5.4.2.1 Human Nox2 transgene was not present in primary VSMCs

It was important to check if the expression of human Nox2 transgene is indeed endothelial specific and not detected in the VSMCs. To confirm this, VSMCs were isolated from wild-type and Nox2 Tg mice, cultured for one week to reach confluence. Cells were passaged and cultured for another week. VSMCs were then counted and plated at a density of 1 x 10^4 cells into 12 well plates. Once the cells reached confluency, they were harvested for RNA extraction. Expression of human Nox2 transgene was examined by qRT-PCR.

As expected, the human Nox2 transgene was not detected in VSMCs isolated from either the wild-type or Nox2 Tg mice (Figure 5.10). There was a minimal detectable level of endogenous mouse Nox2 expression in VSMCs, which was 100 fold less than the mouse Nox2 expression detected in the primary endothelial cells. There was no difference in the gene expression of mouse Nox4 between VSMCs isolated from wild-type and Nox2 Tg mice.

Figure 5.10

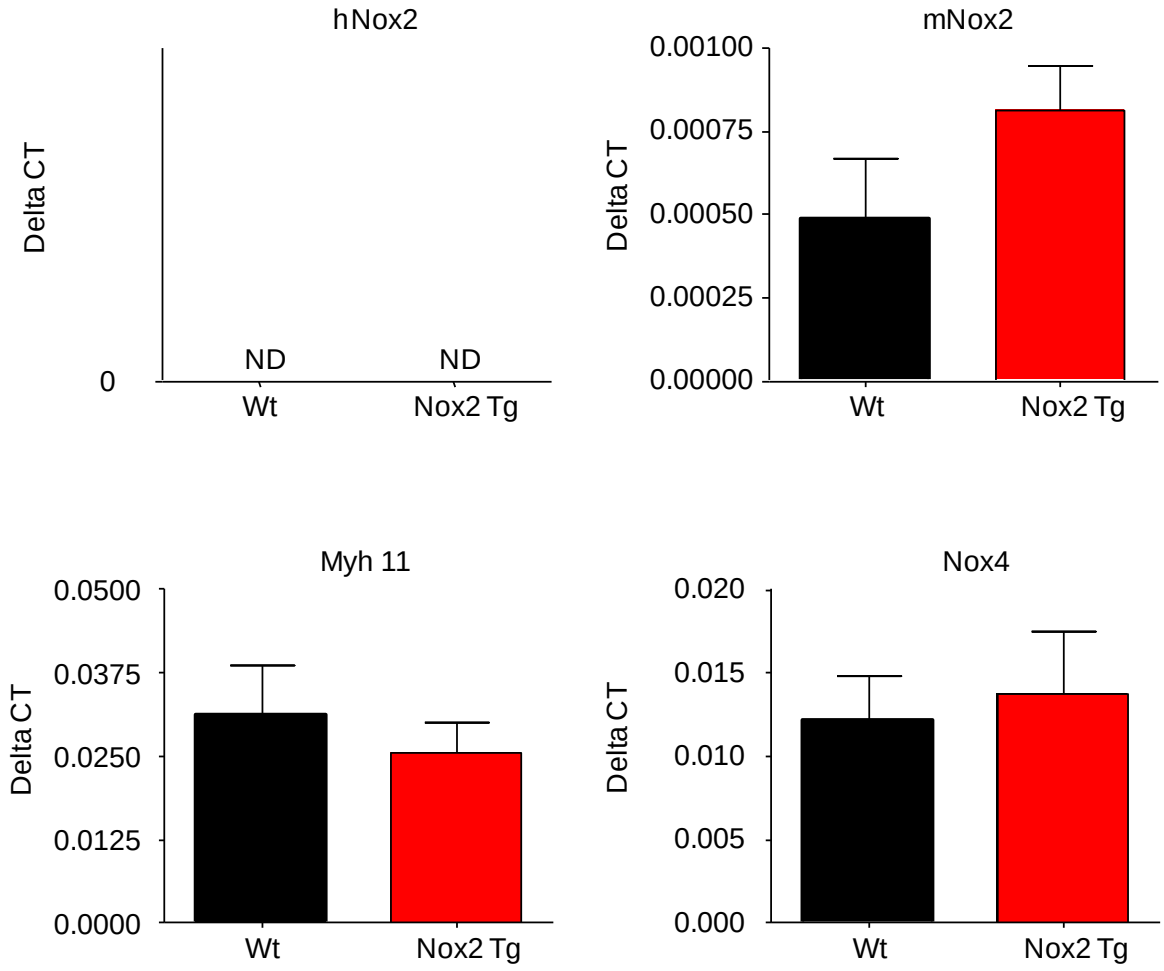


Figure 5.10 No expression of human Nox2 transgene in primary VSMCs

VSMCs were cultured for 2 passages before being used for the detection of gene expression of human Nox2 transgene, mouse Nox2, mouse Nox4 and Myh 11 by qRT-PCR. The results were presented as ΔCT with GADPH as the "housekeeper" gene. Data are expressed as mean±SEM, n=3 independent experiments. ND – not detected. Human Nox2 transgene was undetectable in VSMCs isolated from wild-type and Nox2 Tg mice. There was no significant difference in the gene expression of mouse Nox2, Nox4 and Myh 11 between VSMCs isolated from wild-type and Nox2 Tg mice.

5.4.2.2 Nox2 protein was below detectable level in VSMCs isolated from both wild-type and Nox2 Tg mice

I next investigated the protein levels of Nox2 and Nox4 by western blot. VSMCs were harvested at passage 2, homogenised in lysis buffer and 20µl of the lysates was used for western blots. Antibodies to F4/80 (a macrophage marker), to CD102 (an endothelial marker) and to SM α-actin (a VSMC marker) were used to confirm cell specificity. There was no detectable Nox2 protein in either wild-type or Nox2 Tg VSMCs when compared to endothelial cells and macrophages indicating that protein level of Nox2 expression in VSMCs was very low (Figure 5.11). Similar to mRNA expression, there was no difference in the protein levels of Nox4. As expected, VSMCs expressed SM α-actin (positive control), but not the macrophage marker F4/80 or the endothelial marker CD102, thus confirming the purity of VSMCs.

Figure 5.11

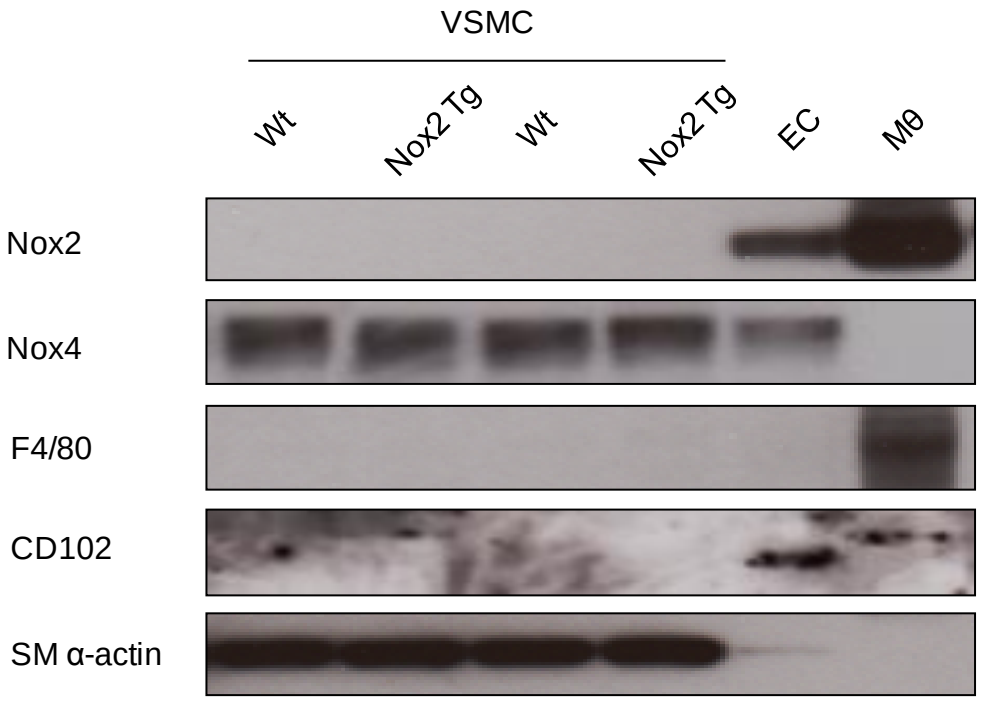


Figure 5.11 No Nox2 protein expression in primary VSMCs

Representative images of western blots for the presence of Nox2, Nox4, F4/80 (a macrophage marker), CD102 (an endothelial cell marker) and SM α-actin (A VSMC marker) in VSMCs. Mθ: primary macrophages. EC: endothelial cells. Primary VSMCs had no Nox2 protein expression (undetectable level). Nox4 protein was similar between wild-type and Nox2 Tg VSMCs. The purity of isolated primary VSMCs was confirmed by expression of SM α-actin and no expression of F4/80 (macrophage marker) or CD102 (endothelial marker).

5.4.2.2.1 No difference in ROS production between primary VSMCs isolated from wild-type and Nox2 Tg mice.

My results so far have demonstrated that VSMCs had very low levels of Nox2 mRNA expression, undetectable levels of Nox2 protein, and no difference in mRNA or protein levels of Nox4. I next examined ROS production by primary VSMCs isolated from wild-type and Nox2 Tg mice using the same protocol as used for the endothelial cells.

Primary VSMCs isolated from wild-type and Nox2 Tg mice were cultured for 2 passages and were seeded at a concentration of 1 x 10^4 cells per well into 12 well plates and grown to confluency. Cells were then pre-incubated with DMEM alone as control or with Peg-SOD before stimulation with or without Ang II (10^{-7} M). O_2^- production was detected by DHE HPLC and was quantified using area under the curve of the 2-hydroxyethidium peak (Figure 5.12).

There was no significant difference in the levels of O_2^- production between wild-type and Nox2 Tg VSMCs either at the baseline (without Ang II stimulation) or after Ang II stimulation (Figure 5.13). Pre-incubation of cells with Peg-SOD inhibited Ang II-induced increase in ROS to a similar degree between wild-type and Nox2 Tg VSMCs.

Figure 5.12

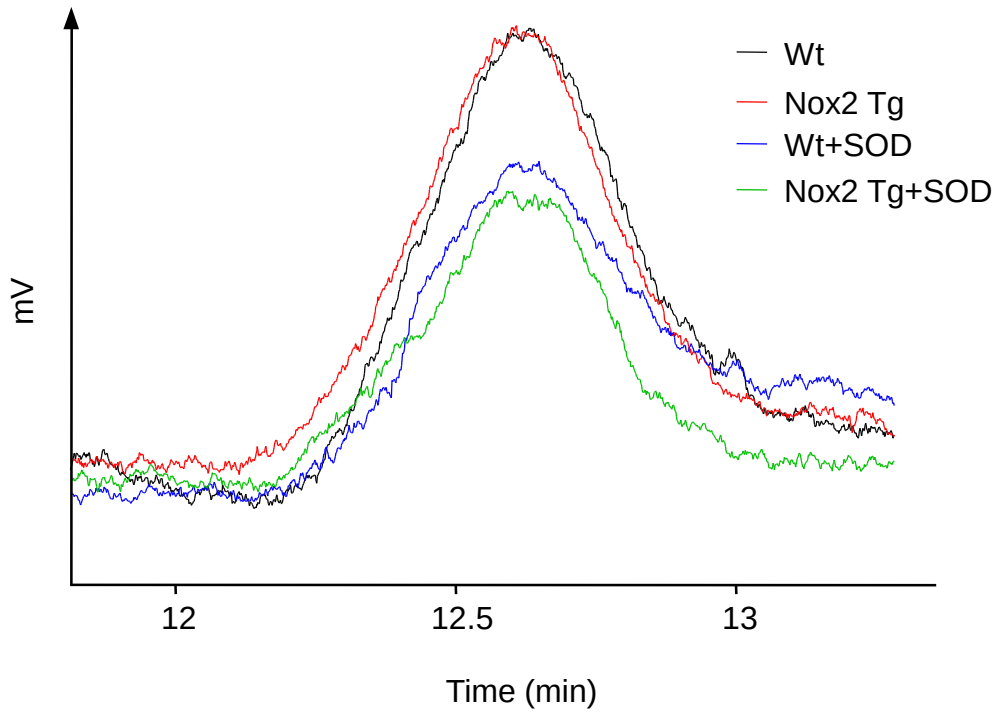


Figure 5.12 No difference in baseline wild-type and Nox2 Tg VSMCs ROS production

Representative traces of 2-hydroxyethidium peak (O_2^- production) in primary VSMCs isolated from wild-type and Nox2 Tg mice detected by DHE HPLC. Pre-incubation of cells with Peg-SOD inhibited the 2-hydroxyethidium peaks in both wild-type and Nox2 Tg VSMCs.

Figure 5.13

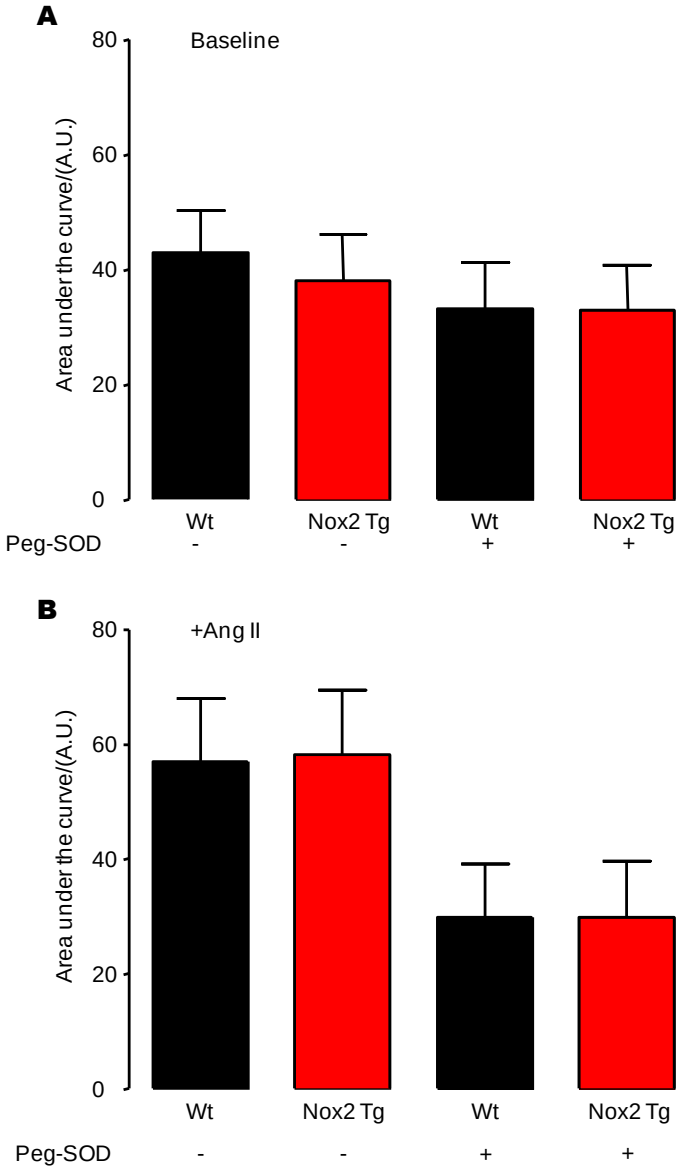


Figure 5.13 No difference in wild-type and Nox2 Tg VSMC ROS production at either baseline or after Ang II stimulation

Primary VSMCs were pre-incubated with or without Peg-SOD and then stimulated with or without Ang II. O_2^- production was detected by DHE HPLC and quantified by area under the curve of the 2-hydroethidium peak. Data are expressed as mean±SEM. A.U. – arbitrary units. n=3 independent experiments and 8 mice per group were used for each experiment. **(A)** Baseline levels of O_2^- production **(B)** Ang II (10^{-7}M) induced O_2^- production. Peg-SOD was used to confirm the assay specificity.

5.4.3 Evidence for secreted factors in the Nox2 Tg endothelial cell conditioned media which act to induce VSMC Erk1/2 phosphorylation and activation.

Having established the characteristics of both primary endothelial cells and VSMCs isolated from Nox2 Tg mice, I next tested the hypothesis that endothelial cells secrete a factor that can activate VSMC by examining conditioned media from wild-type and Nox2 Tg endothelial cells. Erk1/2 phosphorylation is associated with VSMCs activation and commonly used as marker of VSMCs activation (Jin et al., 2000; Liao et al., 2000; Satoh et al., 2008). Conditioned media were prepared as described in Methods. VSMCs were cultured for 2 passages, stimulated with either DMEM control or with conditioned media from wild-type or Nox2 Tg endothelial cells and then examined for Erk1/2 phosphorylation by western blotting.

Nox2 Tg endothelial conditioned media induced significantly greater Erk1/2 phosphorylation in VSMCs compared to DMEM controls or wild-type conditioned media (Figure 5.14). These results suggested that there was a ROS sensitive factor secreted by endothelial cells that was able to activate VSMCs.

Figure 5.14

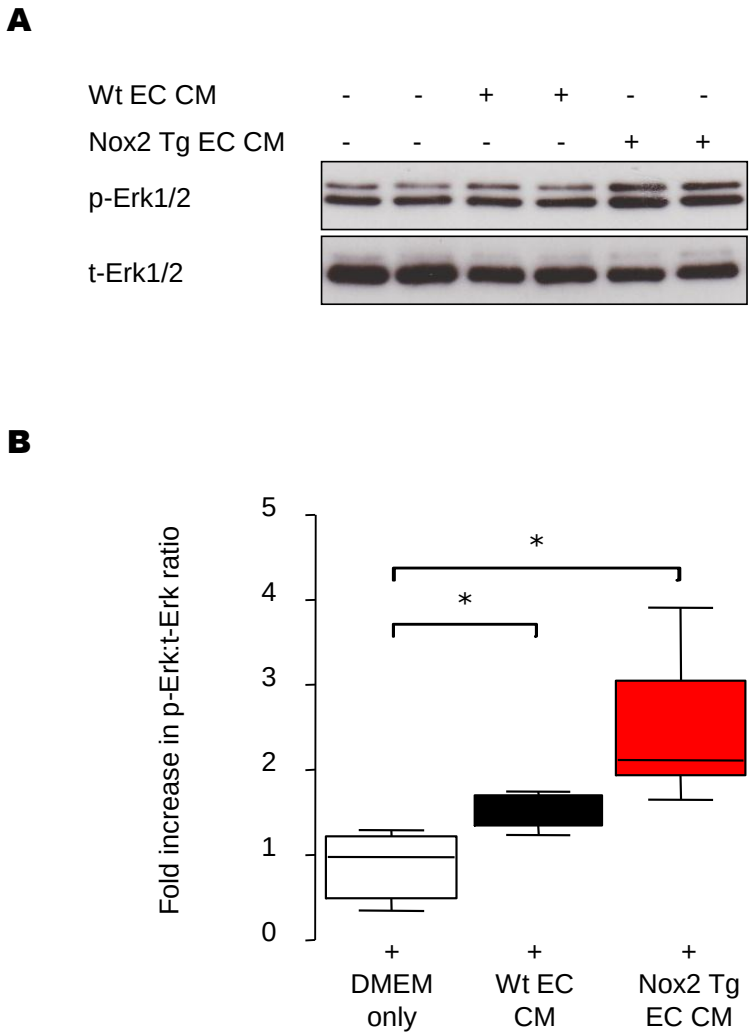


Figure 5.14 Greater VSMCs phosphorylation in cells stimulated with Nox2 Tg endothelial conditioned media

Primary VSMCs were cultured for 2 passages and stimulated for 20 mins with conditioned media from wild-type endothelial cell (Wt EC CM) or conditioned media from Nox2 Tg endothelial cells (Nox2 Tg EC CM). Cells cultured in DMEM only were used as controls. Cell lysates were used to detect Erk1/2 phosphorylation by a phos-Erk1/2 specific antibody. **(A)** Representative images of western blots for phosphorylated Erk1/2 (p-Erk1/2) and total Erk12 (t-Erk1/2). **(B)** Densitometric analysis of Western blots presented as the fold increase in p-Erk1/1 and t-Erk1/2 ratio with baseline defined as 1. Data are expressed as mean±SEM. *$p<0.05$, n=3 independent experiments.

5.5 Discussion

In this chapter I examined and characterised primary endothelial cells and VSMCs isolated from wild-type and Nox2 Tg mice for their biochemistry, mRNA and protein expression of human Nox2 transgene, mouse Nox2 and Nox4. The key findings of this chapter were:

- The human Nox2 transgene was detected only in Nox2 Tg endothelial cells.
- Nox2 transgene expression leads to increased protein levels of Nox2 and increased ROS production by Nox2 Tg endothelial cells at both baseline (without Ang II) and after Ang II stimulation compared to wild-type endothelial cells. There was no significant difference in Nox4 expression at either mRNA or protein levels.
- Nox2 transgene was not detected by qRT-PCR in VSMCs isolated from either wild-type or Nox2 Tg mice.
- Nox2 protein was not detectable in VSMCs and there was no significant difference in the levels of ROS production at either baseline (without Ang II) or after Ang II stimulation.
- Nox2 Tg endothelial cell conditioned media induced greater VSMC Erk1/2 phosphorylation compared to the wild-type.

It is often unclear whether interventions in the in-vivo systems such as a transgene expressed in the animal tissues can be translated into in-vitro systems. Therefore, it was crucial to isolate the primary cells from transgenic mice and characterised these cells to make sure that they retained the some of the same characteristics as observed in-vivo. Previous studies done by Dr R. Rinze in our laboratory have found the human Nox2 transgene in primary endothelial cells to be down regulated progressively during culture and completely undetectable by day 7 of culture with qRT-PCR and Western blotting. My results were in accordance with this previous data and even after only 3 days of culture,

there was a 30 fold decrease in human Nox2 transgene expression as compared to freshly isolated Nox2 Tg endothelial cells. However, my results showed also that such level of human transgene expression was still sufficient to induce an increase in total Nox2 protein expression and more importantly, a significant increase in ROS production by Nox2 Tg endothelial cells at both baseline and after stimulation with Ang II as compared to wild-type endothelial cells.

ROS production was measured by DHE HPLC (Douglas et al., 2012; Fink et al., 2004; Zhao et al., 2005), which is a well-established assay for the specific detection of ROS. It relies on the oxidation of dihydroethidium to the fluorescent DNA binding and membrane permeable compound ethidium and 2-hydroxyethdium which is specific for detecting O_2^- (Benov et al., 1998; Bindokas et al., 1996). Recently evidence has shown the 2-dihydroxyethidium peak to be more specific to O_2^- production especially from NADPH oxidases whereas the ethidium peak corresponds more to H_2O_2 production (Fernandes et al., 2007). This is supported by my data which showed that the 2-dihydroethidium peak but not the ethidium peak was significantly inhibited by Peg-SOD. The specificity of DHE HPLC was further examined using other inhibitors of ROS including DPI and tiron. Tiron is a cell permeable O_2^- scavenger that reduced the 2-dihydroxyethidium peak to a similar degree as Peg-SOD. DPI, however, increased the 2-dihydroxyethidium/ROS peak, and under microscopy it was observed to cause cell death.

As mentioned previously, endothelial cells express both Nox2 and Nox4, but the interactions between Nox2 and Nox4 is largely unknown. It is possible that the over-expression of Nox2 transgene could have affected Nox4 expression which may then alter cellular ROS production. However, I demonstrated in this chapter using both qRT-PCR and western blot that there was no difference in Nox4 expression at both the mRNA and

protein levels between wild-type and Nox2 Tg endothelial cells. These results confirmed that Nox2 transgene was the main contributor to the increase in ROS production.

VSMCs have been studied in many diseases and presumed to have a central role in the development of AAA (Satoh et al., 2009). It was therefore crucial to check if there was leakage of Nox2 transgene expression into VSMCs. My results using isolated primary VSMCs confirmed no expression of the Nox2 transgene in VSMCs from either wild-type or Nox2 Tg mice. A low level of Nox2 mRNA was detected which was consistent with previous reports that VSMCs mainly express Nox1 and Nox4 (Clempus and Griendling, 2006). As expected I found no difference in the levels of ROS production between wild-type and Nox2 Tg VSMCs at either baseline or after Ang II stimulation.

Having confirmed the characteristics of primary endothelial cells and VSMCs, I examined the effects of conditioned media from wild-type and Nox2 Tg endothelial cells on VSMC Erk1/2 activation. The use of conditioned media is an established technique used to examine the function of endogenous factors secreted by cells into culture media (Jin et al., 2000; Jin et al., 2004; Tieu et al., 2009). Erk1/2 belongs to a family of enzymes, the mitogen activated protein kinases (MAPKs), and they have diverse functions in the cell including cell cycle, gene expression and apoptosis. Erk1/2 phosphorylation has been recognised to be associated with VSMCs activation (Jin et al., 2000; Liao et al., 2000; Satoh et al., 2008). Interestingly, I found that conditioned media from both wild-type and Nox2 Tg endothelial cells induced VSMC Erk1/2 phosphorylation. However, conditioned media from Nox2 Tg endothelial cells induced significantly greater Erk1/2 phosphorylation compared to conditioned media from wild-type endothelial cells or DMEM controls. These results strongly suggested that there was a secreted factor in the conditioned media from Nox2 Tg endothelial cells, which was able to induce VSMC

Erk1/2 phosphorylation and activate VSMCs. The identification of this factor was therefore the main focus of the next chapter.

Chapter 6:

The mechanism of endothelial Nox2 regulation of VSMC activation: the role of secreted CypA

Chapter 6. The mechanism of endothelial Nox2 regulation of VSMC activation: the role of secreted CypA

6.1 Introduction

In the previous chapters I have demonstrated an increase in Nox2 protein expression and ROS production in Nox2 Tg endothelial cells; and also discovered the presence of a secreted factor in the conditioned media from endothelial cells that was able to induce Erk1/2 phosphorylation in VSMCs. The question left unanswered is: what is this endothelial secreted factor?

One of the possible candidates for this endothelial secreted factor is Cyclophilin A (CypA), a secreted cytokine that has recently been shown to play a central role in the development of Ang II induced abdominal aortic aneurysm (Satoh et al., 2009). CypA is an 18 kDa protein belonging to a family of highly conserved proteins called immunophilins and is expressed in all eukaryotic cells. It was firstly identified in 1984 intracellularly as the main target for the immunosuppressive drug, cyclosporine A (Handschumacher et al., 1984), which acts to inhibit the cis-trans isomerisation of peptidyl-prolyl catalytic activity (PPIase activity) of CypA (Steinmann et al., 1991). Extracellular secretion of CypA has been demonstrated to be regulated by ROS in VSMCs : it's secretion was increased by ROS inducing agent LY83583 and reduced by ROS scavengers such as tiron (Jin et al., 2000). When secreted, it acts as a potent chemo-attractant for inflammatory cells (Sherry et al., 1992; Xu et al., 1992) and increases VSMC MMP activity which ultimately results in the development of vascular disease such as atherosclerosis and abdominal aortic aneurysm (Satoh et al., 2009). However, most of the previous studies have been focused on VSMCs as the main cellular source of vascular CypA (Jin et al., 2000; Jin et al., 2004). There was only one study that demonstrated

secretion of CypA by primary human umbilical vein endothelial cells in response to lipopolysaccharide stimulation (Kim et al., 2004).

6.2 Hypothesis and aims

Given the evidence from previous studies that CypA:

1) is regulated by ROS
2) plays a central role in Ang II induced vascular disease through activation of VSMCs, recruitment of inflammatory cells and activation of MMPs.
3) can be secreted by endothelial cells

I hypothesize that CypA could be the candidate ROS dependent endothelial factor secreted by Nox2 Tg endothelial cells that regulates VSMC activation.

To test this hypothesis, I aim in this chapter:

- To develop methods to detect CypA in conditioned media of endothelial cells including the generation of negative controls
- To examine whether CypA can be secreted by primary endothelial cells and VSMCs isolated from wild-type and Nox2 Tg mice at baseline and after Ang II stimulation.
- To characterise the functional role of CypA:
    - In the activation of VSMCs and Erk1/2 phosphorylation
    - In the induction of ROS production in primary VSMCs
    - In the induction of other functional differences in VSMCs
- To examine the differences in CypA secretion between wild-type and Nox2 Tg aortas.

6.3 Methods

Most of the methods used in this chapter have been described in details in the previous chapters. Only methods and reagents that were used specifically in the experiments for this chapter are described below.

6.3.1 **Preparation of conditioned media from aorta**

Aortas were harvested from aortic arch to the renal arteries from terminally anaesthetised mice and placed into 12 well plate containing 300µl of serum free DMEM for 4 hours at 37ºC. The culture media was removed, spun sequentially at 1,200, 3,000 and 13,000 rpm to remove cellular debris and 20µl of the media was loaded for western blotting.

For the experiments using aorta segments, aortas were cut into 3 segments of the same size using a scalpel. Each segment was placed into a 12 well plate containing 300µl of serum free DMEM for 4 hours with or without Ang II stimulation. Media were harvested and prepared for western blotting as described above.

6.3.2 **siRNA knockdown of CypA**

siRNA is a commonly used technique to knockdown specific gene expression. sEND.1 cells (1 x 10^5/per well) were seeded into 6 well plates and grown to 80% confluency. CypA siRNA (2 µM) or appropriate controls including scrambled siRNA and GADPH siRNA were added to cells in 3 µl of transfection reagent (Dharmacon, USA) to make a final siRNA concentration of 100 nM per well. The cells were then incubated for 48 hours and lysed for western blot analysis.

6.4 Results

6.4.1 **Detection of CypA**

CypA is a novel cytokine, and there is currently no commercially available ELISA kit for its detection, so western blotting remains the most commonly used method for the detection of CypA. Aortic homogenates were used initially to test the CypA antibody. At antibody concentration of 1:10,000, a single protein band was detected at 18 kDa which corresponded to the predicted size of CypA (Figure 6.1 A). To optimise the protein concentration, the lysates of sEND.1 cells were used at 5, 10 and 20 µg of protein concentration with a commercial human recombinant CypA as positive control. Similar to the aorta homogenates, an 18 kDa band was detected in sEND.1 cell lysates. However, the human recombinant CypA was observed at 24 kDa in contrast to the information given by the company. It was not possible therefore to conclude from these experiments that the 18 kDa bands observed in western blots were CypA.

Figure 6.1

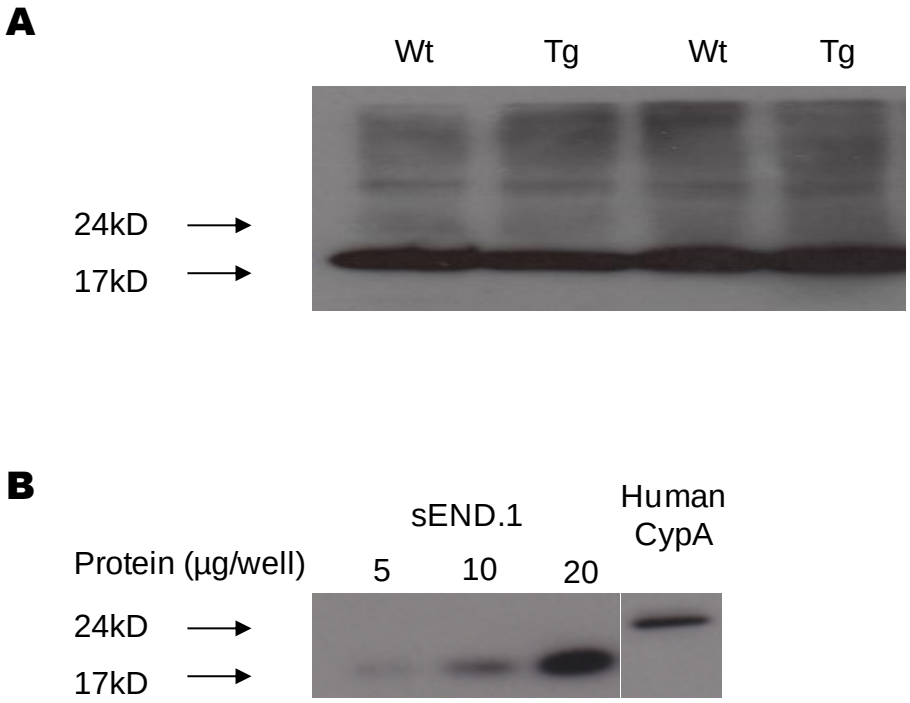


Figure 6.1 CypA antibody detected a protein band at 18 kDa in aortic homogenates and in sEND.1 cell lysates

Representative western blots from aorta homogenates and sEND.1 lysates probed with CypA antibody at 1:10,000 dilutions. **(A)** Aortas from wild-type and Nox2 Tg were homogenised and the protein concentrations were measured as described in Chapter 2. 20µg of proteins/per sample were loaded. **(B)** sEND.1 cell lysates at 5, 10 or 20 µg of proteins were probed with CypA antibody, and a commercially available human recombinant CypA was used as positive control. A protein band at 18 kDa was readily detectable in both aorta homogenates and sEND.1 lysates which corresponded to the predicted size of mouse CypA. The commercial human recombinant CypA was detected at 24kDa.

A negative control of CypA western blot was therefore required in order to confirm that the 18 kDa bands detected in both aorta homogenates and sEND.1 cell lysates were indeed CypA. The negative control was obtained from cells in which CypA expression was knocked down using SiRNA or from tissues isolated from $CypA^{-/-}$ mice.

6.4.1.1 siRNA knockdown of CypA

CypA siRNA, non-targeting siRNA control and GAPDH siRNA control were ordered from Dharmacon. GAPDH was chosen because Dr M. Crabtree (in our laboratory) had previously demonstrated successfully GAPDH knockdown using the same protocol so it was ideal as a positive control for the transfection (Crabtree et al., 2009).

sEND.1 cells were plated into 6 well plates and CypA knockdown was performed as described in Methods. The initial attempt was made using Fugene HD (Promega) as the transfection reagent, but the knockdown experiment was unsuccessful even in the GAPDH control (Figure 6.2 A). A second attempt was made with Dharmafect (Dharmacon, USA) transfection reagent and it was observed that in Dharmafect and GAPDH siRNA treated cells there was a significant reduction of the GADPH protein band indicating successful knockdown of GAPDH. Similarly, in cells treated with CypA siRNA, there was a significant reduction in the 18 kDa protein bands to almost undetectable levels compared to untreated cells, or cells treated with transfection reagent only or cells treated with scrambled siRNA controls (Figure 6.2 B). These experiments suggested that the 18 kDa protein band detected by the western blots was CypA.

Figure 6.2

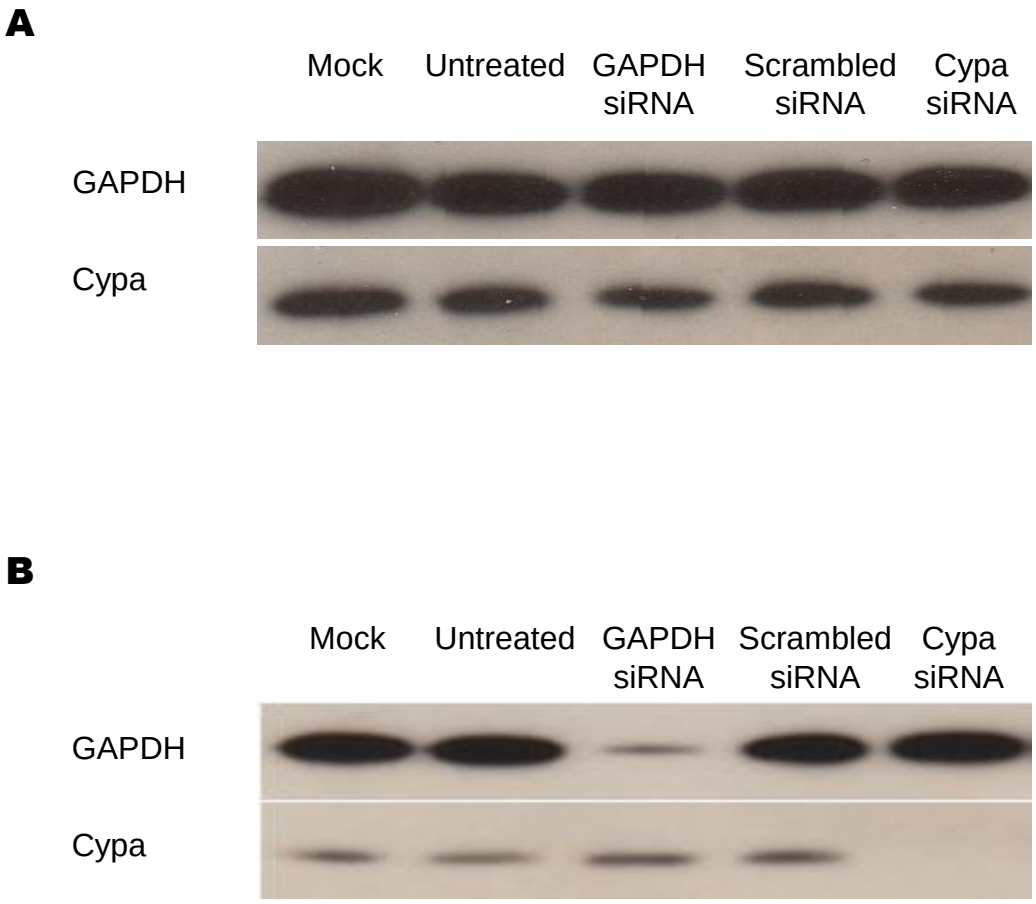


Figure 6.2 siRNA knockdown of CypA in sEND.1 cells detected by Western blot.

Representative western blots of siRNA knockdown of CypA in sEND.1 cells. siRNA was added to each well to a final concentration of 100 nM in 3 µl of transfection agent. Mock – cells treated with transfection agent only; Untreated – cells were not treated with transfection agent or siRNA; Scrambled siRNA – cells treated with non-targeting control siRNA. **(A)** Unsuccessful experiments of siRNA knockdown of GAPDH or CypA using Fugene HD transfection reagent. **(B)** Successful siRNA knock-down of GAPDH or CypA using Dharmafect transfection reagent. Cells treated with CypA siRNA had a significant reduction in the 18 kDa protein band which suggested that 18 kDa band was CypA.

6.4.1.2 CypA$^{-/-}$ mice

To further test whether the 18 kDa western blot band corresponded to CypA, tissues isolated from CypA knockout mice (kind gift from Prof Blomgren, Karolinska Institutet) were used for following experiments. Aortas from CypA$^{-/-}$ mice were homogenised, prepared for western blotting and probed for the presence of CypA along with cell lysates from CypA siRNA knockdown sEND.1 cells, wild-type aortas and control sEND.1 lysates. Similar to what I observed in CypA siRNA knockdown cell lysates, the 18 kDa protein band was absent in aortas from CypA knockout mice thus confirming that the band at 18 kDa was CypA (Figure 6.3).

Figure 6.3

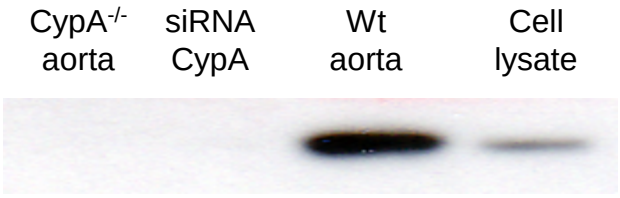


Figure 6.3 Western blot using aorta tissues from CypA knockout mice confirmed that protein band detected at 18 kDa was CypA

Representative western blot of aortas from CypA$^{-/-}$ mice, wild-type mice and cell lysates from control sEND.1 cells or cells after CypA SiRNA knockdown were probed for presence of CypA. The 18 kDa protein band was not detected in either CypA$^{-/-}$ aortas or in siRNA knocked down sEND.1 cell lysates. These results confirmed the 18 kDa band as CypA.

6.4.2 **Ang II induced CypA secretion by sEND.1 cells in low glucose medium but not in high glucose medium (DMEM)**

Having established the method for the detection of CypA using western blot, I next addressed the questions of whether CypA was secreted by endothelial cells and if the secretion was upregulated by Ang II. sEND.1 cells were initially examined to establish the method and the optimum Ang II incubation time required for CypA secretion.

sEND.1 cells were plated at $1x10^4$ cells per well in 12 well plates and incubated only in DMEM as baseline controls or in the presence of Ang II (at concentrations of 10^{-8}, 10^{-7} or 10^{-6} M) for 0, 6, 8, 16 or 24 hours. The DMEM used routinely was high glucose concentration (25mM) and it was observed that sEND.1 cells cultured in high glucose DMEM secreted CypA that was detectable by western blot after 16h of culture (Figure 6.4 A) but Ang II had no significant effect on the levels of CypA secretion. A literature search revealed that high glucose (>20mM) is a potent stimuli for ROS production and caused endothelial activation (Cosentino et al., 1997). This may explain the high endothelial CypA detected even at baseline (unstimulated) (Figure 6.4 A). To investigate this, sEND.1 cells were incubated in low glucose (5.56mM) DMEM. In contrast to the high glucose DMEM, I found that at baseline (without Ang II), even after 24h of incubation CypA was barely detectable (Figure 6.4 B). When cells were stimulated with Ang II there was a dose dependent increase in the levels of CypA secretion (Figure 6.4 B). Wild-type aorta homogenates were used as positive controls, and CypA siRNA knockdown cell lysates were used as negative controls.

Figure 6.4

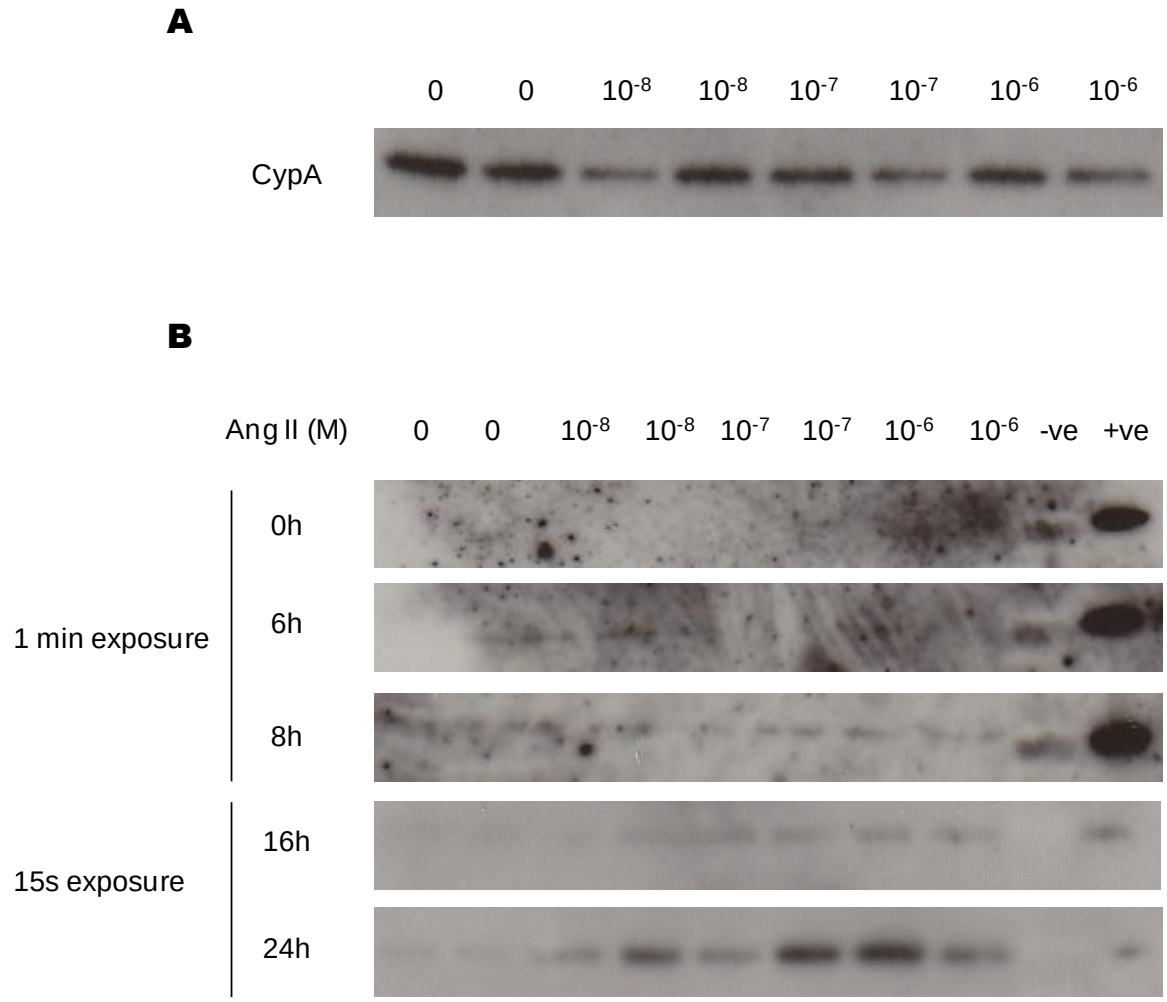


Figure 6.4 Dose and time dependent secretion of CypA in response to Ang II stimulation by sEND.1 cells cultured in low concentration of glucose DMEM.

sEND.1 cells ($1x10^4$/per well) were plated in 12 well plates and treated with Ang II at doses of 10^{-8}, 10^{-7}, and 10^{-6} M over 0, 6, 8, 16 and 24h in either high concentration (25mM) or low concentration (5.56mM) glucose serum free DMEM. **(A)** Representative western blot of sEND.1 cells incubated in high glucose concentration DMEM for 16 h. **(B)** Representative western blots of sEND.1 cells incubated in low concentration of glucose DMEM. The optimal exposure for 0, 6h, 8h blots was for 1 min and 15s for 16 and 24h blots. CypA was readily detectable after 16 h in sEND.1 cells incubated in low glucose DMEM and showed a dose dependent increase in response to Ang II stimulation.

6.4.3 Nox2 Tg endothelial cells secreted higher levels of CypA at baseline compared to wild-type endothelial cells

Having established that sEND.1 endothelial cells secreted CypA, I next examined CypA secretion from primary endothelial cells isolated from wild-type and Nox2 Tg mice after 3 days of culture. On day 3, primary endothelial cells were washed with PBS and incubated in serum free low glucose DMEM for 24h with or without Ang II (10^{-7}M) stimulation. The media was then harvested and prepared for CypA western blot. As CypA is abundantly expressed intracellularly, cell death will release CypA into the media and confound the results. To control for the potential leaking of CypA from dead cells, conditioned media was also western blotted for secreted GAPDH as GAPDH should increase in the event of cell death. After the collection of the media, cells were lysed and western blotted for α-actinin (protein loading control), CD102 (endothelial cell marker) and CypA.

There was a significant 2 fold increase of CypA in Nox2 Tg endothelial conditioned media (CM) at baseline (unstimulated) compared to wild-type controls (Figure 6.5, Figure 6.6). In response to Ang II (10^{-7}M) stimulation, wild-type endothelial cells increased CypA secretion, whereas Nox2 Tg endothelial cells had no further increase in CypA secretion (Figure 6.6). These results indicated that Nox2 Tg endothelial cells were already activated with maximal CypA secretion even at baseline. GAPDH was not detected in the conditioned media from either wild-type or Nox2 Tg endothelial cells indicating the results were not confounded by cell death. As an additional control, the expression of intra-cellular CypA levels was assessed by western blotting. There was no significant difference in intracellular CypA levels between the wild-type and Nox2 Tg endothelial cells suggesting intracellular CypA was not affected by the Nox2 transgene or Ang II stimulation. CD102 (an endothelial cell marker) was used to confirm cell specificity and α-actinin was used as a protein loading control.

Figure 6.5

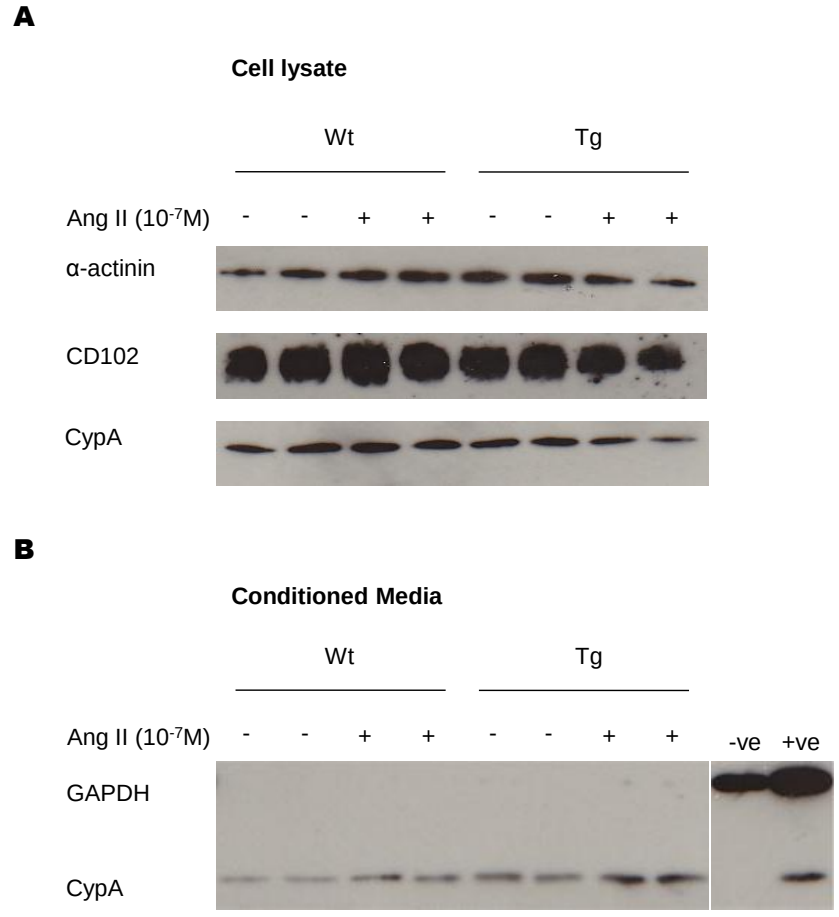


Figure 6.5 Increased CypA in Nox2 Tg primary endothelial conditioned media compared to wild-type endothelial cell conditioned media.

Representative western blots of primary endothelial cells isolated from wild-type and Nox2 Tg mice following 3 days of cell culture and stimulated with or without Ang II (10^{-7}M). **(A)** Cell lysates were probed for α-actinin (protein loading control), CD102 (endothelial cell marker) and CypA. **(B)** Conditioned cell culture media were probed for GAPDH and CypA. CypA siRNA knockdown sEND.1 lysates were used as negative control (-ve), and aorta homogenates from wild-type mice were used as positive control (+ve) for CypA.

Figure 6.6

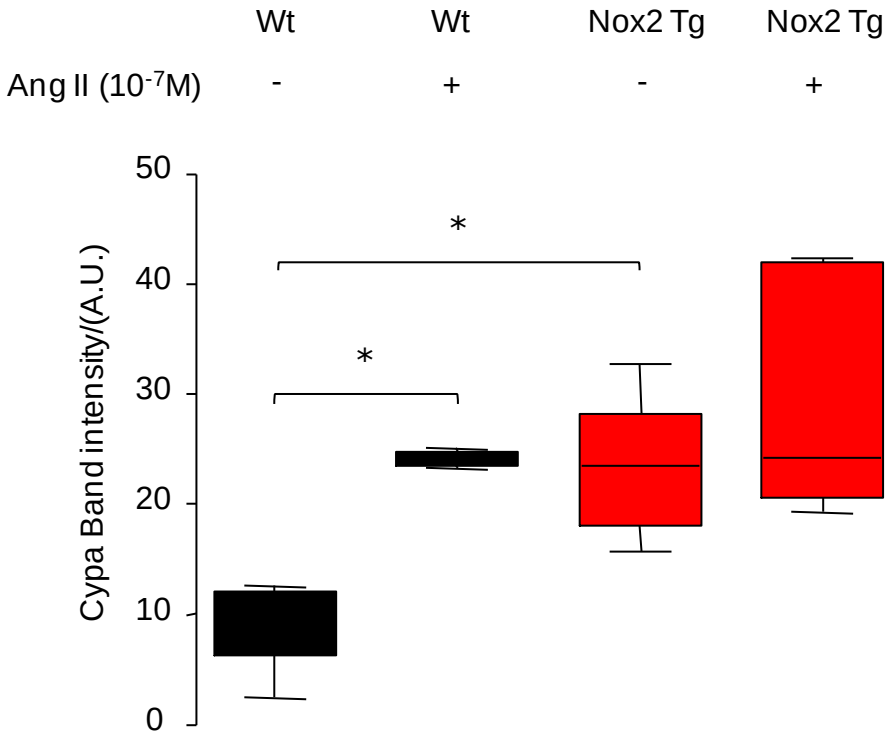


Figure 6.6 Increased CypA secretion in the conditional media of Nox2 Tg endothelial cells compared to wild-type controls at baseline.

Western blots of conditioned media from cultured primary endothelial cells were quantified using band intensity. Data are expressed as median±interquartile range. A.U. – arbitrary units. *$p<0.05$, n=4 independent experiments, and 8 animals per group per experiment. CypA secretion by Nox2 Tg endothelial cells was significantly increased compared to wild-type cells at baseline. Wild-type endothelial cells increased CypA secretion in response to Ang II (10^{-7}M) stimulation, whereas no further elevation in CypA secretion was observed in Nox2 Tg endothelial cells.

6.4.4 Increased CypA secretion is associated with increased Erk1/2 phosphorylation in Nox2 Tg endothelial cells

It had been shown previously by Dr J. Bendall (in our laboratory) that Nox2 Tg aortas had increased Erk1/2 phosphorylation when compared to the wild-type controls. Erk1/2 is involved in many cellular signalling pathways involved in cell proliferation and gene expression, and it is commonly used as a marker of cell activation. Given the increase in ROS and CypA secretion by Nox2 Tg endothelial cells at baseline, it would be interesting to examine if these cells were already in an activated state. Primary endothelial cells were harvested following media collection and lysed in lysis buffer containing protease and phosphatase inhibitors. Cell lysates (20 µl/per sample) were loaded for western blot and probed for phosphorylated Erk1/2 using a phos-Erk1/2 specific antibody. Total Erk1/2 in the same sample was used as controls. A significant 2 fold increase in Erk1/2 phosphorylation in Nox2 Tg endothelial cells was observed at baseline compared to the wild-type control cells (Figure 6.7 A, B). When cells were stimulated with Ang II, wild-type endothelial cells increased Erk1/2 phosphorylation to a similar extent as detected in Nox2 Tg cells at baseline. However, there was no further increase in Erk1/2 phosphorylation in Nox2 Tg endothelial cells stimulated with Ang II (Figure 6.7 A, B), suggesting that Erk1/2 was already activated under basal conditions in endothelial cells over-expressing Nox2.

Figure 6.7

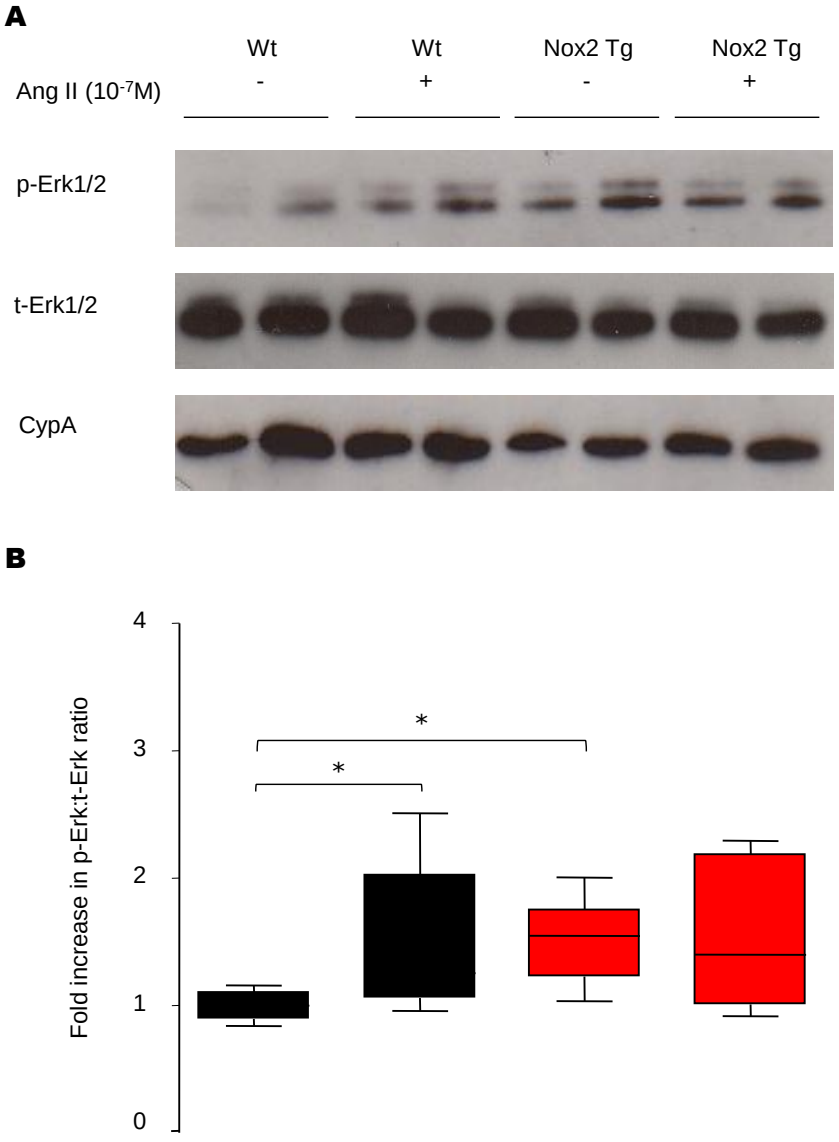


Figure 6.7 Increased Erk1/2 phosphorylation at baseline in Nox2 Tg endothelial cells compared to the wild-type

Primary endothelial cells were cultured for 3 days, incubated for 24 h in serum free DMEM with or without Ang II (10^{-7} M) stimulation. Endothelial cells were then harvested for western blot. **(A)** Representative western blots of endothelial cell lysates probed for phosphorylated Erk1/2 (p-Erk1/2) and total Erk1/2 (t-Erk1/2). **(B)** Densitometric analysis of western blots. Data were presented as fold increase in the ratio of phosphorylated Erk1/2 and total Erk1/2 with baseline defined as 1. Data are expressed as median±interquartile range. *$p<0.05$, n=4 independent experiments, and 2 animals from each genotype per treatment group per experiment. Nox2 Tg endothelial cells had significantly higher levels of phosphorylated Erk1/2 at baseline compared to wild-type endothelial cells.

6.4.5 **No difference CypA secretion between wild-type and Nox2 Tg VSMCs**

Primary VSMCs were tested first for CypA secretion according to established protocol (Jin et al., 2000; Satoh et al., 2009). Primary VSMCs were cultured for 2 passages and then split equally into 6 well plates and grown to confluency. Cells were then incubated in serum free DMEM for 24 h and the culture media was harvested for the detection of CypA using western blot.

No secreted CypA was detected at baseline in the conditioned media from either wild-type or Nox2 Tg VSMCs. When cells were stimulated with Ang II (10^{-6}M), both wild-type and Nox2 Tg VSMCs demonstrated increase in CypA secretion (Figure 6.8 A). There was no increase in CypA at 10^{-4}M most likely due to down-regulation of AT1 receptors from Ang II over-stimulation (Lassegue et al., 1995). Following on from this experiment, the protocol was refined and primary VSMCs were plated in 12 well plates instead of 6 wells which reduced the number of cells (hence aortas) required and was also more comparable to the experimental conditions used for endothelial cells. GADPH was used as a control for possible intracellular protein leakage due to cell death. It was observed that there was significant cell death in some of the VSMCs as indicated by the large GAPDH bands (Figure 6.8 B). Accompanied with increased GAPDH there were high levels of CypA (released by the dead cells) detected in the conditioned media (Figure 6.8 B). CypA siRNA knockdown sEND.1 cell lysates were used as negative controls and normal sEND.1 lysates were used as positive controls.

Figure 6.8

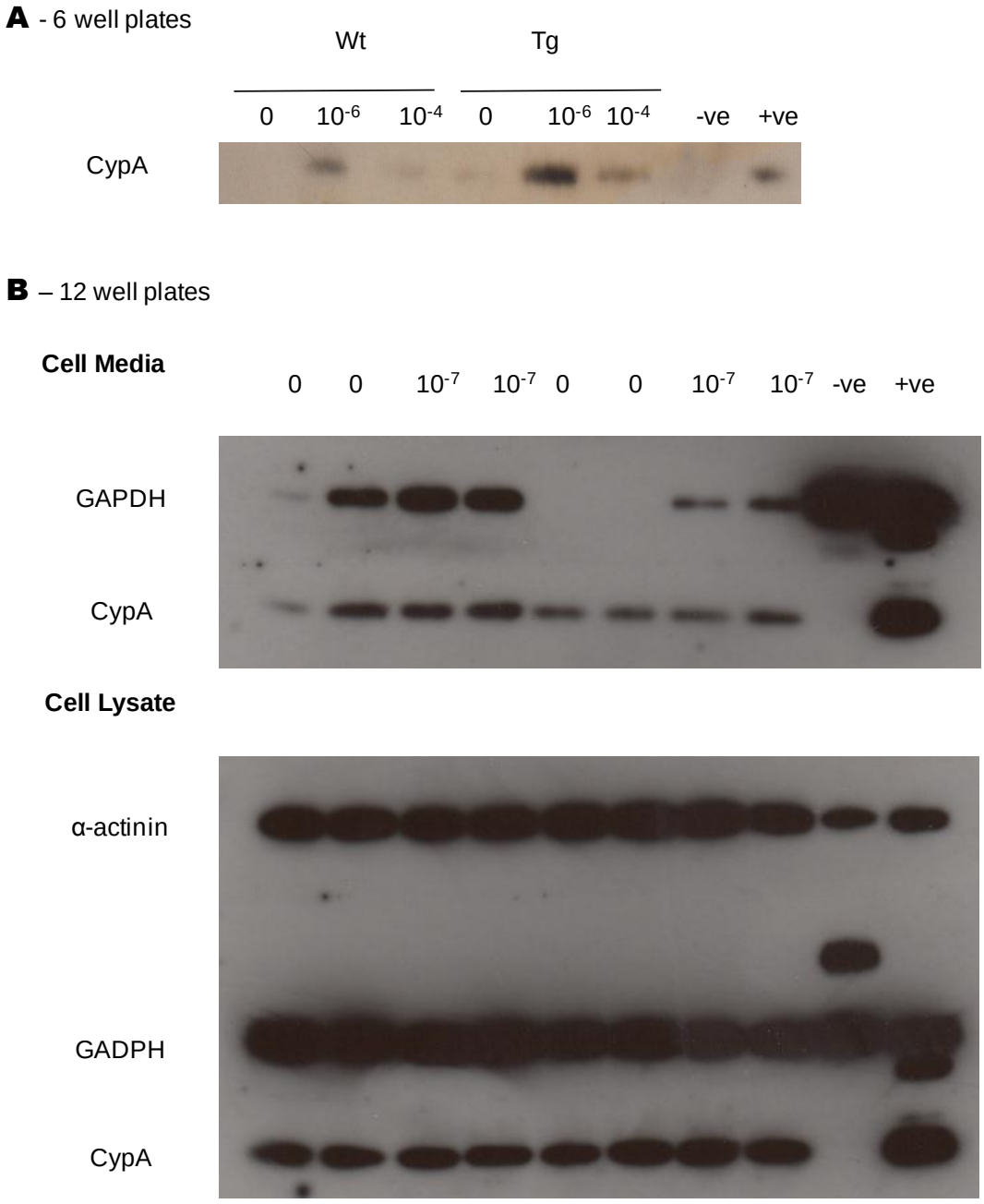


Figure 6.8 Dose dependent increase in CypA secretion by VSMCs in response to Ang II stimulation

Representative western blots of conditioned media from primary VSMCs after 24 h incubation in serum free DMEM with or without Ang II stimulation. **(A)** CypA in conditioned media from VSMCs cultured in 6 well plates stimulated with Ang II at 0, 10^{-6} M and 10^{-4} M. **(B)** CypA in conditioned media from VSMCs cultured in 12 well plates stimulated with Ang II at 10^{-7} M. Incubation of primary VSMCs for 24h in serum free DMEM caused significant cell death in both wild-type and Nox2 Tg VSMCs as indicated by the presence of GADPH protein band detected in the conditioned media.

On reviewing of the methods, it was noted that the VSMCs were grown in 20% FBS DMEM before being incubated in serum free DMEM. The sudden depletion of FBS in the culture medium may have contributed to cell death observed in the above experiments. Therefore, the method of VSMC cell culture was modified for the next experiment such that VSMCs were incubated in 10% FBS for 1 week in 12 well plates before serum starvation. In the conditioned media from these VSMCs, no GAPDH protein band was observed. Secreted CypA was barely detectable. There was no significant difference in the secreted CypA between wild-type and Nox2 Tg VSMCs either at baseline or after Ang II stimulation (Figure 6.9).

Figure 6.9

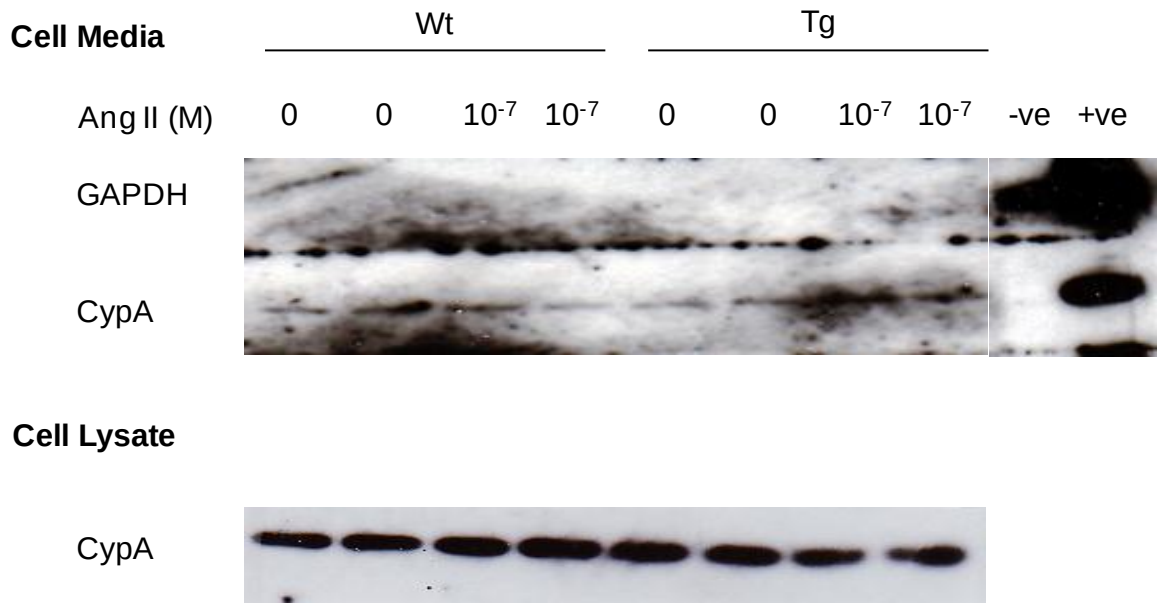


Figure 6.9 No difference in CypA secretion between wild-type and Nox2 Tg VSMCs either at baseline or after Ang II stimulation

VSMCs were isolated and cultured for 1 week in 20% FBS. Cells were then passaged and cultured for another week in 10% FBS before being incubated in serum free DMEM for 24h with or without Ang II (10^{-7}M) stimulation. Top blot: representative western blot of VSMC conditioned media probed for GAPDH and CypA. Bottom blot: representative western blot of VSMC lysates from which conditioned media was harvested. No significant difference in the levels of secreted CypA was observed between wild-type and Nox2 Tg VSMCs at either baseline or after Ang II stimulation.

It can be seen from Figure 6.9 that secreted CypA was difficult to detect by western blot in conditioned media from VSMCs so to improve detection, protein concentrators were used to increase the concentration of CypA (Jin et al., 2000; Satoh et al., 2009). The concentration of proteins in the conditioned media was increased by upto 10 fold using the Amicon Ultra Concentrators. The concentrated conditioned media was then blotted for CypA. The detection of VSMCs CypA improved significantly and it was more apparent that there was no significant difference in the levels of either basal or Ang II-induced CypA secretion between VSMCs isolated from wild-type and Nox2 Tg mice (Figure 6.10)

Figure 6.10

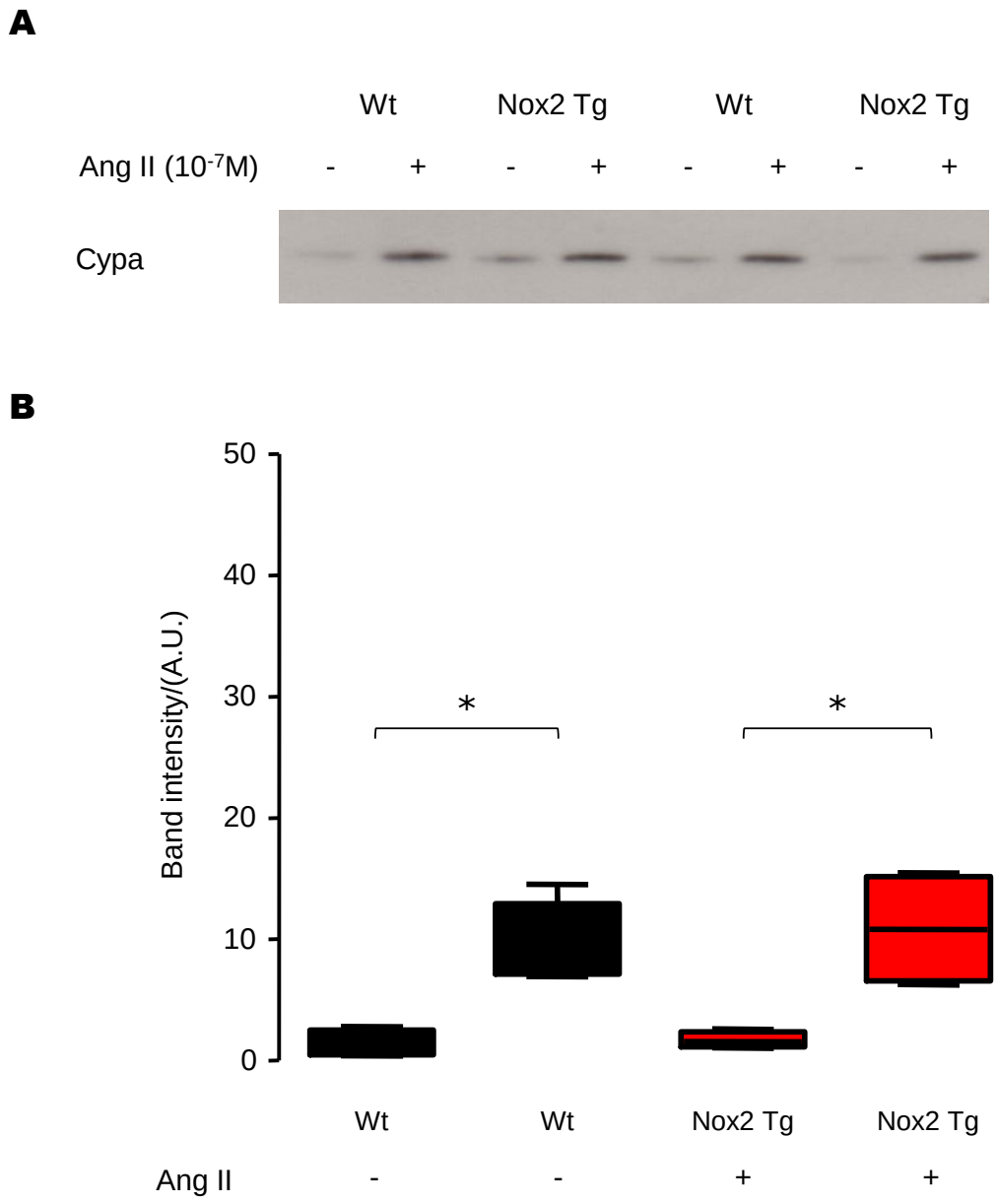


Figure 6.10 No difference in secreted CypA between VSMCs isolated from wild-type and Nox2 Tg mice after using protein concentrator.

Wt and Nox2 Tg conditioned media were concentrated by upto 10 fold using Amicon Ultra concentrators and detected for the presence of CypA by western blot. **(A)** Representative western blot of concentrated VSMC conditioned media for CypA secretion with or without Ang II (10^{-7} M) stimulation. **(B)** Densitometric quantification of CypA protein band. A.U. – arbitrary units. Data are expressed as median±interquartile range. *$p<0.05$, n= 6 independent experiments, and n=4 animals per group per experiment. There was no significant difference in secreted CypA at either baseline or after Ang II stimulation between wild-type and Nox2 Tg VSMCs.

6.4.6 No significant difference Erk1/2 phosphorylation between wild-type and Nox2 Tg VSMCs in response to either acute or chronic Ang II stimulation

Given than there was no significant difference in the levels of CypA secretion by VSMCs isolated from wild-type and Nox2 Tg mice either at baseline or after Ang II stimulation, I next examined whether or not there might be any difference in VSMC activation by looking at the levels of Erk1/2 phosphorylation. Cell lysates of VSMCs from which secreted CypA were examined were probed by western blot for the phosphorylated Erk1/2. Total Erk1/2 from the same samples was used as loading controls.

Similar to what was observed for CypA secretion, there were no significant differences in Erk1/2 phosphorylation between wild-type and Nox2 Tg VSMCs either at baseline or after Ang II stimulation (Figure 6.11 A, B). There was an equal increase in Erk1/2 phosphorylation in response to Ang II stimulation between wild-type and Nox2 Tg VSMCs. To further investigate this observation, VSMCs were serum starved overnight in serum free DMEM and stimulated acutely for 0, 5, 15, or 30 minutes with Ang II (10^{-7}M). An equal time-dependent increase in Erk1/2 phosphorylation was observed in wild-type and Nox2 Tg VSMCs, which confirmed that there was no significant difference in Erk1/2 response to Ang II stimulation between VSMCs isolated from wild-type and Nox2 Tg mice (Figure 6.12 A, B).

Figure 6.11

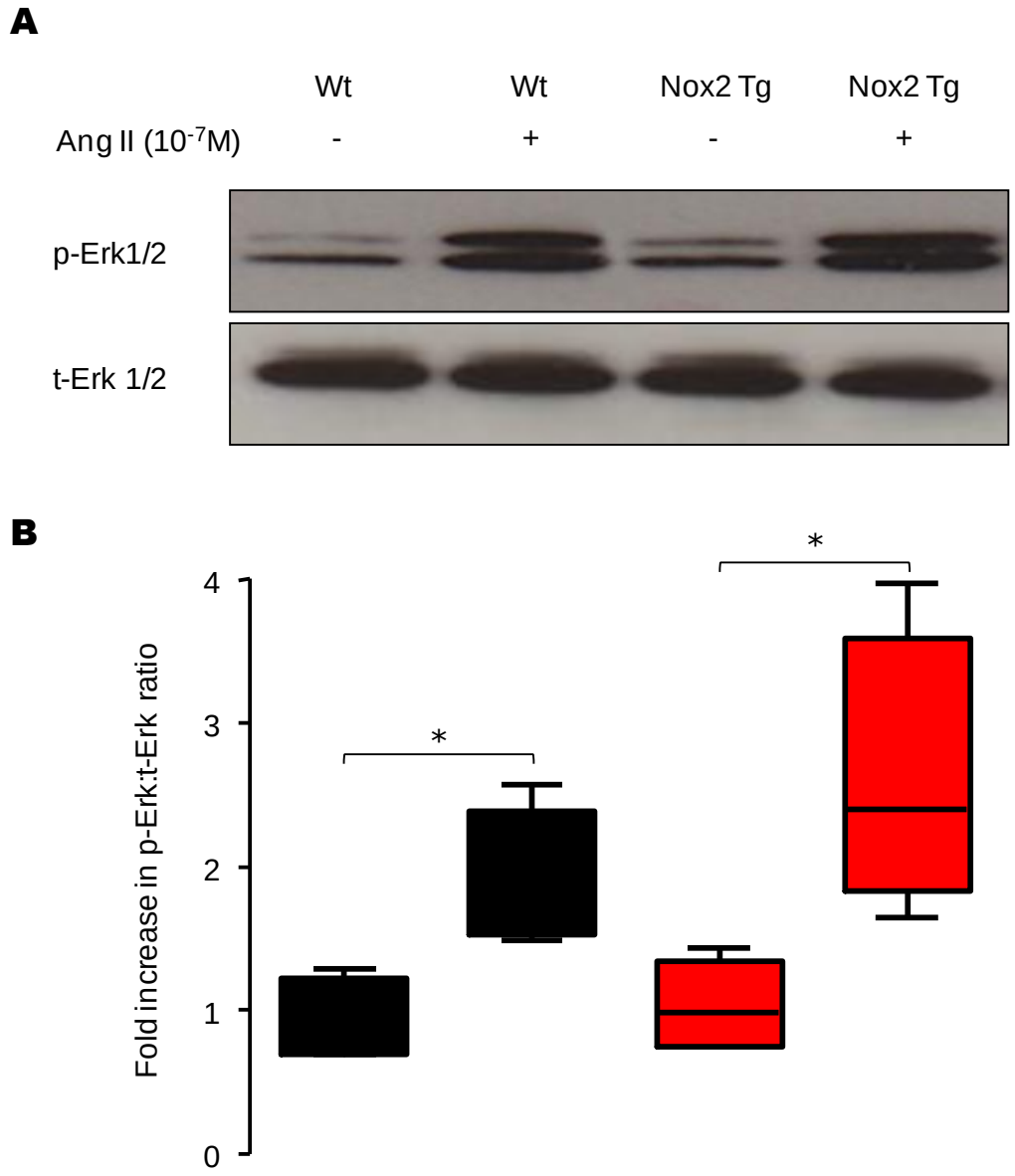


Figure 6.11 No difference in Erk1/2 phosphorylation in VSMCs isolated from wild-type and Nox2 Tg mice either at baseline or after Ang II stimulation.

VSMCs were incubated for 24h in serum free DMEM with or without Ang II (10^{-7}M). Cells were then harvested for the detection of phosphorylated and total Erk1/2 expression by Western blot. **(A)** Representative western blot of VSMCs lysates probed for phosphorylated and total Erk1/2. **(B)** Densitometric analysis of Western blots. Data were presented as thefold increase in the ratio of phosphorylated Erk1/2 and total Erk1/2 with baseline defined as 1. Data expressed as median ± interquartile range. *$p<0.05$, n=4 independent experiments, and 4 animals per group per experiment. No significant difference was observed in the levels of Erk1/2 phosphorylation between wild-type and Nox2 Tg VSMCs either at baseline or after Ang II stimulation.

Figure 6.12

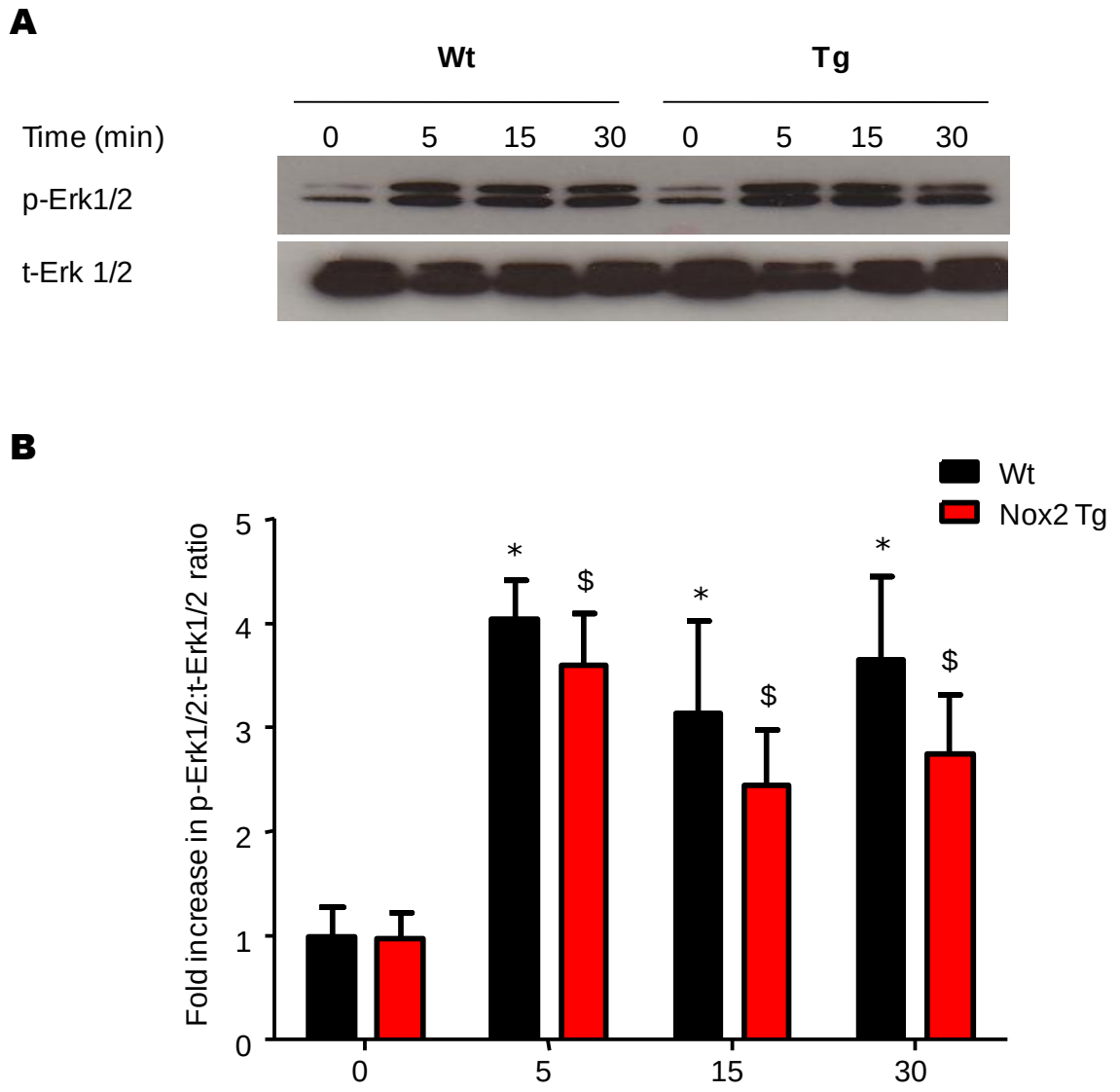


Figure 6.12 Time dependent increase in phosphorylated Erk1/2 in response to acute Ang II stimulation.

VSMCs were serum starved overnight and stimulated with Ang II (10^{-7}M) for 0, 5, 15 and 30 min. Cells were harvested and western blotted for the levels of phosphorylated Erk1/2 and total Erk1/2. **(A)** Representative western blot of VSMC lysates probed for the phosphorylated Erk1/2 and total Erk1/2. **(B)** Densitometric analysis of western blots. Data presented as fold increase in the ratio of phosphorylated Erk1/2 and total Erk1/2 with baseline defined as 1. Data expressed as mean±SEM. *$p<0.05$ for indicated data compared to the data of wild-type VSMCs at time point 0; $^{\$}p<0.05$ for indicated data compared to the data of Nox2 Tg VSMCs at time point 0; n=3 independent experiments, n=4 animals per experiment.

6.4.7 **Exogenous CypA can induce Erk1/2 phosphorylation in VSMCs**

I have shown that Nox2 Tg endothelial cells had increased CypA secretion at both baseline and in response to Ang II stimulation compared to wild-type endothelial cells. I have also shown that there were no significant differences in CypA secretion between wild-type and Nox2 Tg VSMCs. Based on studies indicating that CypA is involved in Ang II-induced VSMCs activation, my hypothesis was that endothelial CypA could be the secreted factor released in the conditioned media which activated VSMCs and caused Erk1/2 phosphorylation in VSMCs.

To test this hypothesis, purified human recombinant CypA was used to stimulate VSMCs. VSMCs were passaged, serum starved overnight and then stimulated with 0, 10 or 50 nM of human recombinant CypA. There was a CypA dose dependent increase in the levels of Erk1/2 phosphorylation in VSMCs (Figure 6.13 A, B). 50 nM of human recombinant CypA was used next to stimulate VSMCs over a time course of 0, 10, 15 and 20 min. There was a time dependent increase in CypA-induced Erk1/2 phosphorylation (Figure 6.14). These data clearly indicated that CypA could directly activate and induce Erk1/2 phosphorylation in VSMCs and further supported the hypothesis that CypA might be the crucial secreted factor in the endothelial conditioned media.

Figure 6.13

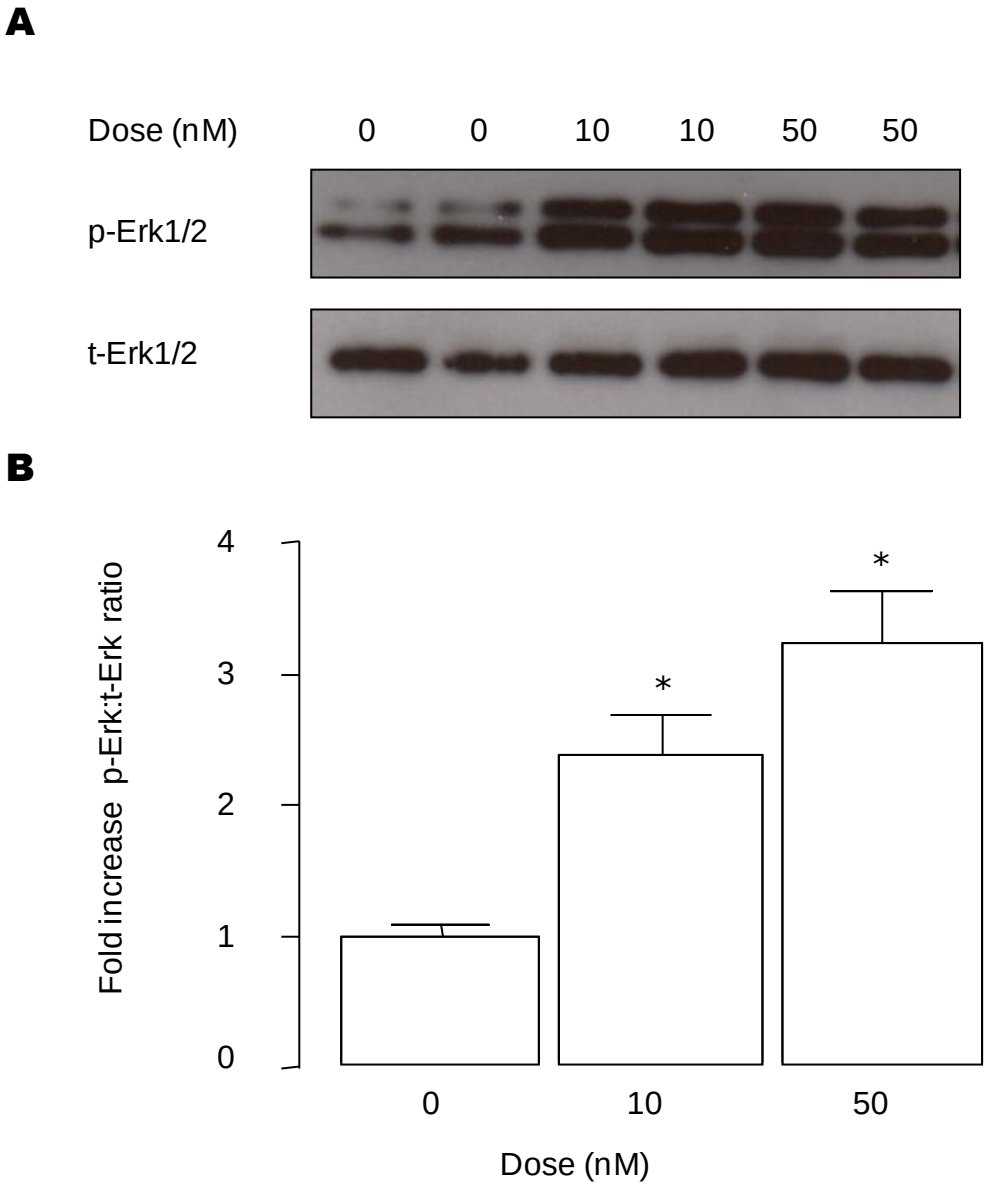


Figure 6.13 Dose dependent VSMC Erk1/2 phosphorylation in response to CypA stimulation

VSMCs isolated from wild-type mice were serum starved overnight and stimulated for 20 min with 0, 10 or 50 nM of human recombinant CypA. **(A)** Representative western blot of VSMCs lysates probed for phosphorylated Erk1/2 and total Erk1/2. **(B)** Densitometric quantification of western blots. Data were presented as fold increase in the ratio of phosphorylated Erk1/2 and total Erk1/2 with baseline defined as 1. Data are expressed as mean±SEM. *$p<0.05$, n=3 independent experiments, and n=4 animals per experiment. A CypA dose dependent response was observed in VSMC Erk1/2 phosphorylation.

Figure 6.14

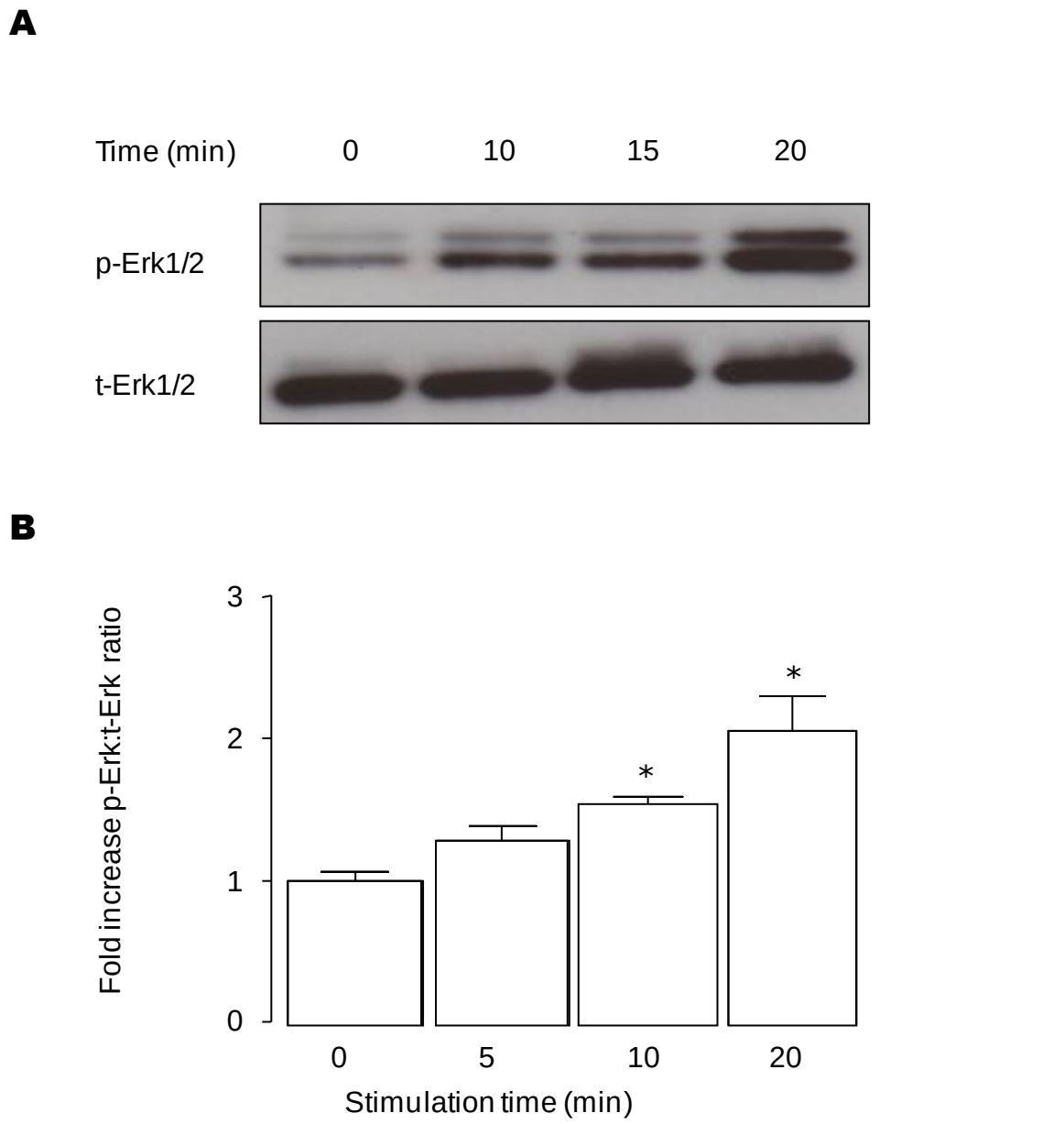


Figure 6.14 Time dependent VSMCs Erk1/2 phosphorylation in response to CypA stimulation

VMSCs isolated from wild-type mice were serum starved overnight and stimulated with 50 nM of human recombinant CypA for 0, 5, 10 and 20 min. **(A)** Representative western blot of VSMC lysates probed for phosphorylated and total Erk1/2. **(B)** Densitometric analysis of western blots. Data were presented as the fold increase in the ratio phosphorylated Erk1/2 and total Erk1/2 with baseline defined as 1. Data are expressed as mean ± SEM. *$p<0.05$, n=3 independent experiments, and n=4 animals per experiment. A time dependent increase in Erk1/2 phosphorylation was observed in VSMCs stimulated with human recombinant CypA.

6.4.8 **sEND.1 endothelial CypA induced Erk1/2 phosphorylation that was abolished by knockdown of CypA.**

My previous experiments indicate that human recombinant CypA can directly induce Erk1/2 phosphorylation and VSMC activation. I next examined whether the same effect could be observed with secreted CypA from sEND.1 endothelial cells. Conditioned media from sEND.1 cells were collected after 24h of culture, concentrated 10 fold using Amicon Ultra concentrator (Millipore, UK) and western blotted for secreted CypA.

As expected, CypA secreted in the conditioned media of sEND.1 was detectable by Western blot (Figure 6.15 A). Primary wild-type VSMCs were serum starved overnight and stimulated with sEND.1 conditioned media for 0, 5, 10 or 20 min. Cells were harvested and Western blotted for phosphorylated Erk1/2 and total Erk1/2. There was a time dependent increase in the levels of Erk1/2 phosphorylation in VSMCs stimulated with sEND.1 conditioned media, which reached the maximum levels around 10 min of stimulation (Figure 6.15 B, C).

Figure 6.15

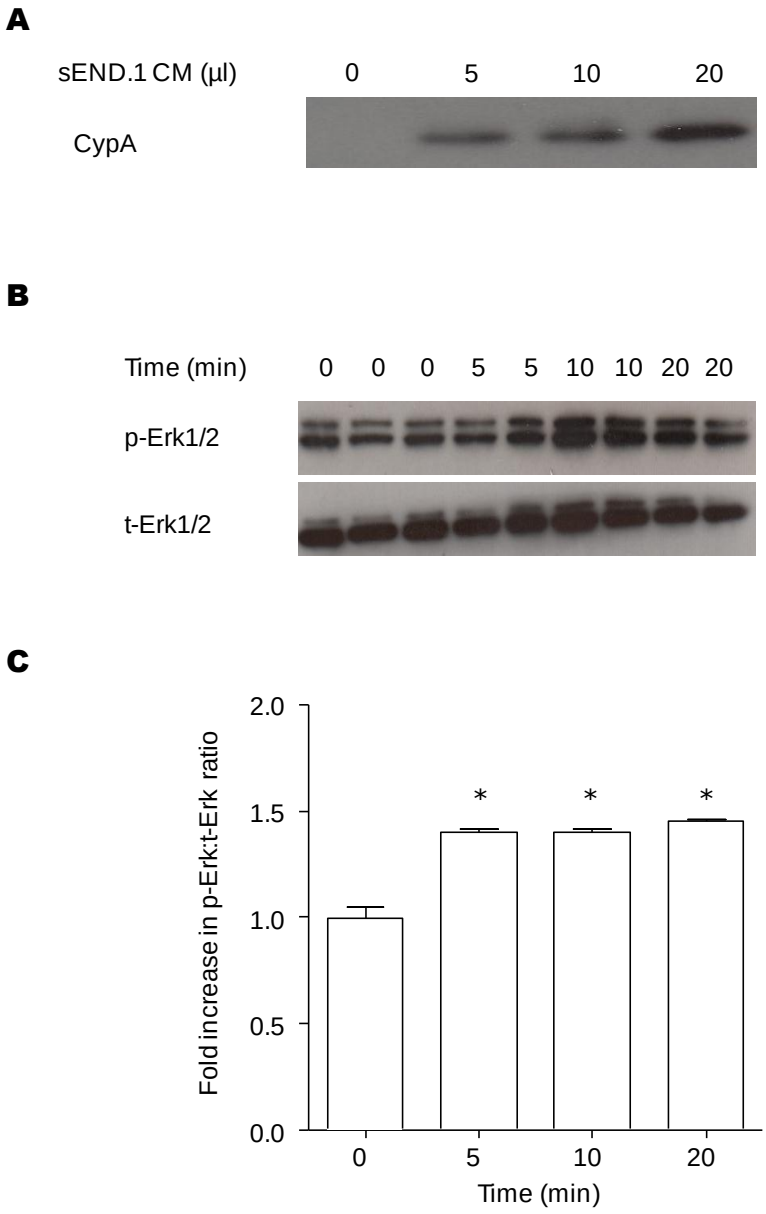


Figure 6.15 Time dependent increase in VSMC Erk1/2 phosphorylation stimulated with sEND.1 CypA

Primary wild-type VMSCs were serum starved overnight and stimulated with sEND.1 conditioned media, CM (20 µl/per well to a total volume 300 µl/well), for 0, 5, 10 or 20 min. Cells were harvested and western blotted for phosphorylated and total Erk1/2. **(A)** Representative western blot of CypA detected in different volumes of sEND.1 conditioned media. **(B)** Representative western blot of phosphorylated Erk1/2 and total Erk1/2 in response to sEND.1 conditioned media stimulation. **(C)** Densitometric analysis of western blots. Data were presented as fold increase in the ratio of phosphorylated Erk1/2 and total Erk1/2 with baseline defined as 1. Data expressed as mean±SEM. *$p<0.05$, n=3 independent experiments.

For knockdown of CypA, sEND.1 cells were incubated with CypA siRNA or controls (untreated, transfection agent only, GADPH siRNA and non-targeting siRNA) as described in Methods for 48 hours. Cells were then washed and incubated in serum free low glucose DMEM for 24h. Cell culture media was harvested and spun sequentially at 1,200, 3,000 and 13,000 RPM. 20µl of the media was loaded to check for knockdown of CypA. Almost complete knockdown of CypA was achieved in both the conditioned media and cell lysate from cells treated with CypA siRNA (Figure 6.16). GAPDH, positive control, was knocked down by >80% in cells treated with GAPDH siRNA.

Figure 6.16

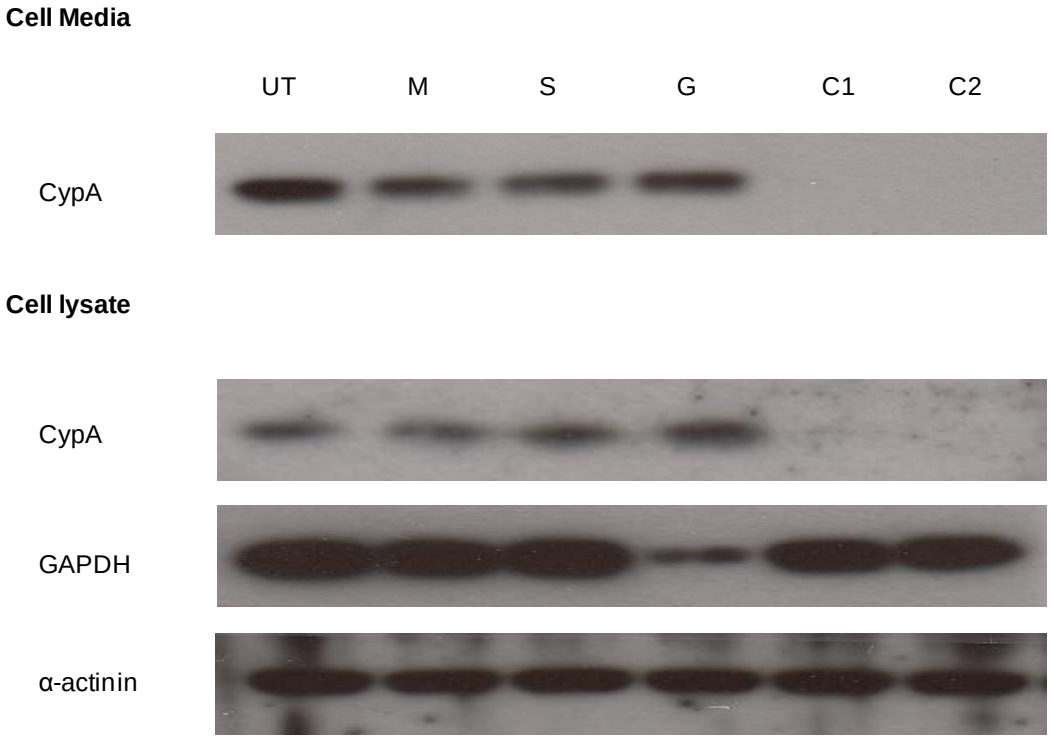


Figure 6.16 Knockdown of CypA in both conditioned media and cell lysate in sEND.1 cells treated with CypA SiRNA

sEND.1 cells were either untreated (UT); or treated with transfection agent only (M), non-targeting siRNA (S), GAPDH siRNA (G) or CypA siRNA (C1 and C2) for 48 hours. Conditioned media were collected and probed for CypA. Cells were lysed in lysis buffer and probed for CypA, GAPDH and α-actinin. CypA was completely knocked down in both conditioned media and cell lysate of sEND.1 cells treated with CypA siRNA.

Media from untreated and CypA siRNA treated sEND.1 cells were concentrated 10 fold using Amicon Ultra Concentrator as described previously. The concentrated stock of conditioned media was then used to treat primary VSMCs to examine the effect of depleting CypA on VSMC Erk1/2 phosphorylation. VSMCs at density of $1x10^4$ were plated in 12 well plates and serum starved overnight. DMEM control, concentrated conditioned media from untreated sEND.1 cells or CypA siRNA treated cells were added to VSMCs and incubated for 10 min. Cells were then harvested and prepared for western blot, probing for phosphorylated and total Erk1/2. Conditioned media from untreated sEND.1 cells (sEND.1 CM) induced a significant increase in Erk1/2 phosphorylation similar to previous experiments when compared to VSMCs treated with DMEM control (Figure 6.17 A, B). This increase in Erk1/2 phosphorylation was abolished when CypA was not present in the conditioned media, indicating CypA is the crucial factor in the conditioned media that mediated the effect on VSMC activation.

Figure 6.17

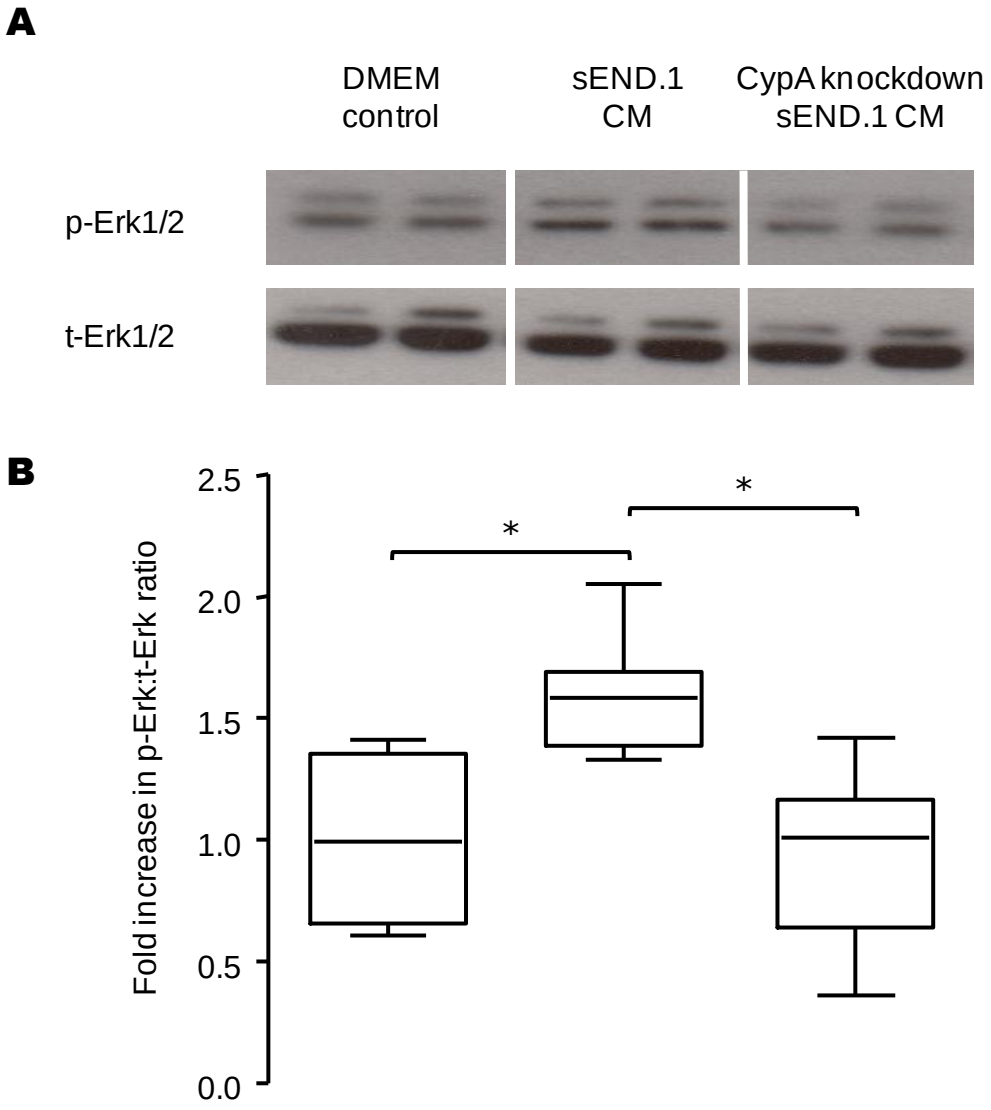


Figure 6.17 sEND.1 conditioned media induced Erk1/2 phosphorylation was abolished by depletion of CypA

Wild-type primary VSMCs ($1x10^4$) were plated in 12 well plates and starved overnight. 10µl of either DMEM control or concentrated conditioned media were added to the VSMCs and incubated for 10 min. VSMCs were then harvested and prepared for western blots probing for phosphorylated and total Erk1/2. **(A)** Representative western blot of cell lysates from VSMCs treated with DMEM control, untreated sEND.1 cell conditioned media (sEND.1 CM) or CypA siRNA treated sEND.1 cell conditioned media (CypA knockdown CM). (B) Densitometric analysis of western blot band intensity presented as the fold increase in the ratio of phosphorylated and total Erk1/2 with baseline defined as 1. Data presented as median±interquartile range. *$p<0.05$, n=3 independent experiments. Untreated sEND.1 CM induced a significant increase in Erk1/2 phosphorylation which was abolished by depletion of CypA.

To confirm the important finding that CypA was the crucial secreted factor from endothelial cells, I repeated the experiment in Chapter 5, Figure 5.14 where I initially demonstrated the presence of a transferable endothelial factor. Human CypA and sEND.1 CypA were used as positive controls.

At the end of the experiment, the conditioned media that were used to stimulate the VSMCs were harvested and examined for the levels of CypA. As expected, conditioned media from Nox2 Tg endothelial cells contained greater secreted CypA compared to conditioned media from wild-type endothelial cells (Figure 6.18 A). Greater secreted CypA in Nox2 Tg endothelial conditioned media was associated with greater Erk1/2 phosphorylation in the VSMCs. Interestingly, human CypA and CypA in sEND.1 conditioned media also induced Erk1/2 phosphorylation to a similar extent observed with Nox2 Tg endothelial conditioned media (Figure 6.18 A, B). These results suggested that increased Erk1/2 phosphorylation was not related to a particular form or preparation of CypA.

Figure 6.18

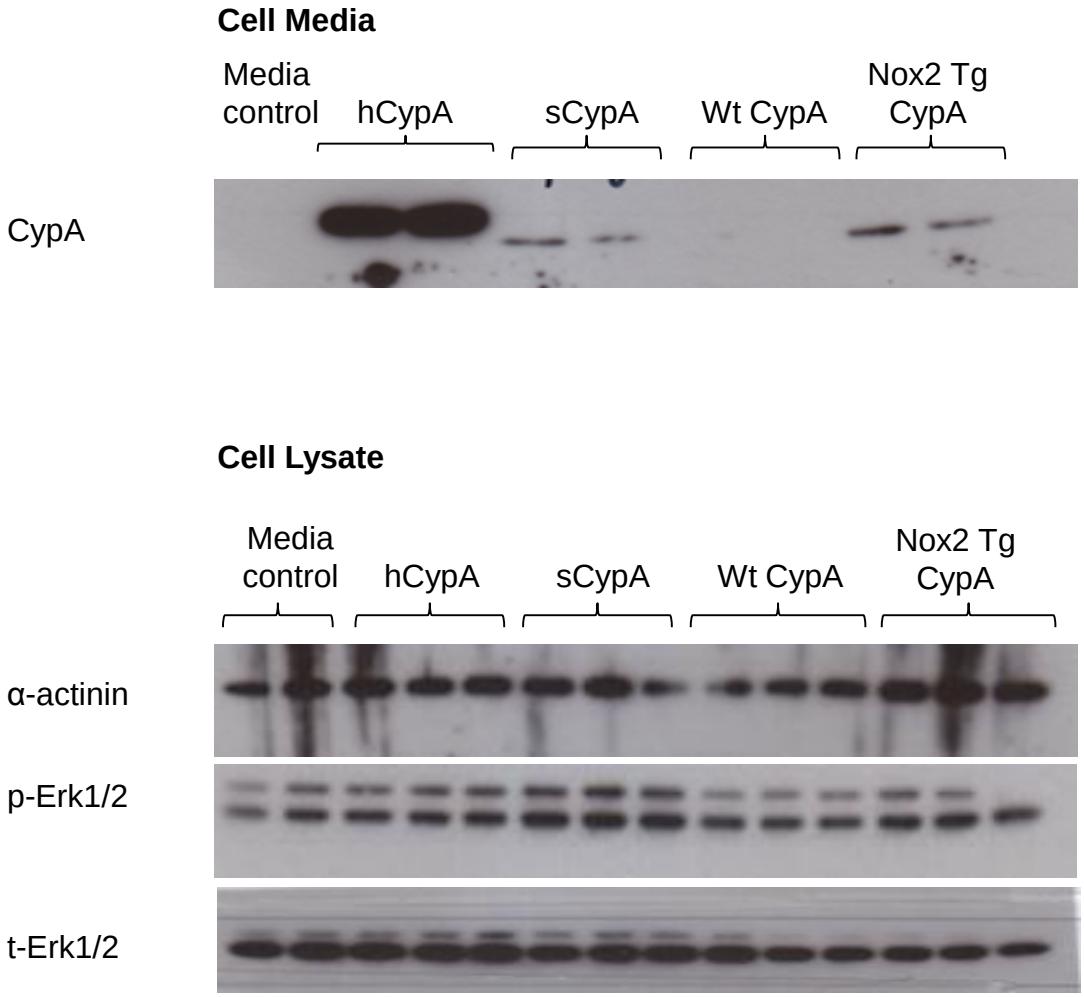


Figure 6.18 Greater secreted CypA in Nox2 Tg endothelial cells was associated with greater VSMC Erk1/2 phosphorylation. Human and sEND.1 CypA induced similar increases in Erk1/2 phosphorylation.

Primary wild-type VSMCs were serum starved and stimulated with either DMEM alone as control, human CypA- hCypA (50 nM); or sEND.1 conditioned media – sCypA (10 µl/well), wild-type endothelial conditioned media (10 µl/well) or Nox2 Tg endothelial conditioned media (10 µl/well) for 15 minutes. Cells were then harvested and western blotted for α-actinin (loading control), phosphorylated Erk1/2 and total Erk1/2. **(A)** Representative western blot of media from which the cells were stimulated. **(B)** Representative western blots of cell lysate probed for α-actinin, phosphorylated and total Erk1/2. Nox2 Tg endothelial conditioned media contained significantly greater secreted CypA than wild-type controls and induced greater Erk1/2 phosphorylation in VSMCs. Human CypA and sEND.1 CypA induced Erk1/2 phosphorylation to a similar extent as Nox2 Tg endothelial conditioned media.

6.4.9 CypA stimulation increased non-superoxide ($O^{\cdot-}$) ROS production

Previous studies have suggested that one of the functional effects of CypA is the activation of ROS production in VSMCs which may provide a positive amplification loop of vascular oxidative stress (Liao et al., 2000; Satoh et al., 2009). To test this hypothesis, I stimulated primary VSMCs with either purified human recombinant CypA or CypA secreted in the conditioned media of sEND.1 cells and examined ROS production by VSMCs.

6.4.9.1 Experiments with human recombinant CypA

VSMCs were plated in 12 well plates, starved overnight in serum free DMEM, preincubated for 30 min with either DMEM alone as control or in the presence of pegylated-superoxide dismutase (Peg-SOD). Cells were then stimulated with 0, 10, 50 or 100 nM of human recombinant CypA for 20 minutes in the presence of DHE. Cells were harvested as described in the previous chapters and detected for the ROS production by DHE HPLC.

There was no significant change in 2-hydroxyethdium peak (representative for O_2^- production), however there was a small but significant increase in Peg-SOD inhibitable fraction. CypA also increased ethidium peak suggesting that CypA increased the production of H_2O_2 or other forms of ROS rather than only superoxide (O_2^-) (Figure 6.19, Figure 6.20). This result was further supported by the fact that the increase in ethidium peak was not inhibited by Peg-SOD when cells were stimulated by 50 and 100 nM dose of CypA but was inhibited by catalase, an enzyme that breaks down H2O2 (Figure 6.19).

Figure 6.19

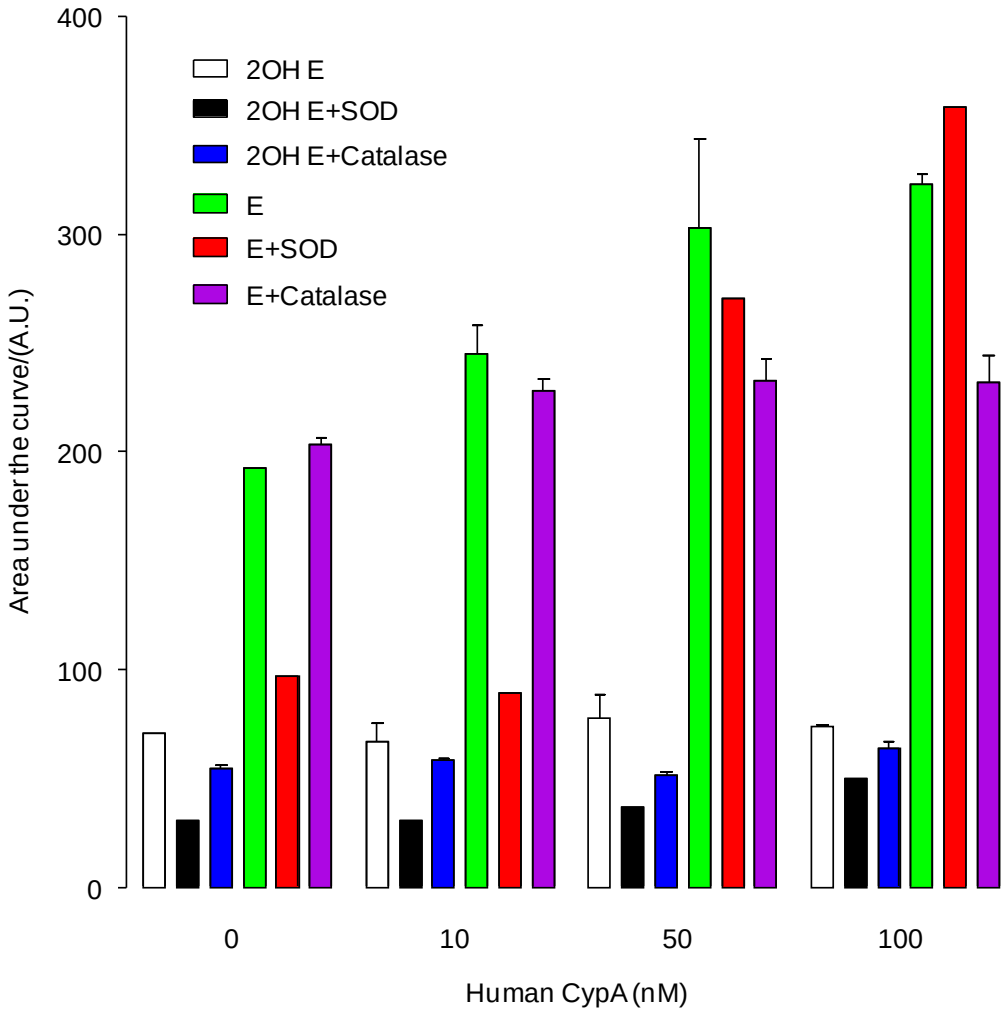


Figure 6.19 Dose dependent increase in VSMC ethidium peak but not 2-hydroxyethidium peak in response to CypA stimulation

Primary VSMCs isolated from wild-type mice were serum starved overnight, pre-incubated with either DMEM control, Peg-SOD (100U/ml) or catalase (100U/ml) and stimulated with purified human CypA at concentrations of 0, 10, 50 and 100 nM. Cells were then harvested for DHE HPLC. 2-hydroxyethidium (2OH-E) and ethidium (E) peaks were quantified using area under the curve. Data expressed as mean±SEM. A dose dependent increase in the ethidium peak but not 2-hydroxyethidium peak was observed in VSMCs in response to human CypA stimulation which was not inhibited by Peg-SOD at higher concentrations of CypA but was inhibited by catalase. A.U. – Arbitrary units.

Figure 6.20

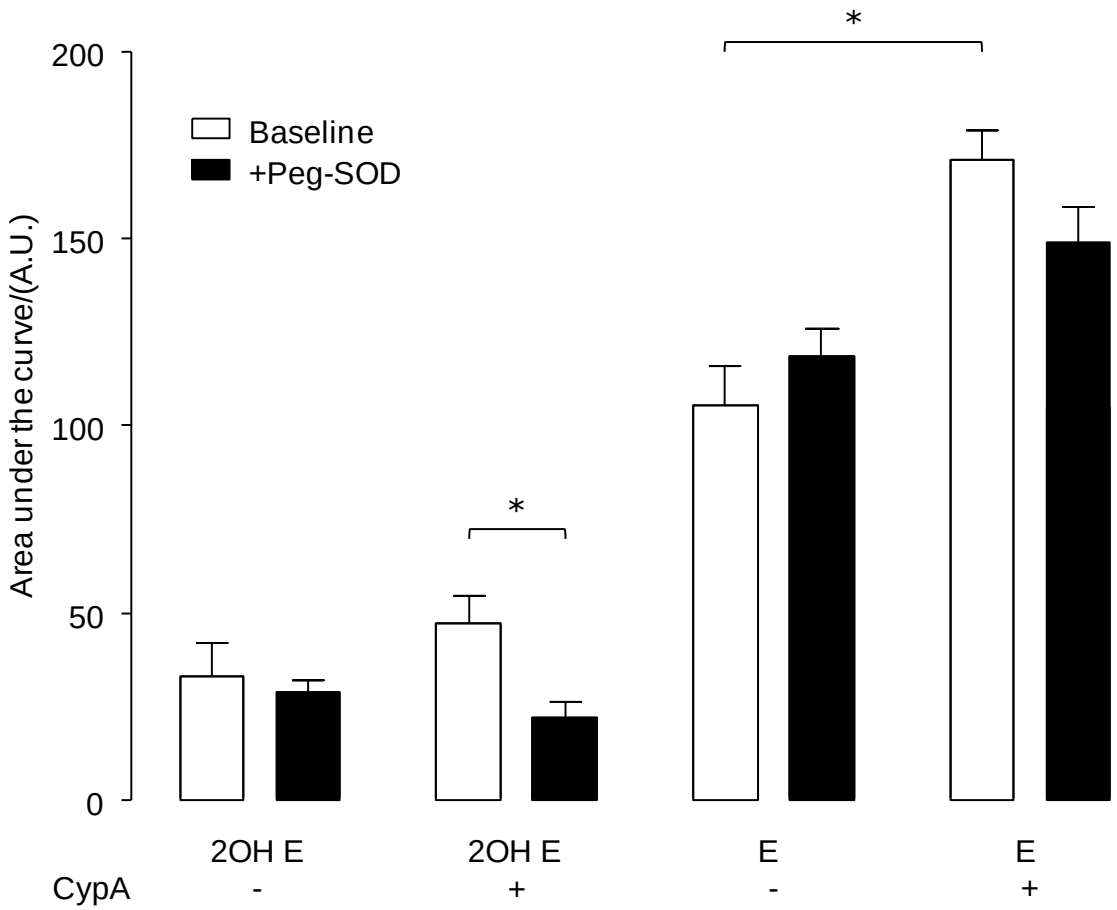


Figure 6.20 Significant increase in VSMC ROS production in response to CypA stimulation

Primary VSMCs were serum starved, pre-incubated with DMEM control or Peg-SOD and stimulated with purified human CypA (50 nM). Cells were then harvested for ROS production measurement using DHE HPLC. 2-hydroxyethidium (2OH-E) and ethidium (E) peaks were quantified using area under the curve. Data presented as mean±SEM. A.U. – arbitrary units. *$p<0.05$, n= 3 independent experiments. CypA induced a significant increase in Peg-SOD inhibitable fraction and also in the ethidium peak which was not inhibited fully by Peg-SOD.

6.4.9.2 CypA in the conditioned media of sEND.1 cells

Purified human CypA is slightly different to mouse CypA in size (24kDa vs. 18kDa), therefore it was important to check whether effects of human CypA on mouse VSMC ROS production was due to the differences in human recombinant CypA to mouse CypA. To test this, conditioned media from sEND.1 cells which contained secreted CypA was used to stimulate VSMCs and the ROS production was measured by DHE HPLC. There was no increase in 2-hydroxyethidium peak (Figure 6.21 A), whereas the ethidium peak showed a dose dependent increase which was similar to that observed with human CypA and was not fully inhibitable by Peg-SOD (Figure 6.21 B).

Figure 6.21

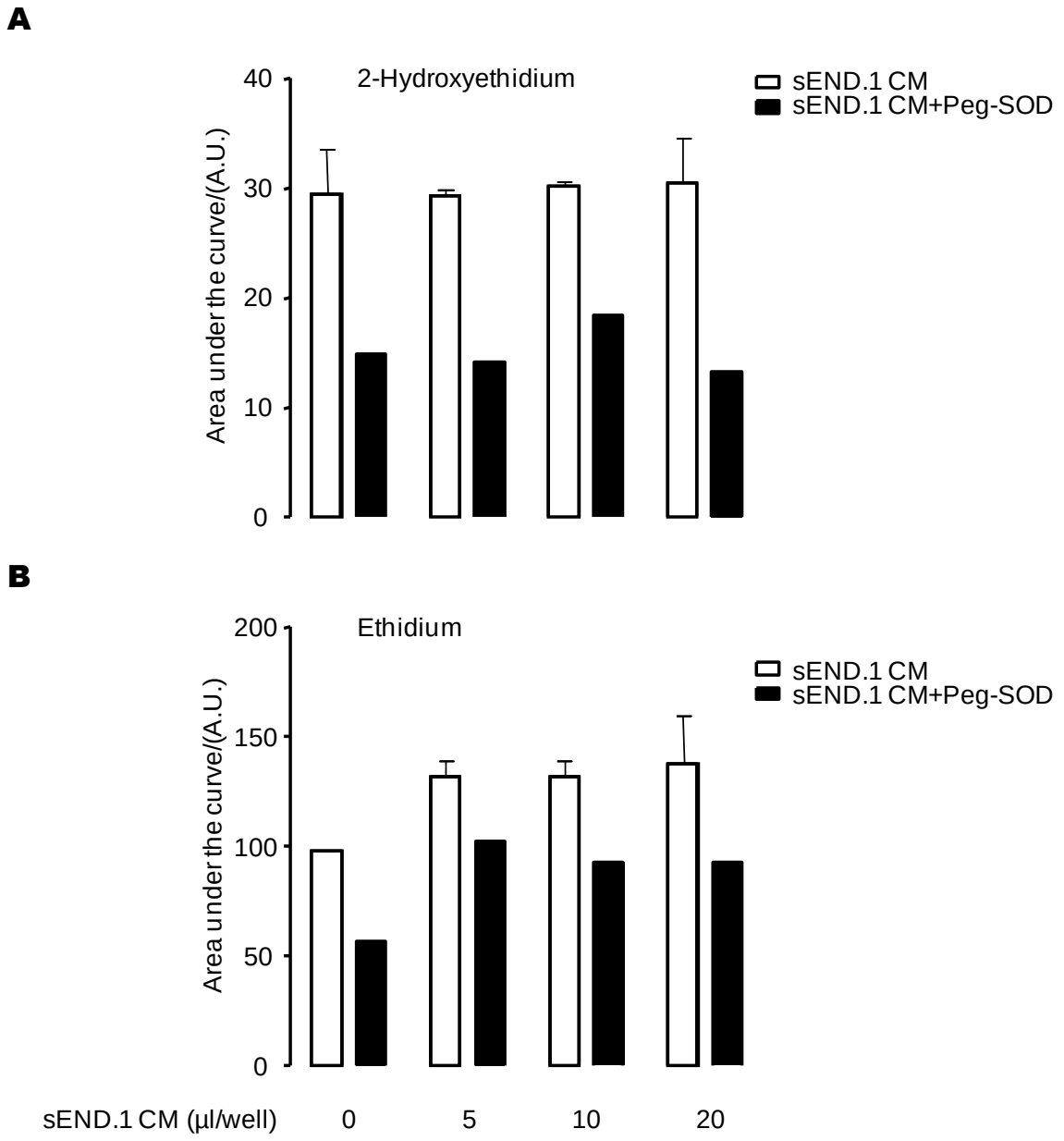
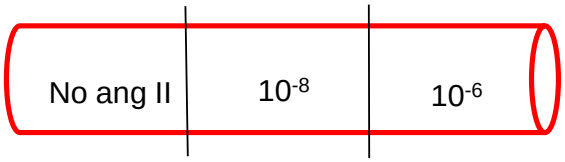


Figure 6.21 Dose dependent in VSMC ethidium peak in response to secreted CypA in the conditioned media of sEND.1 cells.

Primary wild-type VSMCs were serum starved overnight, pre-incubated with DMEM control or peg-SOD and stimulated with sEND.1 conditioned media (0, 5 10 or 20 µl were added per well to a total volume of 300µl). Cells were harvested and prepared for ROS measurement by DHE HPLC. **(A)** Quantification of 2-hydroxyethidium peaks using area under the curve. A.U. – Arbitrary units. Data expressed as mean±SEM. **(B)** Quantification of ethidium peak using area under the curve. Data expressed as mean±SEM. sEND.1 conditioned media induced a dose dependent increase in the ethidium peak but not in the 2-hydroxyethidium peak.

6.4.10 **Increased CypA secretion by Nox2 Tg aortic vessel segments compared to wild-type aortic vessel segments**

I have demonstrated so far that there was greater secretion of CypA in Nox2 Tg endothelial cells which was able to activate Erk1/2 phosphorylation and increase ROS production in VSMCs. Next I investigated whether the difference in the levels of endothelial CypA secretion observed at the cellular level had any pathophysiological significance at the level of whole aortic vessels. Aortas from mice were harvested from the aortic arch to the renal arteries and split into 3 equal segments. Each segment was then incubated in either DMEM alone as control, or in the presence of Ang II at concentrations of 10^{-8}M or 10^{-6}M for 24 hours. Conditioned media from the cultured aortic segments were collected at the end of the experiment and used for CypA western blot.



Aorta 1	10^{-6}	0	10^{-8}
Aorta 2	0	10^{-8}	10^{-6}
Aorta 3	10^{-8}	10^{-6}	0

Diagram 6.1 Aortic segments and experimental design

Aortas from aortic arch to renal arteries were harvested and split into 3 equal segments. Each segment was treated with either DMEM alone (no Ang II) as control, or in the presence of Ang II at the concentration of 10^{-8} or 10^{-6} M for 24 h. At the end of culture, media were collected and used for CypA western blot as described in the method section.

There was greater secreted CypA in the conditioned media from Nox2 Tg aortic segments compared to the wild-type controls (Figure 6.22). Large variability was observed in Ang II treated aortic segments but there appeared to be a trend of a dose dependent increase in CypA secretion by wild-type aortas in response to Ang II stimulation whereas no

significant increase in CypA secretion was observed in Nox2 Tg aortic segments (Figure 6.22).

Figure 6.22

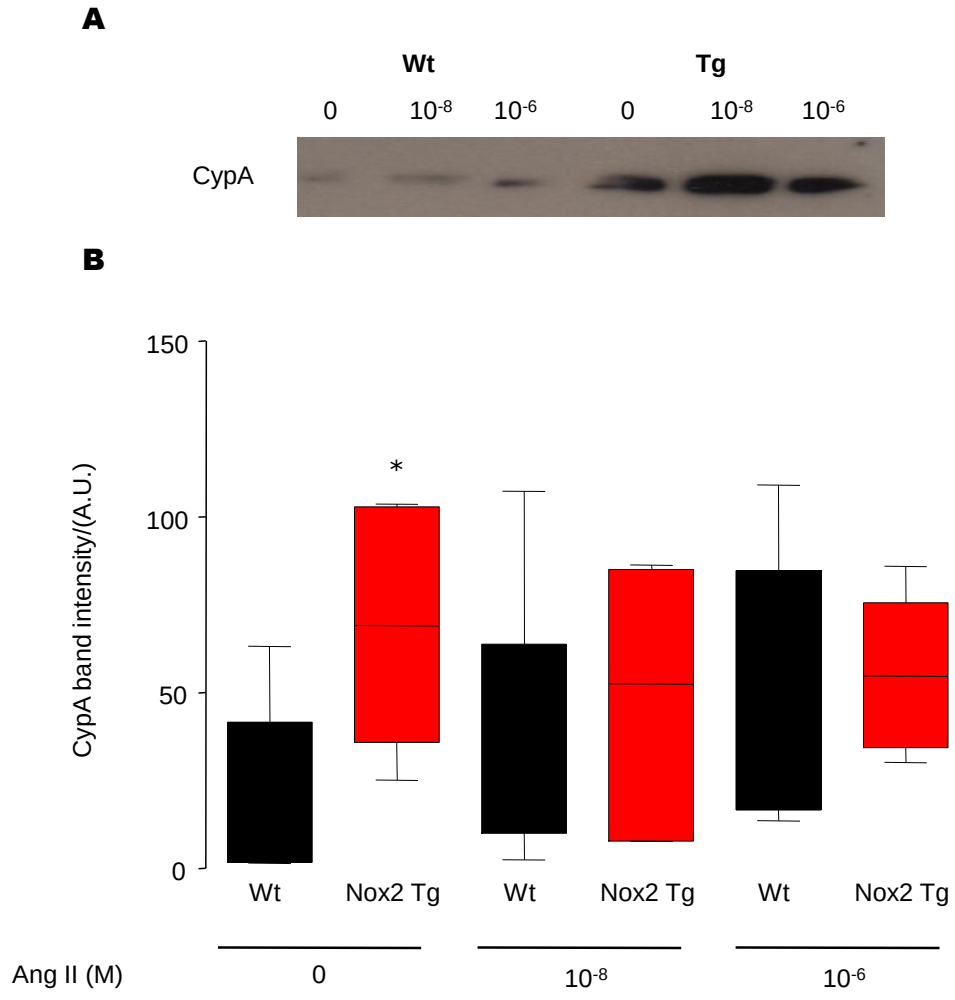


Figure 6.22 Nox2 Tg aortic segments had greater secreted CypA at baseline compared to the wild-type controls

Wt and Nox2 Tg aortas were harvested from aortic arch to the renal arteries and cut into 3 equal segments. Each segment was incubated with DMEM alone as control or in the presence of Ang II (10^{-8} or 10^{-6}M) for 24 hours. Conditioned media from aortic segments were collected and probed for secreted CypA by western blot. **(A)** Representative western blot of CypA in aortic segment conditioned media. **(B)** Densitometric analysis of western blots. A.U. – arbitrary units. Data expressed as median±interquartile range. *$p<0.05$, n=3 aortas per group. Greater secreted CypA were observed in conditioned media of Nox2 Tg aortic segments at baseline compared to the wild-type controls.

6.4.11 **Increased CypA in Nox2 Tg aorta at both baseline and following Ang II infusion**

The large variability in the aortic segment data was likely caused by the splitting of the aorta into segments. In order to reduce the variability, whole aortas were examined for CypA secretion. Wild-type aortas were harvested from the aortic arch to the renal arteries and tested for CypA secretion after incubation with either DMEM alone as control or in the presence of Ang II at 10^{-8} or 10^{-6} M for 24 hours. Conditioned media was then harvested and western blotted for the levels of secreted CypA. Secreted CypA was readily detectable in aortic conditioned media and showed a dose dependent increase in response to Ang II stimulation (Figure 6.23 A, B) similar to the trend observed in primary endothelial cells.

Figure 6.23

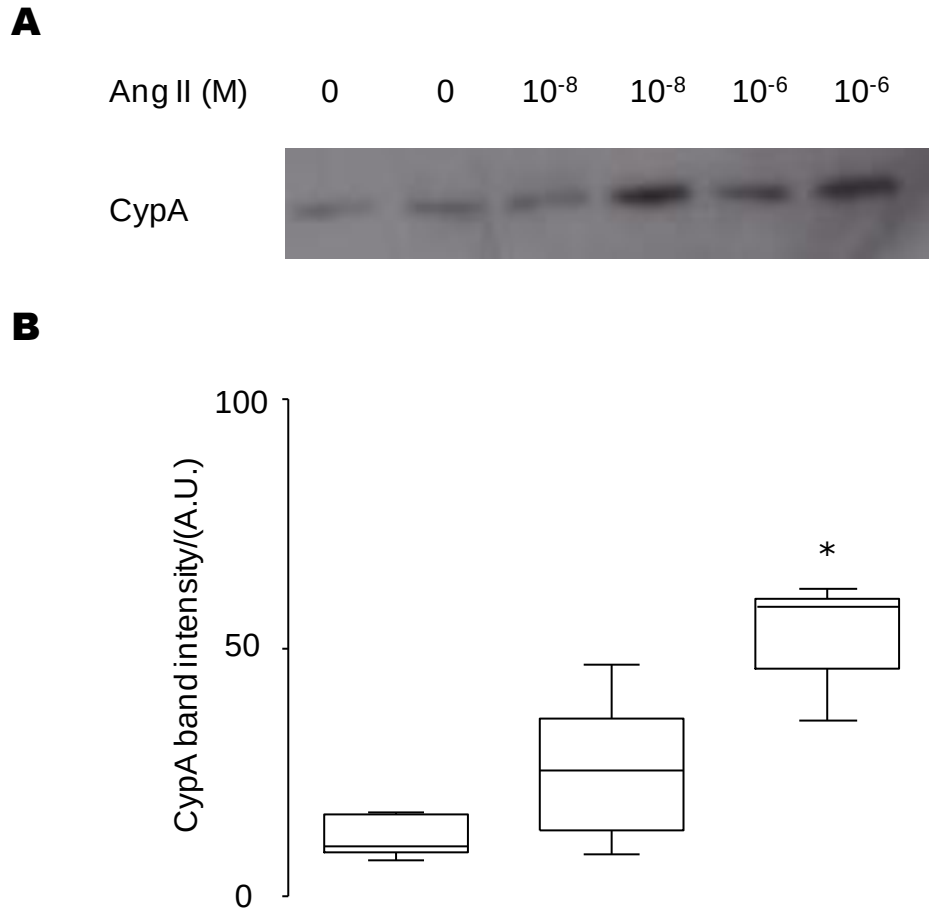


Figure 6.23 Dose dependent increase in wild-type aortic CypA secretion in response to Ang II stimulation

Wild-type aortas were harvested and incubated in either DMEM alone as control or in the presence of Ang II at 10^{-8} or 10^{-6} M for 24 hours. Culture media was harvested and probed for secreted CypA by western blot. **(A)** Representative western blot of CypA in aorta conditioned media. **(B)** Densitometric analysis of Western blots. A.U. – Arbitrary units. Data presented as median ± interquartile range. *$p<0.05$, n=5-6 wild-type mice per treatment group. Dose dependent increase in CypA secretion was observed in the conditioned media from cultured whole aortas stimulated with Ang II.

However, this method of aortic incubation was limited by the fact that aortas were treated with Ang II for only 24 hours, whereas aortic dissection occurred after at least 5 days of Ang II infusion. I therefore, used the method described by Tieu et al where the aorta was cultured following *in-vivo* Ang II infusion (Tieu et al., 2009).

Wild-type and Nox2 Tg supra-renal aortas were harvested following infusion with either saline (baseline) control or Ang II for 5 days and incubated in serum free DMEM for 4 hours. The conditioned media were then harvested and examined for CypA secretion. There was significantly greater secreted CypA in Nox2 Tg aortas at both baseline and after Ang II infusion when compared to the wild-type controls (Figure 6.24). These results confirmed that increased endothelial CypA secretion in Nox2 Tg at the cellular level was able to induce a significant change detectable at the level of the whole of the vessel and further supported the role for CypA as the ROS sensitive mediator of endothelial cells which activated and promoted vessel inflammation.

.

Figure 6.24

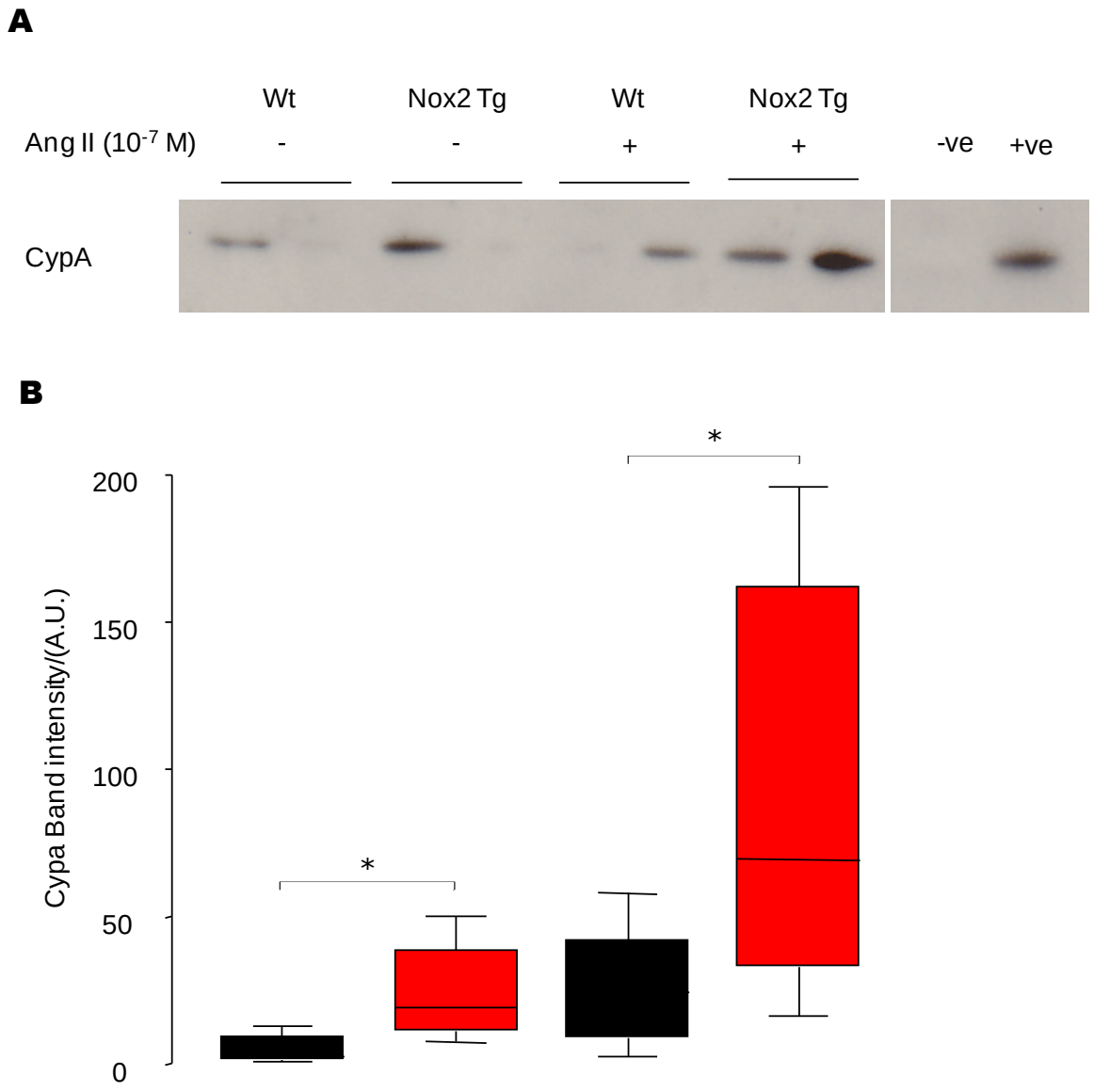


Figure 6.24 Nox2 Tg aortas had greater CypA secretion both at baseline and in response to Ang II infusion compared to wild-type controls

Wild-type and Nox2 Tg mice were infused with either saline control (baseline) or with Ang II (1mg/kg/day) for 5 days. Supra-renal aortas were harvested and incubated in serum free DMEM for 4 hours. Conditioned media were then collected and probed for secreted CypA by western blot. **(A)** Representative western blot of aortic conditioned media probed for CypA. Negative control (-ve): lysates of aorta from $CypA^{-/-}$ mice; positive control (+ve): lysates of wild-type aorta. **(B)** Densitometric analysis of Western blot. A.U. – arbitrary units. Data expressed as median ± interquartile range. *$p<0.05$, n = 4-8 mice per genotype per treatment group. Nox2 Tg aortas secreted significantly higher levels of CypA both at baseline and after Ang II infusion compared to wild-type controls.

6.5 Discussion

In this chapter I investigated the mechanism by which endothelial ROS regulated and activated VSMCs. The key findings were:

1) Primary Nox2 Tg endothelial cells secreted greater levels of CypA both at baseline and after Ang II stimulation as compared to wild-type controls.
2) Greater endothelial secreted CypA was associated with increased endothelial Erk1/2 phosphorylation which was a marker for cell activation.
3) In contrast to endothelial cells, there were no significant differences in the levels of CypA secretion or Erk1/2 phosphorylation between wild-type and Nox2 Tg VSMCs either at baseline or after Ang II stimulation.
4) Purified human CypA and CypA secreted in the conditioned media from an endothelial cell line, sEND.1, were able to induce Erk1/2 phosphorylation and ROS production by VSMCs. Knockdown of CypA in the conditioned media using siRNA abolished the effect of secreted endothelial CypA on VSMC Erk1/2 phosphorylation.
5) Nox2 Tg whole aortas had significantly greater CypA secretion both at baseline and after Ang II infusion for 5 days when compared to the wild-type controls.

There is increasing interest in the role of paracrine factors in the development of vascular diseases. There have been many paracrine factors identified so far including IL-6, MCP-1 and osteopontin, all of which have been shown to play important roles in the development of aortic diseases (Bruemmer et al., 2003; Tieu et al., 2009). One of the new cytokines of interest is Cyclophilin A (CypA), which is a ubiquitous intracellular protein secreted by VSMCs and macrophages in response to external stimuli. Its central role in the

development of abdominal aortic aneurysm was demonstrated by Berk et al. in which knockout of CypA completely abolished AAA in Ang II treated $ApoE^{-/-}$ mice (Satoh et al., 2009). CypA has many other functions as a cytokine including vascular remodelling, chemo-attractant for inflammatory cells (Sherry et al., 1992; Xu et al., 1992) and increasing VSMC MMP activity (Satoh et al., 2009). However, these previous studies had focused on VSMCs as the initiator and producer of CypA that was presumed to orchestrate the vessel response to Ang II and the development of vascular diseases. However, CypA could also be secreted by endothelial cells as suggested by the study from Galis et al. where they showed human umbilical vein endothelial cells secreted CypA in a dose and time dependent manner to LPS stimulation (Kim et al., 2004). No studies, however, had examined the role of endothelial CypA in the context of an *in-vivo* disease model.

In the previous chapter I have demonstrated the presence of a secreted factor in Nox2 Tg conditioned media that was able to activate and induce Erk1/2 phosphorylation in VSMCs, suggesting that endothelial cells regulated the vessel response to Ang II through a paracrine factor. This could be the mechanism for the increased incidence of aortic dissection observed in Nox2 Tg mice. It was reported previously that CypA secretion was ROS dependent and the use of ROS inducing compound significantly increased CypA secretion from VSMCs via a vesicular pathway (Jin et al., 2000). It was therefore logical to hypothesize that Nox2 Tg endothelial cells which had increased ROS production might have increased CypA secretion. This hypothesis was tested by examining secreted CypA in conditioned media from wild-type and Nox2 Tg endothelial cells by western blot. It was found firstly that primary endothelial cells indeed secreted CypA into the culture media and secondly, Nox2 Tg had significantly higher levels of CypA secretion at baseline (unstimulated) when compared to the wild-type controls. Interestingly, the increase in endothelial CypA secretion was associated with increased Erk1/2 phosphorylation

indicating the Nox2 Tg endothelial cells were already activated. This may explain the results found in the *in-vivo* studies with Ang II where there was greater endothelial VCAM-1 expression (a marker of endothelial activation) in Nox2 Tg aorta compared to wild-type controls.

I found also in the current chapter that endothelial secreted CypA was able to activate and induce Erk1/2 phosphorylation in VSMCs. To confirm this, purified human CypA was used to stimulate VSMCs. It was found that VSMCs showed a dose and time dependent increase in Erk1/2 phosphorylation in response to human CypA stimulation. Furthermore, human CypA induced a dose dependent increase in predominantly non-superoxide ROS production in VSMCs. My results were supported by the previous study from Berk et al. which showed an increase in VSMC ROS production when stimulated with CypA using 2',7'-dicloroflurescin (DCF) staining. DCF is a non-specific ROS probe and has been shown to measure mainly H_2O_2 rather than superoxide (Royall and Ischiropoulos, 1993).

The importance of secreted CypA by endothelial cells in the regulation of VSMC function and ROS production was further demonstrated using a molecular approach in which CypA in sEND.1 endothelial cells was knocked down with CypA siRNA. Conditioned media from CypA siRNA treated and untreated sEND.1 cells were used to stimulate VSMCs. The results confirmed that CypA was the crucial factor in endothelial conditioned media as VSMCs stimulated with CypA knocked-down conditioned media had significantly reduced Erk1/2 phosphorylation when compared to conditioned media from control untreated sEND.1 cells.

In-vitro observations often may not translate to the in vivo or ex vivo experiments. It was important therefore, to examine the whole vessel secretion of CypA as it would be difficult to assert an important role for CypA if no difference was observed between wild-type and

Nox2 Tg aortas. This was done using aortic segment stimulated with Ang II ex vivo and whole aortas of animals after 5 days of Ang II infusion. Consistently, Nox2 Tg at baseline in both the aortic segments and the whole aorta had greater secreted CypA compared to the wild type. The consequence is that the whole vessel was at greater activated state as demonstrated by Dr J. Bendall in our laboratory who previously observed greater Erk1/2 phosphorylation in Nox2 Tg whole aortas (Bendall et al., 2007). The translation of cellular observations to observations at the whole organ level provided further evidence for the role of endothelial secreted CypA in the regulation of aortic disease.

The mechanism of CypA signaling is still mostly unknown currently although receptor mediated signaling pathways have been suggested which involved several candidate receptors such as CD147 (Arora et al., 2005; Pushkarsky et al., 2001). Interestingly, in our study two CypA bands (human and mouse) were visible in the Western blot of VSMCs treated with human CypA. It suggested CypA may cross the cell membrane to exert its effects intracellularly. Further detailed studies are required to fully understand CypA signaling pathways.

6.6 Summary

In this chapter I tested the hypothesis that CypA was the secreted endothelial factor that activated and regulated VSMC ROS production. I demonstrated that CypA was the ROS sensitive factor secreted by endothelial cells and was able to activate and induce Erk1/2 phosphorylation in VSMCs. Nox2 Tg, which had greater endothelial ROS and CypA at the cellular level, also had greater secreted CypA at the level of the whole vessel thus providing evidence for CypA as the crucial endothelial mediator involved in promoting vascular inflammation in response to increased endothelial ROS.

Chapter 7:
General Discussions

Chapter 7. General Discussion

7.1 Original hypothesis and aims

Increased endothelial reactive oxygen species (ROS) production is implicated in chronic endothelial dysfunction and the development of cardiovascular diseases including hypertension, atherosclerosis and heart failure (Cai and Harrison, 2000). However, despite recent advances in targeted cell intervention which allow the study for the role of individual cell types in the disease pathology, very few studies have investigated if increases in endothelial specific ROS play a direct role in vascular disease. It is still unclear whether the increase in endothelial ROS observed in many vascular diseases plays a role in the initiation and progression of the disease, or is merely a consequence of disease progression. The answer to this question not only helps to improve our understanding of the basic mechanisms in the pathogenesis of cardiovascular diseases but also focuses the development of future drug therapies.

My original thesis hypothesis is that endothelial Nox2 and Nox2-derived ROS are sufficient to modify the initiation and development of structural vessel disease. To test this hypothesis, a novel mouse model of endothelial Nox2 over-expression was generated in which there was a specific increase in endothelial Nox2-derived ROS and subjected to Ang II infusion as a model of acute vascular inflammation. Accordingly, the aim of this thesis was to investigate the effect of increased endothelial ROS on the development of Ang II induced aortic dissection and the underlying mechanism by which endothelial ROS regulates the aortic response to Ang II.

7.2 Summary of key findings

The work in this thesis demonstrates for the first time a direct role for endothelial Nox2 and ROS in the determination of the susceptibility to aortic dissection in response to Ang II stimulation. The key findings are:

1) Increased endothelial ROS led to significantly increased incidence of aortic dissection in response to Ang II.
2) This was associated with a greater increase in aortic VCAM-1 expression, increased $CD45^+$ inflammatory cell recruitment and MMP activity.
3) Conditioned media from Nox2 Tg primary endothelial cells which had increased ROS production induced greater Erk1/2 phosphorylation in primary VSMCs suggesting the presence of a ROS dependent endothelial secreted factor that was able to activate VSMCs.
4) CypA was identified as a candidate for this secreted factor. There was greater CypA in Nox2 Tg endothelial conditioned media and this was associated with greater Erk1/2 phosphorylation in these cells suggesting increased activation.
5) The increase in endothelial secreted CypA and basal Erk1/2 phosphorylation was not observed in VSMC where the Nox2 transgene was not expressed.
6) Endothelial CypA induced VSMC activation which contributed to aortic dissection. This was supported by: 1) Purified human CypA and sEND.1 CypA directly induced VSMC Erk1/2 phosphorylation; 2) Conditioned media from CypA depleted sEND.1 cells induced significantly less Erk1/2 phosphorylation in VSMCs compared to conditioned media from control SEND.1 cells.
7) In vivo studies demonstrated that CypA was increased in conditioned media from Nox2 Tg aortic segment and whole aorta compared to the wild-type aortas indicating that increased endothelial CypA secretion in Nox2 Tg at the cellular

level was able to induce a significant change detectable at the level of the whole of the vessel

Collectively, the work in this thesis demonstrate that endothelial Nox2 and ROS play a specific role in the initiation of aortic dissection and endothelial CypA is a novel signalling mechanism by which increased endothelial ROS regulates the vessel inflammatory response and susceptibility to aortic dissection.

7.3 Proposed mechanism of endothelial O_2^- and CypA in Ang II induced aortic dissection

From work presented in this thesis and the published literature, I present a "2 hit" model or the role of endothelial Nox2-derived O_2^- in the development of Ang II induced aortic dissection is proposed (Figure 7.1). At the basal state, endothelial cells in Nox2 Tg mice have increased O_2^- production through the over-expression of Nox2 driven by the Tie-2 promoter. The increase in ROS increases endothelial CypA secretion which then activates VSMCs through phosphorylation of Erk1/2 and primes the vascular wall for activation. When Nox2 Tg mice are challenged by Ang II infusion, they express greater endothelial VCAM-1, have increased $CD45^+$ inflammatory cell recruitment and MMP activity. The vessel inflammatory response is further enchanced by the positive feedback from VSMC CypA secretion described by Berk et al. (Satoh et al., 2009) leading ultimately to increased rate of aortic dissection.

7.4 Future directions

The work in this thesis discovered an important role for endothelial Nox2, ROS and endothelial CypA in the pathogenesis of Ang II-induced aortic dissection. It expands upon

the conventional theory whereby VSMCs are the presumed main initiators of pathways leading to the development of aortic dissection in response to Ang II (Dimmeler and Zeiher, 2000; Gavazzi et al., 2007; McCormick et al., 2007; Satoh et al., 2009; Tieu et al., 2009). However, there are some remaining issues that could be investigated further to add to our understanding of the pathological processes leading to aortic dissection.

I have presented CypA as the crucial factor in mediating the changes in endothelial ROS to the regulation of VSMCs using purified human CypA and siRNA knockdown of sEND.1 cells. The limitation here is that although it proves the concept but it may not apply to the primary cells which are different to sEND.1 cells. Removing secreted CypA directly from the primary endothelial cell conditioned media would be a better approach and immunodepletion is one method through which this could be achieved. Berk et al. immune-depleted CypA from their conditioned media and demonstrated complete abolishment of Erk1/2 phosphorylation in VSMCs (Jin et al., 2000). However, initial attempts with immunodepletion using the same protocol and regents were unsuccessful. Significant work on optimisation of the protocol is required to achieve successful immunodepletion. In-vivo approach such as injection of neutralising antibody is currently not feasible due to the lack of antibodies. A more definitive approach would be to generate an endothelial specific CypA knockout mouse. The endothelial $CypA^{-/-}$ mice could then be crossed with Nox2 Tg mice, infused with Ang II and examined for the development of aortic dissection.

VCAM-1 is associated with vessel inflammation and it was observed in this study that the expression was different even within the same region of the aorta. It was not clear however, whether the aortic area with the highest levels of VCAM-1 correlated to the point of rupture later on in the disease development. This is an important question because it could be a powerful tool by which risk of aortic dissection could be assessed. One way to

address this question is through in-vivo imaging of the aorta (McAteer et al., 2008). Mice implanted with Ang II mini-pumps for 5 days could be scanned by MRI under anaesthesia after injection of the VCAM-1 conjugated microparticles to look for microparticle binding. These mice could then be further assessed by MRI at 14 and 28 days of Ang II infusion. The point of rupture could be identified in-vivo and correlated to MRI scan done at 5 days of Ang II infusion to assess if region of highest VCAM-1 expression was indeed the area of rupture.

The other important question is the association between endothelial Nox2 derived O_2^- and endothelial CypA. I have shown an increase in secreted CypA in Nox2 Tg endothelial cells but it does not necessarily indicate causality between the O_2^- production and CypA secretion. A simple way to address this question could be to use the O_2^- inhibitor, superoxide dismutase (peg-SOD) on Nox2 Tg primary endothelial cells and examine the effect on CypA secretion. However, in order to shown definitively the link between Nox2 derived O_2^- and CypA, either over-expression of Nox2 in wild-type endothelial cells or knockdown in Nox2 Tg endothelial cells is required. Transfection of primary cells is difficult for many reasons including the animal cost and the poor transfection efficiency. The use of a cell line could be a more rational approach. For example, Nox2 could be transfected into sEND.1 cells and conditioned media examined for secreted CypA. Alternatively, a stable Nox2 over-expression cell line could be created which would provide greater consistency compared to transient transfection.

Another useful experiment would be to confirm the effect of CypA on the activation of VSMCs. We have inferred by Erk1/2 phosphorylation that VSMCs were activated and therefore respond to a greater extent to Ang II stimulation. One way to confirm this would be to stimulate the VSMCs with Ang II after CypA stimulation and then measure ROS production using DHE HPLC.

7.5 Final conclusion

The work in this thesis has revealed a specific role for endothelial O_2^- in the development of inflammatory vascular disease and also identified CypA as a novel signalling mediator by which endothelial cells regulate the vessel inflammatory response. Many previous studies had looked at the disease process after the disease has occurred. The novelty of this project is the focus on the changes at the initiation of disease. The fact that VCAM-1 expression was significantly elevated in Nox2 Tg after only 3 days of Ang II infusion before any changes in VSMCs or inflammatory cells were observed is highly suggestive of endothelial activation as the first step in the disease process leading to aortic dissection. The findings in this thesis have contributed to the current understanding of the pathways involved in vessel disease initiation and suggest endothelial ROS and CypA as new therapeutic target in the prevention of aortic dissection of which there is no current preventative medical therapy.

Figure 7.1

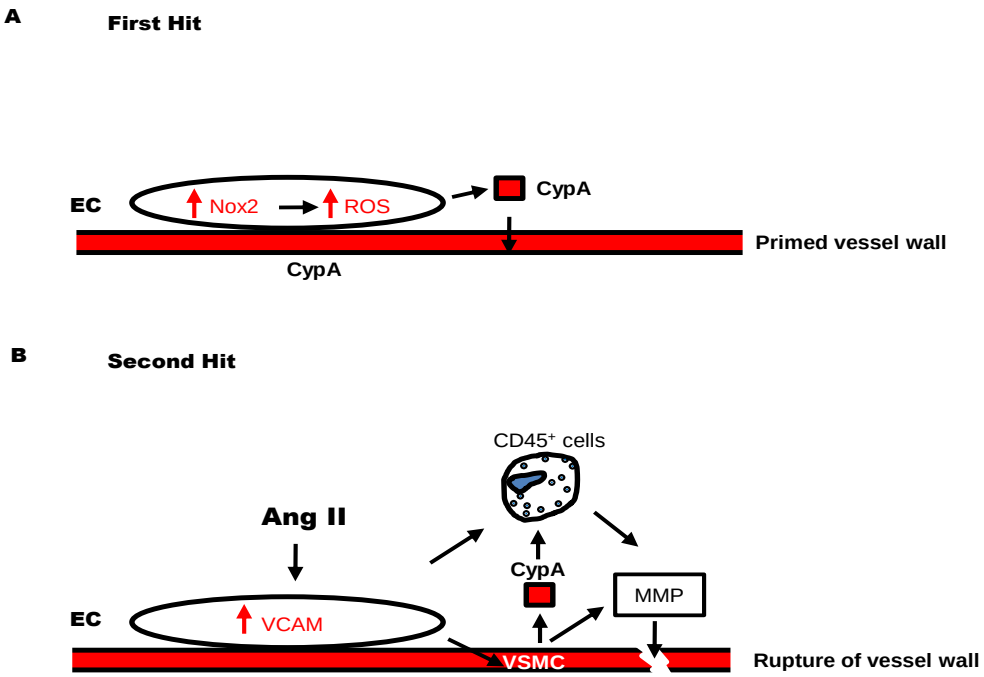


Figure 7.1 "2 hit" model of endothelial O_2^- in Ang II induced aortic dissection

(A) At resting state, endothelial cells in Nox2 Tg mice have increased O_2^- production which leads to increased endothelial CypA secretion that activates VSMCs and primes the vessel for activation. **(B)** On stimulation with Ang II, there is greater VCAM-1 expression, increased $CD45^+$ cell recruitment and MMP activity in Nox2 Tg mice. This is amplified by secreted CypA from VSMCs resulting ultimately in aortic dissection.

References

References

Ago, T., T. Kitazono, H. Ooboshi, T. Iyama, Y.H. Han, J. Takada, M. Wakisaka, S. Ibayashi, H. Utsumi, and M. Iida. 2004. Nox4 as the Major Catalytic Component of an Endothelial NAD(P)H Oxidase. *Circulation* 109:227-233.

Akhtar, A.M., J.E. Schneider, S.J. Chapman, A. Jefferson, J.E. Digby, K. Mankia, Y. Chen, M.A. McAteer, K.J. Wood, and R.P. Choudhury. 2010. In vivo quantification of VCAM-1 expression in renal ischemia reperfusion injury using non-invasive magnetic resonance molecular imaging. *PLoS One* 5:e12800.

Al-Mehdi, A.B., G. Zhao, C. Dodia, K. Tozawa, K. Costa, V. Muzykantov, C. Ross, F. Blecha, M. Dinauer, and A.B. Fisher. 1998. Endothelial NADPH Oxidase as the Source of Oxidants in Lungs Exposed to Ischemia or High K+. *Circulation Research* 83:730-737.

Allaire, E., R. Forough, M. Clowes, B. Starcher, and A.W. Clowes. 1998. Local overexpression of TIMP-1 prevents aortic aneurysm degeneration and rupture in a rat model. *J Clin Invest* 102:1413-1420.

Alp, N.J., and K.M. Channon. 2004. Regulation of endothelial nitric oxide synthase by tetrahydrobiopterin in vascular disease. *Arterioscler Thromb Vasc Biol* 24:413-420.

Alp, N.J., S. Mussa, J. Khoo, T.J. Guzik, S. Cai, A. Jefferson, K.A. Rockett, and K.M. Channon. 2003. Tetrahydrobiopterin-dependent preservation of nitric oxide-mediated endothelial function in diabetes by targeted transgenic GTP-cyclohydrolase I overexpression. *J Clin Invest* 112:725-735.

Ambasta, R.K., P. Kumar, K.K. Griendling, H.H.H.W. Schmidt, R. Busse, and R.P. Brandes. 2004. Direct Interaction of the Novel Nox Proteins with p22phox Is Required for the Formation of a Functionally Active NADPH Oxidase. *Journal of Biological Chemistry* 279:45935-45941.

Anilkumar, N., R. Weber, M. Zhang, A. Brewer, and A.M. Shah. 2008. Nox4 and Nox2 NADPH Oxidases Mediate Distinct Cellular Redox Signaling Responses to Agonist Stimulation. *Arterioscler Thromb Vasc Biol* 28:1347-1354.

Arora, K., W.M. Gwinn, M.A. Bower, A. Watson, I. Okwumabua, H.R. MacDonald, M.I. Bukrinsky, and S.L. Constant. 2005. Extracellular Cyclophilins Contribute to the Regulation of Inflammatory Responses. *The Journal of Immunology* 175:517-522.

Ayabe, N., V.R. Babaev, Y. Tang, T. Tanizawa, A.B. Fogo, M.F. Linton, I. Ichikawa, S. Fazio, and V. Kon. 2006. Transiently heightened angiotensin II has distinct effects on atherosclerosis and aneurysm formation in hyperlipidemic mice. *Atherosclerosis* 184:312-321.

Azumi, H., N. Inoue, S. Takeshita, Y. Rikitake, S. Kawashima, Y. Hayashi, H. Itoh, and M. Yokoyama. 1999. Expression of NADH/NADPH oxidase p22phox in human coronary arteries. *Circulation* 100:1494-1498.

Barisione, C., R. Charnigo, D.A. Howatt, J.J. Moorleghen, D.L. Rateri, and A. Daugherty. 2006. Rapid dilation of the abdominal aorta during infusion of angiotensin II detected by noninvasive high-frequency ultrasonography. *Journal of Vascular Surgery* 44:372-376.

Bedard, K., and K.-H. Krause. 2007. The NOX Family of ROS-Generating NADPH Oxidases: Physiology and Pathophysiology. *Physiological Reviews* 87:245-313.

Bendall, J.K., R. Rinze, D. Adlam, A.L. Tatham, J. de Bono, and K.M. Channon. 2007. Endothelial Nox2 overexpression potentiates vascular oxidative stress and hemodynamic response to angiotensin II: studies in endothelial-targeted Nox2 transgenic mice. *Circ Res* 100:1016-1025.

Benov, L., L. Sztejnberg, and I. Fridovich. 1998. Critical evaluation of the use of hydroethidine as a measure of superoxide anion radical. *Free Radical Biology and Medicine* 25:826-831.

Bindokas, V.P., J. Jordan, C.C. Lee, and R.J. Miller. 1996. Superoxide production in rat hippocampal neurons: selective imaging with hydroethidine. *J Neurosci* 16:1324-1336.

Bondy, S.C., and S. Naderi. 1994. Contribution of hepatic cytochrome P450 systems to the generation of reactive oxygen species. *Biochem Pharmacol* 48:155-159.

Brooke, B.S., J.P. Habashi, D.P. Judge, N. Patel, B. Loeys, and H.C. Dietz. 2008. Angiotensin II Blockade and Aortic-Root Dilation in Marfan's Syndrome. *New England Journal of Medicine* 358:2787-2795.

Bruemmer, D., A.R. Collins, G. Noh, W. Wang, M. Territo, S. Arias-Magallona, M.C. Fishbein, F. Blaschke, U. Kintscher, K. Graf, R.E. Law, and W.A. Hsueh. 2003. Angiotensin II–accelerated atherosclerosis and aneurysm formation is attenuated in osteopontin-deficient mice. *The Journal of Clinical Investigation* 112:1318-1331.

Butler, R., A.D. Morris, J.J.F. Belch, A. Hill, and A.D. Struthers. 2000. Allopurinol Normalizes Endothelial Dysfunction in Type 2 Diabetics With Mild Hypertension. *Hypertension* 35:746-751.

Buul, J.D.V., M. Fernandez-Borja, E.C. Anthony, and P.L. Hordijk. 2005. Expression and Localization of NOX2 and NOX4 in Primary Human Endothelial Cells. *Antioxidants & Redox Signaling* 7:308-317.

Cahilly, C., C.M. Ballantyne, D.S. Lim, A. Gotto, and A.J. Marian. 2000. A variant of p22(phox), involved in generation of reactive oxygen species in the vessel wall, is associated with progression of coronary atherosclerosis. *Circ Res* 86:391-395.

Cai, H., and D.G. Harrison. 2000. Endothelial Dysfunction in Cardiovascular Diseases: The Role of Oxidant Stress. *Circulation Research* 87:840-844.

Cassis, L.A., M. Gupte, S. Thayer, X. Zhang, R. Charnigo, D.A. Howatt, D.L. Rateri, and A. Daugherty. 2009. ANG II infusion promotes abdominal aortic aneurysms independent of increased blood pressure in hypercholesterolemic mice. *Am J Physiol Heart Circ Physiol* 296:H1660-1665.

Chen, H., D. Li, and J.L. Mehta. 2002. Modulation of Matrix Metalloproteinase-1, Its Tissue Inhibitor, and Nuclear Factor-[kappa]B by Losartan in Hypercholesterolemic Rabbits. *Journal of Cardiovascular Pharmacology* 39:332-339.

Chen, Z., L. Mi, J. Xu, J. Yu, X. Wang, J. Jiang, J. Xing, P. Shang, A. Qian, Y. Li, P.X. Shaw, J. Wang, S. Duan, J. Ding, C. Fan, Y. Zhang, Y. Yang, X. Yu, Q. Feng, B. Li, X. Yao, Z. Zhang, L. Li, X. Xue, and P. Zhu. 2005. Function of HAb18G/CD147 in invasion of host cells by severe acute respiratory syndrome coronavirus. *J Infect Dis* 191:755-760.

Cheng, T.H., N.L. Shih, S.Y. Chen, D.L. Wang, and J.J. Chen. 1999. Reactive oxygen species modulate endothelin-I-induced c-fos gene expression in cardiomyocytes. *Cardiovascular Research* 41:654-662.

Chiou, A.C., B. Chiu, and W.H. Pearce. 2001. Murine Aortic Aneurysm Produced by Periarterial Application of Calcium Chloride. *Journal of Surgical Research* 99:371-376.

Cifuentes, M.E., F.E. Rey, O.A. Carretero, and P.J. Pagano. 2000. Upregulation of p67(phox) and gp91(phox) in aortas from angiotensin II-infused mice. *Am J Physiol Heart Circ Physiol* 279:H2234-2240.

Clempus, R.E., and K.K. Griendling. 2006. Reactive oxygen species signaling in vascular smooth muscle cells. *Cardiovascular Research* 71:216-225.

Clempus, R.E., D. Sorescu, A.E. Dikalova, L. Pounkova, P. Jo, G.P. Sorescu, B. Lassègue, and K.K. Griendling. 2007. Nox4 Is Required for Maintenance of the Differentiated Vascular Smooth Muscle Cell Phenotype. *Arteriosclerosis, Thrombosis, and Vascular Biology* 27:42-48.

Cook-Mills, J.M., M.E. Marchese, and H. Abdala-Valencia. 2011. Vascular cell adhesion molecule-1 expression and signaling during disease: regulation by reactive oxygen species and antioxidants. *Antioxid Redox Signal* 15:1607-1638.

Cosentino, F., K. Hishikawa, Z.S. Katusic, and T.F. Luscher. 1997. High glucose increases nitric oxide synthase expression and superoxide anion generation in human aortic endothelial cells. *Circulation* 96:25-28.

Crabtree, M.J., A.L. Tatham, Y. Al-Wakeel, N. Warrick, A.B. Hale, S. Cai, K.M. Channon, and N.J. Alp. 2009. Quantitative regulation of intracellular endothelial nitric oxide synthase (eNOS) coupling by both tetrahydrobiopterin-eNOS stoichiometry and biopterin redox status: Insights from cells with tet-regulated GTP cyclohydrolase I expression. *J Biol Chem* 284:1136-1144.

Craige, S.M., K. Chen, Y. Pei, C. Li, X. Huang, Chen, C. , R. Shibata, K. Sato, K. Walsh, and J.F. Keaney. 2011. NADPH Oxidase 4 Promotes Endothelial Angiogenesis Through Endothelial Nitric Oxide Synthase Activation / Clinical Perspective. *Circulation* 124:731-740.

Cucoranu, I., R. Clempus, A. Dikalova, P.J. Phelan, S. Ariyan, S. Dikalov, and D. Sorescu. 2005. NAD(P)H Oxidase 4 Mediates Transforming Growth Factor-β1–Induced Differentiation of Cardiac Fibroblasts Into Myofibroblasts. *Circulation Research* 97:900-907.

Cui, X.-L., and J.G. Douglas. 1997. Arachidonic acid activates c-jun N-terminal kinase through NADPH oxidase in rabbit proximal tubular epithelial cells. *Proceedings of the National Academy of Sciences* 94:3771-3776.

Curci, J.A., and R.W. Thompson. 1999. "Variable induction of experimental abdominal aortic aneurysms with different preparations of porcine pancreatic elastase". *Journal of vascular surgery : official publication, the Society for Vascular Surgery* 29:385.

Cybulsky, M.I., K. Iiyama, H. Li, S. Zhu, M. Chen, M. Iiyama, V. Davis, J.-C. Gutierrez-Ramos, P.W. Connelly, and D.S. Milstone. 2001. A major role for VCAM-1, but not ICAM-1, in early atherosclerosis. *The Journal of Clinical Investigation* 107:1255-1262.

Daugherty, A., and L. Cassis. 2004. Angiotensin II-mediated development of vascular diseases. *Trends Cardiovasc Med* 14:117-120.

Daugherty, A., L.A. Cassis, and H. Lu. 2011. Complex pathologies of angiotensin II-induced abdominal aortic aneurysms. *Journal of Zhejiang University. Science. B* 12:624-628.

Daugherty, A., M.W. Manning, and L.A. Cassis. 2000. Angiotensin II promotes atherosclerotic lesions and aneurysms in apolipoprotein E-deficient mice. *The Journal of clinical investigation* 105:1605-1612.

Davis, V., R. Persidskaia, L. Baca-Regen, Y. Itoh, H. Nagase, Y. Persidsky, A. Ghorpade, and B.T. Baxter. 1998. Matrix Metalloproteinase-2 Production and Its Binding to the Matrix Are Increased in Abdominal Aortic Aneurysms. *Arteriosclerosis, Thrombosis, and Vascular Biology* 18:1625-1633.

De Keulenaer, G.W., R.W. Alexander, M. Ushio-Fukai, N. Ishizaka, and K.K. Griendling. 1998a. Tumour necrosis factor alpha activates a p22phox-based NADH oxidase in vascular smooth muscle. *The Biochemical journal* 329 (Pt 3):653-657.

De Keulenaer, G.W., D.C. Chappell, N. Ishizaka, R.M. Nerem, R.W. Alexander, and K.K. Griendling. 1998b. Oscillatory and steady laminar shear stress differentially affect human endothelial redox state: role of a superoxide-producing NADH oxidase. *Circ Res* 82:1094-1101.

Dikalov, S.I., A.E. Dikalova, A.T. Bikineyeva, H.H.H.W. Schmidt, D.G. Harrison, and K.K. Griendling. 2008. Distinct roles of Nox1 and Nox4 in basal and angiotensin II-stimulated superoxide and hydrogen peroxide production. *Free Radical Biology and Medicine* 45:1340-1351.

Dikalova, A., R. Clempus, B. Lassegue, G. Cheng, J. McCoy, S. Dikalov, A.S. Martin, A. Lyle, D.S. Weber, D. Weiss, W.R. Taylor, H.H.H.W. Schmidt, G.K. Owens, J.D. Lambeth, and K.K. Griendling. 2005. Nox1 Overexpression Potentiates Angiotensin II-Induced Hypertension and Vascular Smooth Muscle Hypertrophy in Transgenic Mice. *Circulation* 112:2668-2676.

Dikalova, A.E., M.C. Góngora, D.G. Harrison, J.D. Lambeth, S. Dikalov, and K.K. Griendling. 2010. Upregulation of Nox1 in vascular smooth muscle leads to impaired endothelium-dependent relaxation via eNOS uncoupling. *American Journal of Physiology - Heart and Circulatory Physiology* 299:H673-H679.

Dimmeler, S., and A.M. Zeiher. 2000. Reactive oxygen species and vascular cell apoptosis in response to angiotensin II and pro-atherosclerotic factors. *Regul Pept* 90:19-25.

Douglas, G., J.K. Bendall, M.J. Crabtree, A.L. Tatham, E.E. Carter, A.B. Hale, and K.M. Channon. 2012. Endothelial-specific Nox2 overexpression increases vascular superoxide and macrophage recruitment in ApoE−/− mice. *Cardiovascular Research*

Dröge, W. 2002. Free Radicals in the Physiological Control of Cell Function. *Physiological Reviews* 82:47-95.

Du, X.-L., D. Edelstein, L. Rossetti, I.G. Fantus, H. Goldberg, F. Ziyadeh, J. Wu, and M. Brownlee. 2000. Hyperglycemia-induced mitochondrial superoxide overproduction activates the hexosamine pathway and induces plasminogen activator inhibitor-1 expression by increasing Sp1 glycosylation. *Proceedings of the National Academy of Sciences* 97:12222-12226.

Dupont, G.P., T.P. Hueckstead, B.C. Marshall, U.S. Ryan, J.R. Michael, and J.R. Hoidal. 1992. Regulation of xanthine dehydrogenase and xanthine oxidase activity and gene expression in cultured rat pulmonary endothelial cells. *J Clin Invest* 89:197-202.

Ejiri, J., N. Inoue, T. Tsukube, T. Munezane, Y. Hino, S. Kobayashi, K.-i. Hirata, S. Kawashima, S. Imajoh-Ohmi, Y. Hayashi, H. Yokozaki, Y. Okita, and M. Yokoyama. 2003. Oxidative stress in the pathogenesis of

thoracic aortic aneurysm: Protective role of statin and angiotensin II type 1 receptor blocker. *Cardiovasc Res* 59:988-996.

Ernst, C.B. 1993. Abdominal Aortic Aneurysm. *New England Journal of Medicine* 328:1167-1172.

Eskandari, M.K., J.D. Vijungco, A. Flores, J. Borensztajn, V. Shively, and W.H. Pearce. 2005. Enhanced abdominal aortic aneurysm in TIMP-1-deficient mice1. *Journal of Surgical Research* 123:289-293.

Fernandes, D.C., J. Wosniak, Jr., L.A. Pescatore, M.A. Bertoline, M. Liberman, F.R. Laurindo, and C.X. Santos. 2007. Analysis of DHE-derived oxidation products by HPLC in the assessment of superoxide production and NADPH oxidase activity in vascular systems. *Am J Physiol Cell Physiol* 292:C413-422.

Finder, J., W.W. Stark, Jr., D.K. Nakayama, D. Geller, K. Wasserloos, B.R. Pitt, and P. Davies. 1995. TGF-β regulates production of NO in pulmonary artery smooth muscle cells by inhibiting expression of NOS. *Am J Physiol Lung Cell Mol Physiol* 268:L862-L867.

Fink, B., K. Laude, L. McCann, A. Doughan, D.G. Harrison, and S. Dikalov. 2004. Detection of intracellular superoxide formation in endothelial cells and intact tissues using dihydroethidium and an HPLC-based assay. *Am J Physiol Cell Physiol* 287:C895-902.

Finkel, T., and N.J. Holbrook. 2000. Oxidants, oxidative stress and the biology of ageing. *Nature* 408:239-247.

Fisslthaler, B., R. Popp, L. Kiss, M. Potente, D.R. Harder, I. Fleming, and R. Busse. 1999. Cytochrome P450 2C is an EDHF synthase in coronary arteries. *Nature* 401:493-497.

Fleming, I. 2001. Cytochrome P450 and Vascular Homeostasis. *Circulation Research* 89:753-762.

Fleming, I., U.R. Michaelis, D. Bredenkötter, B. Fisslthaler, F. Dehghani, R.P. Brandes, and R. Busse. 2001. Endothelium-Derived Hyperpolarizing Factor Synthase (Cytochrome P450 2C9) Is a Functionally Significant Source of Reactive Oxygen Species in Coronary Arteries. *Circulation Research* 88:44-51.

Forman, H.J., and I. Fridovich. 1973. Superoxide dismutase: A comparison of rate constants. *Archives of Biochemistry and Biophysics* 158:396-400.

Fukai, T., M.R. Siegfried, M. Ushio-Fukai, K.K. Griendling, and D.G. Harrison. 1999. Modulation of extracellular superoxide dismutase expression by angiotensin II and hypertension. *Circ Res* 85:23-28.

Galat, A. 1993. Peptidylproline cis-trans-isomerases: immunophilins. *European Journal of Biochemistry* 216:689-707.

Gavazzi, G., C. Deffert, C. Trocme, M. Schappi, F.R. Herrmann, and K.-H. Krause. 2007. NOX1 Deficiency Protects From Aortic Dissection in Response to Angiotensin II. *Hypertension* 50:189-196.

Gavrila, D., W.G. Li, M.L. McCormick, M. Thomas, A. Daugherty, L.A. Cassis, F.J. Miller, Jr, L.W. Oberley, K.C. Dellsperger, and N.L. Weintraub. 2005. Vitamin E Inhibits Abdominal Aortic Aneurysm Formation in Angiotensin II-Infused Apolipoprotein E-Deficient Mice. *Arterioscler Thromb Vasc Biol* 25:1671-1677.

Gebremedhin, D., A.R. Lange, T.F. Lowry, M.R. Taheri, E.K. Birks, A.G. Hudetz, J. Narayanan, J.R. Falck, H. Okamoto, R.J. Roman, K. Nithipatikom, W.B. Campbell, and D.R. Harder. 2000. Production of 20-HETE and Its Role in Autoregulation of Cerebral Blood Flow. *Circulation Research* 87:60-65.

Goodall, S., M. Crowther, D.M. Hemingway, P.R. Bell, and M.M. Thompson. 2001. Ubiquitous elevation of matrix metalloproteinase-2 expression in the vasculature of patients with abdominal aneurysms. *Circulation* 104:304-309.

Griendling, K.K. 2004. Novel NAD(P)H oxidases in the cardiovascular system. *Heart* 90:491-493.

Griendling, K.K., and G.A. FitzGerald. 2003. Oxidative stress and cardiovascular injury: Part I: basic mechanisms and in vivo monitoring of ROS. *Circulation* 108:1912-1916.

Griendling, K.K., and D.G. Harrison. 1999. Dual role of reactive oxygen species in vascular growth. *Circ Res* 85:562-563.

Griendling, K.K., D. Sorescu, and M. Ushio-Fukai. 2000. NAD(P)H oxidase: role in cardiovascular biology and disease. *Circ Res* 86:494-501.

Grote, K., I. Flach, M. Luchtefeld, E. Akin, S.M. Holland, H. Drexler, and B. Schieffer. 2003. Mechanical stretch enhances mRNA expression and proenzyme release of matrix metalloproteinase-2 (MMP-2) via NAD(P)H oxidase-derived reactive oxygen species. *Circ Res* 92:e80-86.

Guthikonda, S., C. Sinkey, T. Barenz, and W.G. Haynes. 2003. Xanthine Oxidase Inhibition Reverses Endothelial Dysfunction in Heavy Smokers. *Circulation* 107:416-421.

Guzik, T.J., N.E.J. West, E. Black, D. McDonald, C. Ratnatunga, R. Pillai, and K.M. Channon. 2000. Functional effect of the C242T polymorphism in the NAD(P)H oxidase p22phox subunit on vascular superoxide production in atherosclerosis. *Circulation* 102:1744-1747.

Habashi, J.P., D.P. Judge, T.M. Holm, R.D. Cohn, B.L. Loeys, T.K. Cooper, L. Myers, E.C. Klein, G. Liu, C. Calvi, M. Podowski, E.R. Neptune, M.K. Halushka, D. Bedja, K. Gabrielson, D.B. Rifkin, L. Carta, F. Ramirez, D.L. Huso, and H.C. Dietz. 2006. Losartan, an AT1 antagonist, prevents aortic aneurysm in a mouse model of Marfan syndrome. *Science* 312:117-121.

Handschumacher, R.E., M.W. Harding, J. Rice, R.J. Drugge, and D.W. Speicher. 1984. Cyclophilin: a specific cytosolic binding protein for cyclosporin A. *Science* 226:544-547.

Hare, J.M., B. Mangal, J. Brown, C. Fisher, Jr., R. Freudenberger, W.S. Colucci, D.L. Mann, P. Liu, M.M. Givertz, and R.P. Schwarz. 2008. Impact of oxypurinol in patients with symptomatic heart failure. Results of the OPT-CHF study. *J Am Coll Cardiol* 51:2301-2309.

Harris, R.C., M.Z. Zhang, and H.F. Cheng. 2004. Cyclooxygenase-2 and the renal renin–angiotensin system. *Acta Physiologica Scandinavica* 181:543-547.

Herzberg, O., and J. Moult. 1991. Analysis of the steric strain in the polypeptide backbone of protein molecules. *Proteins* 11:223-229.

Hishikawa, K., and T.F. Lüscher. 1997. Pulsatile Stretch Stimulates Superoxide Production in Human Aortic Endothelial Cells. *Circulation* 96:3610-3616.

Howard, A.B., R.W. Alexander, R.M. Nerem, K.K. Griendling, and W.R. Taylor. 1997. Cyclic strain induces an oxidative stress in endothelial cells. *Am J Physiol* 272:C421-427.

Huie, R.E., and S. Padmaja. 1993. The reaction of NO with superoxide. *Free Radic Res Commun* 18:195-199.

Inoue, N., S. Kawashima, K. Kanazawa, S. Yamada, H. Akita, and M. Yokoyama. 1998. Polymorphism of the NADH/NADPH Oxidase p22 phox Gene in Patients With Coronary Artery Disease. *Circulation* 97:135-137.

Irani, K. 2000. Oxidant signaling in vascular cell growth, death, and survival : a review of the roles of reactive oxygen species in smooth muscle and endothelial cell mitogenic and apoptotic signaling. *Circ Res* 87:179-183.

Ishibashi, M., K. Egashira, Q. Zhao, K. Hiasa, K. Ohtani, Y. Ihara, I.F. Charo, S. Kura, T. Tsuzuki, A. Takeshita, and K. Sunagawa. 2004. Bone marrow-derived monocyte chemoattractant protein-1 receptor CCR2 is critical in angiotensin II-induced acceleration of atherosclerosis and aneurysm formation in hypercholesterolemic mice. *Arterioscler Thromb Vasc Biol* 24:e174-178.

Jiménez, E., E.P. de la Blanca, L. Urso, I. González, J. Salas, and M. Montiel. 2009. Angiotensin II induces MMP 2 activity via FAK/JNK pathway in human endothelial cells. *Biochemical and Biophysical Research Communications* 380:769-774.

Jin, Z.-G., M.G. Melaragno, D.-F. Liao, C. Yan, J. Haendeler, Y.-A. Suh, J.D. Lambeth, and B.C. Berk. 2000. Cyclophilin A Is a Secreted Growth Factor Induced by Oxidative Stress. *Circ Res* 87:789-796.

Jin, Z.G., A.O. Lungu, L. Xie, M. Wang, C. Wong, and B.C. Berk. 2004. Cyclophilin A is a proinflammatory cytokine that activates endothelial cells. *Arterioscler Thromb Vasc Biol* 24:1186-1191.

Johnston, K.W., R.B. Rutherford, M.D. Tilson, D.M. Shah, L. Hollier, and J.C. Stanley. 1991. Suggested standards for reporting on arterial aneurysms. *Journal of vascular surgery : official publication, the Society for Vascular Surgery* 13:452-458.

Jones, K.G., D.J. Brull, L.C. Brown, M. Sian, R.M. Greenhalgh, S.E. Humphries, and J.T. Powell. 2001. Interleukin-6 (IL-6) and the Prognosis of Abdominal Aortic Aneurysms. *Circulation* 103:2260-2265.

Judkins, C.P., H. Diep, B.R. Broughton, A.E. Mast, E.U. Hooker, A.A. Miller, S. Selemidis, G.J. Dusting, C.G. Sobey, and G.R. Drummond. 2010a. Direct evidence of a role for Nox2 in superoxide production, reduced nitric oxide bioavailability, and early atherosclerotic plaque formation in ApoE-/- mice. *Am J Physiol Heart Circ Physiol* 298:H24-32.

Judkins, C.P., H. Diep, B.R.S. Broughton, A.E. Mast, E.U. Hooker, A.A. Miller, S. Selemidis, G.J. Dusting, C.G. Sobey, and G.R. Drummond. 2010b. Direct evidence of a role for Nox2 in superoxide production, reduced nitric oxide bioavailability, and early atherosclerotic plaque formation in ApoE−/− mice. *American Journal of Physiology - Heart and Circulatory Physiology* 298:H24-H32.

Jung, O., J.G. Schreiber, H. Geiger, T. Pedrazzini, R. Busse, and R.P. Brandes. 2004. gp91phox-Containing NADPH Oxidase Mediates Endothelial Dysfunction in Renovascular Hypertension. *Circulation* 109:1795-1801.

Juvonen, J., H.M. Surcel, J. Satta, A.M. Teppo, A. Bloigu, H. Syrjala, J. Airaksinen, M. Leinonen, P. Saikku, and T. Juvonen. 1997. Elevated circulating levels of inflammatory cytokines in patients with abdominal aortic aneurysm. *Arterioscler Thromb Vasc Biol* 17:2843-2847.

Karathanassis, D., R.V. Stahelin, J. Bravo, O. Perisic, C.M. Pacold, W. Cho, and R.L. Williams. 2002. Binding of the PX domain of p47phox to phosphatidylinositol 3,4-bisphosphate and phosphatidic acid is masked by an intramolecular interaction. *Embo J* 21:5057-5068.

Kim, S.-H., S.M. Lessner, Y. Sakurai, and Z.S. Galis. 2004. Cyclophilin A as a Novel Biphasic Mediator of Endothelial Activation and Dysfunction. *The American Journal of Pathology* 164:1567-1574.

King, V.L., A.Y. Lin, F. Kristo, T.J. Anderson, N. Ahluwalia, G.J. Hardy, A.P. Owens, 3rd, D.A. Howatt, D. Shen, A.M. Tager, A.D. Luster, A. Daugherty, and R.E. Gerszten. 2009. Interferon-gamma and the interferon-inducible chemokine CXCL10 protect against aneurysm formation and rupture. *Circulation* 119:426-435.

Kirk, E.A., M.C. Dinauer, H. Rosen, A. Chait, J.W. Heinecke, and R.C. LeBoeuf. 2000. Impaired Superoxide Production Due to a Deficiency in Phagocyte NADPH Oxidase Fails to Inhibit Atherosclerosis in Mice. *Arteriosclerosis, Thrombosis, and Vascular Biology* 20:1529-1535.

Klink, A., J. Heynens, B. Herranz, M.E. Lobatto, T. Arias, H.M.H.F. Sanders, G.J. Strijkers, M. Merkx, K. Nicolay, V. Fuster, A. Tedgui, Z. Mallat, W.J.M. Mulder, and Z.A. Fayad. 2011. In Vivo Characterization of a New Abdominal Aortic Aneurysm Mouse Model With Conventional and Molecular Magnetic Resonance Imaging. *J Am Coll Cardiol* 58:2522-2530.

Kunsch, C., and R.M. Medford. 1999. Oxidative Stress as a Regulator of Gene Expression in the Vasculature. *Circulation Research* 85:753-766.

Landing, B.H., and H.S. Shirkey. 1957. A SYNDROME OF RECURRENT INFECTION AND INFILTRATION OF VISCERA BY PIGMENTED LIPID HISTIOCYTES. *Pediatrics* 20:431-438.

Landmesser, U., S. Dikalov, S.R. Price, L. McCann, T. Fukai, S.M. Holland, W.E. Mitch, and D.G. Harrison. 2003. Oxidation of tetrahydrobiopterin leads to uncoupling of endothelial cell nitric oxide synthase in hypertension. *J Clin Invest* 111:1201-1209.

Landmesser, U., S. Spiekermann, S. Dikalov, H. Tatge, R. Wilke, C. Kohler, D.G. Harrison, B. Hornig, and H. Drexler. 2002. Vascular Oxidative Stress and Endothelial Dysfunction in Patients With Chronic Heart Failure. *Circulation* 106:3073-3078.

Lassegue, B., R.W. Alexander, G. Nickenig, M. Clark, T.J. Murphy, and K.K. Griendling. 1995. Angiotensin II down-regulates the vascular smooth muscle AT1 receptor by transcriptional and post-transcriptional mechanisms: evidence for homologous and heterologous regulation. *Mol Pharmacol* 48:601-609.

Lassegue, B., and K.K. Griendling. NADPH oxidases: functions and pathologies in the vasculature. *Arterioscler Thromb Vasc Biol* 30:653-661.

Lassègue, B., A. San Martín, and K.K. Griendling. 2012. Biochemistry, Physiology, and Pathophysiology of NADPH Oxidases in the Cardiovascular System. *Circulation Research* 110:1364-1390.

LeMaire, S.A., and L. Russell. 2011. Epidemiology of thoracic aortic dissection. *Nat Rev Cardiol* 8:103-113.

Li, J.-M., and A.M. Shah. 2004. Endothelial cell superoxide generation: regulation and relevance for cardiovascular pathophysiology. *Am J Physiol Regul Integr Comp Physiol* 287:R1014-1030.

Liao, D.F., Z.G. Jin, A.S. Baas, G. Daum, S.P. Gygi, R. Aebersold, and B.C. Berk. 2000. Purification and identification of secreted oxidative stress-induced factors from vascular smooth muscle cells. *J Biol Chem* 275:189-196.

Liu, P., C.E. Hock, R. Nagele, and P.Y. Wong. 1997. Formation of nitric oxide, superoxide, and peroxynitrite in myocardial ischemia-reperfusion injury in rats. *Am J Physiol* 272:H2327-2336.

Loeys, B.L., U. Schwarze, T. Holm, B.L. Callewaert, G.H. Thomas, H. Pannu, J.F. De Backer, G.L. Oswald, S. Symoens, S. Manouvrier, A.E. Roberts, F. Faravelli, M.A. Greco, R.E. Pyeritz, D.M. Milewicz, P.J. Coucke, D.E. Cameron, A.C. Braverman, P.H. Byers, A.M. De Paepe, and H.C. Dietz. 2006. Aneurysm syndromes caused by mutations in the TGF-beta receptor. *N Engl J Med* 355:788-798.

Longo, G.M., W. Xiong, T.C. Greiner, Y. Zhao, N. Fiotti, and B.T. Baxter. 2002. Matrix metalloproteinases 2 and 9 work in concert to produce aortic aneurysms. *J Clin Invest* 110:625-632.

Luchtefeld, M., K. Grote, C. Grothusen, S. Bley, N. Bandlow, T. Selle, M. Strüber, A. Haverich, U. Bavendiek, H. Drexler, and B. Schieffer. 2005. Angiotensin II induces MMP-2 in a p47phox-dependent manner. *Biochemical and Biophysical Research Communications* 328:183-188.

Mackay, D.J.G., and A. Hall. 1998. Rho GTPases. *Journal of Biological Chemistry* 273:20685-20688.

MacTaggart, J.N., W. Xiong, R. Knispel, and B.T. Baxter. 2007. Deletion of CCR2 but not CCR5 or CXCR3 inhibits aortic aneurysm formation. *Surgery* 142:284-288.

Maiellaro, K., and W.R. Taylor. 2007. The role of the adventitia in vascular inflammation. *Cardiovascular Research* 75:640-648.

Manning, M.W., L.A. Cassis, and A. Daugherty. 2003. Differential Effects of Doxycycline, a Broad-Spectrum Matrix Metalloproteinase Inhibitor, on Angiotensin II–Induced Atherosclerosis and Abdominal Aortic Aneurysms. *Arteriosclerosis, Thrombosis, and Vascular Biology* 23:483-488.

Marchesi, C., P. Paradis, and E.L. Schiffrin. 2008. Role of the renin-angiotensin system in vascular inflammation. *Trends Pharmacol Sci* 29:367-374.

Matsuno, K., H. Yamada, K. Iwata, D. Jin, M. Katsuyama, M. Matsuki, S. Takai, K. Yamanishi, M. Miyazaki, H. Matsubara, and C. Yabe-Nishimura. 2005a. Nox1 Is Involved in Angiotensin II-Mediated Hypertension: A Study in Nox1-Deficient Mice. *Circulation* 112:2677-2685.

Matsuno, K., H. Yamada, K. Iwata, D. Jin, M. Katsuyama, M. Matsuki, S. Takai, K. Yamanishi, M. Miyazaki, H. Matsubara, and C. Yabe-Nishimura. 2005b. Nox1 Is Involved in Angiotensin II–Mediated Hypertension. *Circulation* 112:2677-2685.

McAteer, M.A., J.E. Schneider, Z.A. Ali, N. Warrick, C.A. Bursill, C. von zur Muhlen, D.R. Greaves, S. Neubauer, K.M. Channon, and R.P. Choudhury. 2008. Magnetic resonance imaging of endothelial adhesion

molecules in mouse atherosclerosis using dual-targeted microparticles of iron oxide. *Arterioscler Thromb Vasc Biol* 28:77-83.

McAteer, M.A., J.E. Schneider, K. Clarke, S. Neubauer, K.M. Channon, and R.P. Choudhury. 2004. Quantification and 3D reconstruction of atherosclerotic plaque components in apolipoprotein E knockout mice using ex vivo high-resolution MRI. *Arterioscler Thromb Vasc Biol* 24:2384-2390.

McCormick, M.L., D. Gavrila, and N.L. Weintraub. 2007. Role of Oxidative Stress in the Pathogenesis of Abdominal Aortic Aneurysms. *Arterioscler Thromb Vasc Biol* 27:461-469.

McMillan, W.D., B.K. Patterson, R.R. Keen, and W.H. Pearce. 1995a. In situ localization and quantification of seventy-two – kilodalton type IV collagenase in aneurysmal, occlusive, and normal aorta. *Journal of Vascular Surgery* 22:295-305.

McMillan, W.D., B.K. Patterson, R.R. Keen, V.P. Shively, M. Cipollone, and W.H. Pearce. 1995b. In Situ Localization and Quantification of mRNA for 92-kD Type IV Collagenase and Its Inhibitor in Aneurysmal, Occlusive, and Normal Aorta. *Arteriosclerosis, Thrombosis, and Vascular Biology* 15:1139-1144.

Mehta, R.H., T. Suzuki, P.G. Hagan, E. Bossone, D. Gilon, A. Llovet, L.C. Maroto, J.V. Cooper, D.E. Smith, W.F. Armstrong, C.A. Nienaber, and K.A. Eagle. 2002. Predicting Death in Patients With Acute Type A Aortic Dissection. *Circulation* 105:200-206.

Mehta, S., D.J. Stewart, D. Langleben, and R.D. Levy. 1995. Short-term pulmonary vasodilation with L-arginine in pulmonary hypertension. *Circulation* 92:1539-1545.

Meneshian, A., and G.B. Bulkley. 2002. The Physiology of Endothelial Xanthine Oxidase: From Urate Catabolism to Reperfusion Injury to Inflammatory Signal Transduction. *Microcirculation* 9:161-175.

Meyer, J.W., J.A. Holland, L.M. Ziegler, M.M. Chang, G. Beebe, and M.E. Schmitt. 1999. Identification of a functional leukocyte-type NADPH oxidase in human endothelial cells :a potential atherogenic source of reactive oxygen species. *Endothelium : journal of endothelial cell research* 7:11-22.

Meyer, J.W., and M.E. Schmitt. 2000. A central role for the endothelial NADPH oxidase in atherosclerosis. *FEBS Lett* 472:1-4.

Miller, F.J., Jr, W.J. Sharp, X. Fang, L.W. Oberley, T.D. Oberley, and N.L. Weintraub. 2002. Oxidative Stress in Human Abdominal Aortic Aneurysms: A Potential Mediator of Aneurysmal Remodeling. *Arterioscler Thromb Vasc Biol* 22:560-565.

Mulligan-Kehoe, M.J. 2010. The vasa vasorum in diseased and nondiseased arteries. *American Journal of Physiology - Heart and Circulatory Physiology* 298:H295-H305.

Murphy, H.S., J.A. Shayman, G.O. Till, M. Mahrougui, C.B. Owens, U.S. Ryan, and P.A. Ward. 1992. Superoxide responses of endothelial cells to C5a and TNF-alpha: divergent signal transduction pathways. *Am J Physiol* 263:L51-59.

Nabah, Y.N.A., M. Losada, R. Estellés, T. Mateo, C. Company, L. Piqueras, C. Lopez-Gines, H. Sarau, J. Cortijo, E.J. Morcillo, P.J. Jose, and M.-J. Sanz. 2007. CXCR2 Blockade Impairs Angiotensin II–Induced CC Chemokine Synthesis and Mononuclear Leukocyte Infiltration. *Arteriosclerosis, Thrombosis, and Vascular Biology* 27:2370-2376.

Nathan, C. 2006. Neutrophils and immunity: challenges and opportunities. *Nat Rev Immunol* 6:173-182.

Navalkar, S., S. Parthasarathy, N. Santanam, and B.V. Khan. 2001. Irbesartan, an angiotensin type 1 receptor inhibitor, regulates markers of inflammation in patients with premature atherosclerosis. *Journal of the American College of Cardiology* 37:440-444.

Neptune, E.R., P.A. Frischmeyer, D.E. Arking, L. Myers, T.E. Bunton, B. Gayraud, F. Ramirez, L.Y. Sakai, and H.C. Dietz. 2003. Dysregulation of TGF-beta activation contributes to pathogenesis in Marfan syndrome. *Nat Genet* 33:407-411.

Newman, K.M., Y. Ogata, A.M. Malon, E. Irizarry, R.H. Gandhi, H. Nagase, and M.D. Tilson. 1994. Identification of matrix metalloproteinases 3 (stromelysin-1) and 9 (gelatinase B) in abdominal aortic aneurysm. *Arteriosclerosis, Thrombosis, and Vascular Biology* 14:1315-1320.

Nienaber, C.A., R. Fattori, R.H. Mehta, B.M. Richartz, A. Evangelista, M. Petzsch, J.V. Cooper, J.L. Januzzi, H. Ince, U. Sechtem, E. Bossone, J. Fang, D.E. Smith, E.M. Isselbacher, L.A. Pape, and K.A. Eagle. 2004. Gender-related differences in acute aortic dissection. *Circulation* 109:3014-3021.

Nishiyama, A., M. Yoshizumi, H. Hitomi, S. Kagami, S. Kondo, A. Miyatake, M. Fukunaga, T. Tamaki, H. Kiyomoto, M. Kohno, T. Shokoji, S. Kimura, and Y. Abe. 2004. The SOD Mimetic Tempol Ameliorates Glomerular Injury and Reduces Mitogen-Activated Protein Kinase Activity in Dahl Salt-Sensitive Rats. *Journal of the American Society of Nephrology* 15:306-315.

Okamoto, E.-i., T. Couse, H. De Leon, J. Vinten-Johansen, R.B. Goodman, N.A. Scott, and J.N. Wilcox. 2001. Perivascular Inflammation After Balloon Angioplasty of Porcine Coronary Arteries. *Circulation* 104:2228-2235.

Owens, A.P., III, V. Subramanian, J.J. Moorleghen, Z. Guo, C.A. McNamara, L.A. Cassis, and A. Daugherty. 2010. Angiotensin II Induces a Region-Specific Hyperplasia of the Ascending Aorta Through Regulation of Inhibitor of Differentiation 3. *Circ Res* 106:611-619.

Pannu, H., V.T. Fadulu, J. Chang, A. Lafont, S.N. Hasham, E. Sparks, P.F. Giampietro, C. Zaleski, A.L. Estrera, H.J. Safi, S. Shete, M.C. Willing, C.S. Raman, and D.M. Milewicz. 2005. Mutations in transforming growth factor-beta receptor type II cause familial thoracic aortic aneurysms and dissections. *Circulation* 112:513-520.

Payeli, S.K., C. Schiene-Fischer, J. Steffel, G.G. Camici, I. Rozenberg, T.F. Lüscher, and F.C. Tanner. 2008. Cyclophilin A differentially activates monocytes and endothelial cells: Role of purity, activity, and endotoxin contamination in commercial preparations. *Atherosclerosis* 197:564-571.

Pearlstein, D.P., M.H. Ali, P.T. Mungai, K.L. Hynes, B.L. Gewertz, and P.T. Schumacker. 2002. Role of Mitochondrial Oxidant Generation in Endothelial Cell Responses to Hypoxia. *Arteriosclerosis, Thrombosis, and Vascular Biology* 22:566-573.

Puntarulo, S., and A.I. Cederbaum. 1998. Production of reactive oxygen species by microsomes enriched in specific human cytochrome P450 enzymes. *Free Radic Biol Med* 24:1324-1330.

Pushkarsky, T., G. Zybarth, L. Dubrovsky, V. Yurchenko, H. Tang, H. Guo, B. Toole, B. Sherry, and M. Bukrinsky. 2001. CD147 facilitates HIV-1 infection by interacting with virus-associated cyclophilin A. *Proc Natl Acad Sci U S A* 98:6360-6365.

Pyo, R., J.K. Lee, J.M. Shipley, J.A. Curci, D. Mao, S.J. Ziporin, T.L. Ennis, S.D. Shapiro, R.M. Senior, and R.W. Thompson. 2000. Targeted gene disruption of matrix metalloproteinase-9 (gelatinase B) suppresses development of experimental abdominal aortic aneurysms. *J Clin Invest* 105:1641-1649.

Quie, P.G., E.L. Kaplan, A.R. Page, F.L. Gruskay, and S.E. Malawista. 1968. Defective Polymorphonuclear-Leukocyte Function and Chronic Granulomatous Disease in Two Female Children. *New England Journal of Medicine* 278:976-980.

Raffetto, J.D., and R.A. Khalil. 2008. Matrix metalloproteinases and their inhibitors in vascular remodeling and vascular disease. *Biochemical Pharmacology* 75:346-359.

Rajagopalan, S., S. Kurz, T. Munzel, M. Tarpey, B.A. Freeman, K.K. Griendling, and D.G. Harrison. 1996. Angiotensin II-mediated hypertension in the rat increases vascular superoxide production via membrane NADH/NADPH oxidase activation. Contribution to alterations of vasomotor tone. *J Clin Invest* 97:1916-1923.

Rateri, D.L., J.J. Moorleghen, A. Balakrishnan, A.P. Owens, 3rd, D.A. Howatt, V. Subramanian, A. Poduri, R. Charnigo, L.A. Cassis, and A. Daugherty. 2011. Endothelial cell-specific deficiency of Ang II type 1a receptors attenuates Ang II-induced ascending aortic aneurysms in LDL receptor-/- mice. *Circulation research* 108:574-581.

Ray, R., C.E. Murdoch, M. Wang, C.X. Santos, M. Zhang, S. Alom-Ruiz, N. Anilkumar, A. Ouattara, A.C. Cave, S.J. Walker, D.J. Grieve, R.L. Charles, P. Eaton, A.C. Brewer, and A.M. Shah. 2011. Endothelial Nox4 NADPH Oxidase Enhances Vasodilatation and Reduces Blood Pressure In Vivo. *Arteriosclerosis, Thrombosis, and Vascular Biology* 31:1368-1376.

Rey, F.E., M.E. Cifuentes, A. Kiarash, M.T. Quinn, and P.J. Pagano. 2001. Novel Competitive Inhibitor of NAD(P)H Oxidase Assembly Attenuates Vascular O2− and Systolic Blood Pressure in Mice. *Circulation Research* 89:408-414.

Royall, J.A., and H. Ischiropoulos. 1993. Evaluation of 2′,7′-Dichlorofluorescin and Dihydrorhodamine 123 as Fluorescent Probes for Intracellular H2O2 in Cultured Endothelial Cells. *Archives of Biochemistry and Biophysics* 302:348-355.

Saraff, K., F. Babamusta, L.A. Cassis, and A. Daugherty. 2003. Aortic dissection precedes formation of aneurysms and atherosclerosis in angiotensin II-infused, apolipoprotein E-deficient mice. *Arterioscler Thromb Vasc Biol* 23:1621-1626.

Satoh, K., T. Matoba, J. Suzuki, M.R. O'Dell, P. Nigro, Z. Cui, A. Mohan, S. Pan, L. Li, Z.G. Jin, C. Yan, J. Abe, and B.C. Berk. 2008. Cyclophilin A mediates vascular remodeling by promoting inflammation and vascular smooth muscle cell proliferation. *Circulation* 117:3088-3098.

Satoh, K., P. Nigro, T. Matoba, M.R. O'Dell, Z. Cui, X. Shi, A. Mohan, C. Yan, J.-i. Abe, K.A. Illig, and B.C. Berk. 2009. Cyclophilin A enhances vascular oxidative stress and the development of angiotensin II-induced aortic aneurysms. *Nat Med* 15:649-656.

Schachinger, V., M.B. Britten, and A.M. Zeiher. 2000. Prognostic impact of coronary vasodilator dysfunction on adverse long-term outcome of coronary heart disease. *Circulation* 101:1899-1906.

Schneider, J.E., S.D. Bamforth, S.M. Grieve, K. Clarke, S. Bhattacharya, and S. Neubauer. 2003. High-resolution, high-throughput magnetic resonance imaging of mouse embryonic anatomy using a fast gradient-echo sequence. *Magnetic Resonance Materials in Physics, Biology and Medicine* 16:43-51.

Schneider, J.E., M.A. McAteer, D.J. Tyler, K. Clarke, K.M. Channon, R.P. Choudhury, and S. Neubauer. 2004. High-resolution, multicontrast three-dimensional-MRI characterizes atherosclerotic plaque composition in ApoE-/- mice ex vivo. *J Magn Reson Imaging* 20:981-989.

Schröder, K., M. Zhang, S. Benkhoff, A. Mieth, R. Pliquett, J. Kosowski, C. Kruse, P. Luedike, U.R. Michaelis, N. Weissmann, S. Dimmeler, A.M. Shah, and R.P. Brandes. 2012. Nox4 Is a Protective Reactive Oxygen

Species Generating Vascular NADPH Oxidase / Novelty and Significance. *Circulation Research* 110:1217-1225.

Scott, R.A.P. 2002. The Multicentre Aneurysm Screening Study (MASS) into the effect of abdominal aortic aneurysm screening on mortality in men: a randomised controlled trial. *The Lancet* 360:1531-1539.

Seis, H. 1985. Oxidative Stress: Introductory remarks. *Academic Press* 1-8.

Setacci, F., P. Sirignano, G. de Donato, E. Chisci, A. Perulli, and C. Setacci. 2010. Acute aortic dissection: natural history and classification. *J Cardiovasc Surg (Torino)* 51:641-646.

Sheehan, A.L., S. Carrell, B. Johnson, B. Stanic, B. Banfi, and F.J. Miller Jr. 2011. Role for Nox1 NADPH oxidase in atherosclerosis. *Atherosclerosis* 216:321-326.

Sherry, B., N. Yarlett, A. Strupp, and A. Cerami. 1992. Identification of Cyclophilin as a Proinflammatory Secretory Product of Lipopolysaccharide-Activated Macrophages. *Proceedings of the National Academy of Sciences of the United States of America* 89:3511-3515.

Silence, J., D. Collen, and H.R. Lijnen. 2002. Reduced atherosclerotic plaque but enhanced aneurysm formation in mice with inactivation of the tissue inhibitor of metalloproteinase-1 (TIMP-1) gene. *Circ Res* 90:897-903.

Sorescu, D., M.J. Somers, B. Lassegue, S. Grant, D.G. Harrison, and K.K. Griendling. 2001. Electron spin resonance characterization of the NAD(P)H oxidase in vascular smooth muscle cells. *Free Radic Biol Med* 30:603-612.

Steinmann, B., P. Bruckner, and A. Superti-Furga. 1991. Cyclosporin A slows collagen triple-helix formation in vivo: indirect evidence for a physiologic role of peptidyl-prolyl cis-trans-isomerase. *J Biol Chem* 266:1299-1303.

Suzuki, J., Z.-G. Jin, D.F. Meoli, T. Matoba, and B.C. Berk. 2006. Cyclophilin A Is Secreted by a Vesicular Pathway in Vascular Smooth Muscle Cells. *Circulation Research* 98:811-817.

Suzuki, T., E.M. Isselbacher, C.A. Nienaber, R.E. Pyeritz, K.A. Eagle, T.T. Tsai, J.V. Cooper, J.L. Januzzi, A.C. Braverman, D.G. Montgomery, R. Fattori, L. Pape, K.M. Harris, A. Booher, J.K. Oh, M. Peterson, V.S. Ramanath, and J.B. Froehlich. 2012. Type-Selective Benefits of Medications in Treatment of Acute Aortic Dissection (from the International Registry of Acute Aortic Dissection [IRAD]). *The American journal of cardiology* 109:122-127.

Tangirala, R.K., E.M. Rubin, and W. Palinski. 1995. Quantitation of atherosclerosis in murine models: correlation between lesions in the aortic origin and in the entire aorta, and differences in the extent of

lesions between sexes in LDL receptor-deficient and apolipoprotein E-deficient mice. *J Lipid Res* 36:2320-2328.

Thomas, M., D. Gavrila, M.L. McCormick, F.J. Miller, Jr, A. Daugherty, L.A. Cassis, K.C. Dellsperger, and N.L. Weintraub. 2006. Deletion of p47phox Attenuates Angiotensin II-Induced Abdominal Aortic Aneurysm Formation in Apolipoprotein E-Deficient Mice. *Circulation* 114:404-413.

Thompson, R.W., and B.T. Baxter. 1999. MMP Inhibition in Abdominal Aortic Aneurysms: Rationale for a Prospective Randomized Clinical Trial. *Annals of the New York Academy of Sciences* 878:159-178.

Thompson, R.W., D.R. Holmes, R.A. Mertens, S. Liao, M.D. Botney, R.P. Mecham, H.G. Welgus, and W.C. Parks. 1995. Production and localization of 92-kilodalton gelatinase in abdominal aortic aneurysms. An elastolytic metalloproteinase expressed by aneurysm-infiltrating macrophages. *The Journal of Clinical Investigation* 96:318-326.

Thrasher, A.J., N.H. Keep, F. Wientjes, and A.W. Segal. 1994. Chronic granulomatous disease. *Biochimica et Biophysica Acta (BBA) - Molecular Basis of Disease* 1227:1-24.

Tieu, B.C., C. Lee, H. Sun, W. Lejeune, A. Recinos, 3rd, X. Ju, H. Spratt, D.C. Guo, D. Milewicz, R.G. Tilton, and A.R. Brasier. 2009. An adventitial IL-6/MCP1 amplification loop accelerates macrophage-mediated vascular inflammation leading to aortic dissection in mice. *J Clin Invest* 119:3637-3651.

Touyz, R.M., and E.L. Schiffrin. 1999. Ang II–Stimulated Superoxide Production Is Mediated via Phospholipase D in Human Vascular Smooth Muscle Cells. *Hypertension* 34:976-982.

Uchida, H.A., F. Kristo, D.L. Rateri, H. Lu, R. Charnigo, L.A. Cassis, and A. Daugherty. 2010. Total lymphocyte deficiency attenuates AngII-induced atherosclerosis in males but not abdominal aortic aneurysms in apoE deficient mice. *Atherosclerosis* 211:399-403.

Vasquez-Vivar, J., B. Kalyanaraman, and P. Martasek. 2003. The role of tetrahydrobiopterin in superoxide generation from eNOS: enzymology and physiological implications. *Free Radic Res* 37:121-127.

Wang, H.D., S. Xu, D.G. Johns, Y. Du, M.T. Quinn, A.J. Cayatte, and R.A. Cohen. 2001. Role of NADPH oxidase in the vascular hypertrophic and oxidative stress response to angiotensin II in mice. *Circ Res* 88:947-953.

Wang, P., F. Tang, R. Li, H. Zhang, S. Chen, P. Liu, and H. Huang. 2007. Contribution of different Nox homologues to cardiac remodeling in two-kidney two-clip renovascular hypertensive rats: Effect of valsartan. *Pharmacological Research* 55:408-417.

Wang, Y., H. Ait-Oufella, O. Herbin, P. Bonnin, B. Ramkhelawon, S. Taleb, J. Huang, G. Offenstadt, C. Combadiere, L. Renia, J.L. Johnson, P.L.

Tharaux, A. Tedgui, and Z. Mallat. 2010. TGF-beta activity protects against inflammatory aortic aneurysm progression and complications in angiotensin II-infused mice. *J Clin Invest* 120:422-432.

Williams, R.L., S.A. Courtneidge, and E.F. Wagner. 1988. Embryonic lethalities and endothelial tumors in chimeric mice expressing polyoma virus middle T oncogene. *Cell* 52:121-131.

Wingler, K., S. Wünsch, R. Kreutz, L. Rothermund, M. Paul, and H.H.H.W. Schmidt. 2001. Upregulation of the vascular NAD(P)H-oxidase isoforms Nox1 and Nox4 by the renin-angiotensin system in vitro and in vivo. *Free Radical Biology and Medicine* 31:1456-1464.

Xiong, W., J. Mactaggart, R. Knispel, J. Worth, Z. Zhu, Y. Li, Y. Sun, B.T. Baxter, and J. Johanning. 2009. Inhibition of reactive oxygen species attenuates aneurysm formation in a murine model. *Atherosclerosis* 202:128-134.

Xu, Q., M.C. Leiva, S.A. Fischkoff, R.E. Handschumacher, and C.R. Lyttle. 1992. Leukocyte chemotactic activity of cyclophilin. *Journal of Biological Chemistry* 267:11968-11971.

Yogi, A., C. Mercure, J. Touyz, G.E. Callera, A.C.I. Montezano, A.B. Aranha, R.C. Tostes, T. Reudelhuber, and R.M. Touyz. 2008. Renal Redox-Sensitive Signaling, but Not Blood Pressure, Is Attenuated by Nox1 Knockout in Angiotensin II–Dependent Chronic Hypertension. *Hypertension* 51:500-506.

Yuan, W., H. Ge, and B. He. 2010. Pro-inflammatory activities induced by CyPA-EMMPRIN interaction in monocytes. *Atherosclerosis* 213:415-421.

Zafari, A.M., M. Ushio-Fukai, C.A. Minieri, M. Akers, B. Lassegue, and K.K. Griendling. 1999. Arachidonic acid metabolites mediate angiotensin II-induced NADH/NADPH oxidase activity and hypertrophy in vascular smooth muscle cells. *Antioxid Redox Signal* 1:167-179.

Zhang, Y., J.C. Naggar, C.M. Welzig, D. Beasley, K.S. Moulton, H.-J. Park, and J.B. Galper. 2009. Simvastatin Inhibits Angiotensin II-Induced Abdominal Aortic Aneurysm Formation in Apolipoprotein E-Knockout Mice. *Arteriosclerosis, Thrombosis, and Vascular Biology* 29:1764-1771.

Zhao, H., J. Joseph, H.M. Fales, E.A. Sokoloski, R.L. Levine, J. Vasquez-Vivar, and B. Kalyanaraman. 2005. Detection and characterization of the product of hydroethidine and intracellular superoxide by HPLC and limitations of fluorescence. *Proc Natl Acad Sci U S A* 102:5727-5732.

Zhao, H., S. Kalivendi, H. Zhang, J. Joseph, K. Nithipatikom, J. Vasquez-Vivar, and B. Kalyanaraman. 2003. Superoxide reacts with hydroethidine but forms a fluorescent product that is distinctly different

from ethidium: potential implications in intracellular fluorescence detection of superoxide. *Free Radic Biol Med* 34:1359-1368.

Zhao, L., M.P.W. Moos, R. Grabner, F. Pedrono, J. Fan, B. Kaiser, N. John, S. Schmidt, R. Spanbroek, K. Lotzer, L. Huang, J. Cui, D.J. Rader, J.F. Evans, A.J.R. Habenicht, and C.D. Funk. 2004. The 5-lipoxygenase pathway promotes pathogenesis of hyperlipidemia-dependent aortic aneurysm. *Nat Med* 10:966-973.

Zou, A.P., J.D. Imig, M. Kaldunski, P.R. Ortiz de Montellano, Z. Sui, and R.J. Roman. 1994. Inhibition of renal vascular 20-HETE production impairs autoregulation of renal blood flow. *American Journal of Physiology - Renal Physiology* 266:F275-F282.

Appendices

Appendices

Timing and Venue of Research

The work described in this thesis was conducted between September 2009 to August 2012 in the British Heart Foundation (BHF) Molecular Cardiology Laboratory and Functional Genetics Facility, Department of Cardiovascular Medicine, Wellcome Trust Centre for Human Genetics, Oxford, UK.

Research Funding

The author was funded by the British Heart Foundation Centre of Research Excellence Clinical Training Fellowship. The laboratory of Professor Keith Channon is supported by a programme grant from the British Heart Foundation.

Abstracts presented at scientific conferences

Lampson Fan, Gillian Douglas, Jennifer Bendall, Eileen McNeill. Keith Channon. **Endothelial specific Nox2 Over-expression increases susceptibility to Angiotensin II induced aortic dissection.** *British Cardiovascular Society, Manchester UK, June 2012.* (Finalist oral presentation for Young Research Worker Prize, awarded **runner-up prize**)

Lampson Fan, Gillian Douglas, Jennifer Bendall, Eileen McNeill. Keith Channon. **Endothelial specific redox signalling regulates susceptibility to aortic dissection through Endothelial Cyclophilin A secretion.** *American Heart Association Annual Scientific Sessions, Orlando, Nov 2011.* (Oral Presentation, awarded **ATVB travel grant**. Invited for poster presentation at ATVB Early Career Meeting.)

Lampson Fan, Gillian Douglas, Jennifer Bendall, Eileen McNeill. Keith Channon. **Targeted Endothelial Nox2 Overexpression Potentiates Aortic Dissection In Response to Angiotensin II.** *British Atherosclerosis Society Autumn Meeting, Oxford, September 2010.* (Oral Presentation).

Prepared Manuscript:

Endothelial Cell-Specific ROS Production Determines Susceptibility to Aortic Dissection in Mice. *In submission*